8-8-2024 2:30 PM

Therapeutic Promise and Insights for Parkinson's Disease from the Living Brain

Simon M. Benoit, *University of Western Ontario*

Supervisor: Hebb, Matthew, *The University of Western Ontario*
Co-Supervisor: Schmid, Susanne, *The University of Western Ontario*
A thesis submitted in partial fulfillment of the requirements for the Doctor of Philosophy degree in Neuroscience

Abstract

Background: Parkinson's disease (PD) is a neurodegenerative disorder characterized by the progressive loss of dopaminergic neurons in the brain. To date, no disease-modifying treatments for PD are available and novel insights and therapeutics are essential. This thesis explores a novel substrate for cell-based therapies for PD, brain-derived progenitor cells (BDPCs), derived from living PD brain samples obtained during deep-brain stimulation surgery, while also utilizing this unique tissue source to gain important insights into the molecular underpinnings of the disease. **Methods:** In Chapter 2, human and rat BDPCs were compared, and the latter engineered for longitudinal tracking *in vivo* using bioluminescence imaging(BLI). The engineered cells were implanted in a rodent syngeneic graft model to evaluate BDPCs survival and integration after transplantation, mimicking an autologous therapeutic application. Chapters 3 and 4 utilized RNA sequencing to analyze gene expression and alternative splicing changes in the living PD frontal cortex. A random forest classifier was then trained on a 370-gene signature to discern PD samples from healthy controls. **Results:** Rodent BDPCs exhibited qualities analogous to their human counterparts, including expression and secretion of neurotrophic factors BDNF and GDNF. The rodent BDPC grafts could be tracked effectively with BLI, and showed survival and engraftment in the host brain. Transcriptomic profiling of the living PD brain revealed dysregulation of genes involved in trophic factor signaling, apoptosis, inflammation, and other key pathways. Numerous alternative splicing events were also found to be altered in PD. Building on these findings, a machine learning classifier was developed that could accurately distinguish PD samples from controls using the PD-associated gene expression signature, with potential applications for early diagnosis. **Conclusions:** This thesis establishes a preclinical platform to evaluate autologous BDPCs as a cell-based therapy for PD and provides unprecedented insights into the molecular landscape of the living PD brain. The identification of novel dysregulated pathways and splicing events, as well as the development of a diagnostic classifier, opens new avenues for understanding disease mechanisms and developing targeted (disease-modifying) interventions. The ability to directly access and interrogate the living PD brain represents a powerful approach to advance Parkinson's disease research.

Keywords

Parkinson's disease, cell-based therapy, gene expression, RNA sequencing, bioluminescence imaging, cell tracking, alternative splicing, brain-derived progenitor cells, machine learning, gene signature

Summary for Lay Audience

Parkinson's disease (PD) is a brain disorder that causes problems with movement, balance, and other functions. People with PD gradually lose important brain cells that produce a chemical called dopamine, which is crucial for coordinating movement. Medications can help manage the symptoms for a while, but there is currently no cure. One promising approach being explored to treat PD is cell therapy, where healthy cells are transplanted into the brain to replace or repair the ones that have been lost or support the remaining cells. Unfortunately, researchers have not found suitable conditions and cell types to successfully treat PD in this way. We have discovered a new source of stem-like cells, called brain-derived progenitor cells (BDPCs) that can be isolated from the brain of patients living with PD while they are undergoing surgery. These BDPCs have qualities that make them excellent candidates for cell therapies. In animal studies, we show that these BDPCs can survive and integrate when transplanted into the brain, suggesting they might be useful as a treatment. We also used advanced genetic analysis techniques to examine the activity of genes in the Parkinson's brain tissue. Many genes involved in supporting brain cell health, reducing inflammation, and other key processes had different levels of expression in the Parkinson's samples compared to healthy brains. Interestingly, we also found many changes in how certain genes were being assembled, or "spliced," which can impact their function. Using the data from our genetic analyses, we developed a computer algorithm that could accurately identify Parkinson's patients by looking at the activity of a unique set of genes in brain and even blood samples. This strategy could lead to earlier and more reliable diagnosis of PD in the future. Overall, this work gives us new information about how PD happens and gives us ideas for developing new tools and treatments for PD. It also shows how much valuable information can be gained by studying the living Parkinson's brain.

Co-Authorship Statement

Chapter 3 is reprinted from: Benoit SM, Xu H, Schmid S, Alexandrova R, Kaur G, Thiruvahindrapuram B, Pereira S, Jog M, Hebb MO. (2020) “Expanding the search for genetic biomarkers of Parkinson’s disease into the living brain”. *Neurobiology of Disease*. SMB contributed to experimental design, data collection and analysis, and drafted the manuscript. HX prepared samples for RNA-Seq and assisted with in vitro data collection and analysis. GK and SP completed the RNA-Seq. RA did RNA-Seq data analysis. SS and GK helped with project organization, analysis and manuscript review. MOH participated in experimental design, execution, data analysis, manuscript drafting and review.

Acknowledgements

As with any work on this scale, I have many incredible individuals to thank for helping me along the way.

I want to start by thanking my supervisors Drs. Matthew Hebb and Susanne Schmid for all their consistent support throughout the years, especially when life started throwing wrenches in my carefully laid plans. Dr. Hebb you provided invaluable feedback, a sharp intellect and an infectious curiosity that never seems to wane. Dr. Schmid, you always made me feel welcome in your lab despite my project having truly little to do with your research and provided me with an incredible space to foster relationships with other graduate students and to grow as a researcher.

Hu X., you were the backbone of the Hebb lab, providing assistance to anyone that needed it and performing experiments that bordered on magic.

Cleusa D., your animal handling and surgical skills were invaluable for my project, though your smile probably helped me more.

Andrea D. and Andrew D., you came into the Hebb lab and made what was a noticeably quiet space so much livelier. I learned so much from you both and would not have enjoyed my doctoral experience quite as much without you.

Niveen F. and Faraj H., with Andrew you rounded out a core group of Ph.D. students that I will always be thankful to count as friends. I will never forget our experiences at conferences, at the Grad Club, with SONGS and particularly the chaos of organizing Neuroscience Research Day each year.

To my family, I would not have been who I am without you, and I cannot overstate how much your support has helped along the way, despite many of you only having a vague idea of what I was doing and why it was taking so long.

My partner Jen, just your presence in my life gave me the extra push I needed to bring this thesis to completion. You were there for me when I might have otherwise been alone and needed help that I likely would not have asked for.

Lucie and Caleb, my kids, you were my driving force from the beginning and gave me the determination I needed when it was required, while reminding me that life is a precious thing.

Anyone that I have not mentioned by name, the many friends who were there for me throughout the years, I appreciated you all.

Finally, I need to acknowledge the patient participants who bravely decided that they would take an active role in assisting others suffering with Parkinson’s disease. Your contribution was instrumental to the work that we did in this dissertation.

Table of Contents

List of Tables

List of Figures

List of Appendices

List of Abbreviations

6-OHDA	6-hydroxydopamine
AAV	adeno-associated viral vector
ACSF	artificial cerebrospinal fluid
ALP	autophagy-lysosome pathway
AM	adrenal medullary
AS	alternative splicing
ASE	alternative splicing event
ATP13A2	+ ATPase 13A2
AUC	area under the curve
AXIN2	axin 2
BDNF	brain-derived neurotrophic factor
BDPCs	brain-derived progenitor cells
BLI	bioluminescence imaging
BSA	bovine serum albumin
CBTs	cell-based therapies
CCD	cooled charged coupled device
CDNF	cerebral dopamine neurotrophic factor
cGMP	good manufacturing practice
CLK1	CDC Like Kinase 1
CLK3	CDC Like Kinase 3
CLK4	CDC Like Kinase 4
CNS	central nervous system
CP	ceruloplasmin
CSF	cerebrospinal fluid
CSN1S1	casein alpha S1
CX3CR1	CX3C chemokine receptor 1
DAPI	4,6-diamidino-2-phenylindole
DBS	deep-brain stimulation
DEGs	differentially expressed genes
DJ-1	parkinsonism associated deglycase
DMEM	Dulbecco's modified Eagles medium
DMT	disease-modifying therapies
dPSI	delta percent spliced in
DR4	death receptor 4
EIF4G1	eukaryotic translation initiation factor 4 gamma 1
ER	endoplasmic reticulum
ERBB2	ErbB2 Receptor Tyrosine Kinase 2
ERBB3	ErbB2 Receptor Tyrosine Kinase 3
EVD	extraventricular drain
F5	factor 5
FACS	fluorescence activated cell sorting

FBS	fetal bovine serum
FBX07	F-box protein 7
FGF18	fibroblast growth factor 18
FLuc2	firefly luciferase 2
FOS	Fos proto-oncogene, AP-1 transcription factor subunit
fVM	fetal ventral mesencephalic
GADD45G	growth arrest and DNA damage inducible gamma
GBA	glucocerebrosidase
GDNF	glial-derived neurotrophic factor
hESCs	human embryonic stem cells
HGF	hepatocyte growth factor
HPT	hypothalamic-pituitary-thyroid
IL-1R2	interleukin 1 receptor, type II
iPSC	induced pluripotent stem cells
IRF7	interferon regulatory factor 7
IRF8	interferon regulatory factor 8
LB	Lewy bodies
LRRK2	leucine-rich repeat kinase 2
MANF	mesencephalic astrocyte-derived neurotrophic factor
MPTP	1-methyl-4-phenyl-1,2,3,6-tetrahydropyridine
NF-κBIA	NF-kappaB inhibitor protein A
NG2	neural/glial antigen 2
NGF	nerve growth factor
NGS	next-generation sequencing
NM-MRI	neuromelanin sensitive MRI
NRTN	neurturin
NTFs	neurotrophic factors
OATP1A1	rat organic anion transporting polypeptide 1a1
PAI	plasminogen activator inhibitor 1
PBS	phosphate-buffered saline
PD	Parkinson’s disease
PFA	paraformaldehyde
PINK1	PTEN induced putative kinase 1
PLA2G6	phospholipase A2 group VI
PRKN	parkin RBR E3 ubiquitin ligase
qPCR	quantitative real-time polymerase chain reaction
RDBCTs	randomized double-blind controlled trials
RF	random forest
RNA-seq	Ribonucleic acid sequencing
RT	room temperature
RT-PCR	reverse transcription-polymerase chain reaction
SEPT5	septin 5

SERPINE1	Serpin Family E Member 1
SERPINH1	Serpin family H member 1
SGK1	serum/glucocorticoid regulated kinase 1
SNCA	alpha-synuclein
SNpc	substantia nigra pars compacta
TBS	Tris-buffered saline
TdT	TdTomato
TFAP2D	transcription factor AP-2 delta
TNFRSF10A	tumor necrosis factor receptor superfamily member 10A
TNSFF10	tumor necrosis factor superfamily member 10
TRAIL	tumor necrosis factor-related apoptosis-inducing ligand
TRH	thyrotropin-releasing hormone
trkB	tropomyosin-related kinase type 2
UPDRS	Unified Parkinson's Disease Rating Scale
UPS	ubiquitin-proteasome system
VPS35	vacuolar protein sorting 35
ZFP36	zinc finger protein 36

Chapter 1

1 Introduction

1.1 Motivation and Overview

Parkinson's disease (PD) was first described more than two centuries ago by James Parkinson and is now the fastest growing neurological disorder and the leading source of disability worldwide.[1,2] Efforts to understand the exact mechanisms underlying neurodegeneration in PD are still ongoing, hindered by disease complexity and multiple dysregulated systems that may contribute to varying degrees. At present, we lack the proper tools to accurately diagnose PD, particularly before major neurodegeneration has occurred, and we have yet to develop interventions to slow, halt, or reverse disease progression.

In this thesis, we explored the potential of small cortical biopsies from living patients with PD as a therapeutic vehicle to expand our knowledge of the disease through next-generation sequencing. These samples were obtained during a planned surgical intervention to implant a deep-brain stimulation electrode for the treatment of PD. In Chapter 2, we established an animal model to evaluate the therapeutic potential of what we termed brain-derived progenitor cells (BDPCs), which we had previously shown to be obtainable from human cortical biopsy tissue.[3] In Chapter 3, gene expression in the cortex of patients with PD was examined using next-generation sequencing, for the first time to our knowledge in living humans.[4] Chapter 4 expanded on this work by investigating alternative splicing alterations and the application of machine learning to identify PD based on a signature of differentially expressed genes. Finally, Chapter 5 concludes with a summary of the significant findings of the thesis, limitations of the work, and possibilities for future research.

1.2 Parkinson's disease

Parkinson's disease (PD) is a progressive disorder characterized by widespread loss of neurons and non-neuronal cells of the central nervous system (CNS), particularly dopaminergic neurons of the substantia nigra pars compacta (SNpc). Currently, a spectrum of clinical features is used to diagnose PD, although confirmation is only through postmortem analysis. Clinical diagnosis is based on motor features such as bradykinesia (i.e., slowness of movement), resting tremor and rigidity, and postural instability in later stages of the disease.[5,6] Depression, anxiety, apathy, cognitive dysfunction, hyposmia, constipation, and sleep disorders often accompany the motor symptoms sometimes preceding their appearance by many years.[7] Many of these features of PD are attributed to dopaminergic dysfunction related to neuronal loss in the SNpc and are responsive to dopamine replacement therapy. Other factors, such as olfactory dysfunction, are attributed to widespread pathological CNS and non-CNS changes.

1.2.1 Epidemiological data

PD is the fastest growing neurological disorder presently, second most common after Alzheimer's, affecting 11.86 million people worldwide as of 2021[8] This figure has increased by 273.9% since 1990, a rise in incidence that cannot be entirely explained by an aging worldwide population. It's been estimated that the figure may reach 12 million by 2040 based on current trends and even as high as 17 million when factoring an increase in the use of toxic pesticides associated with PD, a decrease in smoking -a habit which appears to be protective against the disease - and the likelihood that longevity will increase further.[9] The latter figure seems more likely based on the data from 2021. This surge in disease cases is accompanied by a concomitant rise in disability-adjusted life-years and death rates over the same period. If this trend persists, the societal burden of PD will considerably increase in the future. The impact also extends to caregivers who are subject to increasing demands physically, psychologically, socially, and financially.[10]

A study published in 2002 on PD in the USA estimated that the lifetime risk of PD was at 2% for men and 1.3% for women, after adjusting for competing risk factors. More recently, projections of the lifetime risk in France were much higher, estimating a 6.0% chance in men and 5.5% in women in 2010, projected to increase to 7.4% and 6.3%, respectively, by 2030.[11,12] Factors such as pesticide exposure, traumatic brain injury, diabetes, history of melanoma, methamphetamine use, and high dairy intake have been associated with an increased risk of PD in longitudinal studies. Conversely, physical activity, tobacco use, caffeine intake, and high serum urate levels have strong evidence for reducing risk, with lesser quality or conflicting evidence for neuroprotective properties for healthy eating, tea consumption (adjusting for total caffeine), and use of nonsteroidal anti-inflammatory drugs.[13]

Several randomized double-blind controlled trials (RDBCTs) are ongoing or have been completed using these data to guide the treatment of PD. Treatment with a transdermal nicotine patch in early PD did not slow progression as expected and caused a worsening of Unified Parkinson's Disease Rating Scale (UPDRS) scores with and without an 8-week washout period (2.5 and 3.7 mean score decrease treatment vs. control).[14] Caffeine use did not provide a measurable difference in UPDRS score after 6 months of 200 mg twice per day consumption in a cohort of 60 patients with 1-8 years PD duration on stable symptomatic therapy.[15] A phase III trial using Inosine to increase serum urate levels was terminated prematurely after an interim analysis showed ineffectiveness of the drug to mitigate clinical decline (https://clinicaltrials.gov/study/NCT02642393). Based on these studies, lower epidemiological PD risk has yet to be translated into useable therapeutics for the treatment of PD, and further work will be required to establish the complex relationships between these behavioral or environmental factors and the development of PD.

1.2.2 Pathophysiology

From a pathological perspective, the primary postmortem finding in PD is the loss of neurons in the SNpc and the formation of intracellular protein aggregates called Lewy bodies (LB) and smaller Lewy neurite inclusions. It was long thought that the loss of 50-70% of SNpc dopaminergic neurons was what led to the development of clinical motor symptoms, though considerable variability in post-mortem examinations [16] and neuromelanin sensitive MRI (NM-MRI) in early PD do not appear to support that notion.[17–19] A recent imaging study using the pre-synaptic dopamine tracer ^{123}I-ioflupane SPECT reported that the loss of terminals in the striatum corresponded more closely to the progression of motor symptoms in the early stages of PD, while in advanced PD they were inversely correlated to loss of neuromelanin positive cell bodies in the SNpc as detected by NM-MRI.[20] Taken together, these data appear to indicate that the primary loss driving motor symptoms occurs at striatal motor terminals in earlier stages of PD, while the cell bodies in the SNpc tend to consistently degenerate in more advanced stages of the disease, occurring in a manner which can vary considerably in each patient.

Many forms of LB have been reported, though the classic LB consists of a denser inner core composed of a complex mixture of proteins, lipids, metal ions, organelles and an outer filamentous structure.[21,22] While α-synuclein is considered a key component of LB, these pathological deposits contain ubiquitin, neurofilaments and a lesser fraction of proteins also found in Alzheimer's disease or Amyotrophic Lateral Sclerosis including amyloid beta and tau, and organelles such as vesicles and mitochondria.[23,24] Inclusions are found in the highly susceptible SNpc, as well as in extra-nigral dopaminergic, serotoninergic and cholinergic tracts throughout the neocortex, the olfactory bulb; the autonomic nervous system and in epidermal nerves.[25,26] Braak staging proposes a neuroanatomically based staging scheme for PD and suggests that Lewy pathology starts in the olfactory bulb, the central and peripheral nervous system and the lower brainstem, progressing in a caudal to rostral manner to other adjacent structures.[27] Though the validity of Braak staging has been the subject of vigorous debate, there is a consensus for widespread pathophysiological changes in PD.

1.2.3 Etiology

The pathology of PD is consistent and allows for accurate postmortem diagnosis; however, the underlying etiology of PD remains unclear. Pathogenesis appears to be multifactorial, with contributions from environmental and hereditary factors thought to induce changes in many interconnected biological pathways.[28]

Impaired protein processing, including abnormal aggregation, trafficking, and degradation are among the most widely investigated areas of research because of the hallmark presence of alpha (α)-synuclein-containing cytoplasmic inclusions in degenerating brain areas in PD. Both the autophagy-lysosome pathway (ALP) and the ubiquitin-proteasome systems (UPS) are important cellular defense systems responsible for the degradation of toxic misfolded or otherwise damaged proteins. When these homeostatic processes become dysregulated, many of the other areas of intense research—oxidative stress, mitochondrial dysfunction, and protein aggregation to name a few—also come into play and increasing evidence shows together lead to neurodegeneration.[29] Remarkably, 11 of 24 genetic loci associated with PD are involved or modulate functions of the ALP.[30] For example, mutations causing the A53T and A30P forms of α-synuclein are thought to disrupt α-synuclein degradation via chaperone-mediated autophagy. This is hypothesized to occur by blocking the LAMP2A lysosomal receptor, thereby causing the accumulation of both wild-type and mutant α-synuclein leading to cellular toxicity.[31,32] Misfolded α-synuclein can propagate in a self-templating prion-like fashion and can be transmitted between cells *in vitro*[33] and *in vivo* in animals, as evidenced by countless studies(reviewed in [34]). Transmission occurs in such a way that, despite lacking the potential predispositions of host cells, pathological aggregates were detected in implanted fetal and embryonic dopaminergic neurons in human clinical trials. [35–38] However, Lewy body pathology on its own is neither sufficient or required to cause neuronal death as many cases report patients with pathology not developing PD, as well as the inverse where PD patients do not exhibit Lewy pathology.[39]

Mitochondrial dysfunction, particularly mitochondrial bioenergetics, may partly explain the regional susceptibility of neurons, as the large arbors of dopaminergic neurons are more vulnerable to oxidative stress as a result of higher axonal mitochondrial density and basal levels of oxidative phosphorylation.[40] Further implicating mitochondrial dysfunction, the PD associated Parkin and PINK1 genes code for enzymes that cooperate to target damaged mitochondria and mitochondrial membrane components for ubiquitylation and subsequent degradation by the UPS.[41–43] 1-methyl-4-phenyl-1,2,3,6-tetrahydropyridine(MPTP) is an industrial chemical and accidental by-product of illicit drug production which acts as a strong neurotoxin causing severe motor symptoms closely resembling advanced PD in humans and primates.[44,45] It has been used in animal models to replicate disease pathophysiology, along with the pesticide rotenone more recently, both of which interfere with the mitochondrial electron transport chain by disrupting complex I activity leading to oxidative stress, alpha-synuclein aggregation and Lewy pathology producing selective degeneration of the nigrostriatal dopamine system. [46–48]

Whether as a reactive neuroprotective process to other pathology or a distinct degenerative process, neuroinflammation and oxidative stress are believed to play a significant role in the pathophysiology of PD. [49–51] Neuroinflammation is primarily mediated by microglia, phagocytic cells of the innate immune system, which are activated upon immune challenge or after brain injury. [52,53] Activated microglia produce superoxide and nitric oxide, which contribute to oxidative and nitrative stress. They also produce other potentially toxic agents, including glutamate and tumor necrosis factor-alpha, which can promote neurodegeneration. Under normal circumstances, activated microglia repair damaged tissue by clearing toxic agents or cellular debris via phagocytosis and releasing inflammation-mediating cytokines, eventually resolving the inflammatory response.[54] However, under pathological conditions, neuronal cell death releases damaged molecules which further activate microglia, creating a neurotoxic vicious cycle which can cause a chronic proinflammatory state. Based on animal studies, the midbrain likely contains more microglial cells than other brain regions, which can be particularly damaging to dopaminergic neurons.[55]

Despite substantial advances in our understanding of PD pathogenesis, the etiology of PD has yet to be attributed specifically to one pathological process or a combination thereof. Many relationships exist between the cellular processes under investigation, which supports the multi-hit hypothesis of neurodegeneration.[56] This hypothesis proposes that several factors mediate cellular toxicity and that various combinations of these factors can result in cell death leading to pathological neuronal losses. Genetic (discussed in Section 1.4) and environmental factors that increase the risk of developing PD (see Section 1.2.1) modulate these biological pathways in a manner that has yet to be elucidated.

1.2.4 Treatment

1.2.4.1 Pharmacological

Decay of midbrain structures in patients with PD results in a decline in the ability to produce the neurotransmitter dopamine. The dopamine precursor l-3,4-dihydroxyphenylalanine, known as L-dopa or levodopa, has been the mainstay symptomatic treatment for PD since the late 1960s. It is generally used in combination with a peripheral enzyme inhibitor, DOPA decarboxylase, to prevent the synthesis of dopamine outside the central nervous system. As the disease progresses, increases in the frequency and dosage of levodopa are necessary as pathophysiological changes in the brain cause a decreased long-duration and short-duration medication response. The “storage hypothesis” proposes that presynaptic dopaminergic terminals in PD have a reduced dopamine storage capacity and therefore cannot act as a buffer for plasma levodopa levels, effectively causing motor fluctuations.[57] These fluctuations can produce a marked on-off effect whereby symptoms wax and wane cyclically throughout the day, particularly in later stages of the disease. To counter this effect, long-acting levodopa formulations, slow-release intestinal gels, direct-infusion pumps, and inhaled powder targeted at off-peak periods can be helpful. Often, patients will also use adjunct or alternative treatment options to minimize side-effects and limit high medication doses and related adverse events. These can include dopamine agonists, dopamine metabolism inhibitors such as catechol-O-methyl transferase and monoamine oxidase B inhibitors, anticholinergics, and the NMDA receptor antagonist amantadine. While most individuals with PD are responsive to dopaminergic medication, off periods become more prevalent starting as early as 2 years after starting levodopa, and approximately 40% of patients will develop dyskinesias after 4-6 years of treatment.[58]

1.2.4.2 Surgical

Before the introduction of levodopa to treat PD, surgical interventions using ablative techniques were commonly used. The first attempts targeting the motor cortex to treat tremor date back to World War II[59], with further refinement of stereotactic lesions targeting the pallidum and thalamus improving tremor and rigidity without inducing paralysis.[60,61] Without the benefit of modern surgical tools and imaging techniques mortality for these procedures was significant, leading to abandonment for years, particularly after the effectiveness of levodopa was demonstrated for PD. A resurgence of ablative techniques such as caudatomy and pallidotomy, some using new technologies like the Gamma Knife©, has occurred more recently with the realization that levodopa effectiveness diminishes with time and can cause side-effects such as dyskinesia.[62] Pallidotomy can still be performed safely, at lower cost, in less specialized centers and in certain cases when deep-brain stimulation(DBS) surgery is not possible.[63]

DBS is the current surgical treatment of choice for PD. For a subset of patients who meet criteria (e.g. <70 years of age, idiopathic PD duration ≥4-5 years, response to dopaminergic therapy, absence of psychiatric and cognitive concerns), DBS can provide relief for motor symptoms (i.e., bradykinesia, tremor, and rigidity) that might otherwise be intractable with drug therapy alone.[64] Improvement of dyskinesias can also be achieved secondary to a reduction of the need for dopaminergic drugs after DBS. DBS for PD involves placement of an electrode targeting the subthalamic nucleus or the internal portion of the globus pallidus, which provides rhythmic stimulation with titratable parameters specific to each individual. Although DBS has been established as a therapeutic neurosurgical intervention for PD since the 1990s, the mechanism of action is not entirely understood.[65] It was initially proposed that stimulation causes reversible inhibition at the target site similar to that observed with ablation.[66] The effect of DBS may mimic a temporary lesion by creating a depolarization block through electrical entrainment. (Meissner 2005, McIntyre & Anderson 2016) However, the mechanism of action surpasses simple inactivation in the area surrounding the DBS electrode and influences neural networks, neurotransmitters, the adjacent microenvironment (i.e. surrounding astrocytes and microglia) and neuroplasticity.[67] Studies in animal models even suggest a neuroprotective effect, possibly mediated by modulation of neurotrophic factors(NTFs) including brain-derived neurotrophic factor.[68–70] The efficacy, safety and adjustable nature of DBS, combined with a potential neuroprotective effect make it a powerful modern modality for treating PD.

1.2.4.3 Supportive

As discussed in section 1.2.1, some non-pharmacological interventions also show promise, particularly various forms of exercise. A phase II clinical trial in which newly diagnosed patients with PD not on dopaminergic therapy underwent high-intensity treadmill training at 80-85% of maximum heart rate resulted in a mean decrease in UPDRS motor score of only 0.3 compared with 3.2 in the standard care group after 6 months. [71] This corroborates earlier findings of neuroprotection by intensive exercise regimens, including a crossover trial comparing physiotherapy and weight-supported treadmill therapy in which the treadmill intervention resulted in a significant 6 point reduction (vs. 1.1 with physiotherapy) in UPDRS score after 4 weeks.[72] Dance interventions, resistance exercise and multimodal exercise programing also have growing, though largely preliminary and underpowered evidence for disease-modifying effects.[73–76] Effects may not be limited to motor symptoms as improvement in attention and working memory after progressive resistance training have also been noted after 12 and 24 months.[77] Much of the measured protective or beneficial effects are almost certainly related to adaptations to strength, balance and coordination, which would modify the scores for motor components of the UPDRS, one of the primary outcomes of all of these studies. Future work will need to distinguish whether improvements are neuroprotective through mechanisms such as neurotrophic factor release, antioxidative capacity, and promotion of autophagy and neurogenesis, as some preclinical work seems to indicate.[78,79]

1.2.4.4 Clinical Trials

To date, no pharmacological or surgical intervention prevents or delays the progression of PD.[80] However, a 2022 review of pharmacological clinical trials found 147 ongoing trials with 56 focused on disease-modifying therapies (DMT).[81] most of those trials are in early phases, but (1) Exenatide, a glucagon- like peptide-1 receptor agonist that reduces glucose in type 2 diabetes (2) Memantine, an NMDA receptor antagonist used to treat Alzheimer's disease, and (3) Ganoderma, a mushroom used in traditional Chinese medicine, were all in phase III clinical trials. Three phase II trials were due to be completed in 2022. Considering the current treatment regimen for PD, an RDBCT published in 2004 suggests that long-term therapy with levodopa may elicit a decline in dopamine transporter density while potentially slowing the progression of PD.[82] Another recent study supports this notion, showing that motor symptoms scores in the off-drug state declined slower than the projected scores for the natural disease course, independent of disease duration.[83]

Cell-based therapies to replace or support degenerating dopaminergic structures, and therapies with neurotrophic factors, are still ongoing as well (see section 1.3 for more detail). Certainly, many promising avenues of research are being investigated to improve upon or replace the purely symptomatic treatments for PD that, in the case of levodopa, have been the mainstay of therapy for the last half century.

1.3 Cell and neurotrophic factor-based therapies for Parkinson's disease

PD widely affects both neurons and non-neuronal cells throughout the nervous system; however, progressive loss of mesencephalic dopaminergic neurons is the pathological hallmark of PD. With the success of dopamine replacement therapy for treating PD in the 1960s, the prospect of cell-based dopamine replacement by neural grafting of various cell types in the affected brain areas (i.e. striatum), attracted the interest of researchers as the logical next step (see[84,85] for excellent reviews).

1.3.1 Preclinical and early clinical trials of cell-based therapies

Preclinical models first attempted bulk implants of adrenal medullary (AM) or fetal ventral mesencephalic(fVM) tissue grafts into either the lateral ventricle or a preformed cavity in the striatum, followed by cell suspensions in the 1980s. AM grafts circumvented the fVM issues of graft rejection and ethical issues with sourcing cells, however the grafts had low survival and modest effects.[86] Conversely, fVM tissue showed innervation and dopamine release helping to restore deficits caused by 6-hydroxydopamine-induced lesions.[87–92]

Despite poor pre-clinical evidence, the first human open label trial with AM grafts still occurred in 1982[93], followed by another 8 trials over several years.[84] By the early 90s AM grafting was largely abandoned when results from the United Parkinsons Foundation Neurotransplantation registry were published reporting limited benefit from the transplants, combined with complications from surgical intervention leading to psychiatric disturbances among others.[94] Post-mortem examinations also found necrotic adrenal medullary tissue with significant surrounding inflammatory response indicators.[95–99] Open-label trials with fVM were generally more encouraging, with some patients able to stop taking anti-PD medications completely and ^{18}F-dopa scans showing restoration of dopamine signaling in grafted striatum.[100–102] These promising results led to two NIH-funded RDBCTs to address possible placebo effects[103,104], though the design of these trials was considered premature and came to be criticized for their untested grafting protocols, inadequate immune suppression and poor graft quality controls.[105] Even though both trials followed different protocols, parallels could be drawn from their outcomes in that younger patients or patients with milder motor symptoms benefited most from the procedure, graft survival was confirmed in most patients by PET imaging or post-mortem examinations and a significant proportion of grafted patients developed graft-induced dyskinesias (15% and over 50% respectively). The use of fVM tissue was largely abandoned after these trials, but enough patients had significant benefits that a working group was formed to identify trial shortcomings and develop an optimized approach to fVM transplantation. The working group identified that an ideal study would target younger, less clinically advanced patients with preserved ^{18}F-dopa PET signaling and an absence of levodopa-induced dyskinesias, combined with long-term immunotherapy and grafts of more than 100 000 cells per side. These parameters informed a new multicenter, open-label human fVM trial called TRANSEURO.[106] This trial transplanted its first patient in 2015 and reached its clinical end point in 2021 after 11 patients received fVM grafts, although full results have yet to be published(https://clinicaltrials.gov/ct2/show/NCT01898390).

1.3.2 Native and induced pluripotent stem cells

The ability to isolate pluripotent differentiation-capable human embryonic stem cells(hESCs) meaningfully altered the cell-based therapy landscape in the years following this discovery.[107] Human fVM tissue transplants, while promising, did not represent a feasible therapeutic option in the long term because of ethical contention and logistical issues surrounding obtaining the required tissue. hESCs, on the other hand, are more readily available, renewable, and bankable. From a safety perspective, undifferentiated pluripotent stem cells do carry the risk of neoplasia through unchecked proliferative capacity, with some cases of teratoma formation being reported in the literature.[108] With that in mind, good manufacturing practice (cGMP) compliant and scalable cellular protocols were crucial for a safe transition to human clinical trials . as achieved in the following two decades for both undifferentiated hESCs and ventral midbrain dopamine progenitor cells.[109,110]

In 2006, another milestone publication outlined the protocol for induction of fibroblasts into what were termed induced pluripotent stem cells (iPSC), which could be patterned into dopaminergic neurons similar to hESCs.[111,112] iPSCs opened the door to the possibility of generating autologous stem cells for the personalized treatment of various diseases, including PD. Following the discovery that dopaminergic neurons uniquely develop from the floor plate rather than from neuroepithelial progenitors, protocols were further refined to efficiently differentiate iPSCs into functional midbrain dopaminergic neurons. [113,114] Compared with previous iterations, iPSCs derived using these more sophisticated protocols were nontumorigenic and adequately integrated to provide effective functional recovery.[115–118]

Similar to what was achieved with hESCs, midbrain dopaminergic neurons derived from iPSCs can now be produced at scale under conditions that adhere to cGMP guidelines.[118] Now that such cell production pipelines and a sufficient body of pre-clinical literature with efficacy exists, clinical trials have been approved with dopaminergic neurons derived from iPSCs in Japan[119], and parthenogenetic hESCs in Australia and China [120](https://clinicaltrials.gov/study/NCT3119636). Preliminary results from the Australian trial reported 10 successful transplants, with 8 patients completing the active phase.[121] No significant adverse events were reported after 1 year, and patients improved in a dose-dependent manner after 6 months on the Hauser Motor Diary, PD Quality of Life Questionnaire, and Global Clinical Impression measures. The GForce-PD group, a global collaborative initiative collectively using knowledge and experience gathered through previous trials (e.g. TRANSEURO) and a rigorous approach to cell manufacturing and preclinical testing, has also planned four trials in multiple centers using hESCs, allogenic iPSCs, and autologous iPSCs as cell source.[122]

In the last two decades, hESC and iPSC technologies have overcome many of the hurdles of earlier CBT, refining techniques to increase purity and yields of progenitor and mature cells with the A9 midbrain dopaminergic neuron phenotype to scaled production under GMP conditions needed for clinical trials. Overall, it remains to be seen whether any of the proposed cellular substrates and trial protocols will confer enduring benefit and avoid safety issues with tumorigenicity, immune rejection, and graft-induced dyskinesias, but the progress made, and preliminary results are encouraging thus far.

1.3.3 Evidence for a cortical stem cell niche

Contrary to what was considered canon for many years, the adult brain contains progenitor cells capable of producing astrocytes, oligodendrocytes, and neurons, namely in the subventricular zone[123] and dentate gyrus.[124] What is less widely known is that progenitor cells also exist in many other areas of the brain, including the cortex, striatum, and septal regions, as has been described in rodents [125], primates [126] and humans. [127,128] Our laboratory has previously shown that small cortical biopsies can be safely obtained from non-eloquent areas in the frontal lobe of patients with PD (PD) during deep brain stimulation surgery.[3] Primary cultures from these samples can be expanded and yield large numbers of what we have termed brain-derived progenitor cells (BDPCs). Interestingly, these cells endogenously express progenitor and glial lineage markers, as well as brain-derived neurotrophic factor (BDNF), glial-derived neurotrophic factor (GDNF), and cerebral dopamine neurotrophic factor (CDNF).

While cell grafts were initially pursued as a method to replace degenerating dopaminergic circuitry, they also have the potential to confer sustained drug levels to specific diseased brain areas in a way that is not possible through systemic routes. As described in the previous sections, the search is still ongoing for a cell with ideal qualities for replacement strategies, with many of those qualities also lending themselves to use as a substrate for prolonged therapeutic molecule delivery. The colocalization of neurotrophic factors with neural progenitor markers raised the intriguing prospect that BDPCs may effectively integrate back into the host brain as an autologous graft and confer broad and enduring therapeutic function in PD and other neurological diseases.

1.3.4 Neurotrophic factors for the treatment of Parkinson's disease

NTFs are a family of largely peptidic biomolecules that support the growth and differentiation of developing and mature neurons.[129] The first research studies on NTFs were conducted on nerve growth factor(NGF) in the early 1950s.[130] The large number of NTFs that have since been discovered mostly fit into three families: the neurotrophins (BDNF, neurotrophin-3, neurotrophin-4 and NGF); the GDNF-family of ligands (GDNF, neurturin (NRTN), artemin and persephin); and the neuropoietic cytokines. They generally exert their trophic effect through cell signaling that varies by NTF family, eliciting a cellular response that modulates important biological mechanisms for the development, plasticity, regeneration, and survival of neurons and glia.

As a result, NTFs are thought to be some of the most potent protective agents against neurodegeneration. BDNF, CDNF, platelet-derived growth factor, neurturin and GDNF in particular have exhibited strong neuroprotective effects both *in vitro* and *in vivo* preclinically.[131–136] Building on these promising preclinical outcomes, seven clinical trials infusing GDNF, or in the latest case, using an adeno-associated viral vector(AAV) to deliver a GDNF transgene, have been completed to date.[137] Mixed results combined with poor putaminal coverage, and a potent placebo effect precluded the continuation of any of these clinical trials beyond phase II. Ongoing research includes: a newly designed AAV-GDNF trial modified for better coverage(https://clinicaltrials.gov/study/NCT06285643); use of structurally distinct neurotrophins like mesencephalic astrocyte-derived neurotrophic factor (MANF), and CDNF which has achieved safety and tolerability recently in a phase I-II clinical trial[138,139]; and investigation of smaller molecules or peptides with better parenchymal diffusion and neurotrophic effects.[140]

1.4 Tracking cellular grafts using bioluminescence imaging

Bioluminescence imaging (BLI) is a technique that uses genetically engineered organisms that express luciferase, an enzyme capable of generating photons in the presence of its substrate. Since first being reported in 1995, it has been adapted for many fields of preclinical research to study various biological processes due to its advantages as a non-invasive, relatively low-cost, longitudinal technique allowing real-time monitoring of cell viability in vivo.[141] Transplanted cell grafts can be engineered to stably express a Firefly luciferase transgene that converts D-luciferin into light in the presence of ATP and oxygen only available from viable cells. This light is then captured by a cooled charged coupled device (CCD) camera, providing spatially encoded intensity values that can be overlaid on a photo or an alternate imaging modality like CT or X-Ray. Modern BLI devices are capable of capturing the generated photons in deeper tissue than previously possible, particularly with Firefly luciferase, which is red-shifted relative to other types.[142,143] Further signal gains can be obtained by engineering cells with the rat organic anion transporting polypeptide 1a alongside luciferase to increase the uptake of the substrate D-luciferin.[144] However, preclinical use of BLI does have some limitations including (1) being only a two - dimensional technique[143], (2) reliance on the availability of substrate, ATP, magnesium , and oxygen, (3) importantly in the context of this thesis, low intrinsic permeability of the substrate D-luciferin into the brain for imaging grafts[145], and (4) signal attenuating confounders including hemoglobin, fur and skin pigmentation.[145,146] These factors need to be considered during experimental design and can be overcome by the use of complementary techniques depending on the experimental question. As described in Chapter 2, BLI was used to track engineered cell grafts expressing firefly luciferase implanted into the striatum of Fischer rats over a 5-week period.

1.5 Genetics of Parkinson’s disease

PD was long considered largely a sporadic disease, with only approximately 5-10% of cases reflecting a familial origin depending on the study. Genome-wide association studies now suggest a much larger hereditary component ranging from 27% to 41%.[147–149] Monogenic forms of PD are typically characterized by earlier onset than idiopathic PD (i.e. before 50 years of age) and faster progression. The first identified causal mutation for PD was an autosomal dominant mutation reported in 1997 in PARK1 or alpha-synuclein(SNCA).[150] Leucine-rich repeat kinase 2 (LRRK2), eukaryotic translation initiation factor 4 gamma 1(EIF4G1) and encoding vacuolar protein sorting 35 (VPS35) have since been identified as autosomal dominant mutations, whereas recessive mutations include parkin RBR E3 ubiquitin ligase (PRKN), PTEN induced putative kinase 1(PINK1), parkinsonism associated deglycase (DJ-1) + ATPase 13A2 (ATP13A2), F-box protein 7 (FBX07) and phospholipase A2 group VI (PLA2G6).[151] A total of 19 PARK loci, over 40 and possibly up to 90 risk loci identified by genome-wide association, and 11 underlying gene mutations linked to heritable monogenic forms of PD have been identified as of 2019.[152,153]

Mutations in SNCA, LRRK2, PRKN, PINK1 and GBA are the most studied.[6] LRRK2 is the most common cause of autosomal dominant PD worldwide, accounting for 0.1% to 4% of sporadic PD patients of Asian or European descent, and as high as 13% and 30% of sporadic Ashkenazi Jewish and Arab-Berber cases respectively.[154] PRKN and PINK1 mutations are the major autosomal recessive forms of familial PD, particularly early-onset PD. PRKN mutations account for 77% of cases of juvenile PD (<20 years old) and 10-20% of young-onset PD.[155] GBA mutations, responsible for Gaucher's disease, is not considered a causative gene, but rather a strong risk factor. In a large multi-ethnic study of 1100 patients with PD, 8.5% of people had a pathogenic GBA variant.[156] As with idiopathic cases, patient presentation and survival can vary depending on the causative gene. PRKN and LRRK2 mutations had longer survival than idiopathic cases, while SNCA or glucocerebrosidase (GBA) mutations had significantly shorter survival.[157] SNCA mutation carriers also have a younger age at onset than autosomal dominant LRRK2 and VPS35 carriers, and often suffer from additional psychiatric symptoms.[154] Though genetic testing is not standard in current clinical practice, observations such as these give important insights that may guide clinical decision making and with continued research can lead to a more personalized and optimized approach to care for patients with PD.

1.5.1 Transcriptomics to investigate Parkinson's disease

The identification of genes implicated in PD has provided insight into many potential altered pathways involved in the disease. Many of these pathways were also discussed in the section on what we know about the etiology of PD(1.2.3) including mitochondrial function[40] , oxidative stress[49], inflammation[158], impaired protein processing via the ubiquitin-proteasome[159]and autophagy-lysosome[30] systems, and apoptosis.[160] The advent of accessible and affordable genome-wide expression profiling to detect differentially expressed genes using microarrays or, more recently, RNA sequencing (RNA-seq) has provided a powerful tool to confirm or identify pathobiologically relevant alterations in PD. In addition to showing alterations in expression at the gene and functional pathway level, whole transcriptome sequencing also allows the identification of novel transcripts and forms of alternative RNA splicing. Between 2004 and 2018, 63 original studies examining the transcriptome in humans were published.[161] Thirty-three utilized postmortem brain tissue, twenty-six used blood samples, three used cerebrospinal fluid, and one used skin samples. At that time, only eight groups had used RNA-seq to examine the transcriptome, but since then many more studies have used the technology as the cost per sample has dropped significantly.[162–166]

1.5.2 Gene expression in living human brain samples

The SNpc mesencephalic nucleus, which exhibits >70% cell loss at the time of diagnosis, is the canonical site of PD pathology and an anatomical region of obvious interest for transcriptome studies. However, this area is not safely accessible for a living biopsy, and gene expression profiling would likely reflect secondary cell death and reactive processes rather than underlying PD pathology. To date, cadaveric CNS transcriptome studies are still challenged by the rapid degradation of RNA that occurs after death and the detrimental impact of traditional formalin tissue fixation, including poor yields of extractable RNA with strand cleavage and covalent modifications.[167] In addition, quality control analysis typically reflects ribosomal RNA, which is more resistant to breakdown than the mRNA normally used to define differential gene expression. Thus, even with postmortem delays in specimen processing and substantial RNA degradation, these tests may lead to false assurance of sample integrity and unreliable gene profiling data.[168] Peripheral samples would be far better suited to clinical applications, but often an lack adequate signal and are less likely to reflect disease activity in the CNS. [169]

The use of brain tissue from living patients would avert many disadvantages of postmortem specimens, maximizing yield and RNA quality for downstream RNA-seq. Fresh frozen tissue from surgically fit patients would lack exposure to late-stage disease, severe CNS degeneration, and inflammatory changes of the dying process, which markedly influence the transcriptome overshadowing pathogenic processes.[170] In Chapter 3, we used small volume specimens obtained from the prefrontal cortex during otherwise routine DBS surgery. Samples were collected along the mid-pupillary line and coronal suture estimated broadly to be in Brodmann area 8/9 within a reasonable scope of individual variability for surgical planning. Control specimens were obtained from the analogous brain region in patients without PD or intra-axial CNS pathology, again as part of an otherwise standard neurosurgical procedure. This choice to sample the prefrontal cortex was primarily guided by the feasibility and safety of the biopsy procedure, as well as accessibility of the tissue at the site of the burr hole created for insertion of the DBS electrode. However, there is considerable evidence in the literature for cortical involvement in PD making this a region with the potential to provide novel insights. Supporting this idea, the oft cited Braak staging system describes consistent Lewy body and neurite pathology in the neocortex in stages V and VI.[27] A meta-analysis of 15 PET studies assessing neuroinflammation using translocator protein activity, an accepted proxy of microglial activation, reported a significant increase in the frontal cortex of patients with PD as well. [171] Another medical imaging study using structural MRI reported a disease progression-dependant decrease in gyrification in the frontal cortex as PD advanced.[172] At the molecular level, reduced levels of neurotransmitters[173] and tyrosine hydroxylase positive interneurons[174], and altered activity of mitochondrial subunits.[175] Taken together, we hypothesise that genetic expression changes identified from this brain region can yield critical insight not specific to the dopaminergic system or end-stage cell death per se, but more broadly on the degenerative processes of PD.

1.5.3 Role of alternative splicing in PD

Alternative splicing (AS) is a fundamental posttranscriptional process by which a single gene can generate multiple proteins by combining RNA elements (e.g. introns and exons) to generate different mRNA isoforms. This process involves pre-mRNA being processed by the spliceosome to remove introns, and the addition of “caps” which are protective against transcript degradation. The 5’ cap is composed of methylated guanosine triphosphate molecules and a polyadenylated tail is added on the 3’ end, producing a mature mRNA. Alternative forms of splicing can occur at this stage in several ways, including the most common, exon skipping, where an entire exon is spliced out of the primary transcript (or retained). The other four primary forms of alternative splicing are intron retention, mutually exclusive exons, and alternative donor/acceptor sites (see Figure 1-1 for a schematic representation of these alterations), which each result in an altered mature transcript and ultimately a different protein product.

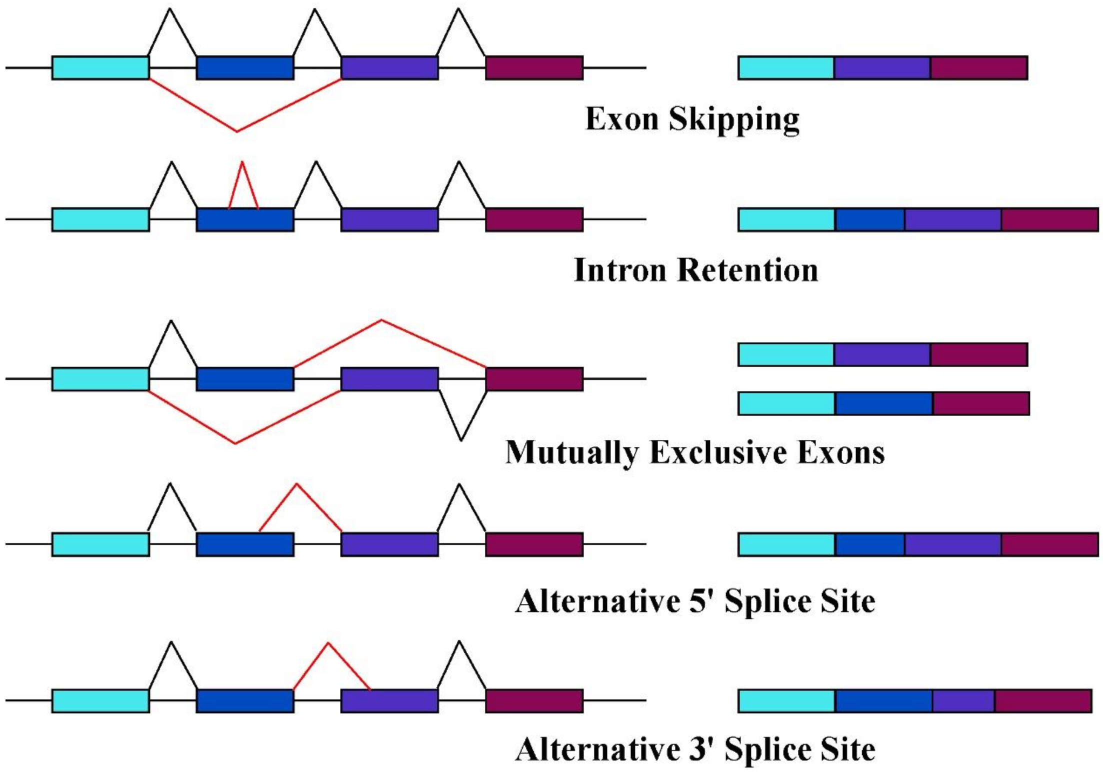

Figure 1-1 – Schematic diagram depicting the five basic forms of alternative splicing (adapted from https://commons.wikimedia.org/wiki/File:Alternative_splicing.jpg)

AS regulates gene expression during development and in response to environmental changes by allowing protein diversity and coding for nonfunctional protein products, which are quickly degraded through nonsense-mediated mRNA decay.[176] The abundance of AS increases with complexity of the organism in eukaryotes and occurs in more than 90% of human genes.[177,178] In neurodegenerative diseases, however, this process may not occur correctly, leading to the production of abnormal proteins that contribute to disease symptoms and progression. In PD, splicing errors and posttranslational modifications can give rise to forms of α-synuclein with a higher propensity for aggregation.[179] Differences in abundance of α-synuclein mRNA transcripts have been observed in brain samples of patients with PD, including an overexpression of full length and 126 amino acid transcripts in the substantia nigra versus controls.[180] Mutations in PINK1, Parkin, DJ-1 and GBA predicted to cause aberrant splicing have recently been described as well.[181–184] Interestingly, a study using iPSCs generated from a patient with a rare mutation DJ-1 that leads to early-onset PD, was able to ascertain that the mutation caused exon skipping and rescued levels of DJ-1 expression and mitochondrial dysfunction *in vitro* using targeted genetic and pharmacological interventions.[185] Studies such as this one make a strong argument for investigating the underlying molecular mechanisms of PD, which can inform therapeutics for broader PD subtypes and also take a significant step towards personalized precision medicine.

1.6 Purpose of the thesis

This thesis utilizes cortical samples from living patients with PD collected during DBS surgery, and from non-PD controls, to explore the potential of BDPCs as a novel substrate for CBT, and to provide a first look at the transcriptomic landscape in the living PD brain. We propose to first establish a rat syngeneic cell graft model as a basis for exploring the therapeutic potential of BDPCs. As a neural cell originating from patients with PD, which endogenously expresses both neural progenitor markers and NTFs, they have properties suitable for effective integration back into the host brain as an autologous graft for CBT. Using next-generation sequencing, we also sought to investigate dynamic changes in gene expression and splicing in the PD cortex to gain a better understanding of the pathways involved in PD pathogenesis and to identify possible new molecular targets. A gene expression profile identified in an initial study of the transcriptome is also used to build a machine learning classifier to discern PD samples from controls . Overall, we aimed to contribute to a better understanding of PD pathophysiology and worked towards developing strategies to facilitate a personalized treatment approach for PD.

1.6.1 Hypotheses

1. Rat BDPCs can be generated like human BDPCs, will exhibit comparable properties, and will survive and integrate to provide a suitable graft substrate in a preclinical CBT model.

2. Cortical tissue samples from living patients with PD will exhibit a novel transcriptomic profile not seen in deceased donor or other tissues.

3. The unique genetic profile of living patients with PD will provide novel data for the development of biomarkers and can be leveraged by computational tools to identify a genetic signature for PD.

In Chapter 2, we used cell culture techniques to isolate and culture BDPCs from rat cortical tissue. After assessing their properties in relation to their human counterpart using molecular and electrophysiological methods, rat BDPCs were engineered to express transgenes necessary for longitudinal tracking in vivo in a syngeneic transplant model. This chapter is in preparation for submission.

In Chapter 3, cortical samples obtained from PD patients and controls during routine surgical procedures were used to perform the first study of the brain transcriptome of living humans in PD. This chapter was published in Neurobiology of Disease (*Benoit SM, et al., "Expanding the search for genetic biomarkers of Parkinson's disease into the living brain ", April 2020)*

In Chapter 4, several bioinformatics tools were employed to further investigate the transcriptomic data from the previous chapter for alternative splicing alterations. Machine learning was then used on our dataset and other datasets to train and assess a classifier for the detection of a Parkinson's disease genetic signature. This chapter is in preparation for submission.

1.7 References

1. Feigin VL, Nichols E, Alam T, et al. Global, regional, and national burden of neurological disorders, 1990–2016: a systematic analysis for the Global Burden of Disease Study 2016. *Lancet Neurol*. 2019;18(5):459-480. doi:10.1016/S1474-4422(18)30499-X

2. Goetz CG. The history of Parkinson's disease: Early clinical descriptions and neurological therapies. *Cold Spring Harb Perspect Med*. 2011;1(1):1-16. doi:10.1101/cshperspect.a008862

3. Xu H, Belkacemi L, Jog M, Parrent A, Hebb MO. Neurotrophic factor expression in expandable cell populations from brain samples in living patients with Parkinson's disease. *FASEB J*. 2013;27(10):4157-4168. doi:10.1096/fj.12-226555

4. Benoit SM, Xu H, Schmid S, et al. Expanding the search for genetic biomarkers of Parkinson's disease into the living brain. *Neurobiol Dis*. 2020;140:104872. doi:10.1016/j.nbd.2020.104872

5. Armstrong MJ, Okun MS. Diagnosis and Treatment of Parkinson Disease: A Review. *JAMA - J Am Med Assoc*. 2020;323(6):548-560. doi:10.1001/jama.2019.22360

6. Bloem BR, Okun MS, Klein C. Parkinson's disease. *Lancet*. 2021;397(10291):2284-2303. doi:10.1016/S0140-6736(21)00218-X

7. Postuma RB, Berg D, Stern M, et al. MDS clinical diagnostic criteria for Parkinson's disease. *Mov Disord*. 2015;30(12):1591-1601. doi:10.1002/mds.26424

8. Steinmetz JD, Seeher KM, Schiess N, et al. Global, regional, and national burden of disorders affecting the nervous system, 1990–2021: a systematic analysis for the Global Burden of Disease Study 2021. *Lancet Neurol*. 2024;23(April):1990-2021. doi:10.1016/s1474-4422(24)00038-3

9. Dorsey ER, Sherer T, Okun MS, Bloemd BR. The emerging evidence of the Parkinson pandemic. *J Parkinsons Dis*. 2018;8(s1):S3-S8. doi:10.3233/JPD-181474

10. Rajiah K, Maharajan MK, Yeen SJ, Lew S. Quality of Life and Caregivers' Burden of Parkinson's Disease. *Neuroepidemiology*. 2017;48(3-4):131-137. doi:10.1159/000479031

11. Elbaz A, Bower JH, Maraganore DM, et al. Risk tables for parkinsonism and Parkinson's disease. *J Clin Epidemiol*. 2002;55(1):25-31. doi:10.1016/S0895-4356(01)00425-5

12. Wanneveich M, Moisan F, Jacqmin-Gadda H, Elbaz A, Joly P. Projections of prevalence, lifetime risk, and life expectancy of Parkinson's disease (2010-2030) in France. *Mov Disord*. 2018;33(9):1449-1455. doi:10.1002/mds.27447

13. Ascherio A, Schwarzschild MA. The epidemiology of Parkinson's disease: risk factors and prevention. *Lancet Neurol*. 2016;15(12):1257-1272. doi:10.1016/S1474-4422(16)30230-7

14. Oertel WH, Müller HH, Unger MM, et al. Transdermal Nicotine Treatment and Progression of Early Parkinson's Disease. *NEJM Evid*. 2023;2(9). doi:10.1056/EVIDoa2200311

15. Postuma RB, Anang J, Pelletier A, et al. Caffeine as symptomatic treatment for Parkinson disease (Café-PD). *Neurology*. 2017;89(17):1795-1803. doi:10.1212/WNL.0000000000004568

16. Kordower JH, Olanow CW, Dodiya HB, et al. Disease duration and the integrity of the nigrostriatal system in Parkinson's disease. *Brain*. 2013;136(8):2419-2431. doi:10.1093/brain/awt192

17. Wang J, Li Y, Huang Z, et al. Neuromelanin-sensitive magnetic resonance imaging features of the substantia nigra and locus coeruleus in de novo Parkinson's disease and its phenotypes. *Eur J Neurol*. 2018;25(7):949-955. doi:10.1111/ene.13628

18. Castellanos G, Fernández-Seara MA, Lorenzo-Betancor O, et al. Automated Neuromelanin Imaging as a Diagnostic Biomarker for Parkinson's Disease. *Mov Disord*. 2015;30(7):945-952. doi:10.1002/mds.26201

19. Huddleston DE, Langley J, Sedlacik J, Boelmans K, Factor SA, Hu XP. In vivo detection of lateral–ventral tier nigral degeneration in Parkinson's disease. *Hum Brain Mapp*. 2017;38(5):2627-2634. doi:10.1002/hbm.23547

20. Furukawa K, Shima A, Kambe D, et al. Motor Progression and Nigrostriatal Neurodegeneration in Parkinson Disease. *Ann Neurol*. 2022;92(1):110-121. doi:10.1002/ana.26373

21. Duffy PE, Tennyson VM. Phase and electron microscopic observations of lewy bodies and melanin granules in the substantia nigra and locus caeruleus in Parkinson's disease. *J Neuropathol Exp Neurol*. 1965;24(3):398-414. doi:10.1097/00005072-196507000-00003

22. Wakabayashi K, Tanji K, Odagiri S, Miki Y, Mori F, Takahashi H. The Lewy body in Parkinson's disease and related neurodegenerative disorders. *Mol Neurobiol*. 2013;47(2):495-508. doi:10.1007/s12035-012-8280-y

23. Lashuel HA. Do Lewy bodies contain alpha-synuclein fibrils? and Does it matter? A brief history and critical analysis of recent reports. *Neurobiol Dis*. 2020;141(April):104876. doi:10.1016/j.nbd.2020.104876

24. Kanazawa T, Uchihara T, Takahashi A, Nakamura A, Orimo S, Mizusawa H. Three-layered structure shared between Lewy bodies and Lewy neurites - Three-dimensional reconstruction of triple-labeled sections. *Brain Pathol*. 2008;18(3):415-422. doi:10.1111/j.1750-3639.2008.00140.x

25. Halliday G, Hely M, Reid W, Morris J. The progression of pathology in longitudinally followed patients with Parkinson's disease. *Acta Neuropathol*. 2008;115(4):409-415. doi:10.1007/s00401-008-0344-8

26. Jellinger KA. Neuropathobiology of non-motor symptoms in Parkinson disease. *J Neural Transm*. 2015;122(10):1429-1440. doi:10.1007/s00702-015-1405-5

27. Braak H, Del Tredici K, Rüb U, De Vos RAI, Jansen Steur ENH, Braak E. Staging of brain pathology related to sporadic Parkinson's disease. *Neurobiol Aging*.

2003;24(2):197-211. doi:10.1016/S0197-4580(02)00065-9

28. Del Rey NLG, Quiroga-Varela A, Garbayo E, et al. Advances in parkinson's disease: 200 years later. *Front Neuroanat*. 2018;12(December):1-14. doi:10.3389/fnana.2018.00113

29. Lynch-day MA, Mao K, Wang K, Zhao M, Klionsky DJ. The Role of Autophagy in Parkinson ' s Disease. *Cold Spring Harb Lab Press*. Published online 2015:1-14. doi:10.1101/cshperspect.a009357

30. Gan-or Z, Dion PA, Rouleau GA, Gan-or Z, Dion PA, Rouleau GA. Genetic perspective on the role of the autophagy-lysosome pathway in Parkinson disease. *Autophagy*. 2016;8627(February):8-13. doi:10.1080/15548627.2015.1067364

31. Xilouri M, Vogiatzi T, Vekrellis K, Park D, Stefanis L. Abberant α-synuclein confers toxicity to neurons in part through inhibition of chaperone-mediated autophagy. *PLoS One*. 2009;4(5):16-20. doi:10.1371/journal.pone.0005515

32. Cuervo AM, Stafanis L, Fredenburg R, Lansbury PT, Sulzer D. Impaired degradation of mutant α-synuclein by chaperone-mediated autophagy. *Science (80-)*. 2004;305(5688):1292-1295. doi:10.1126/science.1101738

33. Sacino AN, Thomas MA, Ceballos-Diaz C, et al. Conformational templating of α-synuclein aggregates in neuronal-glial cultures. *Mol Neurodegener*. 2013;8(1):1. doi:10.1186/1750-1326-8-17

34. Steiner JA, Quansah E, Brundin P. The concept of alpha-synuclein as a prion-like protein: ten years after. *Cell Tissue Res*. Published online 2018:1-13. doi:10.1007/s00441-018-2814-1

35. Kordower JH, Chu Y, Hauser RA, Freeman TB, Olanow CW. Lewy body-like pathology in long-term embryonic nigral transplants in Parkinson's disease. *Nat Med*. 2008;14(5):504-506. doi:10.1038/nm1747

36. Li JY, Englund E, Holton JL, et al. Lewy bodies in grafted neurons in subjects with Parkinson's disease suggest host-to-graft disease propagation. *Nat Med*.

2008;14(5):501-503. doi:10.1038/nm1746

37. Kordower JH, Chu Y, Hauser RA, Olanow CW, Freeman TB. Transplanted dopaminergic neurons develop PD pathologic changes: A second case report. *Mov Disord*. 2008;23(16):2303-2306. doi:10.1002/mds.22369

38. Kurowska Z, Englund E, Widner H, Lindvall O, Li JY, Brundin P. Signs of degeneration in 12-22-year old grafts of mesencephalic dopamine neurons in patients with Parkinson's disease. *J Parkinsons Dis*. 2011;1(1):83-92. doi:10.3233/JPD-2011-11004

39. Surmeier DJ, Obeso JA, Halliday GM. Selective neuronal vulnerability in Parkinson disease. *Nat Rev Neurosci*. 2017;18(2):101-113. doi:10.1038/nrn.2016.178

40. Pacelli C, Gigue N, Slack RS. Elevated Mitochondrial Bioenergetics and Axonal Arborization Size Are Key Contributors to the Vulnerability of Dopamine Neurons Article Elevated Mitochondrial Bioenergetics and Axonal Arborization Size Are Key Contributors to the Vulnerability of Dopamine. Published online 2015:2349-2360. doi:10.1016/j.cub.2015.07.050

41. Iguchi M, Kujuro Y, Okatsu K, et al. Parkin-catalyzed ubiquitin-ester transfer is triggered by PINK1-dependent phosphorylation. *J Biol Chem*. 2013;288(30):22019-22032. doi:10.1074/jbc.M113.467530

42. Kitada T, Asakawa S, Hattori N, et al. Mutations in the parkin gene cause autosomal recessive juvenile parkinsonism. *Nature*. 1998;392(6676):605-608. doi:10.1038/33416

43. Valente EM, Abou-Sleiman PM, Caputo V, et al. Hereditary Early-Onset Parkinson's Disease Caused by Mutations in PINK1. *Science (80-)*. 2004;304(5674):1158-1160. doi:10.1126/science.1096284

44. Kopin IJ. MPTP: An industrial chemical and contaminant of illicit narcotics stimulates a new era in research on Parkinson's disease. *Environ Health Perspect*. 1987;75:45-51. doi:10.1289/ehp.877545

45. Langston JW, Irwin I, Langston EB, Forno LS. 1-Methyl-4-phenylpyridinium ion

(MPP+): Identification of a metabolite of MPTP, a toxin selective to the substantia nigra. *Neurosci Lett*. 1984;48(1):87-92. doi:10.1016/0304-3940(84)90293-3

46. Cannon JR, Tapias V, Na HM, Honick AS, Drolet RE, Greenamyre JT. A highly reproducible rotenone model of Parkinson's disease. *Neurobiol Dis*. 2009;34(2):279-290. doi:10.1016/j.nbd.2009.01.016

47. Tetrud JW, Langston JW. MPTP-induced parkinsonism as a model for Parkinson's disease. *Acta Neurol Scand*. 1989;80(2):35-40. doi:10.1111/j.1600-0404.1989.tb01780.x

48. Betarbet R, Canet-Aviles RM, Sherer TB, et al. Intersecting pathways to neurodegeneration in Parkinson's disease: Effects of the pesticide rotenone on DJ-1, α-synuclein, and the ubiquitin-proteasome system. *Neurobiol Dis*. 2006;22(2):404-420. doi:10.1016/j.nbd.2005.12.003

49. Guo JD, Zhao X, Li Y, Li GR, Liu XL. Damage to dopaminergic neurons by oxidative stress in Parkinson's disease (Review). *Int J Mol Med*. 2018;41(4):1817-1825. doi:10.3892/ijmm.2018.3406

50. Liu C, Liang MC, Soong TW. Nitric Oxide, Iron and Neurodegeneration. *Front Neurosci*. 2019;13(February):1-10. doi:10.3389/fnins.2019.00114

51. Dias V, Junn E, Mouradian MM. The Role of Oxidative Stress in Parkinson's Disease. *J Parkinsons Dis*. 2013;3(4):461-491. doi:10.3233/JPD-130230

52. Lull ME, Block ML. Microglial Activation and Chronic Neurodegeneration. *Neurotherapeutics*. 2010;7(4):354-365. doi:10.1016/j.nurt.2010.05.014

53. Block ML, Zecca L, Hong JS. Microglia-mediated neurotoxicity: Uncovering the molecular mechanisms. *Nat Rev Neurosci*. 2007;8(1):57-69. doi:10.1038/nrn2038

54. Xu L, He D, Bai Y. Microglia-Mediated Inflammation and Neurodegenerative Disease. *Mol Neurobiol*. 2016;53(10):6709-6715. doi:10.1007/s12035-015-9593-4

55. Kim WG, Mohney RP, Wilson B, Jeohn GH, Liu B, Hong JS. Regional difference in

susceptibility to lipopolysaccharide-induced neurotoxicity in the rat brain: Role of microglia. *J Neurosci*. 2000;20(16):6309-6316. doi:10.1523/jneurosci.20-16-06309.2000

56. Post MR, Lieberman OJ, Mosharov E V. Can interactions between α-synuclein, dopamine and calcium explain selective neurodegeneration in Parkinson's disease? *Front Neurosci*. 2018;12(MAR):1-11. doi:10.3389/fnins.2018.00161

57. Chou KL, Stacy M, Simuni T, et al. The spectrum of "off" in Parkinson's disease: What have we learned over 40 years? *Park Relat Disord*. 2018;51:9-16. doi:10.1016/j.parkreldis.2018.02.001

58. Ahlskog JE, Muenter MD. Frequency of levodopa-related dyskinesias and motor fluctuations as estimated from the cumulative literature. *Mov Disord*. 2001;16(3):448-458. doi:10.1002/mds.1090

59. Bucy PC, Case TJ. Tremor: Physiologic mechanism and abolition by surgical means. *Arch Neurol Psychiatry*. 1939;41(4):721-746. doi:10.1001/archneurpsyc.1939.02270160077007

60. Hassler R. Sagittal Thalamotomy for Relief of Motor Disorders in Cases of Double Athetosis and Cerebral Palsy. *Confin Neurol*. 1972;34(1-4):18-28. doi:10.1159/000103026

61. Spiegel EA, Wycis HT. Thalamotomy and pallidotomy for treatment of choreic movements. *Acta Neurochir (Wien)*. 1952;2(3-4):417-422. doi:10.1007/BF01405833

62. Pereira GM, Soares NM, Rieder CR de M, Alva TAP. Stereotatic radiosurgery for the treatment of motor symptoms in Parkinson's disease: A systematic review. *J Med Imaging Radiat Sci*. 2024;55(1):146-157. doi:10.1016/j.jmir.2024.01.001

63. Spindola B, Leite MA, Orsini M, Fonoff E, Landeiro JA, Pessoa BL. Ablative surgery for Parkinson's disease: Is there still a role for pallidotomy in the deep brain stimulation era? *Clin Neurol Neurosurg*. 2017;158(April):33-39. doi:10.1016/j.clineuro.2017.04.018

64. Artusi CA, Lopiano L, Morgante F. Deep brain stimulation selection criteria for parkinson's disease: Time to go beyond capsit-pd. *J Clin Med*. 2020;9(12):1-14. doi:10.3390/jcm9123931

65. Brück D, Wenning GK, Stefanova N, Fellner L. Glia and alpha-synuclein in neurodegeneration: A complex interaction. *Neurobiol Dis*. 2016;85:262-274. doi:10.1016/j.nbd.2015.03.003

66. Montgomery EB. Deep Brain Stimulation: Mechanisms of Action. In: John Wiley & Sons, Ltd; 2013:1-19. doi:10.1002/9781118346396.ch1

67. Jakobs M, Fomenko A, Lozano AM, Kiening KL. Cellular, molecular, and clinical mechanisms of action of deep brain stimulation—a systematic review on established indications and outlook on future developments. *EMBO Mol Med*. 2019;11(4):1-18. doi:10.15252/emmm.201809575

68. Musacchio T, Rebenstorff M, Fluri F, et al. Subthalamic nucleus deep brain stimulation is neuroprotective in the A53T α-synuclein Parkinson's disease rat model. *Ann Neurol*. 2017;81(6):825-836. doi:10.1002/ana.24947

69. Fischer DL, Kemp CJ, Cole-Strauss A, et al. Subthalamic Nucleus Deep Brain Stimulation Employs trkB Signaling for Neuroprotection and Functional Restoration. *J Neurosci*. 2017;37(28):6786-6796. doi:10.1523/JNEUROSCI.2060-16.2017

70. Fischer DL, Sortwell CE. BDNF provides many routes toward STN DBS-mediated disease modification. *Mov Disord*. 2019;34(1):22-34. doi:10.1002/mds.27535

71. Schenkman M, Moore CG, Kohrt WM, et al. Effect of High-Intensity Treadmill Exercise on Motor Symptoms in Patients With De Novo Parkinson Disease: A Phase 2 Randomized Clinical Trial. *JAMA Neurol*. 2018;75(2):219-226. doi:10.1001/jamaneurol.2017.3517

72. Miyai I, Fujimoto Y, Ueda Y, et al. Treadmill training with body weight support: Its effect on Parkinson's disease. *Arch Phys Med Rehabil*. 2000;81(7):849-852. doi:10.1053/apmr.2000.4439

73. Corcos DM, Robichaud JA, David FJ, et al. A two-year randomized controlled trial of progressive resistance exercise for Parkinson's disease. *Mov Disord*. 2013;28(9):1230-1240. doi:10.1002/mds.25380

74. Landers MR, Navalta JW, Murtishaw AS, Kinney JW, Pirio Richardson S. A High-Intensity Exercise Boot Camp for Persons with Parkinson Disease: A Phase II, Pragmatic, Randomized Clinical Trial of Feasibility, Safety, Signal of Efficacy, and Disease Mechanisms. *J Neurol Phys Ther*. 2019;43(1):12-25. doi:10.1097/NPT.0000000000000249

75. Volpe D, Signorini M, Marchetto A, Lynch T, Morris ME. A comparison of Irish set dancing and exercises for people with Parkinson ' s disease : A phase II feasibility study. Published online 2013.

76. Duncan RP, Earhart GM. Randomized controlled trial of community-based dancing to modify disease progression in Parkinson disease. *Neurorehabil Neural Repair*. 2012;26(2):132-143. doi:10.1177/1545968311421614

77. David FJ, Robichaud JA, Leurgans SE, et al. Exercise improves cognition in Parkinson's disease: The PRET-PD randomized, clinical trial. *Mov Disord*. 2015;30(12):1657-1663. doi:10.1002/mds.26291

78. Jang Y, Kwon I, Song W, Cosio-Lima LM, Lee Y. Endurance Exercise Mediates Neuroprotection Against MPTP-mediated Parkinson's Disease via Enhanced Neurogenesis, Antioxidant Capacity, and Autophagy. *Neuroscience*. 2018;379:292-301. doi:10.1016/j.neuroscience.2018.03.015

79. Tuon T, Valvassori SS, Pont GCD, et al. Physical training prevents depressive symptoms and a decrease in brain-derived neurotrophic factor in Parkinson ' s disease. *Brain Res Bull*. 2014;108:106-112. doi:10.1016/j.brainresbull.2014.09.006

80. Church FC. Review treatment options for motor and non-motor symptoms of parkinson's disease. *Biomolecules*. 2021;11(4). doi:10.3390/biom11040612

81. McFarthing K, Rafaloff G, Baptista M, et al. Parkinson's Disease Drug Therapies in

the Clinical Trial Pipeline: 2022 Update. *J Parkinsons Dis*. 2022;12(4):1073-1082. doi:10.3233/JPD-229002

82. Fahn S, Oakes D, Shoulson I, et al. Levodopa and the progression of Parkinson's disease. *N Engl J Med*. 2004;351(24):2498-2508. doi:10.1056/NEJMoa033447

83. Cilia R, Cereda E, Akpalu A, et al. Natural history of motor symptoms in Parkinson's disease and the long-duration response to levodopa. *Brain*. 2020;143(8):2490-2501. doi:10.1093/brain/awaa181

84. Barker RA, Drouin-Ouellet J, Parmar M. Cell-based therapies for Parkinson disease-past insights and future potential. *Nat Rev Neurol*. 2015;11(9):492-503. doi:10.1038/nrneurol.2015.123

85. Parmar M, Torper O, Drouin-Ouellet J. Cell-based therapy for Parkinson's disease: A journey through decades toward the light side of the Force. *Eur J Neurosci*. 2019;49(4):463-471. doi:10.1111/ejn.14109

86. Freed WJ, Morihisa JM, Spoor E, et al. Transplanted adrenal chromaffin cells in rat brain reduce lesion-induced rotational behaviour. *Nature*. 1981;292(5821):351-352. doi:10.1038/292351a0

87. Perlow MJ, Freed WJ, Hoffer BJ, Seiger A, Olson L, Wyatt RJ. Brain grafts reduce motor abnormalities produced by destruction of nigrostriatal dopamine system. *Science (80-)*. 1979;204(4393):643-647. doi:10.1126/science.571147

88. Björklund A, Stenevi U. Reconstruction of the nigrostriatal dopamine pathway by intracerebral nigral transplants. *Brain Res*. 1979;177(3):555-560. doi:10.1016/0006-8993(79)90472-4

89. Freed WJ, Perlow MJ, Karoum F, et al. Restoration of dopaminergic function by grafting of fetal rat substantia nigra to the caudate nucleus: Long-term behavioral, biochemical, and histochemical studies. *Ann Neurol*. 1980;8(5):510-519. doi:10.1002/ana.410080508

90. Björklund A, Dunnett SB, Stenevi U, Lewis ME, Iversen SD. Reinnervation of the

denervated striatum by substantia nigra transplants: Functional consequences as revealed by pharmacological and sensorimotor testing. *Brain Res*. 1980;199(2):307-333. doi:10.1016/0006-8993(80)90692-7

91. Björklund A, Stenevi U, Dunnett SB, Iversen SD. Functional reactivation of the deafferented neostriatum by nigral transplants. *Nature*. 1981;289(5797):497-499. doi:10.1038/289497a0

92. Hoffer B, Freed W, Olson L, Wyatt RJ. Transplantation of Dopamine-containing Tissues to the Central Nervous System. *Neurosurgery*. 1984;31(Supplement 1):404-416. doi:10.1093/neurosurgery/31.CN_suppl_1.404

93. Backlund EO, Granberg PO, Hamberger B, et al. Transplantation of adrenal medullary tissue to striatum in parkinsonism. *J Neurosurg*. 1985;62(2):169-173. doi:10.3171/jns.1985.62.2.0169

94. Goetz CG, Tanner CM, Klawans HL, et al. United Parkinson Foundation Neurotransplantation Registry on adrenal medullary transplants: Presurgical, and 1- and 2-year follow-up. *Neurology*. 1991;41(11):1719-1722. doi:10.1212/wnl.41.11.1719

95. Hurtig H, Joyce J, Sladek Jr JR, Trojanowski JQ. Postmortem analysis of adrenal-medulla-to-caudate autograft in a patient with parkinson's disease. *Ann Neurol*. 1989;25(6):607-614. doi:10.1002/ana.410250613

96. Kompoliti K, Chu Y, Shannon KM, Kordower JH. Neuropathological study 16 years after autologous adrenal medullary transplantation in a Parkinson's disease patient. *Mov Disord*. 2007;22(11):1630-1633. doi:10.1002/mds.21528

97. Kordower JH, Cochran E, Penn RD, Goetz CG. Putative chromaffin cell survival and enhanced host-derived TH-Fiber innervation following a functional adrenal medulla autograft for Parkinson's disease. *Ann Neurol*. 1991;29(4):405-412. doi:10.1002/ana.410290411

98. Waters CH, Itabashi HH, Apuzzo MLJ, Weiner LP. Adrenal to caudate

transplantation-postmortem study. *Mov Disord*. 1990;5(3):248-250. doi:10.1002/mds.870050312

99. Peterson DI, Price ML, Small CS. Autopsy findings in a patient who had an adrenal-to-brain transplant for parkinson's disease. *Neurology*. 1989;39(2):235-238. doi:10.1212/wnl.39.2.235

100. Brundin P, Pogarell O, Hagell P, et al. Bilateral caudate and putamen grafts of embryonic mesencephalic tissue treated with lazaroids in Parkinson's disease. *Brain*. 2000;123(7):1380-1390. doi:10.1093/brain/123.7.1380

101. Lindvall O, Sawle G, Widner H, et al. Evidence for long-term survival and function of dopaminergic grafts in progressive Parkinson's disease. *Ann Neurol*. 1994;35(2):172-180. doi:10.1002/ana.410350208

102. Wenning GK, Odin P, Morrish P, et al. Short- and long-term survival and function of unilateral intrastriatal dopaminergic grafts in Parkinson's disease. *Ann Neurol*. 1997;42(1):95-107. doi:10.1002/ana.410420115

103. Freed CR, Greene PE, Breeze RE, et al. Transplantation of Embryonic Dopamine Neurons for Severe Parkinson's Disease. *N Engl J Med*. 2001;344(10):710-719. doi:10.1056/NEJM200103083441002

104. Olanow CW, Goetz CG, Kordower JH, et al. A Double-blind Controlled Trial of Bilateral Fetal Nigral Transplantation in Parkinson ' s Disease. *Ann Neurol*. Published online 2003:403-414. doi:10.1002/ana.10720

105. Widner H. NIH neural transplantation funding. *Science*. 1994;263(5148):737. doi:10.1126/science.8303281

106. Barker RA, Farrell K, Guzman NV, et al. Designing stem-cell-based dopamine cell replacement trials for Parkinson's disease. *Nat Med*. 2019;25(7):1045-1053. doi:10.1038/s41591-019-0507-2

107. Thomson JA, Itskovitz-Eldor J, Shapiro SS, et al. Embryonic Stem Cell Lines Derived from Human Blastocysts. *Science (80-)*. 1998;282(5391):1145-1147.

doi:10.1126/science.282.5391.1145

108. Lehnen D, Barral S, Cardoso T, et al. IAP-Based Cell Sorting Results in Homogeneous Transplantable Dopaminergic Precursor Cells Derived from Human Pluripotent Stem Cells. *Stem Cell Reports*. 2017;9(4):1207-1220. doi:10.1016/j.stemcr.2017.08.016

109. Kirkeby A, Nolbrant S, Tiklova K, et al. Predictive Markers Guide Differentiation to Improve Graft Outcome in Clinical Translation of hESC-Based Therapy for Parkinson's Disease. *Cell Stem Cell*. 2017;20(1):135-148. doi:10.1016/j.stem.2016.09.004

110. Nolbrant S, Heuer A, Parmar M, Kirkeby A. Generation of high-purity human ventral midbrain dopaminergic progenitors for in vitro maturation and intracerebral transplantation. *Nat Protoc*. 2017;12(9):1962-1979. doi:10.1038/nprot.2017.078

111. Soldner F, Hockemeyer D, Beard C, et al. Parkinson's Disease Patient-Derived Induced Pluripotent Stem Cells Free of Viral Reprogramming Factors. *Cell*. 2009;136(5):964-977. doi:10.1016/j.cell.2009.02.013

112. Takahashi K, Yamanaka S. Induction of Pluripotent Stem Cells from Mouse Embryonic and Adult Fibroblast Cultures by Defined Factors. *Cell*. 2006;126(4):663-676. doi:10.1016/j.cell.2006.07.024

113. Bonilla S, Hall AC, Pinto L, et al. Identification of midbrain floor plate radial glia-like cells as dopaminergic progenitors. *Glia*. 2008;56(8):809-820. doi:10.1002/glia.20654

114. Ono Y, Nakatani T, Sakamoto Y, et al. Differences in neurogenic potential in floor plate cells along an anteroposterior location: midbrain dopaminergic neurons originate from mesencephalic floor plate cells. *Dev*. 2007;134(17):3213-3225. doi:10.1242/dev.02879

115. Doi D, Magotani H, Kikuchi T, et al. Pre-clinical study of induced pluripotent stem cell-derived dopaminergic progenitor cells for Parkinson's disease. *Nat Commun*. 2020;11(1). doi:10.1038/s41467-020-17165-w

116. Kikuchi T, Morizane A, Doi D, et al. Human iPS cell-derived dopaminergic neurons function in a primate Parkinson’s disease model. *Nature*. 2017;548(7669):592-596. doi:10.1038/nature23664

117. Nakamura R, Nonaka R, Oyama G, et al. A defined method for differentiating human iPSCs into midbrain dopaminergic progenitors that safely restore motor deficits in Parkinson’s disease. *Front Neurosci*. 2023;17(July):1-13. doi:10.3389/fnins.2023.1202027

118. Song B, Cha Y, Ko S, et al. Human autologous iPSC-derived dopaminergic progenitors restore motor function in Parkinson’s disease models. *J Clin Invest*. 2020;130(2):904-920. doi:10.1172/JCI130767

119. Takahashi J. iPS cell-based therapy for Parkinson’s disease: A Kyoto trial. *Regen Ther*. 2020;13:18-22. doi:10.1016/j.reth.2020.06.002

120. Garitaonandia I, Gonzalez R, Sherman G, Semechkin A, Evans A, Kern R. Novel Approach to Stem Cell Therapy in Parkinson’s Disease. *Stem Cells Dev*. 2018;27(14):951-957. doi:10.1089/scd.2018.0001

121. Kern R, Garitaonandia I, Gonzalez R, et al. Results of an Open Label, Dose Escalating, Phase 1 Clinical Trial Evaluating the Safety of a Human Neural Stem Cell Based Therapy in Parkinson’s Disease (P1.8-016). *Neurology*. 2019;92(15 Supplement):P1.8-016. http://n.neurology.org/content/92/15_Supplement/P1.8-016.abstract

122. Barker RA, Parmar M, Studer L, Takahashi J. Human Trials of Stem Cell-Derived Dopamine Neurons for Parkinson’s Disease: Dawn of a New Era. *Cell Stem Cell*. 2017;21(5):569-573. doi:10.1016/j.stem.2017.09.014

123. Reynolds BA, Weiss S. Generation of Neurons and Astrocytes from Isolated Cells of the Adult Mammalian Central Nervous System. *Science (80-)*. 1992;255(5052):1707-1710. http://www.jstor.org/stable/2876641

124. Gage FH, Coates PW, Palmer TD, et al. Survival and differentiation of adult neuronal

progenitor cells transplanted to the adult brain. *Proc Natl Acad Sci U S A*. 1995;92(25):11879-11883. doi:10.1073/pnas.92.25.11879

125. Palmer TD, Ray J, Gage FH. FGF-2-responsive neuronal progenitors reside in proliferative and quiescent regions of the adult rodent brain. *Mol Cell Neurosci*. 1995;6:474-486. doi:10.1006/mcne.1995.1035

126. Bloch J, Brunet JF, Mcentire CRS, Redmond DE. Primate adult brain cell autotransplantation produces behavioral and biological recovery in 1-methyl-4-phenyl-1,2,3,6-tetrahydropyridine-induced parkinsonian St. Kitts monkeys. *J Comp Neurol*. 2014;2740:2729-2740. doi:10.1002/cne.23579

127. Arsenijevic Y, Villemure JG, Brunet JF, et al. Isolation of multipotent neural precursors residing in the cortex of the adult human brain. *Exp Neurol*. 2001;170(1):48-62. doi:10.1006/exnr.2001.7691

128. Nunes MC, Roy NS, Keyoung HM, et al. Identification and isolation of multipotential neural progenitor cells from the subcortical white matter of the adult human brain. *Nat Med*. 2003;9(4):439-447. doi:10.1038/nm837

129. Huttunen HJ, Saarma M. CDNF Protein Therapy in Parkinson’s Disease. *Cell Transplant*. 2019;28(4):349-366. doi:10.1177/0963689719840290

130. Rocco ML, Soligo M, Manni L, Aloe L. Nerve Growth Factor: Early Studies and Recent Clinical Trials. *Curr Neuropharmacol*. 2018;16(10):1455-1465. doi:10.2174/1570159X16666180412092859

131. Allen SJ, Watson JJ, Shoemark DK, Barua NU, Patel NK. GDNF, NGF and BDNF as therapeutic options for neurodegeneration. *Pharmacol Ther*. 2013;138(2):155-175. doi:10.1016/j.pharmthera.2013.01.004

132. Lu B, Nagappan G, Guan X, Nathan PJ, Wren P. BDNF-based synaptic repair as a disease-modifying strategy for neurodegenerative diseases. *Nat Rev Neurosci*. 2013;14(6):401-416. doi:10.1038/nrn3505

133. Garea-Rodríguez E, Eesmaa A, Lindholm P, et al. Comparative Analysis of the Effects

of Neurotrophic Factors CDNF and GDNF in a Nonhuman Primate Model of Parkinson's Disease. *PLoS One*. 2016;11(2). doi:10.1371/journal.pone.0149776

134. Deng X, Liang Y, Lu H, et al. Co-transplantation of GDNF-overexpressing neural stem cells and fetal dopaminergic neurons mitigates motor symptoms in a rat model of parkinson's disease. *PLoS One*. 2013;8(12):1-10. doi:10.1371/journal.pone.0080880

135. Hickey P, Stacy M. AAV2-neurturin (CERE-120) for Parkinson ' s disease. *Expert Opin Biol Ther*. 2013;13(1):137-145.

136. Bondarenko O, Saarma M. Neurotrophic Factors in Parkinson's Disease: Clinical Trials, Open Challenges and Nanoparticle-Mediated Delivery to the Brain. *Front Cell Neurosci*. 2021;15(June):1-18. doi:10.3389/fncel.2021.682597

137. Gash DM, Gerhardt GA, Bradley LH, Wagner R, Slevin JT. GDNF clinical trials for Parkinson's disease: a critical human dimension. *Cell Tissue Res*. 2020;382(1):65-70. doi:10.1007/s00441-020-03269-8

138. Lindholm P, Saarma M. Cerebral dopamine neurotrophic factor protects and repairs dopamine neurons by novel mechanism. *Mol Psychiatry*. 2022;27(3):1310-1321. doi:10.1038/s41380-021-01394-6

139. Lõhelaid H, Saarma M, Airavaara M. CDNF and ER stress: Pharmacology and therapeutic possibilities. *Pharmacol Ther*. 2024;254. doi:10.1016/j.pharmthera.2024.108594

140. Barker RA, Björklund A, Gash DM, et al. GDNF and Parkinson's Disease: Where Next? A Summary from a Recent Workshop. *J Parkinsons Dis*. 2020;10(3):875-891. doi:10.3233/JPD-202004

141. Contag CH, Contag PR, Mullins JI, Spilman SD, Stevenson DK, Benaron DA. Photonic detection of bacterial pathogens in living hosts. *Mol Microbiol*. 1995;18(4):593-603. doi:10.1111/j.1365-2958.1995.mmi_18040593.x

142. Contag PR, Nick Olomu I, Stevenson DK, Contag CH. Bioluminescent indicators in living mammals. *Nat Med*. 1998;4(2):245-247. doi:10.1038/nm0298-245

143. Contag CH, Spilman SD, Contag PR, et al. Visualizing Gene Expression in Living Mammals Using a Bioluminescent Reporter. *Photochem Photobiol*. 1997;66(4):523-531. doi:10.1111/j.1751-1097.1997.tb03184.x

144. Nyström NN, Hamilton AM, Xia W, Liu S, Scholl TJ, Ronald JA. Longitudinal Visualization of Viable Cancer Cell Intratumoral Distribution in Mouse Models Using Oatp1a1 -Enhanced Magnetic Resonance Imaging. *Invest Radiol*. 2019;54(5):302-311. doi:10.1097/RLI.0000000000000542

145. Kim M, Gupta SK, Zhang W, et al. Factors Influencing Luciferase-Based Bioluminescent Imaging in Preclinical Models of Brain Tumor. *Drug Metab Dispos*. 2022;50(3):277-286. doi:10.1124/dmd.121.000597

146. Aswendt M, Adamczak J, Couillard-Despres S, Hoehn M. Boosting Bioluminescence Neuroimaging: An Optimized Protocol for Brain Studies. *PLoS One*. 2013;8(2):1-9. doi:10.1371/journal.pone.0055662

147. Baranzini SE, Wang J, Gibson RA, et al. Genome-wide association analysis of susceptibility and clinical phenotype in multiple sclerosis. *Hum Mol Genet*. 2009;18(4):767-778. doi:10.1093/hmg/ddn388

148. Hamza TH, Payami H. The heritability of risk and age at onset of Parkinson's disease after accounting for known genetic risk factors. *J Hum Genet*. 2010;55(4):241-243. doi:10.1038/jhg.2010.13

149. Keller MF, Saad M, Bras J, et al. Using genome-wide complex trait analysis to quantify "missing heritability" in Parkinson's disease. *Hum Mol Genet*. 2012;21(22):4996-5009. doi:10.1093/hmg/dds335

150. Polymeropoulos MH, Lavedan C, Leroy E, Ide SE, Dutra A. Mutation in the alpha-synuclein gene identified in families with Parkinson's disease Mihel H. Polymeropoulos, Christian Lavedan, Elisabeth Leroy, Susan E. Ide, Anindya Dehejia and Amalia Dutra. *Science (80-)*. 1997;5321(4):2045.

151. Puschmann A. New Genes Causing Hereditary Parkinson's Disease or Parkinsonism.

Curr Neurol Neurosci Rep. 2017;17(9). doi:10.1007/s11910-017-0780-8

152. Reed X, Bandrés-Ciga S, Blauwendraat C, Cookson MR. The role of monogenic genes in idiopathic Parkinson's disease. *Neurobiol Dis*. 2019;124(November 2018):230-239. doi:10.1016/j.nbd.2018.11.012

153. Nalls MA, Blauwendraat C, Vallerga CL, et al. Identification of novel risk loci, causal insights, and heritable risk for Parkinson's disease: a meta-analysis of genome-wide association studies. *Lancet Neurol*. 2019;18(12):1091-1102. doi:10.1016/S1474-4422(19)30320-5

154. Trinh J, Zeldenrust FMJ, Huang J, et al. Genotype-phenotype relations for the Parkinson's disease genes SNCA, LRRK2, VPS35: MDSGene systematic review. *Mov Disord*. 2018;33(12):1857-1870. doi:10.1002/mds.27527

155. Kasten M, Hartmann C, Hampf J, et al. Genotype-Phenotype Relations for the Parkinson's Disease Genes Parkin, PINK1, DJ1: MDSGene Systematic Review. *Mov Disord*. 2018;33(5):730-741. doi:10.1002/mds.27352

156. Skrahina V, Gaber H, Vollstedt EJ, et al. The Rostock International Parkinson's Disease (ROPAD) Study: Protocol and Initial Findings. *Mov Disord*. 2021;36(4):1005-1010. doi:10.1002/mds.28416

157. Lanore A, Casse F, Tesson C, et al. Differences in survival across monogenic forms of Parkinson's disease. *Ann Neurol*. Published online 2023:123-132. doi:10.1002/ana.26636

158. Pajares M, I. Rojo A, Manda G, Boscá L, Cuadrado A. Inflammation in Parkinson's Disease: Mechanisms and Therapeutic Implications. *Cells*. 2020;9(7):1687. doi:10.3390/cells9071687

159. Martins-Branco D, Esteves AR, Santos D, et al. Ubiquitin proteasome system in Parkinson's disease: a keeper or a witness? *Exp Neurol*. 2012;238(2):89-99. doi:10.1016/j.expneurol.2012.08.008

160. Lev N, Melamed E, Offen D. Apoptosis and Parkinson's disease. *Prog Neuro-*

Psychopharmacology Biol Psychiatry. 2003;27(2):245-250. doi:10.1016/S0278-5846(03)00019-8

161. Borrageiro G, Haylett W, Seedat S, Kuivaniemi H, Bardien S. A review of genome-wide transcriptomics studies in Parkinson's disease. *Eur J Neurosci*. 2018;47(1):1-16. doi:10.1111/ejn.13760

162. Craig DW, Hutchins E, Violich I, et al. RNA sequencing of whole blood reveals early alterations in immune cells and gene expression in Parkinson's disease. *Nat aging*. 2021;1(8):734-747. doi:10.1038/s43587-021-00088-6

163. Kern F, Fehlmann T, Violich I, et al. Deep sequencing of sncRNAs reveals hallmarks and regulatory modules of the transcriptome during Parkinson's disease progression. *Nat aging*. 2021;1(3):309-322. doi:10.1038/s43587-021-00042-6

164. Irmady K, Hale CR, Qadri R, et al. Blood transcriptomic signatures associated with molecular changes in the brain and clinical outcomes in Parkinson's disease. *Nat Commun*. 2023;14(1). doi:10.1038/s41467-023-39652-6

165. Cappelletti C, Henriksen SP, Geut H, et al. Transcriptomic profiling of Parkinson's disease brains reveals disease stage specific gene expression changes. *Acta Neuropathol*. 2023;146(2):227-244. doi:10.1007/s00401-023-02597-7

166. Kurvits L, Lättekivi F, Reimann E, et al. Transcriptomic profiles in Parkinson's disease. *Exp Biol Med*. 2021;246(5):584-595. doi:10.1177/1535370220967325

167. David LE, Fowler CB, Cunningham BR, Mason JT, O'Leary TJ. The effect of formaldehyde fixation on RNA: Optimization of formaldehyde adduct removal. *J Mol Diagnostics*. 2011;13(3):282-288. doi:10.1016/j.jmoldx.2011.01.010

168. Sidova M, Tomankova S, Abaffy P, Kubista M, Sindelka R. Effects of post-mortem and physical degradation on RNA integrity and quality. *Biomol Detect Quantif*. 2015;5:3-9. doi:10.1016/j.bdq.2015.08.002

169. Prieto C, Risueño A, Fontanillo C, De Las Rivas J. Human gene coexpression landscape: Confident network derived from tissue transcriptomic profiles. *PLoS One*.

2008;3(12). doi:10.1371/journal.pone.0003911

170. Franz H, Ullmann C, Becker A, et al. Systematic analysis of gene expression in human brains before and after death. *Genome Biol*. 2005;6(13):1-9. doi:10.1186/gb-2005-6-13-r112

171. Zhang PF, Gao F. Neuroinflammation in Parkinson's disease: a meta-analysis of PET imaging studies. *J Neurol*. 2022;269(5):2304-2314. doi:10.1007/s00415-021-10877-z

172. Sterling NW, Wang M, Zhang L, et al. Stage-dependent loss of cortical gyrification as Parkinson disease "unfolds." *Neurology*. 2016;86(12):1143-1151. doi:10.1212/WNL.0000000000002492

173. Scatton B, Javoy-Agid F, Rouquier L, Dubois B, Agid Y. Reduction of cortical dopamine, noradrenaline, serotonin and their metabolites in Parkinson's disease. *Brain Res*. 1983;275(2):321-328. doi:10.1016/0006-8993(83)90993-9

174. Fukuda T, Takahashi J, Tanaka J. Tyrosine hydroxylase-immunoreactive neurons are decreased in number in the cerebral cortex of Parkinson's disease. *Neuropathology*. 1999;19(1):10-13. doi:10.1046/j.1440-1789.1999.00196.x

175. Garcia-Esparcia P, Koneti A, Rodríguez-Oroz MC, Gago B, del Rio JA, Ferrer I. Mitochondrial activity in the frontal cortex area 8 and angular gyrus in Parkinson's disease and Parkinson's disease with dementia. *Brain Pathol*. 2018;28(1):43-57. doi:10.1111/bpa.12474

176. Lareau LF, Green RE, Bhatnagar RS, Brenner SE. The evolving roles of alternative splicing. *Curr Opin Struct Biol*. 2004;14(3):273-282. doi:10.1016/j.sbi.2004.05.002

177. Wang ET, Sandberg R, Luo S, et al. Alternative isoform regulation in human tissue transcriptomes. *Nature*. 2008;456(7221):470-476. doi:10.1038/nature07509

178. Keren H, Lev-Maor G, Ast G. Alternative splicing and evolution: Diversification, exon definition and function. *Nat Rev Genet*. 2010;11(5):345-355. doi:10.1038/nrg2776

179. Beyer K, Ariza A. α-Synuclein posttranslational modification and alternative splicing as a trigger for neurodegeneration. *Mol Neurobiol*. 2013;47(2):509-524. doi:10.1007/s12035-012-8330-5

180. McLean JR, Hallett PJ, Cooper O, Stanley M, Isacson O. Transcript expression levels of full-length alpha-synuclein and its three alternatively spliced variants in Parkinson's disease brain regions and in a transgenic mouse model of alpha-synuclein overexpression. *Mol Cell Neurosci*. 2012;49(2):230-239. doi:10.1016/J.MCN.2011.11.006

181. Samaranch L, Lorenzo-Betancor O, Arbelo JM, et al. PINK1-linked parkinsonism is associated with Lewy body pathology. *Brain*. 2010;133(4):1128-1142. doi:10.1093/BRAIN/AWQ051

182. Asselta R, Rimoldi V, Siri C, et al. Glucocerebrosidase mutations in primary parkinsonism. *Parkinsonism Relat Disord*. 2014;20(11):1215. doi:10.1016/J.PARKRELDIS.2014.09.003

183. Bras JM, Guerreiro RJ, Teo JTH, et al. Atypical Parkinsonism-Dystonia Syndrome Caused by a Novel DJ1 Mutation. *Mov Disord Clin Pract*. 2014;1(1):45. doi:10.1002/MDC3.12008

184. Ghazavi F, Fazlali Z, Banihosseini SS, et al. PRKN, DJ-1, and PINK1 screening identifies novel splice site mutation in PRKN and two novel DJ-1 mutations. *Mov Disord*. 2011;26(1):80-89. doi:10.1002/mds.23417

185. Boussaad I, Obermaier CD, Hanss Z, et al. A patient-based model of RNA mis-splicing uncovers treatment targets in Parkinson's disease. *Sci Transl Med*. 2020;12(560). doi:10.1126/SCITRANSLMED.AAU3960

Chapter 2

2 Establishing a rodent syngeneic graft model to examine the potential of novel cell-based therapeutics for Parkinson's disease

Background: Current treatments for Parkinson's disease (PD) only address symptoms and do not modify disease progression. Cell-based therapies (CBT) using various cell types have shown limited success due to ethical concerns, standardization issues and potential immune rejection, among others. Cortical biopsies safely obtained from living PD patients during deep brain stimulation yield large numbers of brain-derived progenitor cells (BDPCs) with key merits for CBT by being of brain origin and expressing multiple neurotrophic factors (NTF; e.g., GDNF, BDNF, CDNF) along with progenitor and neural proteins. These attributes raise the prospect that BDPCs may provide an effective substrate for enduring therapeutic function in PD, but a preclinical transplant model is a necessary step to evaluate this potential. Human BDPCs have been characterized (Xu et al 2013) but analogous cells from other mammals have not been described. **Methods:** Rat BDPCs were isolated and cultured using a protocol adapted from human BDPCs. Markers of cell type, endogenous NTF production and electrophysiological properties were evaluated and compared to human cells. Rat BDPCs were engineered to express luciferase/OATP1A1/TdTomato, then 15k, 60k or 240k cells were implanted into the striatum of syngeneic rats and tracked longitudinally for 5 weeks with bioluminescence imaging (BLI), before brain extraction for histology. **Results:** Rat BDPCs expressed comparable neural progenitor and mesenchymal markers as human BDPCs. Electrophysiological analysis revealed differences in resting membrane potential and membrane time constant. Expression and secretion of NTFs BDNF and GDNF was confirmed by Western blot in human and rat BDPCs. Engineered rat BDPC syngeneic grafts with 15k and 60k cells showed successful engraftment for 5 weeks, however 240k grafts had a sharp decline in BLI signal after 2 weeks. Histological examination revealed striatal grafts integrated into the surrounding brain parenchyma. **Conclusions:** This study establishes the possibility of generating BDPCs from rat cortex and provides a proof-of

concept pre-clinical syngeneic model in rats that allows longitudinal tracking in vivo, an ideal platform for future testing of therapeutic interventions for PD.

2.1 Introduction

Parkinson's disease (PD) is a progressive neurodegenerative disease with an estimated prevalence of 1% in individuals over the age of 60.[1] The disease is diagnosed clinically using a characteristic motor symptom profile which includes tremor and bradykinesia, often accompanied by other symptoms such as gait and postural instability, cognitive impairment, hyposmia and mood disturbances. The current standard-of-care for PD consists primarily of dopamine replacement therapy to counter the loss of the dopamine producing neurons of the substantia nigra. A subset of patients may also be candidates for surgical intervention to treat inadequately controlled motor symptoms by implanting a deep-brain stimulation (DBS) electrode. All forms of treatment to date are purely symptomatic, doing nothing to slow, halt or reverse the progression of the disease. As such, researchers continue to pursue any form of disease-modifying treatment with the broad objectives of improving the bioavailability of dopamine in the relevant brain circuitry, preventing further cell death, and promoting regeneration. Among the most widely investigated forms of therapy are cell-based therapies (CBTs) and therapies based on the use of potently cytoprotective neurotrophic factors (NTFs).[2]

CBTs have been explored over the last several decades using various cell types and grafting strategies, with the objective of restoring the dopaminergic supply lost to disease by replacing lost cells or repairing and supporting remaining functional neurons. Initial trials with bulk tissue adrenal medullary cells implants into preformed cavities in the lateral ventricle or striatum failed to show any benefit.[3,4] However, refinement of surgical technique and continued trials using fetal nigral grafts, native stem cells, induced pluripotent stem cells and their differentiated progeny led to some signs of therapeutic benefit, including improved [^{18}F]dopa uptake in grafted tissue. Despite progress and refinement of surgical techniques many hurdles still exist to the use of CBT. The use of fetal cells - most recently seen in the TRANSEURO trial[3]- has been hampered by ethical concerns, non-standardized source tissue and logistical issues obtaining necessary tissue for transplants.[5] Native and induced pluripotent stem-cells are more readily expanded and preserved, but they raise their own apprehensions from a standardization, safety and tumorigenicity perspective. Furthermore, concerns of immunogenicity of allogeneic cell grafts remain, despite the relative immunological privilege of the brain. Recent evidence showing active patrol of the central nervous system (CNS) by the immune system and the possibility of generating an immune response[6], combined with in vivo studies showing a rejection response to grafts[7–9], appear to support those concerns.

NTFs are trophic biomolecules - typically proteins with a molecular weight between 10 and 35 kDa – that support survival, growth and differentiation of neurons.[10] They are mostly grouped into three families: the neurotrophins (BDNF, neurotrophin-3, neurotrophin-4 and NGF); the GDNF-family of ligands (GDNF, neurturin (NRTN), artemin and persephin); and the neuropoietic cytokines. Mechanisms of trophic action vary by family, but most NTFs support neurons in the mature nervous system via signaling through receptor tyrosine kinases. Decreased levels of NTFs have been found in the brains and blood of patients with PD.[11–13] Early experimental models of NTF therapy for PD, particularly those using glial-derived neurotrophic factor (GDNF), demonstrated the neuroprotective and neurorestorative effects of NTFs against toxic insults to dopaminergic neurons.[14–20] In humans, initial clinical trials directly infusing GDNF into the putamen reported no serious adverse effects and promising results in open-labeled studies[21,22], but failed to meet their endpoints in randomized, double-blind, placebo-controlled trials, despite showing measurable clinical benefit in some cases.[23–26] The unconventional endoplasmic reticulum(ER) protein and NTF cerebral dopamine neurotrophic factor (CDNF) demonstrated safety in a trial completed in 2020 and can act extracellularly and in the ER to protect neurons and other cells against stress-induced unfolded response.[27,28] Trials using adeno-associated virus (AAV) mediated gene therapy to generate expression of both neurturin and GDNF in the putamen have also proved to be safe for patients.[29–32] However, meaningful translation of a therapeutic effect to humans has been plagued with difficulties obtaining coverage of the irregular volume of the putamen leading to only modest benefits on a subset of patients. Research is still ongoing with a planned new AAV-GDNF trial with improved delivery protocol for better putaminal coverage planned for early 2024 (https://clinicaltrials.gov/study/NCT06285643).

The current state of therapeutics for PD does show promise, though several clear hurdles still exist demanding the continued exploration of novel approaches. Prior work from our lab has shown that small cortical biopsies can be obtained from PD patients during deep-brain stimulation (DBS) surgery. These tissue biopsies are invaluable biological samples that can yield an expandable cell population we have termed brain-derived progenitor cells (BDPCs).[33] BDPCs are expandable *in vitro*; brain-derived and have been shown to endogenously express both neural progenitor markers like Olig1 and Nestin, as well as the NTFs BDNF, GDNF and CDNF. The combination of progenitor cells from a neural source with endogenous NTF expression is inherently advantageous for use as a substrate for CBT for PD, circumventing many of the issues raised in experimental models and clinical trials to date. As a novel non-immunogenic source of cells, they could provide a long-term substrate for endogenous NTF delivery or alternatively, could be modified for use as a delivery vehicle for therapeutic molecules. However, the therapeutic potential of BDPCs has yet to be thoroughly evaluated. To begin to examine their potential, this study first sought to determine if rat BDPCs could be derived and expanded from frontal cortical brain tissue, like human BDPCs, with the goal of establishing a pre-clinical model. Properties of derived rat BDPCs could then be systematically compared to human BDPCs with an emphasis on the neural progenitor markers and neurotrophic factors previously confirmed to be present in the human cells. Once phenotype was established, we also sought to establish the basic electrophysiological properties of human and rat BDPCs, and whether NTFs were secreted from rat BDPCs. Finally, we worked to develop a syngeneic graft model in Fischer rats in preparation for future preclinical studies to assess the therapeutic potential of BDPCs, mimicking an autologous transplant model in humans while keeping a functional immune system. We expected that derivation of rat BDPCs would be possible, and they would exhibit a similar phenotype to human BDPCs. Furthermore, we hypothesized that rat BDPCs would survive and integrate to provide a suitable graft substrate in a preclinical model. With the establishment of a derivation protocol for rat BDPCs, evaluation of their phenotype and properties, and examination of survival and engraftment of BDPC in a syngeneic animal model, we lay the groundwork for further development of this innovative cell-based therapy approach.

2.2 Materials and Methods

2.2.1 Isolation and culture of rodent brain-derived progenitor cells

Brain-derived progenitor cells were generated from rat cortical tissue by adapting the same protocol previously described for human brain samples.[33] Brain tissue from Fischer rats (Charles-River, Wilmington, MA, USA) ranging from 4-6 months of age with a mean weight of 326.18g (SD 15.31g) was collected in phosphate-buffered saline (PBS) with 5% fetal bovine serum (FBS). To emulate the sampling location in the frontal cortex in humans, ~100 mm^3 (50 mm^3 per hemisphere) of frontal cortical tissue was carefully dissected (away from pial or ventricular surfaces) and rinsed twice with PBS to remove FBS and blood. Tissue was digested with 0.25% Trypsin and 75µl DNase at 37°C for 20 minutes, then 5ml of Dulbecco's modified Eagle's medium (DMEM; Thermo Fisher Scientific, Waltham, MA, USA) with 10% FBS, 1% penicillin/streptomycin and 1% non-essential amino acids was added (standard medium). The resulting suspension was triturated and filtered through a 100µm cell strainer (BD Biosciences, San Jose, CA, USA), then centrifuged at 800 rpm for 15 minutes. The pellet, resuspended in fresh medium, was plated to a 35 mm dish. After 2 hours at 37°C, the supernatant was transferred to four 15 mm wells in a 24-well plate coated with poly-l-lysine (Trevigen Inc., Gaithersburg, MD, USA) and allowed to grow 2-3 weeks to confluence before first passage. Cultures were grown at 37 °C in a humidified chamber with 5% CO2, with the medium changed twice a week and cells passaged at approximately 80% confluence using a 1:2 ratio. Experiments, including the transplant model were all conducted with either human or rat BDPCs from passages 3 to 8.

2.2.2 Immunocytochemistry for lineage markers and growth factors

BDPCs (3x10e4) were seeded onto uncoated glass coverslips, incubated for 48 hours, and fixed with 4% paraformaldehyde (PFA) in PBS for 20 minutes at room temperature (RT). Cells were permeabilized with 0.25% Triton X-100 for 12 minutes and non-specific binding was blocked with 1% bovine serum albumin (BSA) for 30 minutes at RT. Primary antibodies (Supplementary Table 2-1) diluted in PBS with 1% BSA were incubated with cells overnight at 4°C. Secondary antibodies (Alexa Fluor© 488 goat anti-mouse or Alexa Fluor © 546 goat anti-rabbit; 1:200, Thermo Fisher) were applied for 1 hour at RT and nuclei counterstained with 4,6-diamidino-2-phenylindole (DAPI). PBS was used as a no primary control. All experiments were repeated twice with distinct BDPC cultures. Coverslips were mounted with antifade solution and sealed. Imaging was performed on a Leica TCS SP8 confocal microscope.

2.2.3 Western blot analysis

Protein expression was evaluated with Western-blot analysis of whole cell extracts and cell media filtrate to determine both intracellular expression and secretion of target proteins. Protein extracts from media were obtained by incubating cells overnight in 4ml fresh DMEM without any additives. Media was then removed and centrifuged in a 15ml conical filter tube (Amicon Ultra-4, Sigma-Aldrich, St. Louis, MO, USA; 4,000 x g, 20 min, 4°C) to concentrate protein. For whole cell protein extracts, cells were collected in media using a cooled cell scraper and centrifuged (2,200 x g, 5 min, 4°C). The pellet was resuspended in PBS and centrifuged again (2,200 x g, 5 min, 4°C). The pellet was incubated on ice for 30 min in lysis buffer (50 mM Tris-HCl, 150 mM NaCl and 1% Nonidet P40 substitute, pH 7.4) with fresh protease inhibitor cocktail (1:10, Sigma-Aldrich). Lysate was then centrifuged (16,100 x g, 15 min, 4°C) and supernatant was collected for analysis. The concentration of protein lysates was measured using the DC Protein Assay (Bio-Rad Laboratories Ltd., Mississauga, ON, Canada) read at 750 nm on an Epoch spectrophotometer (Biotek Instruments Inc., Winooski, VT, USA) and fractions were frozen at -20°C until needed. Samples in Laemmli buffer (40μg total protein) were loaded in 8-15% polyacrylamide gels depending on target protein size and transferred to Immun-Blot PVDF membranes (Bio-Rad Laboratories). Membranes were blocked with 5% skim milk in Tris-buffered saline (TBS) for 15 minutes at RT, then incubated overnight at 4°C with primary antibodies in the same solution with 0.1% Tween 20 added (Supplementary Table 2-2). Membranes were washed with TBS with 0.1% Tween 20 and incubated with either IRDye® 680LT goat anti-mouse or IRDye® 800CW donkey anti-rabbit secondary antibodies (LI-COR Inc., Lincoln, NE, USA) for 1 hour at RT. Cutting membranes and using both infrared secondary antibodies allowed probing of up to four distinct proteins per Western blot lane. A minimum of two technical replicates (up to a maximum of five) per protein of interest were run using two distinct cultures of BDPCs. Membrane images were taken on a LI-COR Odyssey infrared imaging system and analyzed using the packaged Image Studio software. Blots were stripped and re-probed using 1x membrane stripping buffer (Gene Bio-Application Ltd., Yavne, Israel) following the manufacturer's instructions.

2.2.4 Reverse transcription polymerase chain reaction

The presence of mRNA for neurotrophic factors was confirmed using reverse transcription-polymerase chain reaction (RT-PCR). Total RNA was isolated from $1x10^6$ rat BDPC cells using a PureLink™ RNA Mini Kit (Thermo Fisher). Sample cDNA was generated from approximately 1 µg of extracted RNA with qScript cDNA SuperMix (Quanta Biosciences, Beverly, MA, USA) following the manufacturer's protocol. Samples were prepared for RT-PCR by combining 2 µl of template cDNA, 0.5 µM dNTP, 2 µl of the forward/reverse oligonucleotide primer (0.5 µM), and 0.25 µl *Taq*DNA polymerase, adding dH_2O for a final volume of 20 µl. cDNA was then amplified using three custom primers designed for rodent CNDF, GDNF and BDNF mRNA (Thermo Fisher, see Supplementary Table 2-1) for 40 cycles with an annealing step adjusted to each primers' melting temperature. Electrophoresis was performed on a 4% agarose gel and visualized with RedSafe™ Nucleic Acid Staining Solution (iNTron Biotechnology, Seongnam, South Korea) using a FluorChem Q digital imaging system (Alpha Innotech Corp., San Leandro, CA, USA). Samples lacking *Taq*DNA polymerase and template cDNA were loaded as negative controls.

2.2.5 Flow cytometry for lineage markers

Fischer rat BDPCs from passage 5-8 were gently dissociated from culture dishes with TrypLE Express (Thermo Fisher) for 10 minutes, resuspended as a $1x10^6$ cells/ml single cell suspension and divided to generate all experimental and compensation control tubes in parallel. Cells were first incubated with ZombieRed(BioLegend, San Diego, CA, USA) viability dye on ice for 30 minutes, then fixed in a 4% PFA solution for 10 minutes at RT. A 0.1% Triton X-100 solution was used to permeabilize cells for 10 minutes at RT. Cells were incubated for 30 minutes at 4°C with mouse primary antibodies for neural progenitor markers anti-Olig1 (Millipore, Burlington, MA, USA; 1:200), anti-Nestin (Proteintech, Rosemont, IL, USA; 1:200) or PBS for no primary controls. After washing, cells were incubated with an anti-mouse Alexa Fluor 488/647 secondary or PBS for 30 minutes at 4°C prior to resuspension in PBS with 3% BSA. Cytometry was performed on a FACSCanto flow cytometer (BD Biosciences), and results were analyzed with FlowJo X (v.10.0.7r2).

2.2.6 Electrophysiological analysis

Cells were placed in artificial cerebrospinal fluid (ACSF) containing (in mM): 3 KCl, 1.25 NaH2PO4-H2O, 3 MgSO4, 26 NaHCO3, 124 NaCl, 10 glucose and CaCl2 (2mM); equilibrated with 95% O2/5% CO2. Before the coverslips were transferred from the cell culture dish to the ACSF perfused recording chamber, the media was gradually replaced with ACSF over 15 minutes. The whole-cell patch clamp recordings were done at room temperature with continuous ACSF perfusion (1-2 ml/min). Cells were visualized through an upright microscope (Axioskop; Zeiss, Oberkochen, Germany) and an EMCCD camera (Evolve 512; Photometric, Huntington Beach, CA, USA). Micropipettes used for the recordings had 4-7 MOhm resistance and were filled with an intracellular solution containing (in mM): 140 K-gluconate, 10 KCl, 1 MgCl2, 0.2 EGTA, 10 HEPES, 3 Mg-ATP, and 0.5 Na-GTP, pH adjusted to 7.3, 290-300 mOsm/L. Signals were be sampled at 10 kHz, amplified with Axopatch 200B, digitized with Digidata-1550, and analyzed using pClamp 10.4 (Molecular Devices, San Jose, CA, USA). Data acquisition, analysis, and presentation were performed using pClamp10.4 (Molecular Devices), and GraphPad Prism 6.

2.2.7 Engineering cells for bioluminescence imaging

Isolated BDPCs from early passages (3 or 4) were engineered with a custom lentiviral vector to stably express firefly luciferase 2(FLuc2) for bioluminescence imaging (BLI); the rat organic anion transporting polypeptide 1a1 (OATP1A1) to increase the uptake of the luciferase substrate D-luciferin permitting detection of smaller cell grafts; and the red fluorophore TdTomato (TdT), driven by the human elongation factor 1α promoter (p-HEF1).[34] Briefly, pUltra-Chili-Luc vector was modified to express p-HEF1 and FLuc2, with a P2A self-cleaving peptide sequence separating them. OATP1A1, preceded by a E2A sequence was then inserted into the transfer vector downstream of FLuc2, generating a p-HEF1-TdT(P2A)FLuc2(E2A)OATP1A1 lentiviral vector. Cells were transduced with this vector at a multiplicity of infection of 50 and FACS sorted based on TdT expression using a FACSAria III flow cytometric cell sorter (BD Biosciences). Resultant BDPCs expressing TdT/FLuc2/OATP1A1 were maintained in the same culture medium as above until surgical implantation.

2.2.8 In vivo syngeneic graft model, BLI imaging and histology

Animal studies were conducted in accordance with the standards of the Canadian Council on Animal Care and approved by the Animal Care committee at the University of Western Ontario (protocol 2018-026). Unilateral grafts were established by stereotaxically implanting 15 000, 60 000 or 240 000 Fischer rat BDPCs into conspecific rats (n=4 per group). Rats were first anesthetized with isoflurane and placed in a stereotaxic frame. BDPCs were then injected into the dorsolateral striatum in 3µl PBS using a 10 µl Hamilton syringe at the following coordinates relative to bregma: anteroposterior: -1.0 mm, lateral: +5.0mm, dorsoventral: -6.5 mm. To assess graft survival, the bioluminescent signal of BDPCs was captured one week after implantation and weekly for another 4 weeks using an IVIS Lumina BLI system (Perkin-Elmer, Waltham, MA, USA) Animals were injected with D-luciferin (30 mg/mL solution at 150mg/kg) immediately prior to isoflurane anesthesia for imaging. BLI signal was then captured using a 60 second exposure window until signal peak. As ATP is required as a cofactor for this reaction, BLI provides a direct readout of implanted cells' viability. At 5 weeks rats were quickly perfused transcardially with 0,9% saline, followed by a 4% solution of PFA. Brains were extracted and post-fixed in 4% PFA for 1 hour at 4ºC and transferred to 30% sucrose for 3 days before cryopreservation. Brains were then sectioned into 15 µm coronal sections on a Leica cryostat and mounted onto charged slides for imaging. Sections were counterstained with DAPI to label cell nuclei. Grafted cells were located using the TdTomato fluorophore included in the BLI construct on a Nikon Eclipse Ni-E microscope and photomicrographs were taken with a DS-Qi2 camera (Nikon Instruments Inc, Melville, NY, USA).

2.3 Results

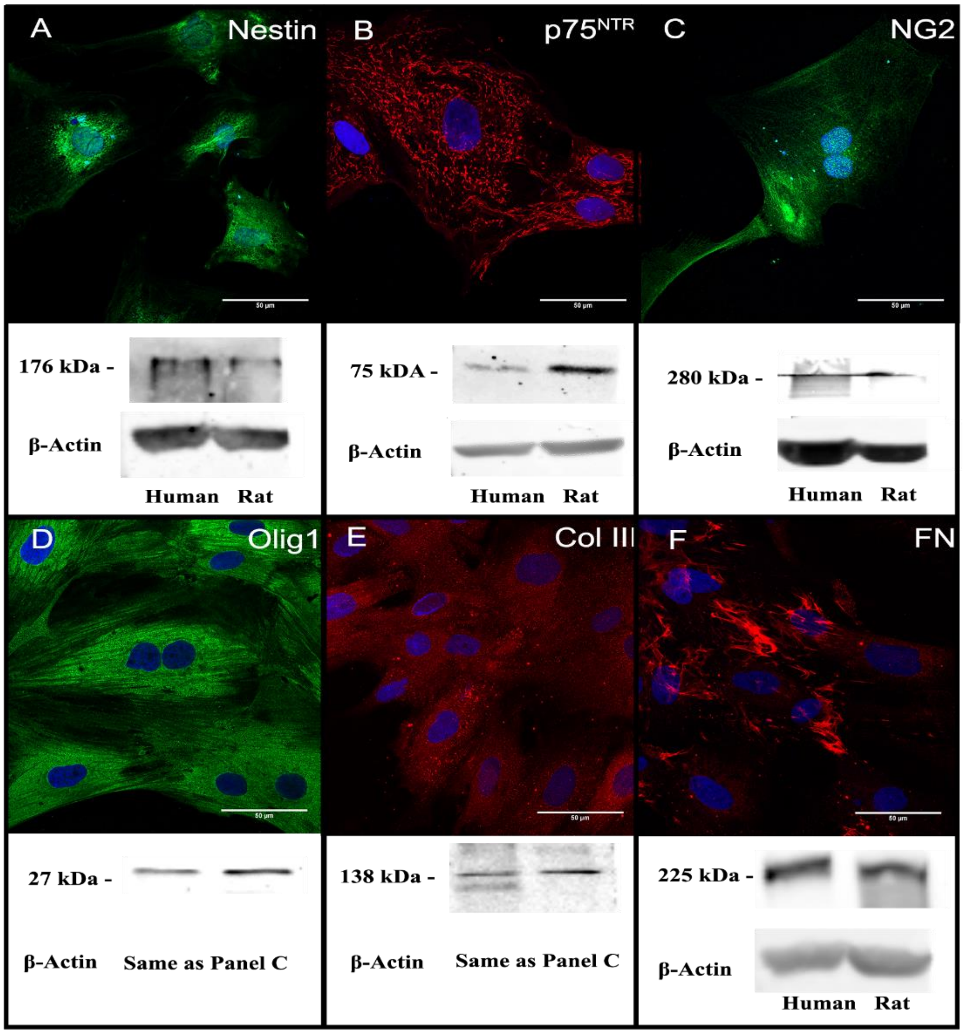

Figure 2-1 Immunocytochemistry for rodent BDPC lineage markers and comparison to human BDPC with Western blot

Representative photomicrographs (63x objective, scale = 50 μm) and accompanying Western blots showing expression of (A-C) progenitor markers nestin, p75NTR and neural/glial antigen 2 (NG2); (D) the oligodendrocyte precursor marker Olig1; and (E-F) the mesenchymal markers collagen III (Col III) and fibronectin (FN) in rodent BDPCs. Western blots were run with protein extracts from human and rodent BDPC in parallel for comparison and show bands of expected size for each marker. B-Actin was used as a loading control and is shown below each set of bands (Panels C-E share a loading control from the same lane).

2.3.1 Derivation and comparison of rodent BDPCs to human analogues

Robust cultures of rat BDPCs were derived from 12 unique brain tissue samples yielding cells with morphological characteristics consistent with their human analogues. Cells exhibited a flat polygonal shape at subconfluence and at approximately 80% confluence had a narrower spindle-like morphology, more closely resembling mesenchymal stem-cells or fibroblasts (Supplementary Fig. 2-1). These showed growth consistently through 10-12 passages before proliferation slowed, were readily frozen for storage and subsequently recovered up to 4 years after initial freezing.

Expression of proteins linked to neural progenitor, precursor and mesenchymal phenotypes were strategically evaluated and compared to those in human BDPCs. The neural progenitor markers nestin; p75 neurotrophin receptor ($p75^{NTR}$), and neural/glial antigen 2 (NG2) were all present as evidenced by immunocytochemistry and Western blot (Fig. 2-1, A-C). Expression of the oligodendrocyte progenitor markers Olig1 and the mesenchymal markers collagen III and fibronectin were also robustly expressed (Fig. 2-1, D-F). FACS analysis was conducted to assess the homogeneity of Nestin and Olig1 expression in cultures as previously observed in human BDPCs. After screening out any dead or dying cells using the ZombieRed viability dye, to eliminate non-specific binding of antibodies that is observed in dead cells and ensure accurate and reproducible results, we observed >99% of viable cells had immunolabelling for Nestin and Olig1 (Fig. 2-2, A-B).

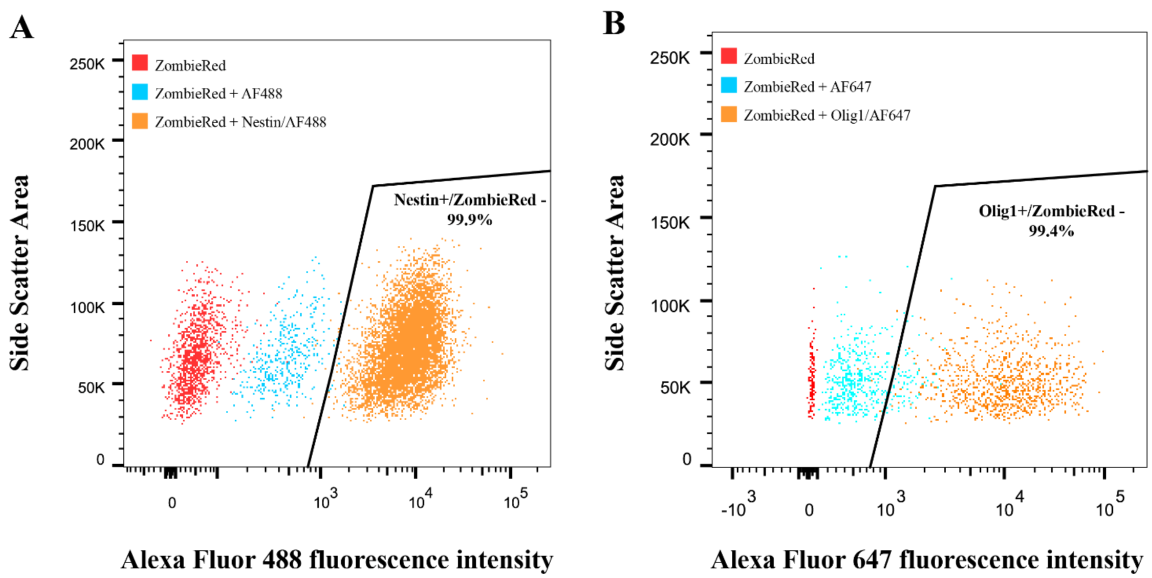

Figure 2-2 Homogenous expression of neural progenitor and early oligodendrocyte markers in viable BDPCs.

FACS scatterplots depicting the proportion in orange of (A) Nestin-positive and (B) Olig1-positive cells which did not show measurable expression of the viability marker ZombieRed. ZombieRed only (red) and secondary only (blue) control cells are also shown for comparison, as well as the gate used to select Nestin/Olig1+ cells. Cells are separated on the X-axis by secondary fluorescence intensity and on the Y-axis by their side-scatter area, a measure of cellular complexity. Approximately 10,000 cells were run for each fully stained sample.

2.3.2 Electrophysiological characteristics of human and rat BDPCs

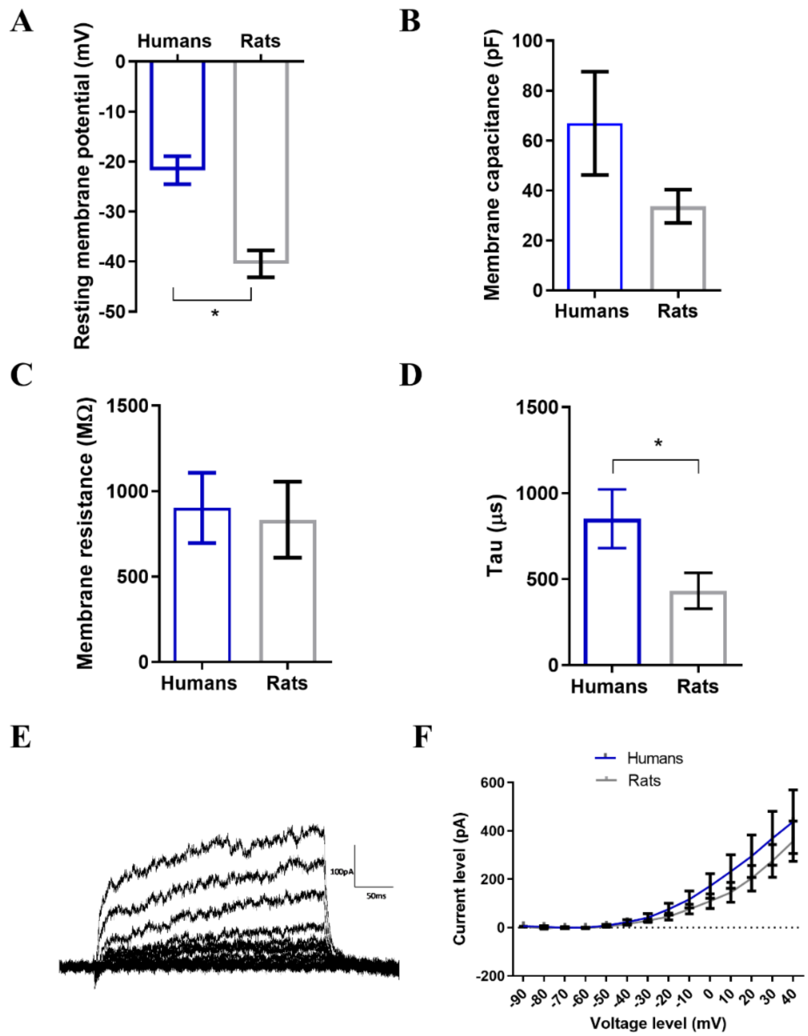

Figure 2-3 Whole cell patch clamp of human and rat derived BDPCs

Whole cell patch clamp recording results from human (blue, n=11) and rat (gray, n=12) derived BDPCs. (A) Resting membrane potential is more negative in rat derived cells compared to human derived ones. (B) Membrane capacitance and (C) membrane resistance are not different between the two population of cells. (D) The membrane time constant, Tau, as measured by applying a 10mV step is significantly lower in the rat derived cells. (E) Sample voltage clamp trace where current response is measured for increasing voltages, -90mV to +40mV in 10 mV increments, which is plotted in an (F) IV curve. All data are represented as mean ± standard error, and an asterisk indicates significant difference (P<0.05).

The intrinsic electrophysiological properties of human derived and rat derived BDPCs were compared with whole-cell patch clamp electrophysiology. Analysis showed that both rat and human derived BDPCs maintained a negative resting membrane potential, with rat derived BDPCs exhibiting a more negative resting membrane potential than human BDCPs (Fig. 2-3C, Supplementary 2-2 for average traces). They also had smaller membrane time constants (tau) than their human counterparts, while there were no differences in membrane capacitance and membrane resistance (Fig. 2-3A-D; independent samples t-tests: RMP: $t(21) = 0.049$, $p < 0.0001$; tau: $t(16.74) = 10.025$, $p = 0.027$; Cm: $t(21) = 3.136$, $p = 0.0635$; Rm: $t(21) = 1.301$, $p = 0.1295$). Analysis of the current-voltage profile through voltage-ramp recordings of these cells revealed a main effect of voltage ramp level (2-way RM ANOVA; Voltage level × cell type: $F(1.047, 19.895) = 26.937$, $p < 0.0001$) but no significant differences between the cell types ($F(1, 19) = 0.786$, $p = 0.386$; Fig. 3E and 3F).

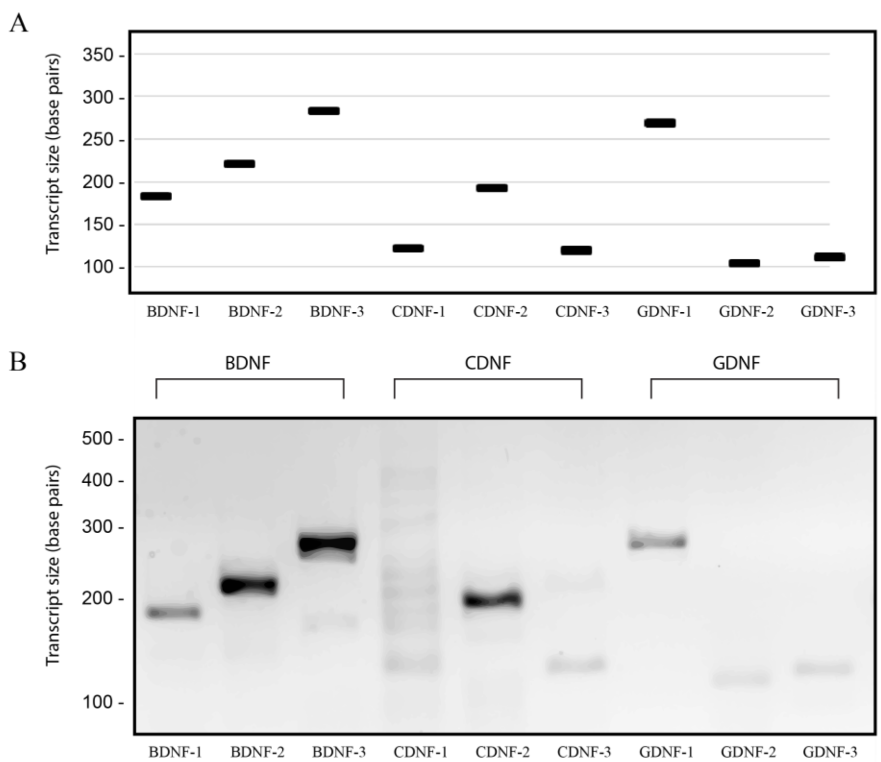

Figure 2-4 RT-PCR analysis for neurotrophic factors

(A) Expected gel for three custom-designed primers each for rodent BDNF (Lanes 1-3, expected sizes 182bp, 220bp and 282bp), CDNF(Lanes 4-6, expected sizes 121bp, 192bp and 119bp) and GDNF mRNA(Lanes 7-9, expected sizes 268bp, 104bp and 111bp) and (B) the resulting gel of the PCR products.

2.3.3 Rodent BDPCs endogenously express and secrete neurotrophic factors

Using RT-PCR with three custom designed primers per neurotrophic factor, mRNA for CDNF, BDNF and GDNF were detected in rat BDPC whole cell lysates (Fig. 2-4). Protein expression evaluated using immunocytochemistry also showed BDNF and GDNF in the cell cytoplasm, with a higher density of staining in the perinuclear space - likely in the endoplasmic reticulum - and in association with the cytoskeleton (Fig. 2-5, A-B). The presence of BDNF and GDNF in cell media and intracellularly were also examined by Western blot. proBDNF (32 kDa), truncated BDNF and mature BDNF (28 kDa and 14 kDa) were observed in whole cell lysates, while only the monomer was detected in conditioned cell media (Fig. 2-5C). For GDNF, bands of approximately 24 kDa and 15 kDa, corresponding to proGDNF and mature GDNF respectively, were detected in whole cell lysate (Fig. 2-5D). In the cell media, secreted mature BDNF bands were observed as well as a larger band corresponding to roughly 18kDa. This larger band appears to be β-pro-GDNF one of 8 known isoforms of the GDNF protein.[35]

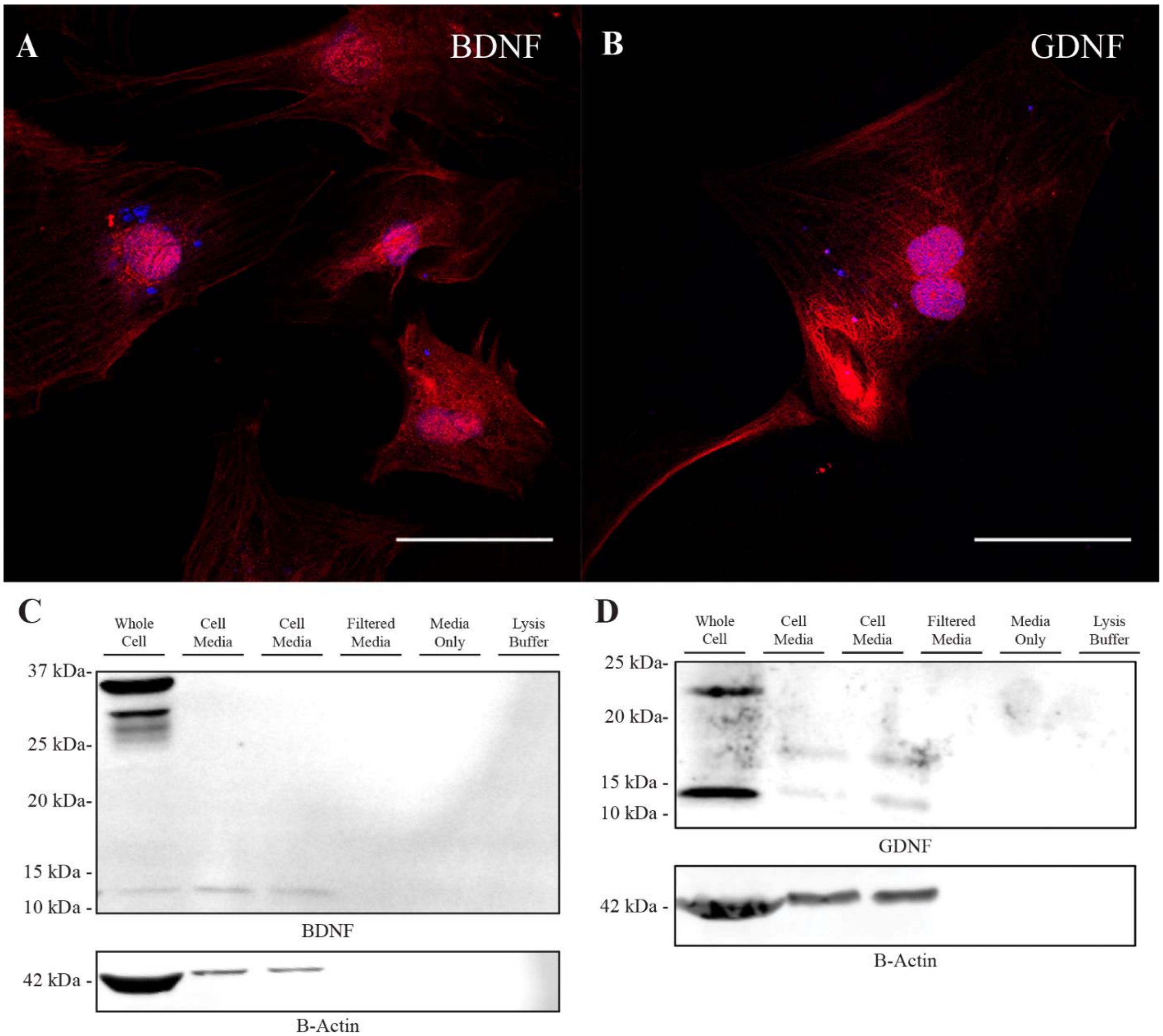

Figure 2-5 Neurotrophic factor expression in rodent BDPCs

Representative confocal photomicrographs (63x objective, scale = 50µm) showing rodent BDPCs labeled by immunocytochemistry for (A) brain-derived neurotrophic factor (BDNF), and (B) glial-derived neurotrophic factor (GDNF) (red). Nuclei are counterstained with DAPI (blue). Western Blot analysis for (C) BDNF showing expression of 32kDa proBDNF band and the 28 kDa truncated form in the whole cell protein extract as well as the mature 14kDa BDNF. Mature BDNF was detected in filtrated conditioned cell medium. Probing for GDNF (D) the ~25kDa proGDNF is observed in whole cell extract and 15 kDa mature GDNF is visible in media and whole cell lanes. An additional slightly larger band (approx. 18kda) can be seen in the media which may correspond to a unglycosylated proGDNF. Filtered DMEM from an empty culture dish, DMEM alone and lysis buffer were run as negative controls and B-Actin was included as a loading control.

2.3.4 Engineered rodent BDPCs are readily tracked in vivo using bioluminescence imaging

Having established that the overall cellular profile of rat BDPCs was like human BDPCs - including the production and newly confirmed secretion of NTFs - we sought to look at survival of cells in a syngeneic implantation model. Cells engineered through lentiviral transduction to stably express TdTomato, firefly luciferase 2 and the transporter Oatp1a1 were implanted in the striatum of Fischer rats with grafts consisting of either 15, 60 or 240 thousand cells (n=4 per group). Overall, 10 of 12 grafts still had a detectable BLI signal at 5 weeks, with two grafts no longer exhibiting detectable signal at 2 and 4 weeks respectively in the 240k cell graft cohort only (Fig. 2-6A, Supplementary Fig. 2-2 for individual peak signals). Consistent with this observation, the overall trend of graft luminescent signal in the 240k cell group decreased over 5 weeks, while the 15k and 60k groups had a generally stable signal (Fig. 2-6B). Interestingly, all three groups showed a temporary, but marked decrease in signal two weeks after engraftment. Histological sections of the striatal tissue reveal engrafted cells in the brain parenchyma visible via fluorescence microscopy of the engineered TdTomato label and with a density corresponding qualitatively to the size of graft (Fig. 2-6C).

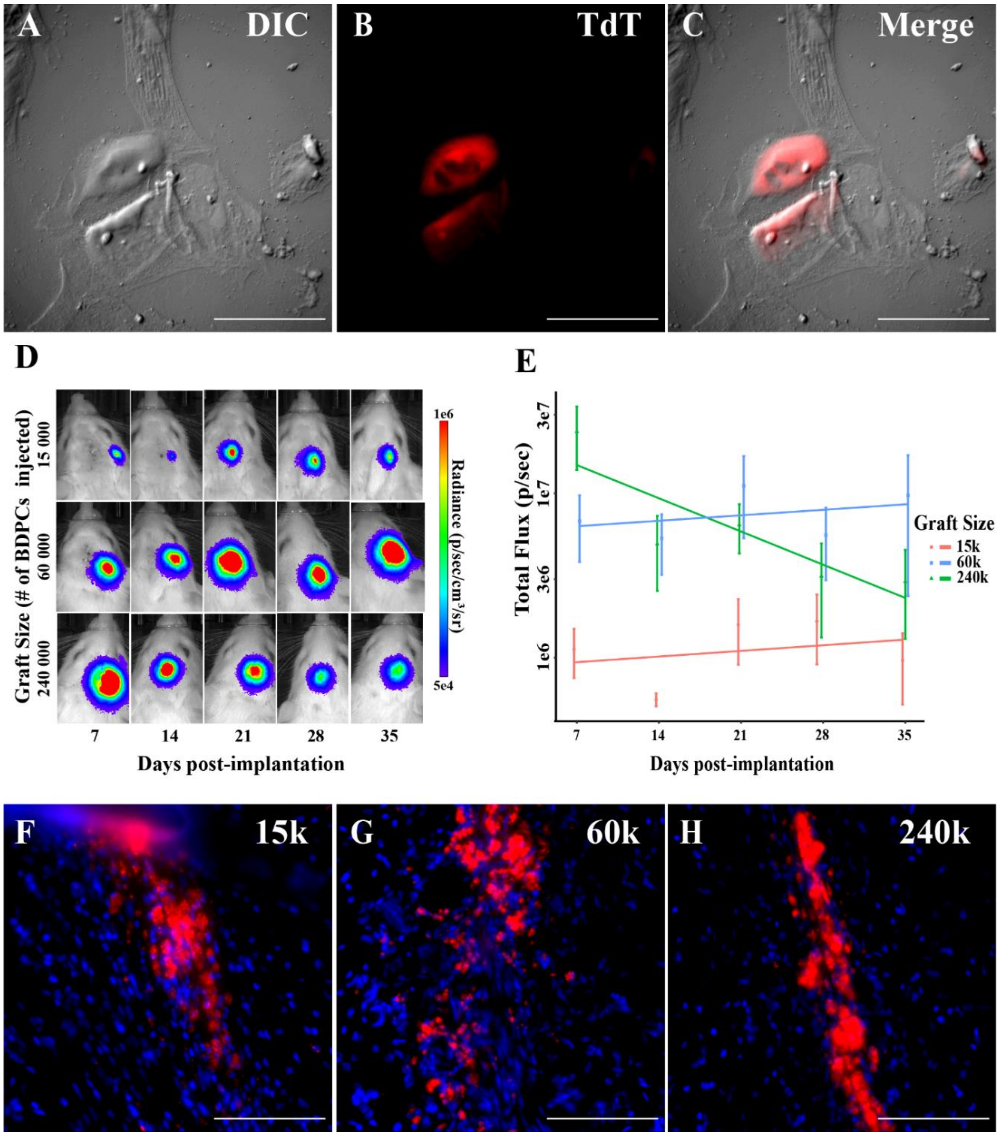

Figure 2-6 Syngeneic grafts show survival *in vivo* for 5 weeks

Photomicrograph of engineered BDPCs in culture shown using (A) differential interference contrast (DIC), (B) the fluorescent marker TdTomato (TdT) and (C) merged at 400X magnification. (D) Implanted BDPC grafts of 15k, 60k and 240k cells were detected with bioluminescence imaging over 5 weeks (n=4 per group). Weekly imaging of one representative animal from each group is shown with peak radiance signal overlaid on a static image. (E) Average peak radiance measures for animals grouped by graft size are shown with standard error at each time point. A linear model is overlaid showing the overall trend for luminescence signal over time by graft size grouping. Representative histological sections at 400X magnification of grafts of (F) 15k, (G) 60k and (H) 240k cells, respectively. Implanted cells are engineered cells from panels A-C with fluorescently labelled TdT (red) and nuclei counterstained with DAPI (blue, scale bars = 100µm).

2.4 Discussion

Previous work from our group demonstrated feasibility of generating an expandable population of cells from small-volume brain biopsies harvested from PD patients during DBS surgery.[33] These cultures exhibited mixed lineage markers characteristic of glial progenitors and expressed a panel of NTFs that are known protective molecules against PD neurodegeneration in preclinical models.[15,18,36–39] Those qualities are the foundation necessary for the development of a novel form of cell-based therapeutic which required a pre-clinical model for early therapeutic testing. As a logical first step towards that goal, the current work provides evidence that BDPC can be generated from rodent cortical tissue similarly to humans. Notably, these rat BDPCs express a profile of progenitor and neural lineage markers consistent with those seen in human BDPC cultures, including nestin, an intermediate filament protein best known for its presence in dividing cells of the nervous system; and Olig1, a transcription factor necessary for oligodendrocyte differentiation. Neurotrophic factors BDNF and GDNF were detected intracellularly in rodent BDPC as previously seen in human derived cells and we here show that they are also present in cell media (Fig. 2-4). This suggests that NTFs are likely secreted by BDPC at least partially via the constitutive pathway, as has been observed in neural and mesenchymal stem cells.[40,41] However, the presence of B-Actin in the conditioned media does raise questions about the viability of cells in the presence of serum-free media. B-Actin should not have been present in the media under normal circumstances. Inclusion of a viability verification step prior to collecting conditioned media would strengthen the argument that neurotrophic factors are being secreted rather than released by dead or dying cells. Future experiments will need to address this limitation and takes steps such as using semi-quantitative Western Blot methods; or a combination of cell culture well inserts to isolate cells, only allowing molecules smaller than membrane pores to enter the experimental media and enzyme-linked immunosorbent assay to obtain a quantitative measure of neurotrophic factors. This would allow assessment of the biological relevance of BDNF and GDNF secreted by BDPCs.

Comparison of the electrophysiological properties of human and rat BDPCs does however highlight some differences, unlike the consistent expression of lineage markers and NTFs observed above. A smaller membrane time constant, combined with a smaller membrane capacitance (although not significant) in the rat derived BDPCs indicates the cells are smaller in size than human derived BDPCs (Fig. 2-3). Both cell populations do not express rapid inward currents when depolarized, indicating they are unable to fire action potentials. However, they do have sustained outward currents, presumably predominantly K+ currents, seen in immature neurons or neural precursor cells.[42,43] A lack of difference in the voltage-current profile as well as no significant differences in the membrane resistance indicate they express relatively similar ionic currents overall. Moreover, a more negative resting membrane potential of the rat BDPCs indicates these cells are likely more mature in culture than human derived ones. A more precise analysis of the ion channel compositions of these cells would require recordings with pharmacological applications. Despite the differences observed, rodent BDPC generated in this study bear striking similarities to human BDPC.

2.4.1 Engineering BDPC to assess graft survival longitudinally in vivo

Striatal transplants, such as the ones piloted in this study, are relevant in disease models for PD.[44] The ability to monitor grafts longitudinally over the course of experimental treatment has previously been difficult in the rat due to the scale of the brain, skull and surrounding tissue compared to the more commonly used mouse. The current experiments with BDPCs showed they could be engineered to stably express a fluorescent marker and the necessary enzymes for bioluminescence imaging. With the addition of the OATP1A1 transporter they were detectable in grafts as small as fifteen thousand cells implanted in the striatum for 5 weeks in vivo. Detection of grafts of $1.5x10^4$ cells with a 60 second BLI exposure represents an important increase in sensitivity compared to previous rat models where grafts of the same order of magnitude were undetectable.[45] This result could translate to the use of BLI in preclinical studies with larger animals. For example, BLI in a larger animal model like a non-human primate could assist in getting a better understanding of cell survival *in vivo* while also bringing us phylogenetically closer to the intended application in humans.

The process of grafting exogenous cells into the CNS generates a response from the host immune system; one that is relative to the phylogenetic distance between donor and host among other things, and determines whether the graft is rejected or not.[46–48] We hypothesize that the diminished BLI signal measured 2 weeks after implantation across graft sizes is associated to initial loss of cells due to the mechanical stress of implantation, and eventual clearance of some of the grafted cells. However, subsequent rapid loss of BLI signal in 50% of the 240k cell grafts is more suggestive of a rejection response. As a syngeneic transplant, which are generally accepted to only induce short-term local inflammation and phagocytic recruitment, this result was unexpected.[46] The response was potentially triggered by the combination of a 4 to 16-fold increase in BDPCs versus smaller grafts, a parallel increase in size of the hypoxic core of the graft and disruption of the blood-brain barrier post-transplantation, and the presence of exogenous genetic material in our manipulated cells which are considered potent antigens for the peripheral immune system.[49] Hypoxia and anoikis-induced cell-death in the hours following transplantation would generate danger signals triggering an influx of neutrophils and possibly a peripheral immune response with the BBB altered by the surgical procedure.[50] This is an important consideration going forward, one that will need to be investigated further in a larger cohort. Finding a balance between adequate graft size for therapeutic benefit and increased potential for graft rejection will have to be addressed in the future.

2.5 Conclusions

Human BDPCs, by avoiding host defense mechanisms and the physiological incompatibilities of cells from outside the CNS, could offer an excellent alternative graft substrate. These characteristics, in combination with their potential for innate cytoprotective influence through NTF secretion in the CNS, are promising for development of novel therapies for PD and other neurological diseases. In this study, we show that derivation of rodent BDPCs analogous to the human cells is possible, as is modification using a lentiviral vector to assess long-term survival and localization of transplanted cells using BLI. This provides the basis for further exploration of the utility of BDPCs as an autologous, non-immunogenic, brain-derived substrate for cell-based therapies for PD and other neurodegenerative disorders. Future work will have to further characterize BDPCs and establish whether their innate characteristics are sufficient to offer therapeutic potential in animal models of PD or if these cells are better suited as a therapeutic delivery vehicle.

2.6 References

1. Lee A, Gilbert RM. Epidemiology of Parkinson Disease. *Neurol Clin*. 2016;34(4):955-965. doi:10.1016/j.ncl.2016.06.012

2. Parmar M, Torper O, Drouin-Ouellet J. Cell-based therapy for Parkinson's disease: A journey through decades toward the light side of the Force. *Eur J Neurosci*. 2019;49(4):463-471. doi:10.1111/ejn.14109

3. Barker RA, Farrell K, Guzman NV, et al. Designing stem-cell-based dopamine cell replacement trials for Parkinson's disease. *Nat Med*. 2019;25(7):1045-1053. doi:10.1038/s41591-019-0507-2

4. Staudt MD, Di Sebastiano AR, Xu H, et al. Advances in neurotrophic factor and cell-based therapies for Parkinson's disease: A mini-review. *Gerontology*. 2016;62(3):371-380. doi:10.1159/000438701

5. Harris JP, Burrell JC, Struzyna LA, et al. Emerging regenerative medicine and tissue engineering strategies for Parkinson's disease. *npj Park Dis*. 2020;6(1). doi:10.1038/s41531-019-0105-5

6. Huss A, Mojib-Yezdani F, Bachhuber F, et al. Association of cerebrospinal fluid kappa free light chains with the intrathecal polyspecific antiviral immune response in multiple sclerosis. *Clin Chim Acta*. 2019;498(December 2018):148-153. doi:10.1016/j.cca.2019.08.016

7. Olanow CW, Goetz CG, Kordower JH, et al. A Double-blind Controlled Trial of Bilateral Fetal Nigral Transplantation in Parkinson ' s Disease. *Ann Neurol*. Published online 2003:403-414. doi:10.1002/ana.10720

8. Kordower JH, Sortwell CE. Neuropathology of fetal nigra transplants for Parkinson's disease. *Prog Brain Res*. 2000;127:333-344. doi:10.1016/S0079-6123(00)27016-7

9. Morizane A, Kikuchi T, Hayashi T, et al. MHC matching improves engraftment of iPSC-derived neurons in non-human primates. *Nat Commun*. 2017;8(1):1-12. doi:10.1038/s41467-017-00926-5

10. Huttunen HJ, Saarma M. CDNF Protein Therapy in Parkinson's Disease. *Cell Transplant*. 2019;28(4):349-366. doi:10.1177/0963689719840290

11. Jiang L, Zhang H, Wang C, Ming F, Shi X, Yang M. Serum level of brain-derived neurotrophic factor in Parkinson's disease: a meta-analysis. *Prog Neuro-Psychopharmacology Biol Psychiatry*. 2019;88(March 2018):168-174. doi:10.1016/j.pnpbp.2018.07.010

12. Chauhan NB, Siegel GJ, Lee JM. Depletion of glial cell line-derived neurotrophic factor in substantia nigra neurons of Parkinson's disease brain. *J Chem Neuroanat*. 2001;21(4):277-288. doi:10.1016/S0891-0618(01)00115-6

13. Mogi M, Togari A, Kondo T, et al. Brain-derived growth factor and nerve growth factor concentrations are decreased in the substantia nigra in Parkinson's disease.

Neurosci Lett. 1999;270(1):45-48. doi:10.1016/S0304-3940(99)00463-2

14. Garea-Rodríguez E, Eesmaa A, Lindholm P, et al. Comparative Analysis of the Effects of Neurotrophic Factors CDNF and GDNF in a Nonhuman Primate Model of Parkinson's Disease. *PLoS One*. 2016;11(2). doi:10.1371/journal.pone.0149776

15. Deng X, Liang Y, Lu H, et al. Co-transplantation of GDNF-overexpressing neural stem cells and fetal dopaminergic neurons mitigates motor symptoms in a rat model of parkinson's disease. *PLoS One*. 2013;8(12):1-9. doi:10.1371/journal.pone.0080880

16. Deng X, Liang Y, Lu H, et al. Co-transplantation of GDNF-overexpressing neural stem cells and fetal dopaminergic neurons mitigates motor symptoms in a rat model of parkinson's disease. *PLoS One*. 2013;8(12):1-10. doi:10.1371/journal.pone.0080880

17. Sadan O, Bahat-Stromza M, Barhum Y, et al. Protective Effects of Neurotrophic Factor–Secreting Cells in a 6-OHDA Rat Model of Parkinson Disease. *Stem Cells Dev*. 2009;18(8):1179-1190. doi:10.1089/scd.2008.0411

18. Allen SJ, Watson JJ, Shoemark DK, Barua NU, Patel NK. GDNF, NGF and BDNF as therapeutic options for neurodegeneration. *Pharmacol Ther*. 2013;138(2):155-175. doi:10.1016/j.pharmthera.2013.01.004

19. Palasz E, Wysocka A, Gasiorowska A, Chalimoniuk M, Niewiadomski W, Niewiadomska G. BDNF as a promising therapeutic agent in parkinson's disease. *Int J Mol Sci*. 2020;21(3). doi:10.3390/ijms21031170

20. Barker RA, Björklund A, Gash DM, et al. GDNF and Parkinson's Disease: Where Next? A Summary from a Recent Workshop. *J Parkinsons Dis*. 2020;10(3):875-891. doi:10.3233/JPD-202004

21. Gill SS, Patel NK, Hotton GR, et al. Direct brain infusion of glial cell line-derived neurotrophic factor in Parkinson disease. *Nat Med*. 2003;9(5):589-595. doi:10.1038/nm850

22. Slevin JT, Gerhardt GA, Smith CD, Gash DM, Kryscio R, Young B. Improvement of bilateral motor functions in patients with Parkinson disease through the unilateral intraputaminal infusion of glial cell line-derived neurotrophic factor. *J Neurosurg*. 2005;102(2):216-222. doi:10.3171/jns.2005.102.2.0216

23. Lang AE, Gill S, Patel NK, et al. Randomized controlled trial of intraputamenal glial cell line-derived neurotrophic factor infusion in Parkinson disease. *Ann Neurol*. 2006;59(3):459-466. doi:10.1002/ana.20737

24. Patel NK, Bunnage M, Plaha P, Svendsen CN, Heywood P, Gill SS. Intraputamenal infusion of glial cell line-derived neurotrophic factor in PD: A two-year outcome study. *Ann Neurol*. 2005;57(2):298-302. doi:10.1002/ana.20374

25. Patel NK, Pavese N, Javed S, Hotton GR, Brooks DJ, Gill SS. Benefits of putaminal GDNF infusion in Parkinson disease are maintained after GDNF cessation. *Neurology*. 2013;81(13):1176-1178.

doi:10.1212/wnl.0b013e3182a55ea5

26. Whone A, Luz M, Boca M, et al. Randomized trial of intermittent intraputamenal glial cell line-derived neurotrophic factor in Parkinson's disease. *Brain*. 2019;142(3):512-525. doi:10.1093/brain/awz023

27. Lindholm P, Saarma M. Cerebral dopamine neurotrophic factor protects and repairs dopamine neurons by novel mechanism. *Mol Psychiatry*. 2022;27(3):1310-1321. doi:10.1038/s41380-021-01394-6

28. Lõhelaid H, Saarma M, Airavaara M. CDNF and ER stress: Pharmacology and therapeutic possibilities. *Pharmacol Ther*. 2024;254. doi:10.1016/j.pharmthera.2024.108594

29. Marks WJ, Bartus RT, Siffert J, et al. Gene delivery of AAV2-neurturin for Parkinson's disease: A double-blind, randomised, controlled trial. *Lancet Neurol*. 2010;9(12):1164-1172. doi:10.1016/S1474-4422(10)70254-4

30. Olanow CW, Bartus RT, Baumann TL, et al. Gene Delivery of Neurturin to Putamen and Substantia Nigra in Parkinson Controlled Trial. *Ann Neurol*. 2015;(78):248-257. doi:10.1002/ana.24436

31. Heiss JD, Lungu C, Hammoud DA, et al. Trial of magnetic resonance–guided putaminal gene therapy for advanced Parkinson's disease. *Mov Disord*. 2019;34(7):1073-1078. doi:10.1002/mds.27724

32. Gash DM, Gerhardt GA, Bradley LH, Wagner R, Slevin JT. GDNF clinical trials for Parkinson's disease: a critical human dimension. *Cell Tissue Res*. 2020;382(1):65-70. doi:10.1007/s00441-020-03269-8

33. Xu H, Belkacemi L, Jog M, Parrent A, Hebb MO. Neurotrophic factor expression in expandable cell populations from brain samples in living patients with Parkinson's disease. *FASEB J*. 2013;27(10):4157-4168. doi:10.1096/fj.12-226555

34. Nyström NN, Hamilton AM, Xia W, Liu S, Scholl TJ, Ronald JA. Longitudinal Visualization of Viable Cancer Cell Intratumoral Distribution in Mouse Models Using Oatp1a1 -Enhanced Magnetic Resonance Imaging. *Invest Radiol*. 2019;54(5):302-311. doi:10.1097/RLI.0000000000000542

35. Lonka-Nevalaita L, Lume M, Leppänen S, Jokitalo E, Peränen J, Saarma M. Characterization of the intracellular localization, processing, and secretion of two glial cell line-derived neurotrophic factor splice isoforms. *J Neurosci*. 2010;30(34):11403-11413. doi:10.1523/JNEUROSCI.5888-09.2010

36. Garea-rodríguez E, Eesmaa A, Lindholm P, Schlumbohm C, Fuchs E. Comparative Analysis of the Effects of Neurotrophic Factors CDNF and GDNF in a Nonhuman Primate Model of Parkinson ' s Disease. Published online 2016. doi:10.1371/journal.pone.0149776

37. Lu B, Nagappan G, Guan X, Nathan PJ, Wren P. BDNF-based synaptic repair as a disease-modifying strategy for neurodegenerative diseases. *Nat Rev Neurosci*. 2013;14(6):401-416. doi:10.1038/nrn3505

38. Turconi G, Kopra J, Võikar V, et al. Chronic 2-Fold Elevation of Endogenous GDNF Levels Is Safe and Enhances Motor and Dopaminergic Function in Aged Mice. *Mol Ther Methods Clin Dev*. 2020;17(June):831-842. doi:10.1016/j.omtm.2020.04.003

39. Terse PS, Kells AP, Noker P, Wright JF, Bankiewicz KS. Safety Assessment of AAV2-hGDNF Administered Via Intracerebral Injection in Rats for Treatment of Parkinson's Disease. *Int J Toxicol*. 2021;40(1):4-14. doi:10.1177/1091581820966315

40. Lu P, Jones LL, Snyder EY, Tuszynski MH. Neural stem cells constitutively secrete neurotrophic factors and promote extensive host axonal growth after spinal cord injury. *Exp Neurol*. 2003;181(2):115-129. doi:10.1016/S0014-4886(03)00037-2

41. Pan HC, Cheng FC, Chen CJ, et al. Post-injury regeneration in rat sciatic nerve facilitated by neurotrophic factors secreted by amniotic fluid mesenchymal stem cells. *J Clin Neurosci*. 2007;14(11):1089-1098. doi:10.1016/j.jocn.2006.08.008

42. Cai J, Cheng A, Luo Y, et al. Membrane properties of rat embryonic multipotent neural stem cells. *J Neurochem*. 2004;88(1):212-226. doi:10.1046/j.1471-4159.2003.02184.x

43. Moe MC, Varghese M, Danilov AI, et al. Multipotent progenitor cells from the adult human brain: Neurophysiological differentiation to mature neurons. *Brain*. 2005;128(9):2189-2199. doi:10.1093/brain/awh574

44. Zimmermann T, Remmers F, Lutz B, Leschik J. ESC-Derived BDNF-Overexpressing Neural Progenitors Differentially Promote Recovery in Huntington's Disease Models by Enhanced Striatal Differentiation. *Stem Cell Reports*. 2016;7(4):693-706. doi:10.1016/j.stemcr.2016.08.018

45. Bernau K, Lewis CM, Petelinsek AM, et al. In vivo tracking of human neural progenitor cells in the rat brain using bioluminescence imaging. *J Neurosci Methods*. 2014;228(8):67-78. doi:10.1016/j.jneumeth.2014.03.005

46. Duan WM, Widner H, Brundin P. Temporal pattern of host responses against intrastriatal grafts of syngeneic, allogeneic or xenogeneic embryonic neuronal tissue in rats. *Exp Brain Res*. 1995;104(2):227-242. doi:10.1007/BF00242009

47. Mirza B, Krook H, Andersson P, Larsson LC, Korsgren O, Widner H. Intracerebral cytokine profiles in adult rats grafted with neural tissue of different immunological disparity. *Brain Res Bull*. 2004;63(2):105-118. doi:10.1016/j.brainresbull.2004.01.009

48. Bergwerf I, Tambuyzer B, De Vocht N, et al. Recognition of cellular implants by the brain's innate immune system. *Immunol Cell Biol*. 2011;89(4):511-516. doi:10.1038/icb.2010.141

49. Stripecke R, Del Carmen Villacres M, Skelton DC, Satake N, Halene S, Kohn DB. Immune response to green fluorescent protein: Implications for gene therapy. *Gene*

Ther. 1999;6(7):1305-1312. doi:10.1038/sj.gt.3300951

50. Hoornaert CJ, Le Blon D, Quarta A, et al. Concise review: Innate and adaptive immune recognition of allogeneic and xenogeneic cell transplants in the central nervous system. *Stem Cells Transl Med*. 2017;6(5):1434-1441. doi:10.1002/sctm.16-0434

Chapter 3 [1]

3 Expanding the search for genetic biomarkers of Parkinson's disease into the living brain

Altered gene expression related to Parkinson's Disease (PD) has not been described in the living brain, yet this information may support novel discovery pertinent to disease pathophysiology and treatment. This study compared the transcriptome in brain biopsies obtained from living PD and Control patients. To evaluate the novelty of this data, a comprehensive literature review also compared differentially expressed gene (DEGs) identified in the current study with those reported in PD cadaveric brain and peripheral tissues. RNA was extracted from rapidly cryopreserved frontal lobe specimens collected from PD and Control patients undergoing neurosurgical procedures. RNA sequencing (RNA-Seq) was performed and validated using quantitative polymerase chain reaction. DEG data was assessed using bioinformatics and subsequently included within a comparative analysis of PD RNA-Seq studies. 370 DEGs identified in living brain specimens reflected diverse gene groups and included key members of trophic signaling, apoptosis, inflammation, and cell metabolism pathways. The comprehensive literature review yielded 7 RNA-Seq datasets generated from blood, skin, and cadaveric brain but none from a living brain source. From the current dataset, 123 DEGs were identified only within the living brain and 267 DEGs were either newly found or had distinct directional change in living brain relative to other tissues. This is the first known study to analyze the transcriptome in brain tissue from living PD and Control patients. The data produced using these methods offer a unique, unexplored resource with potential to advance insight into the genetic associations of PD.

---

[1] A version of this chapter has been published: Benoit SM, Xu H, Schmid S, et al. Expanding the search for genetic biomarkers of Parkinson's disease into the living brain. Neurobiol Dis. 2020;140:104872. doi:10.1016/j.nbd.2020.104872

3.1 Introduction

The changes in gene expression associated with Parkinson's Disease (PD) remain poorly understood and a priority in the search for disease biomarkers and novel therapeutic strategies. Ribonucleic acid sequencing (RNA-Seq) provides sensitive, unbiased definition of regional transcriptome variations and has been reported in PD using diverse tissue sources including blood [1–4], skin [5,6], cerebral spinal fluid[7] (CSF) and cadaveric brain [8–13]. Each tissue source has advantages and limitations that impact outcome reliability and potential for use in clinical applications. For example, blood and skin are readily accessible for diagnostic and surveillance testing, however, genetic indicators of central nervous system (CNS) pathology may be poorly represented in peripheral transcriptomes[14,15] (e.g., low signal to noise). CSF is in closer physical proximity to PD neuropathology and has been used as an accessible surrogate to brain tissue. This fluid is a nearly cell-free plasma ultrafiltrate and, while extracellular fragmented RNA has been sequenced from patient CSF, neither the CNS origin nor the accuracy of transcriptome representation is known [7,16,17]. Cadaveric brain offers advantages of accessibility and potential for multi-region tissue sampling but also has considerable limitations for RNA-Seq analysis. For example, post-mortem brains often have been subject to a long disease history with transcriptomes biased by inflammation and severe neurodegeneration [18]. Patients with end-stage PD are also more likely to have multiple co-morbidities and poly-pharmacy, and their brains exposed to prolonged ischemic times during the dying process, all of which markedly influence gene expression. Moreover, RNA is rapidly degraded after death and traditional formalin fixation can yield poor isolates, further reducing specimen integrity and quantity. Variable tissue processing delays and methods may be key confounders in cadaveric brain transcriptome studies [19].

RNA-Seq using live brain as the source tissue may more accurately reflect disease-relevant gene expression in PD compared to cadaveric brain or peripheral tissues. Although the principal obstacle for this strategy has historically been lack of tissue access, the now routine use of deep brain stimulation (DBS) for PD may provide opportunity to advance this field. The frontal lobe exposure required for DBS electrode placement is a low risk biopsy site in most patients and small volume specimens are adequate for extraction of high quality genetic material [20]. Notable advantages of brain biopsies for RNA-Seq include analyzing a viable CNS region known to be affected by PD yet not laden with the marked degeneration manifest in canonical target areas such as the substantia nigra [21]. These patients are medically fit for surgery and typically in early to mid- stages of disease, increasing the chance of identifying causative, rather than consequential, genetic changes. The collection of fresh tissue also avoids formalin fixation and permits immediate cryopreservation in the operating room, maintaining integrity of the genetic material and allowing variability in processing time without compromising outcome data. The present study sought to demonstrate the feasibility of RNA-Seq in brain biopsies from living PD patients and to compare the transcriptomes generated within PD and Control patient cohorts. To determine if the current methods provided new data over published peripheral or cadaveric CNS studies, the differentially expressed genes (DEGs) identified presently were compared to those identified in all available PD RNA-Seq datasets.

3.2 Methods

3.2.1 Patient Brain Biopsies

This study was approved by the Research Ethics Board at Western University with informed consent obtained from all patients. Individuals referred for DBS surgery had a diagnosis of idiopathic PD based on the validated UK Parkinson's Disease Society Brain Bank Clinical Diagnostic Criteria**.** [22] The modified Hoehn and Yahr scale was used to measure preoperative PD clinical status while off medications**.**[23,24] DBS access was obtained through 14 mm burr holes created over the frontal cortex at or near the intersection of the coronal suture and mid-pupillary line. A microdissector was used to remove a ~0.5 cc biopsy from directly beneath the cortical surface after which standard DBS procedures continued. Control biopsies were obtained from the analogous frontal lobe region in patients without PD during resection of a low grade, skull base tumor (e.g., meningioma). The control biopsy sites were remote from the tumor location, exhibited no radiographic or intraoperative evidence of pathology and served as the cortical entry site to place a silicone catheter, called an external ventricular drain (EVD), into the lateral ventricle for CSF drainage during the surgical procedure. Control brain specimens were collected prior to catheter placement. All brain tissue was promptly frozen in the operating room using liquid nitrogen.

3.2.2 RNA Sequencing

RNA-Seq was performed by The Centre for Applied Genomics, The Hospital for Sick Children, Toronto, Canada. Total RNA was extracted from individual brain biopsies using the Invitrogen Ambion Purelink RNA Mini Kit (ThermoFisher Scientific, Waltham, MA, USA). RNA concentration was measured by Qubit RNA HS Assay on a Qubit fluorometer (ThermoFisher Scientific) and sample quality assessed using a Bioanalyzer 2100 RNA Nano chip (Agilent Technologies, Santa Clara, CA, USA). A poly(A) mRNA RNA library was prepared from 800 ng of total RNA using the NEBNext Ultra II Directional Library Preparation kit (New England Biolabs, Ipswich, MA, USA). Each unique sample was amplified with a different barcoded adapter to allow for multiplex sequencing. To verify library insert size, 1µl of the final RNA libraries was loaded on a Bioanalyzer 2100 DNA High Sensitivity chip (Agilent Technologies). Equimolar quantities of all libraries were pooled and paired-end sequenced on 4 lanes of a High Throughput Run Mode flow cell with V4 sequencing chemistry on an Illumina HiSeq 2500 platform to generate paired-end reads of 126-bases in length.

3.2.3 Differential Gene Expression Analysis

Raw RNA-Seq data were converted to FASTQ format with bcl2fastq2 v2.17. Sequences were assessed for quality of reads with FastQC v.0.11.2 (http://www.bioinformatics.babraham.ac.uk/projects/fastqc/). Illumina adapters, bases with low quality scores near the end of the sequencing reaction (i.e., > 1% probability of inaccuracy) and reads < 40 nucleotides long were removed with TrimGalore v.0.4.0 (http://www.bioinformatics.babraham.ac.uk/projects/trim_galore/). Remaining sequences were re-assessed with FastQC to ensure post-trimming quality. Depletion of ribosomal RNA and the presence of mitochondrial RNA were assessed using FastQ-Screen v.0.4.3. [25] TopHat v.2.0.11 [26] was used for alignment to the human genome (build hg19) and read distribution, positional read duplication and strandedness of alignment were evaluated using RSeQC package v.2.3.7 (http://resqc.sourceforge.net). Quantification of nuclear transcripts was performed using RefSeq gene annotations (National Center for Biotechnology Information, NCBI) to which definitions for the known mitochondrial DNA protein coding genes were added from Gencode v.28/lift 37. Raw count data was generated with these annotations using htseq-count v.0.6.1p2 (HTSeq, http://www-huber.embl.de/users/anders/HTSeq/doc/overview.html).

Two-condition differential expression analysis was performed using the R package edgeR v.3.8.6. This analysis produces a false discovery rate, referred to below as the corrected *P*-value, generated using the Benjamini-Hochberg procedure to minimize false positives, while correcting for multiple comparisons.[27] DEGs with a corrected *P*-value < 0.05 were deemed significant. Low copy genes (i.e., < 10 reads per sample in at least 2 of the 11 samples) were excluded from the analysis to reduce the negative impact of weakly expressed transcripts on post-correction power.[28,29] Heatmap representation was generated using the superheat package for R to qualitatively parse DEG patterns and group patient samples using an unbiased similarity algorithm.

3.2.4 PCR Validation of Differential Gene Expression

Quantitative real-time polymerase chain reaction (qPCR) was used to validate the expression of six randomly selected DEGs with an absolute fold change > 1.5 measured using RNA-Seq. Primers were designed using the NCBI Primer-Blast tool (Supplementary Table 3-1).[30] cDNA was synthesized using the qScript cDNA synthesis kit (Quantabio, Beverly, MA, USA) and qPCR performed with SYBR Green Master Mix (Bio-Rad, Mississauga, ON, Canada). Briefly, 10µl reactions were run in quadruplicate in a 96-well plate following the manufacturer's protocol with annealing and extension at a temperature between 55-60°C adjusted to the melting temperature of the primers. The average cycle threshold (Ct) values for each DEG and the housekeeping gene, glyceraldehyde 3-phosphate dehydrogenase, were determined by regression analysis (CFX Manager v.3.1, Bio-Rad) and relative DEG fold change obtained using the comparative □□Ct method.[31,32] PCR products were run on an agarose gel to verify the expected size based on primer design specifications. Correlation analysis between RNA-Seq and qPCR fold changes was performed using a linear model regression in the ggplot2 package in R.

3.2.5 Comparative Literature Review of PD RNA-Seq Datasets

A PubMed review was conducted using the search terms: Parkinson’s disease, transcriptome, RNA-Seq and RNA sequencing. Returned articles were filtered using the following inclusion criteria: (i) idiopathic PD; (ii) human study and (iii) original research. Comparison of published DEG lists with the current dataset was performed using custom R scripts which extracted common entries and generated a new dataset for each study containing only common genes. A master set of all overlapping genes was also compiled from all common gene lists for the final comparative analysis.

3.3 Results

Table 3-1 PD and Control patient cohorts.

Age (Years)	Sex	Primary Disease	Time Since PD Diagnosis (Years)	Side of Brain Biopsy	Modified Hoehn & Yahr (off-state)	Co-morbidities
38	M	Parkinson's disease	4	left	3	nil
40	M	Parkinson's disease	15	right	3	paroxysmal atrial fibrillation, cardiomyopathy
56	M	Parkinson's disease	10	left	3	coronary artery disease, hyperlipidemia, inguinal hernia, anxiety
57	F	Parkinson's disease	5	right	2	nil
62	M	Parkinson's disease	11	left	2	hypertension
68	F	Parkinson's disease	17	right	3	hypertension
32	M	Craniopharyngioma	N/A	right	N/A	gastroesophageal reflux disease
60	M	Sphenoid wing meningioma	N/A	right	N/A	nil
61	M	Craniopharyngioma	N/A	right	N/A	hypertension, hyperlipidemia, basal cell ca

61	M	Sphenoid wing meningioma	N/A	left	N/A	nil
70	F	Planum sphenoidale meningioma	N/A	left	N/A	nil

3.3.1 Patient Demographics and Biopsy Outcomes

6 PD (4 male/2 female; mean age 53.5 years) and 5 Control patients (4 male/1 female; mean age 56.8 years) were recruited to this study. PD patients had a mean disease duration of 10.3 years and were receiving levodopa therapy which was held at midnight prior to surgery. Control patients had low grade, extra-axial tumors remote from the biopsy location and received a single dose of dexamethasone immediately prior to the surgical procedure. There were no other common pharmacotherapy distinctions within or between cohorts and all patients were medically fit for surgery with minimal co-morbidities (Table 1). Biopsies were obtained from 3 right/3 left PD, and 3 right/2 left Control frontal lobes. There were no perioperative complications related to the brain biopsy in any patient (Fig. 1).

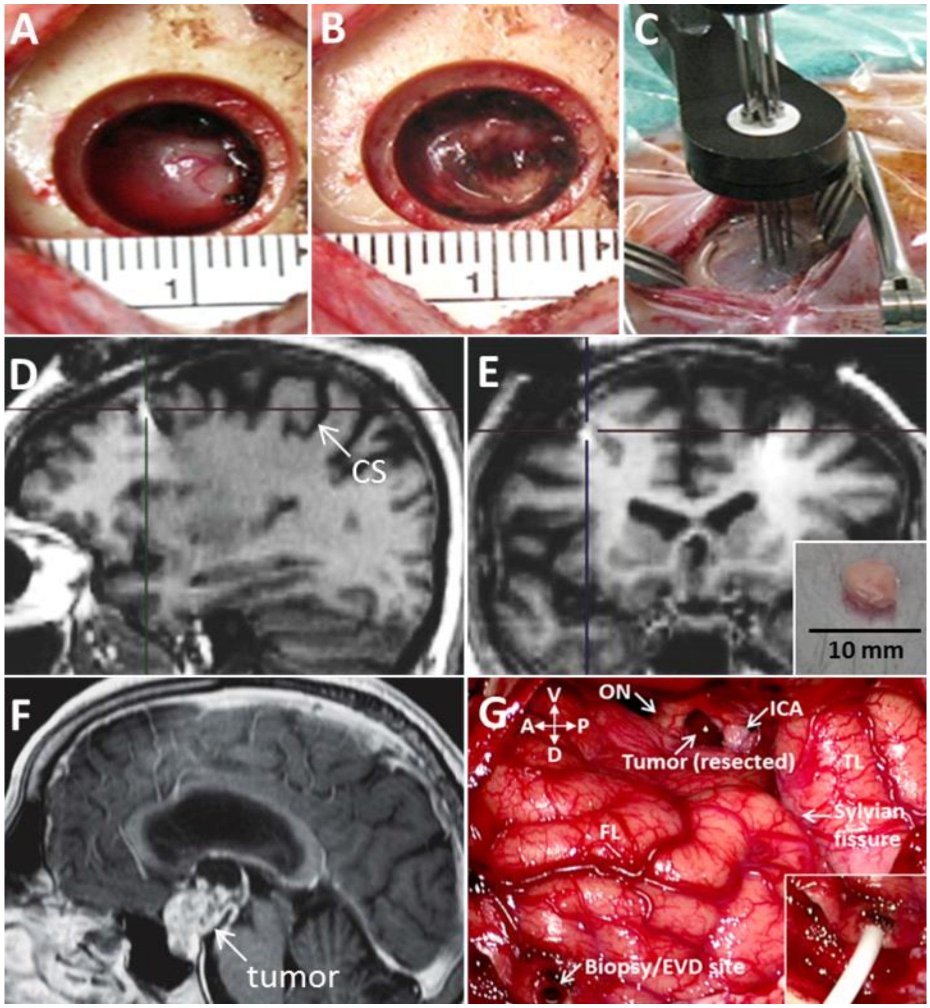

Figure 3-1 Brain biopsies in PD and Control patients

A) Consenting PD patients underwent a frontal lobe biopsy through a standard 14 mm burr hole used in the DBS procedure. B, C) The biopsy site served as the entry location of microelectrodes used for electrophysiological recording as part of the normal surgical procedure. Postoperative MRI in D) sagittal and E) coronal planes show the biopsy and electrode insertion site in the synchronized crosshairs. The inset in E) shows a typical biopsy specimen. Control patients had an extra-axial, low grade, skull base tumor that required insertion of an external ventricular drain (EVD) to reduce brain volume and widen the surgical corridor. The EVD insertion site served as the biopsy location in the frontal lobe of Control patients, was remote from the tumor location and analogous to the DBS electrode insertion site in the frontal lobe of PD patients. F) Sagittal MRI showing an example of a tumor at the skull base of a Control patient. G) Intraoperative photograph showing a right-sided exposure of the frontotemporal cortex used to resect tumors in Control patients. This is a surgical view with the brain upside down and the skull base at the top of the image. The site of frontal lobe biopsy and EVD insertion is shown with the EVD in situ (inset) and after removal (large image). A, anterior; CS, central sulcus; D,

dorsal; FL, frontal lobe; ICA, internal carotid artery; ON, optic nerve; P, posterior; TL, temporal lobe; V, ventral

3.3.2 Differential Gene Expression in PD

RNA-Seq generated ~90 million pairs of reads of predominantly messenger RNA (Supplementary Table 3-2). Approximately ~18,000 genes were detected with appropriate sequencing depth across samples and retained for downstream analysis. Differential expression analysis revealed 370 significant DEGs (172 up-regulated, 198 down-regulated) that distinguished PD and Control cohorts. Disparate expression profiles were visualized using heatmap representation and unbiased hierarchical clustering confirmed similarity of samples within each group (Fig. 2).

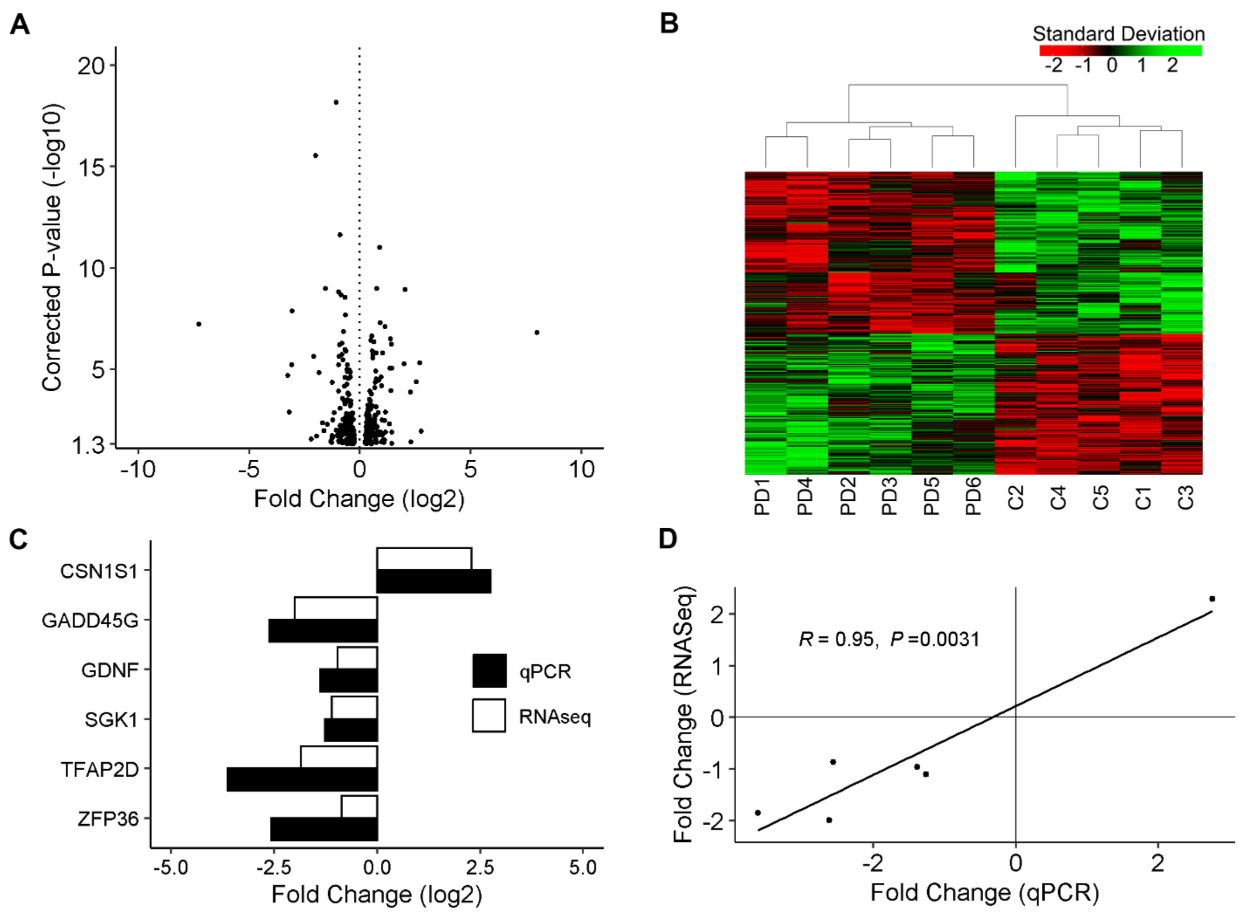

Figure 3-2 Differential gene expression in living PD frontal lobe biopsies

PD-associated DEGs are displayed A) per gene as a volcano plot and B) per sample as a heat map of read values transformed to show standard deviation from the mean (red = down-regulation; green = up-regulation). The ordinate origin (i.e., 1.3) of the volcano plot corresponds to the maximum corrected p-value of significance (i.e., p = 0.05). DEGs segregated PD from Control cohorts with 99% of fold changes between ± 4 and a nearly equal number of up-regulated (172) and down-regulated (198) genes. The dendrogram above the heatmap depicts sample similarity by hierarchical clustering. C) Six randomly selected DEGs provided qPCR validation of RNA-Seq data, as indicated by the corresponding fold change values defined using these techniques. D) Correlation analysis revealed a strong positive linear relationship between qPCR and RNA-Seq data for the six genes shown in C).

RNA-Seq data was sampled for validation using qPCR to measure transcript levels of six randomly selected DEGs: casein alpha S1 (CSN1S1), growth arrest and DNA damage inducible gamma (GADD45G), glial cell-derived neurotrophic factor (GDNF), serum/glucocorticoid regulated kinase 1 (SGK1), transcription factor AP-2 delta (TFAP2D) and zinc finger protein 36 (ZFP36). DEGs were selected arbitrarily to evaluate RNA-Seq accuracy across a range of expression levels and fold changes. RNA-Seq and qPCR results aligned for each DEG with significant linear relationships demonstrated between outcome measures generated using both techniques (Fig 2). No significant changes were found in mitochondrial genes or those associated with inheritable forms of PD (Supplementary Tables 3-3, 3-4), however numerous altered genes were identified with prominent or presumed links to PD pathogenesis and therapeutics (Fig. 3; Supplementary Table 3-5). Examples of notable DEGs included the down-regulated trophic signaling elements GDNF (-1.94-fold), fibroblast growth factor 18 (FGF18, -1.80-fold) and hepatocyte growth factor (HGF) receptor, c-MET (-1.90-fold). PD samples had significantly elevated levels of the pro-apoptotic cytokine, tumor necrosis factor-related apoptosis-inducing ligand (TRAIL; +1.61-fold; also called tumor necrosis factor superfamily member 10, TNFSF10) and its death receptor 4 (DR4; +1.96-fold; also called tumor necrosis factor receptor superfamily member 10A, TNFRSF10A). Other DEGs included the inflammation regulators interferon regulatory factor 8 (IRF8; +1.61-fold), NF-kappaB inhibitor protein A (NF-κBIA; -1.84-fold), interleukin 1 receptor, type II (IL-1R2; -4.56-fold), and CX3C chemokine receptor 1 (CX3CR1; +1.63-fold). There were also significant changes in expressed levels of the coagulation cascade elements, factor 5 (F5, +2.02-fold) and plasminogen activator inhibitor 1 (PAI-1; -4.25-fold; also called Serpin

Family E Member 1, SERPINE1), as well as thyrotropin-releasing hormone (TRH; +1.92-fold) and the ferroxidase ceruloplasmin (CP; -2.23-fold). A complete DEG list is provided in Supplementary Table 3-5.

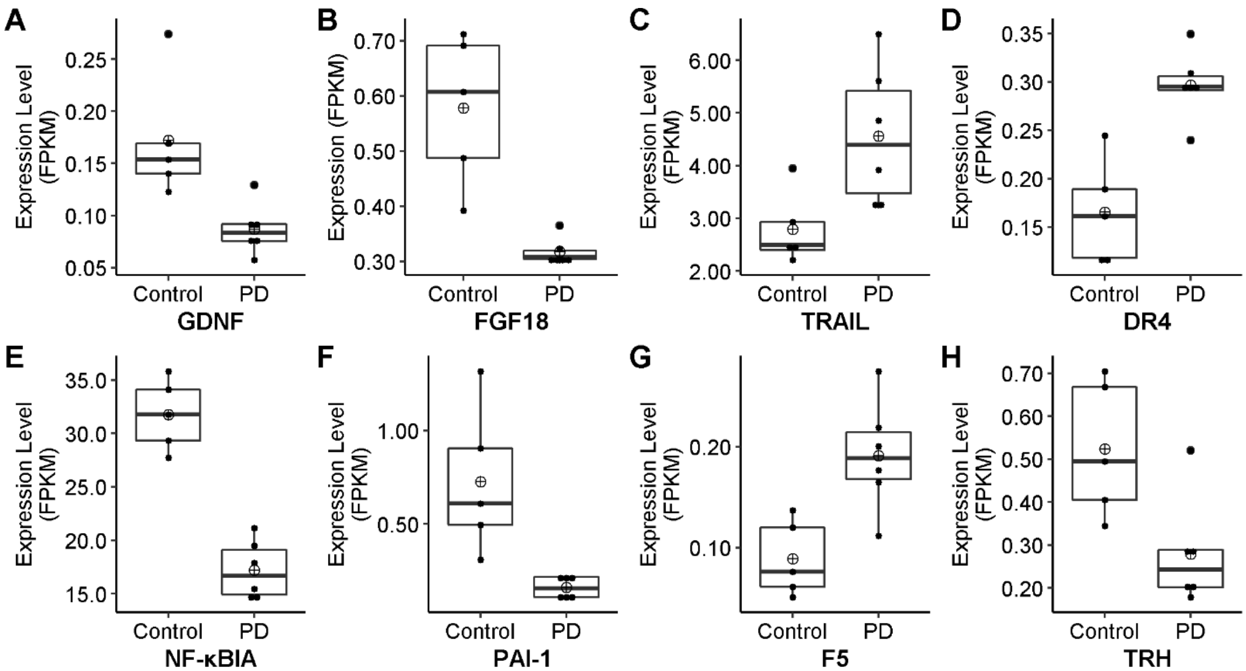

Figure 3-3 PD-associated DEGs reflect changes across diverse gene groups in the living frontal lobe

Box plot representation of DEGs with prominent or presumed links to neurodegenerative disease as measured using RNA-Seq in living PD and Control brain samples. Shown are DEG examples of growth factors (A, B), apoptosis mediators (C, D) and regulators of inflammation (D), coagulation (F, G) and hormone production (H) in fragments per kilobase per million (FPKM) as a measure of expression normalized for sequencing depth and read length. Boxes represent the upper and lower quartile values for each group, and the median value is denoted by a horizontal black bar, with a crosshair to indicate the mean. Individual data points corresponding to values for each patient are overlaid as black points.

3.3.3 Comparative Analysis of PD Transcriptome Datasets

The literature review identified 6 RNA-Seq studies using human idiopathic PD source tissue, including cadaveric brain [11–13], whole blood [2], skin fibroblasts [5] and CSF.[7] DEG information from the CSF report was not available but the remaining studies yielded 7 RNA-Seq datasets that were included in the current analysis. Of the 370 DEGs identified in the living frontal lobe, 123 genes were newly identified and unique to this study (Tables 3-2, Supplementary 3-6). The remaining 247 genes had been reported in at least one of the past studies, with 103 (42%) showing corresponding directional changes (i.e., increased or decreased expression) in all studies which identified that specific gene (Tables 3-2, Supplementary 3-7). However, many of these genes were reported only in a single study with 35, 6 and 2 DEGs from the current list having corresponding directional changes in ≥2, ≥3 and ≥4 of the published datasets, respectively. Comparing the present DEG dataset from living brain specimens to those of other non-cadaveric studies (i.e., blood and skin) identified 10 genes in common with blood, and 23 with skin. Of these, only 6 (60%) and 9 (39%) had the same directional change in expression, respectively (Supplementary Table 3-8). There were no DEGs found in living brain that were common to both blood and skin datasets.

Table 3-2 The 25 most significant DEGs uniquely identified in brain specimens from living PD patients

Symbol	Gene Name	Fold Change (log2)	Corrected *P*-value
ARRDC3	arrestin domain containing 3	-0.54	3.32E-04
CCDC38	coiled-coil domain containing 38	2.01	5.53E-06
CNTN6	contactin 6	0.67	8.37E-05
CTAG2	cancer/testis antigen 2	-7.27	5.97E-08
DUSP6	dual specificity phosphatase 6	0.72	1.24E-05
F2RL3	F2R like thrombin/trypsin receptor 3	-3.06	6.08E-06
FAM13B	family with sequence similarity 13 member B	-0.42	2.41E-05
FAM212B	family with sequence similarity 212 member B	-0.43	1.38E-05
FRAT1	frequently rearranged in advanced T-cell lymphomas 1	-0.70	4.01E-04
GADD45G	growth arrest and DNA damage inducible gamma	-2.00	2.97E-16
GPX3	glutathione peroxidase 3	0.49	3.71E-07
IDH1	isocitrate dehydrogenase) 1, cytosolic	0.43	3.20E-04
LAMA2	laminin subunit alpha 2	0.51	1.72E-04

MIR3648	microRNA 3648-1	2.54	4.18E-05
MIR3687	microRNA 3687-1	2.70	4.90E-06
PCDH11X	protocadherin 11 X-linked	-0.70	7.16E-05
PER1	period circadian clock 1	-0.53	4.01E-04
PLEKHO2	pleckstrin homology domain containing O2	0.49	3.70E-04
RASD1	ras related dexamethasone induced 1	-0.57	6.08E-06
REM2	RRAD and GEM like GTPase 2	-0.97	1.22E-04
SNAR-C3	small ILF3/NF90-associated RNA C3	8.00	1.55E-07
SPRY4	sprouty RTK signaling antagonist 4	0.73	1.57E-06
TFAP2D	transcription factor AP-2 delta	-1.85	1.49E-05
TSHZ3	teashirt zinc finger homeobox 3	-0.67	2.90E-09
USP2	ubiquitin specific peptidase 2	-0.62	1.31E-06

3.4 Discussion

This is the first known study to profile a regional CNS transcriptome in living PD patients. The frontal cortex was chosen based on accessibility and previous experience with safe biopsies in this area during DBS surgery (Fig. 3-1).[20] Based on previous cadaveric studies of the transcriptome in the healthy brain and in PD mRNA expression in the frontal cortex should vary from that of other brain regions.[33,34] Despite these regional variations, there is evidence for an underlying profile in PD that spans regions, as best evidenced by the multi-regional study included in our comparative literature review.[13] Comparing the expression profile in the cortex, substantia nigra and striatum they highlighted both a unique regional profile and a smaller shared component across regions numbering 80 genes. RNA-Seq identified 370 DEGs associated with PD, approximately one third of which were unique to the living brain and not reported in past cadaveric brain or peripheral tissue studies (Tables 3-2, Supplementary 3-7). Moreover, 267 DEGs were either new or exhibited distinct directional change in the living brain relative to other source tissues. Although there were no expression changes in MT genes or those associated with hereditary forms of PD, the current DEG dataset contained a broad spectrum of gene groups and many with established or presumed contributions to neurodegenerative disease.

3.4.1 Trophic Factor and Apoptosis Signaling

The potent neural support conferred through trophic signaling mechanisms has driven longstanding interest in therapeutic applications for PD.[36–39] However, it remains to be established whether and to what extent abnormalities in these molecular pathways contribute to the neurodegenerative process. GDNF is one of the most widely investigated trophic agents in PD, recognized for robust preclinical benefits in dopaminergic neuron survival and regeneration. [39,40] The current study provides new evidence for significant GDNF deficiency in the frontal lobe of living PD patients using RNA-Seq (-1.94-fold) and qPCR (-2.60-fold); a finding not previously reported in PD transcriptomes from blood, skin or cadaveric brain (Figs. 3-2, 3-3).[2,5,11–13] Other down-regulated trophic signaling proteins included FGF18 and the HGF receptor, c-Met. Although less characterized in PD than GDNF, both proteins exert neuroprotection in preclinical models and were identified as reduced DEGs in 2 of the past 3 cadaveric PD cortex RNA-Seq datasets (FGF18: -2.11 and -2.39-fold; c-Met: -1.97 and -5.54-fold), but neither in blood nor skin. [2,5,11–13]

The known mechanisms of neuronal death in PD largely relate to the intrinsic (mitochondrial) apoptosis pathway whereas the role of the extrinsic pathway is less established. [41] TRAIL is a pro-apoptotic cytokine and principal activator of the extrinsic pathway through binding cell surface death receptors that trigger caspase-dependent programmed cell death. The abnormalities in trophic support currently found in the living PD frontal lobe were accompanied by heightened levels of TRAIL/TNFSF10 (+1.61-fold) and its death receptor DR4/TNFRSF10A (+1.96-fold). TRAIL up-regulation has not been reported in past PD RNA-Seq datasets and the current DR4 overexpression corroborated similar findings in a single cadaveric PD brain study. [12]

3.4.2 Inflammation Regulators

The inflammatory response in the brain is mediated largely by activated glial cells and a significant but poorly understood contribution to PD pathology. This study identified numerous changes in pro- and anti-inflammatory genes with prominent roles in neuroinflammation. For example, a key inflammatory hub is the NF-κB signaling network in neurons and glial cells. [42] Under homeostatic conditions, the inhibitor protein, NF-κBIA, also known as IκBα, sequesters NF-κB proteins in the cytoplasm to block nuclear localization and render them inactive. This system is disrupted when an appropriate stimulus (e.g., oxidative stress) triggers IκBα degradation, freeing NF-κB to activate transcription of pro-inflammatory genes. [43] In the present cohort of living PD patients, expression of the NF-κBIA inflammatory brake was significantly reduced (-1.84-fold), concordant with 1 of 3 reports of cadaveric cortex RNA-Seq transcriptomes. [11–13] Other inflammation-related DEGs identified in the current study included the transcription factor IRF8 (+1.61-fold) which regulates microglial activation and pro-inflammatory phenotype [44,45], IL-1R2 (-4.55-fold), a decoy receptor that reduces activity of the pro-inflammatory cytokine IL-1, and the chemokine receptor CX3CR1 (+1.63-fold) expressed in microglia that binds neuronal fractalkine, promotes monocyte survival and reduces microglial expression of pro-inflammatory genes and reactivity. [46,47]

3.4.3 Coagulation Factors and Protease Inhibitors

There is widely conflicting evidence regarding a potential association between coronary artery disease or stroke, and PD. [48–51] In the present study, PD patients exhibited a 2.02-fold increase in F5, a procoagulant molecule that, when activated, catalyzes thrombin production to convert soluble fibrinogen to a fibrin clot (Fig. 3-3). Mutations that produce chronic F5 activation (i.e., Factor V Leiden) manifest a hypercoagulable state that increases thrombosis and stroke risk. [52] The present data corroborates a prior report of F5 up-regulation (+2.19-fold) in cadaveric PD cortex but notably this DEG was not identified in a blood RNA-Seq dataset. [2,12]

Another DEG in this group is PAI-1/SERPINE1, the principal inhibitor of tissue plasminogen activator (tPA). tPA converts plasminogen to the plasmin protease which breaks down blood clots through fibrinolysis. Elevated PAI-1 levels reduce plasmin activity and present a risk factor for thrombosis and atherosclerosis. [53] PAI-1-regulated plasmin activity also impacts other functional systems and can degrade extracellular α-synuclein, a major component of pathological Lewy bodies, to potentially limit its prion-like spread. [54] Additionally, PAI-1 activity affects processing of the neurotrophin, brain-derived neurotrophic factor (BDNF). The proBDNF peptide is cleaved by plasmin to a mature form that signals through the tropomyosin-related kinase type 2 (trkB) receptor to exert neuronal protection and stimulate neurite growth, among other functions. [55] Uncleaved proBDNF has an opposing effect acting through the p75 nerve growth factor receptor to promote apoptosis. Through these various mechanisms, alterations in the PAI-1 system have been implicated in numerous neurological disorders. [55–60] Although plasma PAI-1 protein has been reported elevated in PD patients, this was not an identified DEG in the only published blood PD RNA-Seq analysis. [2,57] In the current study, PAI-1 was markedly reduced (-4.25-fold) in living PD brain samples, corroborating the down-regulation (-2.62-fold) found in one cadaveric cortex PD RNA-Seq dataset [13] but contrasting the up-regulation (+1.93-fold) reported in another (Fig. 3-3, Supplementary Table 3-7).[12] It remains to be proven whether the reduced PAI-1 observed in the present living PD brain specimens promotes plasmin-mediated fibrinolysis, active BDNF levels and α-synuclein degradation.

3.4.4 Thyrotropin Releasing Hormone (TRH)

TRH is a central regulator of the hypothalamic-pituitary-thyroid (HPT) axis, primarily synthesized in the hypothalamus but found widely throughout the CNS where it confers diverse neuromodulatory and protective functions. [61] Sensitization of the TRH response has been demonstrated in PD models and patients [62–65] and the interactions between TRH and dopamine in the HPT axis and other CNS regions is well documented. [66] TRH or analogues thereof produce neurotrophic effects and significantly attenuate apoptosis in models of ischemia and neurodegenerative disease, including PD.[62,67–70] Moreover, TRH can directly stimulate release of dopamine in the striatum and reduce PD-related symptoms in experimental models. [71] In the present study, TRH was significantly reduced (-1.92-fold) in the frontal lobe of living PD patients (Fig. 3-3). This gene was also reported as down-regulated (-2.71-fold) in a single RNA-Seq study that analyzed cadaveric PD cortex. [13]

3.4.5 Ceruloplasmin (CP)

Dysregulated cerebral iron metabolism has long been postulated to heighten oxidative stress associated with PD. [72] CP is a ferroxidase enzyme that facilitates iron egress from the cell thereby reducing the risk of iron accumulation and oxidative free radical production. [73] Low CP-ferroxidase activity was identified in the substantia nigra, serum and CSF of patients with idiopathic PD and reduced serum CP levels has been associated with earlier PD onset. [74] Iron chelation to mitigate this deficiency may offer potential as a therapeutic strategy for PD. [74–76] Consistent with these findings, the present study revealed a significant reduction (-2.23-fold) in CP levels in living PD patient cortex yet was discordant with the CP up-regulation reported in RNA-Seq analyses using cadaveric cortex. [12,13]

3.5 Conclusions

This proof-of-concept study demonstrated the feasibility of regional CNS transcriptome analysis and the unique, unexplored DEG composition of the frontal lobe in living PD patients. The data generated using small cohorts with minor variance in medical history was supported by numerous DEGs with known association to neurodegenerative disease, as well as a substantial overlap with RNA-Seq datasets from peripheral and cadaveric PD tissues. The emergence of DBS as a standard of surgical care in PD has created a broad patient population that could facilitate adequately powered and controlled CNS transcriptome studies. Future efforts may also be expanded to identify genomic mutations, epigenetic changes as well as alterations in micro- and non-coding RNA. Genetic analysis using living brain tissue offers new potential for molecular discovery and refined pursuit of disease-relevant peripheral biomarkers in PD.

3.6 References

1. Soreq L, Bergman H, Israel Z, Soreq H. Exon arrays reveal alternative splicing aberrations in Parkinson's disease leukocytes. Neurodegener Dis. 2012;10(1–4):203–6.

2. Infante J, Prieto C, Sierra M, Sánchez-Juan P, González-Aramburu I, Sánchez-Quintana C, et al. Comparative blood transcriptome analysis in idiopathic and LRRK2 G2019S-associated Parkinson's disease. Neurobiol Aging [Internet]. 2015;38:214.e1-214.e5. Available from: http://dx.doi.org/10.1016/j.neurobiolaging.2015.10.026

3. Infante J, Prieto C, Sierra M, Sánchez-Juan P, González-Aramburu I, Sánchez-Quintana C, et al. Identification of candidate genes for Parkinson's disease through blood transcriptome analysis in LRRK2-G2019S carriers, idiopathic cases, and controls. Neurobiol Aging [Internet]. 2015;36(2):1105–9. Available from: http://dx.doi.org/10.1016/j.neurobiolaging.2014.10.039

4. Mutez E, Nkiliza A, Belarbi K, de Broucker A, Vanbesien-Mailliot C, Bleuse S, et al. Involvement of the immune system, endocytosis and EIF2 signaling in both genetically determined and sporadic forms of Parkinson's disease. Neurobiol Dis. 2014;63:165–70.

5. Planken A, Kurvits L, Reimann E, Kadastik-eerme L, Kingo K, Kõks S, et al. Looking beyond the brain to improve the pathogenic understanding of Parkinson's disease: implications of whole transcriptome profiling of Patients' skin. BMC Neurol [Internet]. 2017;17(1):6. Available from: http://bmcneurol.biomedcentral.com/articles/10.1186/s12883-016-0784-z

6. González-Casacuberta I, Morén C, Juárez-Flores DL, Esteve-Codina A, Sierra C, Catalán-García M, et al. Transcriptional alterations in skin fibroblasts from Parkinson's disease patients with parkin mutations. Neurobiol Aging [Internet]. 2018;65:206–16. Available from: https://doi.org/10.1016/j.neurobiolaging.2018.01.021

7. Hossein-Nezhad A, Fatemi RP, Ahmad R, Peskind ER, Zabetian CP, Hu SC, et al. Transcriptomic Profiling of Extracellular RNAs Present in Cerebrospinal Fluid Identifies Differentially Expressed Transcripts in Parkinson's Disease. J Parkinsons Dis. 2016;6(1):109–17.

8. Hauser MA, Li Y-J, Xu H, Noureddine MA, Shao YS, Gullans SR, et al. Expression Profiling of Substantia Nigra in Parkinson Disease, Progressive Supranuclear Palsy, and Frontotemporal Dementia With Parkinsonism. Arch Neurol [Internet]. 2005;62(6). Available from: http://archneur.jamanetwork.com/article.aspx?doi=10.1001/archneur.62.6.917

9. Moran LB, Duke DC, Deprez M, Dexter DT, Pearce RKB, Graeber MB. Whole genome expression profiling of the medial and lateral substantia nigra in Parkinson's disease. Neurogenetics. 2006;7(1):1–11.

10. Elstner M, Morris CM, Heim K, Bender A, Mehta D, Jaros E, et al. Expression analysis of dopaminergic neurons in Parkinson's disease and aging links transcriptional dysregulation of energy metabolism to cell death. Acta Neuropathol. 2011;122(1):75–86.

11. Dumitriu A, Golji J, Labadorf AT, Gao B, Beach TG, Myers RH, et al. Integrative analyses of proteomics and RNA transcriptomics implicate mitochondrial processes, protein folding pathways and GWAS loci in Parkinson disease. BMC Med Genomics [Internet]. 2016;9(1):1–17. Available from: http://dx.doi.org/10.1186/s12920-016-0164-y

12. Henderson-Smith A, Corneveaux JJ, De Both M, Cuyugan L, Liang WS, Huentelman M, et al. Next-generation profiling to identify the molecular etiology of Parkinson dementia. Neurol Genet. 2016;2(e75).

13. Riley BE, Gardai SJ, Emig-Agius D, Bessarabova M, Ivliev AE, Schüle B, et al. Systems-based analyses of brain regions functionally impacted in Parkinson's disease reveals underlying causal mechanisms. PLoS One. 2014;9(8).

14. LeDoux MS, Xu L, Xiao J, Ferrell B, Menkes DL, Homayouni R. Murine central and peripheral nervous system transcriptomes: Comparative gene expression. Brain Res. 2006;1107(1):24–41.

15. Prieto C, Risueño A, Fontanillo C, De Las Rivas J. Human gene coexpression landscape: Confident network derived from tissue transcriptomic profiles. PLoS One. 2008;3(12).

16. Saugstad JA, Lusardi TA, Van Keuren-Jensen KR, Phillips JI, Lind B, Harrington CA, et al. Analysis of extracellular RNA in cerebrospinal fluid. J Extracell Vesicles [Internet]. 2017;6(1). Available from: https://doi.org/10.1080/20013078.2017.1317577

17. Parnetti L, Castrioto A, Chiasserini D, Persichetti E, Tambasco N, El-Agnaf O, et al. Cerebrospinal fluid biomarkers in Parkinson disease. Nat Rev Neurol [Internet]. 2013;9(3):131–40. Available from: http://dx.doi.org/10.1038/nrneurol.2013.10

18. Franz H, Ullmann C, Becker A, Ryan M, Bahn S, Arendt T, et al. Systematic analysis of gene expression in human brains before and after death. Genome Biol. 2005;6(13):1–9.

19. David LE, Fowler CB, Cunningham BR, Mason JT, O'Leary TJ. The effect of formaldehyde fixation on RNA: Optimization of formaldehyde adduct removal. J Mol Diagnostics [Internet]. 2011;13(3):282–8. Available from: http://dx.doi.org/10.1016/j.jmoldx.2011.01.010

20. Xu H, Belkacemi L, Jog M, Parrent A, Hebb MO. Neurotrophic factor expression in expandable cell populations from brain samples in living patients with Parkinson's disease. FASEB J. 2013;27(10):4157–68.

21. Jellinger KA. Neuropathobiology of non-motor symptoms in Parkinson disease. J Neural Transm. 2015;122(10):1429–40.

22. Hughes AJ, Daniel SE, Kilford L, Lees AJ. Accuracy of clinical diagnosis of idiopathic Parkinson's disease: a clinico-pathological study of 100 cases. J Neurol

Neurosurg Psychiatry. 1992;55:181–4.

23. Goetz CG, Poewe W, Rascol O, Sampaio C, Stebbins GT, Counsell C, et al. Movement Disorder Society Task Force report on the Hoehn and Yahr staging scale: Status and recommendations. Mov Disord. 2004;19(9):1020–8.

24. Jankovic J, McDermott M, Carter J, Gauthier S, Goetz C, Golbe L, et al. Variable expression of Parkinson's disease: A base-line analysis of the DAT ATOP cohort. Neurology [Internet]. 1990 Oct 1;40(10):1529–1529. Available from: http://www.neurology.org/cgi/doi/10.1212/WNL.40.10.1529

25. Wingett SW, Andrews S. FastQ Screen: A tool for multi-genome mapping and quality control. F1000Research [Internet]. 2018;7(0):1338. Available from: https://f1000research.com/articles/7-1338/v1

26. Trapnell C, Pachter L, Salzberg SL. TopHat: Discovering splice junctions with RNA-Seq. Bioinformatics. 2009;25(9):1105–11.

27. Ferreira JA, Zwinderman AH. On the Benjamini-Hochberg method. Ann Stat. 2006;34(4):1827–49.

28. Anders S, McCarthy DJ, Chen Y, Okoniewski M, Smyth GK, Huber W, et al. Count-based differential expression analysis of RNA sequencing data using R and Bioconductor. Nat Protoc [Internet]. 2013 Sep 22;8(9):1765–86. Available from: http://www.nature.com/articles/nprot.2013.099

29. Bourgon R, Gentleman R, Huber W. Independent filtering increases detection power for high-throughput experiments. Proc Natl Acad Sci [Internet]. 2010 May 25;107(21):9546–51. Available from: http://www.pnas.org/cgi/doi/10.1073/pnas.0914005107

30. Ye J, Coulouris G, Zaretskaya I, Cutcutache I, Rozen S, Madden TL. Primer-BLAST : A tool to design target-specific primers for polymerase chain reaction. BMC Bioinformatics. 2012;13(134).

31. Schmittgen TD, Livak KJ. Analyzing real-time PCR data by the comparative Ct method. Nat Protoc. 2008;3(6):1101–8.

32. Coulson DTR, Brockbank S, Quinn JG, Murphy S, Ravid R, Brent GB, et al. Identification of valid reference genes for the normalization of RT qPCR gene expression data in human brain tissue. BMC Mol Biol. 2008;9:1–11.

33. Hegarty S V., Lee DJ, O'Keeffe GW, Sullivan AM. Effects of intracerebral neurotrophic factor application on motor symptoms in Parkinson's disease: A systematic review and meta-analysis. Park Relat Disord [Internet]. 2017;38:19–25. Available from: http://dx.doi.org/10.1016/j.parkreldis.2017.02.011

34. Kordower JH, Bjorklund A. Trophic Factor Gene Therapy for Parkinson's Disease. Mov Disord. 2013;28(1):96–109.

35. Paul G, Sullivan AM. Trophic factors for Parkinson's disease: Where are we and where do we go from here? Eur J Neurosci. 2019;49(4):440–52.

36. Staudt MD, Di Sebastiano AR, Xu H, Jog M, Schmid S, Foster P, et al. Advances in neurotrophic factor and cell-based therapies for Parkinson's disease: A mini-review. Gerontology. 2016;62(3):371–80.

37. Tenenbaum L, Humbert-Claude M. Glial Cell Line-Derived Neurotrophic Factor Gene Delivery in Parkinson's Disease: A Delicate Balance between Neuroprotection, Trophic Effects, and Unwanted Compensatory Mechanisms. Front Neuroanat [Internet]. 2017;11(April):1–12. Available from: http://journal.frontiersin.org/article/10.3389/fnana.2017.00029/full

38. Alves da Costa C, Checler F. Apoptosis in Parkinson's disease: Is p53 the missing link between genetic and sporadic Parkinsonism? Cell Signal [Internet]. 2011;23(6):963–8. Available from: http://dx.doi.org/10.1016/j.cellsig.2010.10.020

39. Gilmore TD. Introduction to NF-κB: Players, pathways, perspectives. Oncogene. 2006;25(51):6680–4.

40. Perkins ND. Integrating cell-signalling pathways with NF-κB and IKK function. Nat Rev Mol Cell Biol. 2007;8(1):49–62.

41. Masuda T, Tsuda M, Yoshinaga R, Tozaki-Saitoh H, Ozato K, Tamura T, et al. IRF8 Is a Critical Transcription Factor for Transforming Microglia into a Reactive Phenotype. Cell Rep [Internet]. 2012;1(4):334–40. Available from: http://dx.doi.org/10.1016/j.celrep.2012.02.014

42. Zhou N, Liu K, Sun Y, Cao Y, Yang J. Transcriptional mechanism of IRF8 and PU.1 governs microglial activation in neurodegenerative condition. Protein Cell. 2019;10(2):87–103.

43. Finneran DJ, Nash KR. Neuroinflammation and fractalkine signaling in Alzheimer's disease. J Neuroinflammation. 2019;16(1):1–8.

44. Landsman L, Liat BO, Zernecke A, Kim KW, Krauthgamer R, Shagdarsuren E, et al. CX3CR1 is required for monocyte homeostasis and atherogenesis by promoting cell survival. Blood. 2009;113(4):963–72.

45. Patel M, Coutinho C, Emsley HCA. Prevalence of radiological and clinical cerebrovascular disease in idiopathic Parkinson's disease. Clin Neurol Neurosurg [Internet]. 2011;113(10):830–4. Available from: http://dx.doi.org/10.1016/j.clineuro.2011.05.014

46. Zambito Marsala S, Gioulis M, Pistacchi M, Lo Cascio C. Parkinson's disease and cerebrovascular disease: is there a link? A neurosonological case–control study. Neurol Sci. 2016;37(10):1707–11.

47. Huang Y-P, Chen L, Yen M-F, Fann C, Chiu Y, Chen H-H, et al. Parkinson's Disease Is Related to an Increased Risk of Ischemic Stroke—A Population-Based Propensity Score-Matched Follow-Up Study. PLoS One [Internet]. 2013;8(9):e68314. Available from: http://dx.plos.org/10.1371/journal.pone.0068314

48. Li Q, Wang C, Tang H, Chen S, Ma J. Stroke and Coronary Artery Disease Are

Associated with Parkinson's Disease. Can J Neurol Sci. 2018;45(5):559–65.

49. Connell JRO, Stine OC, Wozniak MA. Genetics of early onset stroke (GEOS) study. J Stroke Cerebrovasc Dis. 2014;22(4):419–23.

50. Dawson S. The status of PAI-1 as a risk factor for arterial and thrombotic disease: a review. Atherosclerosis. 1992 Aug;95(2–3):105–17.

51. Kim KS, Choi YR, Park JY, Lee JH, Kim DK, Lee SJ, et al. Proteolytic cleavage of extracellular α-synuclein by plasmin: Implications for Parkinson disease. J Biol Chem. 2012;287(30):24862–72.

52. Gerenu G, Martisova E, Ferrero H, Carracedo M, Rantamäki T, Ramirez MJ, et al. Modulation of BDNF cleavage by plasminogen-activator inhibitor-1 contributes to Alzheimer's neuropathology and cognitive deficits. Biochim Biophys Acta - Mol Basis Dis. 2017;1863(4):991–1001.

53. Pelisch N, Dan T, Ichimura A, Sekiguchi H, Vaughan DE, Van Ypersele De Strihou C, et al. Plasminogen activator inhibitor-1 antagonist TM5484 attenuates demyelination and axonal degeneration in a mice model of multiple sclerosis. PLoS One. 2015;10(4):1–17.

54. Pan H, Zhao Y, Zhai Z, Zheng J, Zhou Y, Zhai Q, et al. Role of plasminogen activator inhibitor-1 in the diagnosis and prognosis of patients with Parkinson's disease. Exp Ther Med. 2018;15(6):5517–22.

55. Angelucci F, Čechová K, Průša R, Hort J. Amyloid beta soluble forms and plasminogen activation system in Alzheimer's disease: Consequences on extracellular maturation of brain-derived neurotrophic factor and therapeutic implications. CNS Neurosci Ther. 2019;25(3):303–13.

56. Savoy C, Van Lieshout RJ, Steiner M. Is plasminogen activator inhibitor-1 a physiological bottleneck bridging major depressive disorder and cardiovascular disease? Acta Physiol. 2017;219(4):715–27.

57. Tsai SJ. Role of tissue-type plasminogen activator and plasminogen activator inhibitor-1 in psychological stress and depression. Oncotarget. 2017;8(68):113258–68.

58. Gary KA, Sevarino KA, Yarbrough GG, Prange AJJ, Winokur A. The thyrotropin-releasing hormone (TRH) hypothesis of homeostatic regulation: implications for TRH-based therapeutics. J Pharmacol Exp Ther. 2003 May;305(2):410–6.

59. Cantuti-Castelvetri I, Hernandez LF, Keller-McGandy CE, Kett LR, Landy A, Hollingsworth ZR, et al. Levodopa-Induced Dyskinesia Is Associated with Increased Thyrotropin Releasing Hormone in the Dorsal Striatum of Hemi-Parkinsonian Rats. Cookson MR, editor. PLoS One [Internet]. 2010 Nov 10;5(11):e13861. Available from: https://dx.plos.org/10.1371/journal.pone.0013861

60. Otake K. Hypothalamic dysfunction in Parkinson's disease patients. Acta Med Hung. 1994;50(1–2):3–13.

61. Lestingi L, Bonifati V, Stocchi F, Antonozzi I, Meco G. TRH test and the continuous dopaminergic stimulation in complicated Parkinson's disease. Eur Neurol. 1992;32(2):65–9.

62. Kihara M, Kihara Y, Tukamoto T, Nishimura Y, Watanabe H, Hanakago R, et al. Assessment of sudomotor dysfunction in early Parkinson's disease. Eur Neurol. 1993;33(5):363–5.

63. Singh O, Pradhan DR, Nagalakashmi B, Kumar S, Mitra S, Sagarkar S, et al. Thyrotropin-releasing hormone (TRH) in the brain and pituitary of the teleost, Clarias batrachus and its role in regulation of hypophysiotropic dopamine neurons. J Comp Neurol. 2019;527(6):1070–101.

64. Faden AI, Movsesyan VA, Knoblach SM, Ahmed F, Cernak I. Neuroprotective effects of novel small peptides in vitro and after brain injury. Neuropharmacology. 2005 Sep;49(3):410–24.

65. Jaworska-Feil L, Jantas D, Leskiewicz M, Budziszewska B, Kubera M, Basta-Kaim A, et al. Protective effects of TRH and its analogues against various cytotoxic agents in retinoic acid (RA)-differentiated human neuroblastoma SH-SY5Y cells. Neuropeptides. 2010 Dec;44(6):495–508.

66. Luo L, Stopa EG. Thyrotropin releasing hormone inhibits tau phosphorylation by dual signaling pathways in hippocampal neurons. J Alzheimers Dis [Internet]. 2004 Oct;6(5):527–36. Available from: http://www.ncbi.nlm.nih.gov/pubmed/15505375

67. Zheng C, Chen G, Tan Y, Zeng W, Peng Q, Wang J, et al. TRH Analog, Taltirelin Improves Motor Function of Hemi-PD Rats Without Inducing Dyskinesia via Sustained Dopamine Stimulating Effect. Front Cell Neurosci. 2018;12(November):1–16.

68. Ogata A, Nagashima K, Yasui K, Matsuura T, Tashiro K. Sustained release dosage of thyrotropin-releasing hormone improves experimental Japanese encephalitis virus-induced parkinsonism in rats. J Neurol Sci. 1998 Aug;159(2):135–9.

69. Medeiros MS, Schumacher-Schuh A, Cardoso AM, Bochi GV, Baldissarelli J, Kegler A, et al. Iron and oxidative stress in Parkinson’s disease: An observational study of injury biomarkers. PLoS One. 2016;11(1):1–12.

70. Bonaccorsi di Patti MC, Cutone A, Polticelli F, Rosa L, Lepanto MS, Valenti P, et al. The ferroportin-ceruloplasmin system and the mammalian iron homeostasis machine: regulatory pathways and the role of lactoferrin. BioMetals [Internet]. 2018;31(3):399–414. Available from: https://doi.org/10.1007/s10534-018-0087-5

71. Grolez G, Moreau C, Sablonniere B, Garcon G, Devedjian J-C, Meguig S, et al. Ceruloplasmin activity and iron chelation treatment of patients with Parkinson’s disease. BMC Neurol. 2015 May;15:74.

72. Martin-Bastida A, Ward RJ, Newbould R, Piccini P, Sharp D, Kabba C, et al. Brain iron chelation by deferiprone in a phase 2 randomised double-blinded

placebo controlled clinical trial in Parkinson's disease. Sci Rep. 2017 May;7(1):1398.

73. Liu C, Liang MC, Soong TW. Nitric oxide, iron and neurodegeneration. Front Neurosci. 2019;13(FEB):1–10.

Chapter 4

4 Alternative splicing in the living Parkinson's disease brain: probing for novel events and the development of a random forest classifier

Background Parkinson's disease (PD) is a neurodegenerative disorder with a complex etiology involving genetic and environmental factors. Alternative splicing (AS) is a key regulatory mechanism that generates diverse protein isoforms from a single gene, and alterations in AS have been linked to neurodegenerative diseases. AS occurs rapidly *in vivo* and has not yet been investigated in the living PD brain in humans. Samples obtained from the frontal cortex of patients with PD during surgery for deep-brain stimulation offer an invaluable opportunity to study this highly dynamic process and should provide new insights into disease pathophysiology. **Methods** RNA sequencing was performed on frontal cortex tissue samples from six patients with PD and five controls to investigate AS. SpliceSeq and DEXSeq packages were used to identify differentially spliced genes using two different computational approaches . Four AS events were validated using quantitative real-time PCR. In addition, a random forest classifier was trained using a previously identified 370-gene differential expression signature to distinguish PD samples from controls in four publicly available datasets (postmortem brain tissue, laser-captured dopaminergic neurons, and blood samples). **Results** SpliceSeq identified 646 significant AS events in 505 genes, whereas DEXSeq detected 721 AS events in 571 genes. Only 10 genes with 14 AS events overlapped with differentially expressed genes identified in a previous study. Four validated AS events showed consistent changes in PD samples compared to controls. The random forest classifier trained on the 370-gene signature achieved moderate accuracy in classifying PD samples in all four public datasets, with area under the curve (AUC) values ranging from 0.667 to 0.875. **Conclusions** This study provides the first comprehensive analysis of AS events in the living PD brain, identifying several genes with altered splicing patterns. The trained random forest classifier based on the 370-gene signature showed promising performance in distinguishing PD samples from controls in different tissue types,

suggesting its potential as a diagnostic tool. Further research is required to investigate the functional consequences of these AS events and their role in PD pathogenesis.

4.1 Introduction

Considerable progress has been made in the last 30 years on the etiology of Parkinson's disease (PD) with the discovery of the causative genes LRRK2, SNCA, VPS35, Parkin, PINK1, and DJ-1. These monogenic causes of PD account for only 3-5% of cases, with an estimated 16-36% of disease risk explained collectively by approximately 90 risk variants, according to a recent meta-analysis of 17 genome-wide association studies.[1] Epigenetic factors impacting gene expression can also completely modify cellular function, although the underlying DNA may not be altered. Expression can be modulated directly by influencing promoter regions (i.e. downregulation by transcription factors), altering the accessibility of DNA for transcription through DNA methylation and splicing mechanisms such as nonsense-mediated decay. Alternative gene splicing(AS) is thought to occur in >95% of human protein-coding genes and is the primary mechanism through which an estimated four times as many proteins can be generated as there are genes.[2] The transcript diversity conferred by AS plays an essential role in organismal development and cellular differentiation, particularly in complex eukaryotes where it is thought to have played a role in evolution.[3] Alterations in the functioning of the complex machinery involved in posttranslational regulation of AS can lead to diseases such as cancer, muscular dystrophies, and neurodegenerative diseases.[4] Mutations resulting in aberrant splicing of messenger RNA, which lead to altered or non-functional proteins, have been described in PD -associated genes PINK1, Parkin, DJ-1, and GBA.[5–8]

In addition to genetic and epigenetic risk factors, environmental risks, including pesticide exposure, traumatic brain injury, diabetes, history of melanoma, and methamphetamine use, have been associated with an increased risk of PD.[9] With the wide range of genetic and environmental factors that lead to the development of PD, disease presentation and progression is unsurprisingly heterogeneous. Currently, the diagnosis of PD is clinical and relies on a battery of symptoms, namely the motor symptoms of bradykinesia, tremor, and rigidity. Nonmotor symptoms, including depression, anxiety, cognitive issues, apathy, autonomic dysfunction, and sleep disorders, are some of the earliest to present, causing major decreases in quality of life for individuals with PD.[10] In early PD (<5 years), it has been estimated that patients are diagnosed accurately just over 50% of the time, a troublingly low figure that underlines the need for better diagnostic and prognostic tools for PD.[11] A better understanding of the dynamic processes underpinning the development of PD, combined with advanced computational tools, could accelerate early diagnosis, perhaps pushing our ability to detect PD into early or prodromal stage disease.

To that end, we have previously applied next-generation sequencing (NGS) technology, RNA sequencing (RNA-Seq), to investigate gene expression in PD in cortical tissue obtained from living patients during planned surgical intervention to implant a DBS electrode. Utilizing this approach we identified a genetic profile comprising 370 differentially expressed genes (DEGs) compared to controls, 123 of which were unique and had not been previously reported.[12] The current study sought to apply modern computational tools to perform a comprehensive unbiased assessment of AS events in the PD frontal cortex using the previously acquired RNA-Seq data. Differential expression and alternative splicing are thought to occur independantly[13], therefore we hypothesize that AS analysis of the transcriptome found in the living brain will uncover a new layer of transcriptional dysregulation distinct from differential expression in PD. Building on the foundational work from our previous study on differential expression, we also used the previously identified 370-gene signature to develop a random forest classifier capable of distinguishing PD based on gene expression data. Random-forest classification is a supervised machine learning algorithm that subdivides data and builds multiple decisions trees using these subsets. These trees are then aggregated and used to predict an outcome, in this case whether the gene expression data submitted belonged to someone with PD or not. The expectation was that by utilizing the 370-gene profile, with 123 novel genes not identified in other gene expression profiling studies, our classifier would provide unique features that might reflect primarily the disease state changes rather than gene expression confounders that have plagued previous studies (e.g. late-stage disease, death, post-mortem processing intervals, etc.). Random forest classifiers also have the added benefit of providing some insight into which of its features, in this case genes, were most informative in the decision-making process. Recognizing that both classifier generalizability and clinically accessible biomarkers are essential, we also applied that classification strategy to four other publicly available datasets in blood , post-mortem cortex, and substantia nigra dopaminergic neurons. Together this work represents another important glimpse into the complex pathophysiology of this disorder, using tissue from the living PD brain as a window. The identification of alternative splicing events associated with PD, coupled with the continued refinement of gene expression-based diagnostic classifiers, has the potential to significantly advance both our understanding of the disease and our ability to detect and manage it in the clinic.

4.2 Methods

4.2.1 Tissue collection and RNA sequencing

Ethics approval for the study was obtained from the Research Ethics Board at Western University, and all patients provided informed consent for study participation. Tissue collection and sequencing were performed as previously described.[12] In brief, frontal cortex samples were obtained from patients with PD diagnosed on the basis of the UK Parkinson's Disease Society Brain Bank Clinical Diagnostic Criteria[14] and control samples were from patients undergoing resection of benign skullbase tumors with no radiological or intraoperative evidence of tumor invasion. After biopsy, tissue samples were immediately snap-frozen in liquid nitrogen and transferred to the laboratory for processing. Total RNA was extracted from individual brain biopsies and paired-end sequenced on the Illumina HiSeq 2500 platform to an average depth of approximately 90 million reads per sample, generating paired-end reads of 126 bases in length.

4.2.2 Splicing analysis using SpliceSeq and DEXSeq

Initial processing of raw RNA-Seq data was performed as previously described to generate quality-controlled transcript files in FASTQ format. These files were used as input for two distinct differential splicing software packages for initial pipeline comparison, SpliceSeq(v2.1)[15], and DEXseq(v.1.32.0).[16,17] SpliceSeq aligns reads to a preconstructed gene graph representing exons and splice sites, then calculates a delta percent spliced in (PSI) value that compares average PSI values for each group (PD vs. control) for a given feature and outputs a *p* value calculated using a two-tailed t-test of unequal variance on the PSI values of individual samples. DEXSeq identifies differentially retained introns and splicing junctions at the exon level using generalized linear models. Read count data were generated for DEXSeq with Ensembl gene annotation GRCh37 release 75 using htseq-count v.0.11.2 (HTSeq, http://www.huber.embl.de/users/anders/HTSeq/doc/overview.html). The Overlap of alternative splicing events identified by SpliceSeq and DEXseq was analyzed using the ggVennDiagram package (v.1.2.3) in R(v.4.3.3).

4.2.3 PCR validation of alternative splicing events

Four alternative splicing events were selected for validation using quantitative real-time polymerase chain reaction (qPCR). Custom primers for the AS site and an adjacent stably expressed sequence were designed using the NCBI Primer-Blast tool(Table S1).[18] cDNA was synthesized from RNA samples using the qScript cDNA synthesis kit (Quantabio, Beverly, MA, USA), and qPCR was performed with SYBR Green Master Mix (Bio-Rad, Mississauga, ON, Canada). 10µl reactions were run in triplicate in a 96-well plate following the manufacturer's protocol for 40 cycles of annealing and extension at a temperature between 55 °C and 60°C adjusted to the melting temperature of the primers. The average cycle threshold (Ct) values for each targeted splicing event and the adjacent unaltered site, normalized to glyceraldehyde 3-phosphate dehydrogenase, were determined by regression analysis (CFX Manager v.3.1, Bio-Rad) and relative AS fold change obtained using the comparative ΔΔCt method.[19,20] Correlation analysis between qPCR and RNA-Seq fold changes was performed using a linear model regression in the ggplot2 package(v. 3.5.0) in R(v. 4.3.3).

4.2.4 Random Forest analysis using differentially expressed gene signature

Bulk post-mortem Broadman Area 8 or 9 tissue (GSE68719[21] & GSE216281[22]), laser-capture microdissected midbrain dopaminergic neurons (GSE182622[23]) and blood (GSE165082[24]) datasets containing RNA-seq gene expression data with normalized counts were obtained from the GEO database for analysis and training of a random forest classifier. For the GSE216281 dataset only Braak stage V and VI samples were retained as cases to provide features consistent with later stage PD found in the other datasets. Feature counts from the 370 significant DEGs from our previous study were retained resulting in 312-370 features used for training each model, as some genes were not present in each dataset.[12] Data was then imported into R (v.4.3.3) and split randomly using rsample, but stratified to maintain the same proportion of control and PD samples in the test and training data. Test data comprised 10% of the dataset for studies with >40 samples or >5 in smaller datasets to retain sufficient samples for testing and reduce overfitting of the model to small samples. A cartesian grid search was then performed with randomForest (v.4.7-1.1) to determine the best performing hyperparameters (e.g. ntree, mtry, etc.) based on the smallest aggregate training and test error. Because of significant variation in data collection, determination of the best classifier parameters and training the RF model were performed separately for each study. Model accuracy was evaluated with retained test data for each study(see Table 4-2 for summary). ROC curves showing specificity and sensitivity of the trained classifier on test samples were generated using pROC[25](v.1.18.5). The area under the curve (AUC) of the ROCs was used to assess diagnostic power with values over 0.7 being considered acceptable.

4.3 Results

Our study included 11 participants, 6 patients with PD and 5 controls. RNA samples were isolated from the frontal cortex of individuals during planned surgical intervention.(for demographic and surgical details see[12]) Samples were sequenced at ~90 million reads per sample, sufficient depth to examine differential alternative splicing events (ASE). This study builds on our previous work highlighting a unique profile of 370 DEGs in the living brain and examines ASEs with DEXSeq and SpliceSeq. ASEs identified by each pipeline were compared to each other and SpliceSeq results compared to the DEGs from our previous study. Four randomly selected ASEs in genes formerly identified as DEGs were validated by qPCR. Using the unique DEG profile, we trained a random forest classifier to identify PD samples based on expression data and applied the same technique to RNA-seq data available publicly in the GEO database.

4.3.1 Alternative splicing events identified by multiple analysis pipelines in PD

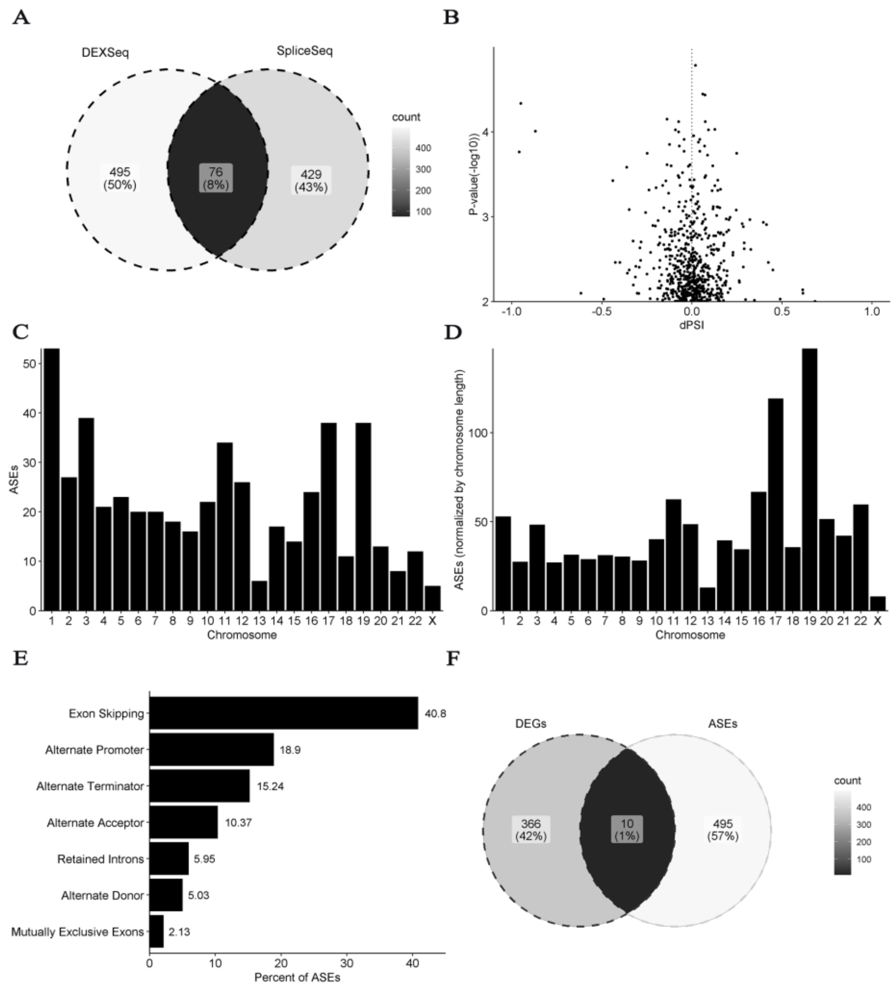

Figure 4-1 Differential alternative splicing events identified in the living PD frontal cortex

A) Venn diagram showing the intersection of genes with alternative splicing events as identified by SpliceSeq(505 genes) and DEXSeq (571 genes). SpliceSeq results B) as a Volcano plot of significant ASEs ($p < 0.01$), with dPSI on the x-axis and ASE significance on the y-axis. Counts of C) ASEs by chromosome and D) ASEs by chromosome normalized to length. E) Percentage of each type of ASE with nearly half being exon skipping events (40.8%). F) Overlap of genes with ASEs and 370 DEGs identified in previous work is less than 1% (10 total). Abbreviations: ASE, alternative splicing event; DEG, differentially expressed gene; dPSI, delta percent spliced in.

SpliceSeq identified 646 significant ASEs in 505 unique genes (p<0.01; Fig. 4-1, B; Supplementary Table 4-2) and DEXSeq detected 721 ASEs in 571 known genes (corrected p value<0.05; Supplementary Table 4-3). SpliceSeq and DEXSeq analyses had 76 genes in common representing 109 significant ASEs according to SpliceSeq (Fig. 4-1, A; Supplementary 4-4). SpliceSeq significant events spanned all chromosomes, with more observations of ASEs in chromosomes 1, 3, 11, 17, and 19, the last two particularly when normalized for chromosome length (Fig. 4-1, C-D). Of these, exon skipping was the most frequently observed at 40.8%, followed by alternate promoter (18.9%), alternate terminator (15.24%), alternate acceptor (10.37%), retained introns (5.95%), alternate donor (5.03%), and mutually exclusive exons (2.13%, Fig. 4-1, E). Seventeen significant ASEs identified by SpliceSeq had a dPSI greater than 0.2 and a magnitude - which represents the proportion of the overall reads occurring in the ASE region- greater than 0.8 (Table 4-1). Notable genes with ASEs include: three members of the CDC Like Kinase family(CLK1, CLK3 and CLK4), a family of protein kinases involved in the control of RNA splicing whose dysregulation has been linked to aberrant splicing in neurodegenerative diseases; glucosylceramidase beta 2 (GBA2), which encodes for a nonlysosomal enzyme functionally related to the glucocerebrosidase GBA, a major genetic risk factor for PD[26,27]; the epidermal growth factor receptor family members ErbB2 Receptor Tyrosine Kinase 2 and 3 (ERBB2/3), more commonly referred to as HER2 and HER3, which have been explored as predictive biomarkers for PD *in vitro*[28,29]; interferon regulatory factor 7 (IRF7) involved in neuroinflammatory processes; RELA, which codes the protein p65, a subunit of the NFκB complex involved in immune/inflammatory response and apoptosis; and septin 5 (SEPT5), a parkin substrate with growing evidence for a role in AD and PD pathogenesis.[30,31] Only 10 genes with 14 ASEs overlapped with DEGs from our previous study (Fig. 4-1, F; Supplementary Table 4-5).

Table 4-1 Significant alternative splicing events identified by SpliceSeq with a dPSI >0.2 and magnitude >0.8

Symbol	Gene Name	RPKM Controls	RPKM PD	Splice Type	Exons	dPSI	Magnitude	*P*-value
ADAMTS16	ADAM metallopeptidase with thrombospondin type 1 motif 16	0.29	0.31	AT	23	-0.23	0.91	2.64E-03
APOLD1	Apolipoprotein L domain containing 1	12.74	12.38	AT	4	-0.25	1	1.79E-04
APOLD1	Apolipoprotein L domain containing 1	12.74	12.38	AT	17	0.25	1	1.79E-04
CLK4	CDC like kinase 4	6.58	6.8	ES	2.3:3	-0.33	0.87	9.04E-04
FGF5	Fibroblast growth factor 5	0.37	0.35	ES	2	-0.22	0.85	1.27E-03
FOS	Fos proto-oncogene, AP-1 transcription factor subunit	2.96	6.61	RI	2.3	0.21	0.8	7.04E-03
HES2	Hes family bHLH transcription factor 2	0.01	0	AT	5	-0.62	0.8	7.95E-03
IRF7	Interferon regulatory factor 7	0.43	0.4	RI	2.4	-0.35	0.94	4.24E-03
IRF7	Interferon regulatory factor 7	0.43	0.4	ES	4	0.29	0.9	1.31E-03
POU2F2	POU class 2 homeobox 2	0.49	0.34	AA	5.1	0.35	1	9.67E-03
SLC26A6	Solute carrier family 26 member 6	0.92	0.93	AA	18.2	-0.36	0.81	2.61E-04
SLC43A1	Solute carrier family 43 member 1	0.42	0.4	ES	7:08	0.2	0.97	1.44E-03
ZGLP1	Zinc finger GATA like protein 1	0.93	0.93	RI	1.4	0.29	0.98	2.03E-03
ZNF222	Zinc finger protein 222	1.05	0.86	ES	2	-0.21	1	4.07E-03
ZNF449	Zinc finger protein 449	1.33	1.47	RI	2.2	0.26	0.96	5.93E-03
ZNF792	Zinc finger protein 792	0.16	0.15	AP	1	0.42	0.82	3.47E-03
ZNF837	Zinc finger protein 837	0.33	0.35	AD	2.2	0.26	1	5.67E-03

Abbreviations: AD, alternate donor; AP, alternate promoter; AT, alternate terminator; dPSI, delta percent spliced in; ES, exon skipping; RI, retained intron; RPKM, reads per kilobase of transcript per million aligned reads.

4.3.2 Quantitative PCR validation of ASEs

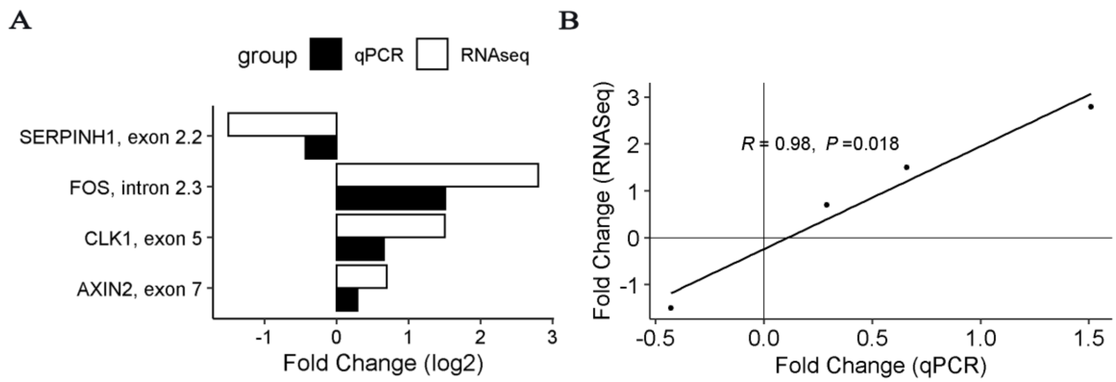

Figure 4-2 Validation of alternative splicing events using qPCR

A) Four ASEs in genes that were also identified as differentially expressed by RNA-seq were validated by qPCR. Corresponding fold changes with both techniques showed a B) strong linear relationship by correlation analysis (*R*=0.98, *p* =0.018) with a smaller fold change detected by qPCR across all queried ASEs.

Four ASEs were validated using qPCR: Serpin Family H Member 1 (SERPINH1), a serine proteinase inhibitor that plays a role in collagen biosynthesis; Fos Proto-Oncogene, AP-1 Transcription Factor Subunit (FOS), a transcription factor and immediate early gene involved in gene repression and activation in response to various cellular stimuli; CDC Like Kinase 1(CLK1), a kinase regulating gene splicing; and Axin 2 (AXIN2), an inhibitor of the Wnt signaling pathway. ASEs were selected from the 10 events that overlapped with DEGs in our previous study. Primers were designed to compare fold changes of the predicted splice sites against adjacent stably expressed sites (Supplementary Table 4-1). Of the four validated genes, three were exon skipping events, whereas one was an intron retention (FOS). At the splice sites for FOS, CLK1, and AXIN2, log2 fold changes were positive relative to the adjacent no-splice sites, indicating overexpression of the retained intron or exon in PD, consistent with the RNA-Seq findings. For SERPINH1, the fold change was negative, which was representative of increased exon skipping, as predicted. All qPCR results confirmed the RNA-seq ASE findings, albeit with more modest fold changes, and demonstrated a significant linear relationship between the results obtained using both techniques (Fig. 4-2).

4.3.3 Training a random forest classifier to identify PD signature in brain, neurons, and blood samples

Table 4-2 Random Forest classification datasets, model design, and results

Study	Tissue Type	Samples	Training data	Test data	Model features	Model Predicted Error (%)	Accuracy (%)
This Study	Frontal cortex	11	6	5	370	0	100.00
GSE68719	Post-mortem BA9 cortex	73	65	8	311	18.46	87.50
GSE216281	Post-mortem BA8/9 cortex	42	37	5	330	32.43	80.00
GSE182622	Laser-captured SN dopaminergic neurons	192	172	20	331	27.91	80.00
GSE165082	Blood	26	20	6	350	35.00	66.67

Abbreviations: BA, Broadman area; SN, substantia nigra

Our RNA-seq gene expression data and four datasets available from the Gene Expression Omnibus database (GSE68719, GSE216281, GSE182622, GSE165082, see Table 4-2 and methods for more details) were selected to train a random forest (RF) classifier to distinguish PD samples from Controls based on a gene expression signature. Datasets were first filtered to include only genes from the 370 genes found to be significantly differentially expressed in our previous study, resulting in between 312 and 370 training features per model. Data were then subdivided into training and test data, retaining 10%

of the data for datasets with more than 40 samples or at least 5 samples for the smaller datasets (This study and GSE165082).

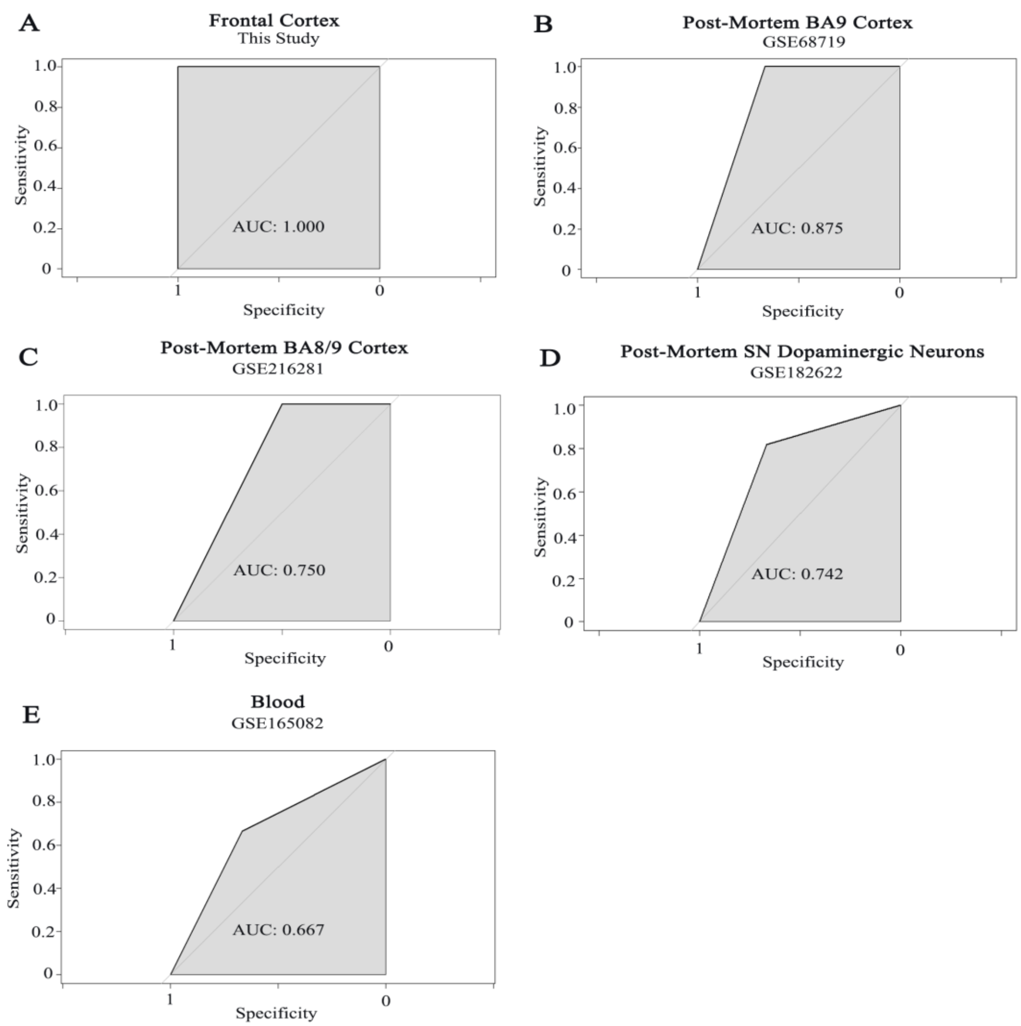

Figure 4-3 Receiver operating characteristic curves (ROC) of Random Forest classifier in the analyzed datasets

ROC analysis of a random forest classifier applied to public transcriptomic data corresponding to our 370-gene DEG profile in A) our data from the living frontal cortex, B) BA9 postmortem bulk tissue, C) BA8/9 postmortem bulk tissue, C) postmortem laser microdissected dopaminergic neurons from the substantia nigra, and D) blood samples from patients with PD and controls. Specificity is represented on the x-axis, and sensitivity is plotted on the y-axis. The area under the curve (AUC) value represents the predictive power of the model with a score ranging from 0 (no specificity or sensitivity) to 1 (perfect classifier). Abbreviations: BA, Broadman Area

As expected, because feature selection was guided by the gene signature from our data, the model predicted error for data from this study was 0% and the test set accuracy was 100%. For GSE68719 and GSE216281, both studies of postmortem frontal cortex samples, model predicted errors were 18.46% and 32.43%. The Accuracy of predictions in the test samples was 87.50% and 80.00%. The Predicted error in substantia nigra dopaminergic neurons captured by laser microdissection (GSE182622) was 27.91% with an accuracy of 80.00% and in blood samples(GSE165082) predicted error was 35.00% with an accuracy of 66.67%. ROC curves, where the sensitivity or true positive rate is plotted on the y-axis and the specificity or false positive rate is plotted on the x-axis, were used to further evaluate the models. Values above 0.5 are better than chance, with classifiers scoring above 0.7 considered acceptable.[32] The resulting area under the curve (AUC) metric for the classifiers using ROC analysis were all above 0.7, except for the blood dataset with a value of 0.667 (Fig. 4-3).

4.4 Discussion

4.4.1 Role of alternative splicing in Parkinson's disease

In this study, we investigated alternative splicing events in cortical brain samples from living patients with Parkinson's disease using RNA-seq. Building on our previous work examining gene expression in rapidly frozen fresh brain tissue from the prefrontal cortex obtained during routine DBS surgery, this study exhibits many of the same strengths. As the first of its kind study, it offers the following benefits: (1) safe sampling of a brain region known to be affected by PD in living patients, (2) avoiding the challenges associated with cadaveric brain transcriptome studies and formalin fixation[33], (3) obtaining samples not influenced by late-stage disease, death, and the related degeneration and inflammatory changes that may dwarf disease pathogenesis[34], and (4) offering an acceptable mix of accessibility and proximity to disease process circumventing the signal-to-noise issues seen in peripheral tissue sources.[35] Furthermore, with brain cells exhibiting pervasive alternative splicing relative to other tissues[36–38], identification of ASEs in the frontal cortex of living patients provides a broader snapshot of the highly dynamic transcriptomic landscape in PD. Interestingly, our study revealed that alternative splicing events largely occurred in genes that were not previously identified in the same samples as differentially expressed. Although related, alternative splicing and gene expression are thought to be largely independent processes.[13] The results from our analysis with SpliceSeq indicate that less than 1% of the genes identified previously as significantly DEGs also had differential alternative splicing in PD (Fig. 4-1F, Supplementary Table 4-5). This observation underlines the importance of examining alternative splicing events for a comprehensive view of the molecular alterations involved in Parkinson's disease, which may not be captured by traditional differential expression analysis alone.

Dysregulated alternative splicing has been implicated in various neurodegenerative disorders, including PD[39,40]. This study identified several genes related to PD with significant ASEs including: CLK 1,3 and 4; GBA2; ERBB2 and ERBB3; and RELA. The CDC-like kinases figured prominently with three of the four family members identified by SpliceSeq(CLK1 and CLK4 were also significant with DEXSeq). CLK1 reportedly plays an important role in dopaminergic neuron survival shown both in vitro and in an animal model of PD with CLK-1$^{+/-}$ mice.[26,27] The authors proposed that CLK1 was protective by regulating autophagy and modulating microglia-mediated neuroinflammation. Here, CLK1 showed increased use of an alternate promoter in exon 1 (dPSI 0.086, magnitude 0.31, *p*= 7.07E-03) and skipping of exon 5 in PD samples(dPSI 0.408, magnitude 0.40, *p*=5.57E-05). GBA2, the nonlysosomal counterpart to GBA1(the well-known genetic risk factor for PD), exhibited decreased retention of intron 14.5 (dPSI 0.058, magnitude 0.97, *p*= 0.0067). Despite being discovered in 1992, little is known about the amino acid sequence, structure, and posttranslational state of GBA2, making interpretation of this retained intron difficult.[41] However, GBA2 loss-of-function mutations have been found in several neurological disorders.[42–44] In addition, decreased levels of GBA2 in induced pluripotent stem cells from patients with PD with GBA1 mutations, despite no change in gene expression, suggest a role for altered splicing of GBA2 in PD.[45] ErbB signaling, mediated by human epidermal growth factor family receptors including ERBB2 and ERBB3, is important for the maintenance and development of the central nervous system. For ERBB2, exon 5 was skipped (dPSI -0.131, magnitude 0.36, *p*=0.005), whereas ERBB3 had an alternate promoter ASE in exon 24.1 with a more modest effect (dPSI -0.047, magnitude 0.07, *p*=0.002). ERBB2s exon 5 translates a growth factor receptor domain involved in signal transduction by receptor tyrosine kinases. Further research is needed to determine the impact of exon 5 omission on signal transduction. Disruption of ErbB neurotrophin signaling has previously been highlighted in postmortem PD brain samples and in the 6-hydroxydopamine rat model of PD.[46] This 2005 study reported a significant decrease in ErbB1 and ErbB2 protein levels and its ligand EGF in brain homogenates from the prefrontal cortex and striatum. Perhaps altered splicing, as observed in our study, leads to nonsense-mediated mRNA decay in PD, resulting in diminished levels of functional ERBB receptors. RELA encodes the p65 protein, a subunit of the NFκB transcription factor complex. The NFκB complex plays an important role in cell proliferation and differentiation, and more importantly in the context of PD, inflammation, immune response, and apoptosis.[47] Interestingly, we observed increased retention of intron 10.2 (dPSI 0.086, magnitude 0.87 and p=0.008), which was the same retention observed in PD with dementia by Henderson-Smith and colleagues.[48] They predicted that this retained intron would result in the overproduction of a truncated inactive protein. Further investigations are warranted to explore the functional consequences of the identified alternative splicing events in Parkinson's disease. Elucidating the specific roles of these splicing events in disease pathogenesis may provide new therapeutic targets or biomarkers.

4.4.2 Machine learning models as diagnostic tools for Parkinson's disease

The application of machine learning techniques to genomic data shows great promise in the field of Parkinson's disease research. High-throughput sequencing technologies have been available for two decades and produce rich genetic and transcriptomic data with increased speed, accuracy, and lower cost than ever possible.[49] Multiple repositories have also been created with transcriptomic data, including GEO[50], ArrayExpress[51] and the PD specific ParkDB[52], rendering training of classifiers on large transcriptomic datasets far more feasible. In the literature, machine learning approaches have already been applied to classification in PD, using voice recordings, movement data, handwriting and imaging data, or a combination of features to distinguish known PD patients from healthy controls with high accuracy.[53]

The choice was made to use a random forest (RF) classifier based on its reported robustness, resistance to noise and overfitting relative to other machine learning algorithms, high accuracy in classification tasks - including gene expression data classification[54] - and ability to identify key genes through feature importance. Using the 370 significant DEGs we had previously identified as training features, our random forest classifier was able to consistently distinguish between Parkinson's disease patients and healthy individuals, with AUC values from ROC analysis of 0.742 or above in all but the blood transcriptome datasets(Figure 4-3). Comparison of these results with the literature is not straightforward because our classifier was trained using gene expression signature data from the brain, whereas the blood transcriptome has primarily been studied because of improved access. The correlation between the blood and brain transcriptome has been estimated to be between 0.25 and 0.64, depending on the study.[55] Pantaleo et al. recently conducted a large-scale study on whole blood transcriptome in 390 early-onset PD samples, before the initiation of dopaminergic therapy, and 189 age-matched healthy controls.[56] They used a combination of differential expression analysis and a random forest classification algorithm to select 493 genes as training features and with an XGBoost classification algorithm achieved a comparable AUC of 0.72. Another large cohort study of 205 idiopathic PD samples and 233 healthy controls, using expression data obtained from the analysis of blood samples by microarray, used 100 features and a support vector machine algorithm. This strategy achieved an AUC of 0.79 in a validation set of 75 samples and 0.74 in an independent test set of 70 samples. Their signature and SVM method were also able to distinguish between PD and combined samples of healthy controls and 48 samples from a variety of non-PD neurodegenerative disease samples, including Huntington's disease, multiple system atrophy, and corticobasal degeneration. Comparatively, our RF classifier using the 370 DEG signature performed at a similar level with AUC values ranging from 0.667 to 1, showing robustness across multiple types of brain samples and blood.

4.4.3 Considerations and future directions

While informative, as a proof-of-concept study, the insights gained from analyzing 11 samples are insufficient both (a) to generalize our findings of alternative splicing more broadly and to determine any functional consequences without further studies and (b) to provide sufficient power to train a machine learning classifier capable of performing reproducibly across sites, heterogeneous genetic backgrounds, and varying sample preparation methods, among others. This is an ongoing challenge for the field of PD research and one acknowledged in other fields as well.[57,58] This challenge was visible in the results obtained in the same samples analyzed by the two analysis methods we initially used (DEXSeq, SpliceSeq), which only shared 76 genes or 8% of genes (Fig. 4-1, A). Ideally, for both alternative splicing and the purposes of developing clinically relevant and accurate diagnostic tools, using larger datasets or aggregating data from many sources would overcome many of the challenges presented. Issues such as low quality input samples, different library preparation methods, and analysis pipelines could be lessened by incorporating diverse patient cohorts and a better cross-section of the heterogeneous PD patient population.[59] Furthermore, the incorporation of multiomics data, including epigenomics and proteomics, would enhance our understanding of PD and, in the case of classification, could improve accuracy and predictive power.

4.5 Conclusions

In conclusion, although alternative splicing occurs as a gene regulation mechanism under normal conditions, our study highlights novel alternative splicing events in the living cortex of patients with Parkinson’s disease with consistently altered function that could be a result of the disease state. Alternatively, the identified aberrant transcripts could have a more direct impact on the functioning of downstream pathways directly contributing to disease onset or progression. The identification of alternative splicing events in genes distinct from differentially expressed genes also suggests a unique role for this regulatory mechanism in the disease. Furthermore, the successful application of machine learning classification to identify PD, using RNA-seq data guided by transcriptomic alterations from the living brain, demonstrates a new strategy that could aid in disease diagnosis and stratification. Continued research in this direction has the potential to uncover novel insights into the molecular mechanisms underlying Parkinson's disease and may facilitate the development of targeted therapeutic strategies.

4.6 References

1. Nalls MA, Blauwendraat C, Vallerga CL, et al. Identification of novel risk loci, causal insights, and heritable risk for Parkinson's disease: a meta-analysis of genome-wide association studies. *Lancet Neurol*. 2019;18(12):1091-1102. doi:10.1016/S1474-4422(19)30320-5

2. Gámez-Valero A, Beyer K. Alternative splicing of alpha- and beta-synuclein genes plays differential roles in synucleinopathies. *Genes (Basel)*. 2018;9(2). doi:10.3390/genes9020063

3. Lareau LF, Green RE, Bhatnagar RS, Brenner SE. The evolving roles of alternative splicing. *Curr Opin Struct Biol*. 2004;14(3):273-282. doi:10.1016/j.sbi.2004.05.002

4. Montes M, Sanford BL, Comiskey DF, Chandler DS. RNA Splicing and Disease : Animal Models to Therapies. *Trends Genet*. 2019;35(1):68-87. doi:10.1016/j.tig.2018.10.002

5. Asselta R, Rimoldi V, Siri C, et al. Glucocerebrosidase mutations in primary parkinsonism. *Parkinsonism Relat Disord*. 2014;20(11):1215. doi:10.1016/J.PARKRELDIS.2014.09.003

6. Bras JM, Guerreiro RJ, Teo JTH, et al. Atypical Parkinsonism-Dystonia Syndrome Caused by a Novel DJ1 Mutation. *Mov Disord Clin Pract*. 2014;1(1):45. doi:10.1002/MDC3.12008

7. Ghazavi F, Fazlali Z, Banihosseini SS, et al. PRKN, DJ-1, and PINK1 screening identifies novel splice site mutation in PRKN and two novel DJ-1 mutations. *Mov Disord*. 2011;26(1):80-89. doi:10.1002/mds.23417

8. Samaranch L, Lorenzo-Betancor O, Arbelo JM, et al. PINK1-linked parkinsonism is associated with Lewy body pathology. *Brain*. 2010;133(4):1128-1142. doi:10.1093/BRAIN/AWQ051

9. Ascherio A, Schwarzschild MA. The epidemiology of Parkinson’s disease: risk factors and prevention. *Lancet Neurol*. 2016;15(12):1257-1272. doi:10.1016/S1474-4422(16)30230-7

10. Barone P, Antonini A, Colosimo C, et al. The PRIAMO study: A multicenter assessment of nonmotor symptoms and their impact on quality of life in Parkinson’s disease. *Mov Disord*. 2009;24(11):1641-1649. doi:https://doi.org/10.1002/mds.22643

11. Adler CH, Beach TG, Shill HA, et al. Low clinical diagnostic accuracy of early vs advanced Parkinson disease. *Neurology*. 2014;83(83):406-412. www.brainandbodydonationprogram.org

12. Benoit SM, Xu H, Schmid S, et al. Expanding the search for genetic biomarkers of Parkinson’s disease into the living brain. *Neurobiol Dis*. 2020;140:104872. doi:10.1016/j.nbd.2020.104872

13. Merkin J, Russell C, Chen P, Burge CB. Evolutionary Dynamics of Gene and Isoform Regulation in Mammalian Tissues. *Science (80-)*. 2012;338(6114):1593-1599. doi:10.1126/science.1228186

14. Hughes AJ, Daniel SE, Kilford L, Lees AJ. Accuracy of clinical diagnosis of idiopathic Parkinson’s disease: a clinico-pathological study of 100 cases. *J Neurol Neurosurg Psychiatry*. 1992;55:181-184.

15. Ryan MC, Cleland J, Kim RG, Wong WC, Weinstein JN. SpliceSeq: A resource for analysis and visualization of RNA-Seq data on alternative splicing and its functional impacts. *Bioinformatics*. 2012;28(18):2385-2387. doi:10.1093/bioinformatics/bts452

16. Anders S, Reyes A, Huber W. Detecting differential usage of exons from RNA-seq data. *Genome Res*. 2012;22(10):2008-2017. doi:10.1101/gr.133744.111

17. Reyes A, Anders S, Weatheritt RJ, Gibson TJ, Steinmetz LM, Huber W. Drift and conservation of differential exon usage across tissues in primate species. *Proc Natl*

Acad Sci U S A. 2013;110(38):15377-15382. doi:10.1073/pnas.1307202110

18. Ye J, Coulouris G, Zaretskaya I, Cutcutache I, Rozen S, Madden TL. Primer-BLAST : A tool to design target-specific primers for polymerase chain reaction. *BMC Bioinformatics*. 2012;13(134).

19. Coulson DTR, Brockbank S, Quinn JG, et al. Identification of valid reference genes for the normalization of RT qPCR gene expression data in human brain tissue. *BMC Mol Biol*. 2008;9:1-11. doi:10.1186/1471-2199-9-46

20. Schmittgen TD, Livak KJ. Analyzing real-time PCR data by the comparative Ct method. *Nat Protoc*. 2008;3(6):1101-1108.

21. Dumitriu A, Golji J, Labadorf AT, et al. Integrative analyses of proteomics and RNA transcriptomics implicate mitochondrial processes, protein folding pathways and GWAS loci in Parkinson disease. *BMC Med Genomics*. 2016;9(1):1-17. doi:10.1186/s12920-016-0164-y

22. Cappelletti C, Henriksen SP, Geut H, et al. Transcriptomic profiling of Parkinson's disease brains reveals disease stage specific gene expression changes. *Acta Neuropathol*. 2023;146(2):227-244. doi:10.1007/s00401-023-02597-7

23. Tiklová K, Gillberg L, Volakakis N, et al. Disease Duration Influences Gene Expression in Neuromelanin-Positive Cells From Parkinson's Disease Patients. *Front Mol Neurosci*. 2021;14(November):1-12. doi:10.3389/fnmol.2021.763777

24. Henderson AR, Wang Q, Meechoovet B, et al. DNA Methylation and Expression Profiles of Whole Blood in Parkinson's Disease. *Front Genet*. 2021;12(April):1-17. doi:10.3389/fgene.2021.640266

25. Turck N, Vutskits L, Sanchez-Pena P, et al. pROC: an open-source package for R and S+ to analyze and compare ROC curves. *BMC Bioinformatics*. 2011;8:12-77. http://link.springer.com/10.1007/s00134-009-1641-y

26. Gu R, Zhang F, Chen G, et al. Clk1 deficiency promotes neuroinflammation and

subsequent dopaminergic cell death through regulation of microglial metabolic reprogramming. *Brain Behav Immun*. 2017;60:206-219. doi:10.1016/j.bbi.2016.10.018

27. Yan Q, Han C, Wang G, Waddington JL, Zheng L, Zhen X. Activation of AMPK/mTORC1-mediated autophagy by metformin reverses Clk1 deficiency-sensitized dopaminergic neuronal death. *Mol Pharmacol*. 2017;92(6):640-652. doi:10.1124/mol.117.109512

28. Jin M, Shi R, Gao D, et al. ErbB2pY-1248 as a predictive biomarker for Parkinson's disease based on research with RPPA technology and in vivo verification. *CNS Neurosci Ther*. 2024;30(2):1-12. doi:10.1111/cns.14407

29. Wang V, Chuang TC, Kao MC, Shan DE, Soong BW, Shieh TM. Polymorphic Ala-allele carriers at residue 1170 of HER2 associated with Parkinson's disease. *J Neurol Sci*. 2013;325(1-2):115-119. doi:10.1016/j.jns.2012.12.017

30. Son JH, Kawamata H, Yoo MS, et al. Neurotoxicity and behavioral deficits associated with Septin 5 accumulation in dopaminergic neurons. *J Neurochem*. 2005;94(4):1040-1053. doi:10.1111/j.1471-4159.2005.03257.x

31. Marttinen M, Kurkinen KM, Soininen H, Haapasalo A, Hiltunen M. Synaptic dysfunction and septin protein family members in neurodegenerative diseases. *Mol Neurodegener*. 2015;10(1):1-12. doi:10.1186/s13024-015-0013-z

32. Mandrekar JN. Receiver operating characteristic curve in diagnostic test assessment. *J Thorac Oncol*. 2010;5(9):1315-1316. doi:10.1097/JTO.0b013e3181ec173d

33. David LE, Fowler CB, Cunningham BR, Mason JT, O'Leary TJ. The effect of formaldehyde fixation on RNA: Optimization of formaldehyde adduct removal. *J Mol Diagnostics*. 2011;13(3):282-288. doi:10.1016/j.jmoldx.2011.01.010

34. Franz H, Ullmann C, Becker A, et al. Systematic analysis of gene expression in human brains before and after death. *Genome Biol*. 2005;6(13):1-9.

doi:10.1186/gb-2005-6-13-r112

35. Prieto C, Risueño A, Fontanillo C, De Las Rivas J. Human gene coexpression landscape: Confident network derived from tissue transcriptomic profiles. *PLoS One*. 2008;3(12). doi:10.1371/journal.pone.0003911

36. Porter RS, Jaamour F, Iwase S. Neuron-specific alternative splicing of transcriptional machineries: Implications for neurodevelopmental disorders. *Mol Cell Neurosci*. 2018;87(October 2017):35-45. doi:10.1016/j.mcn.2017.10.006

37. Yeo G, Holste D, Kreiman G, Burge CB. Variation in alternative splicing across human tissues. *Genome Biol*. 2004;5(10):1-15. doi:10.1186/gb-2004-5-10-r74

38. Pan Q, Shai O, Lee LJ, Frey BJ, Blencowe BJ. Deep surveying of alternative splicing complexity in the human transcriptome by high-throughput sequencing. *Nat Genet*. 2008;40(12):1413-1415. doi:10.1038/ng.259

39. Fu RH, Liu SP, Huang SJ, et al. Aberrant alternative splicing events in Parkinson's disease. *Cell Transplant*. 2013;22(4):653-661. doi:10.3727/096368912X655154

40. Soreq L, Bergman H, Israel Z, Soreq H. Exon arrays reveal alternative splicing aberrations in Parkinson's disease leukocytes. *Neurodegener Dis*. 2012;10(1-4):203-206. doi:10.1159/000332598

41. Massimo A, Maura S, Nicoletta L, et al. Current and novel aspects on the non-lysosomal β-glucosylceramidase GBA2. *Neurochem Res*. 2016;41(1-2):210-220. doi:10.1007/s11064-015-1763-2

42. Citterio A, Arnoldi A, Panzeri E, et al. Mutations in CYP2U1, DDHD2 and GBA2 genes are rare causes of complicated forms of hereditary spastic paraparesis. *J Neurol*. 2014;261(2):373-381. doi:10.1007/s00415-013-7206-6

43. Hammer MB, Eleuch-Fayache G, Schottlaender L V, et al. Mutations in GBA2 cause autosomal-recessive cerebellar ataxia with spasticity. *Am J Hum Genet*. 2013;92(2):245-251. doi:10.1016/j.ajhg.2012.12.012

44. Sultana S, Reichbauer J, Schüle R, Mochel F, Synofzik M, Van Der Spoel AC. Lack of enzyme activity in GBA2 mutants associated with hereditary spastic paraplegia/cerebellar ataxia (SPG46). *Biochem Biophys Res Commun*. 2015;465(1):35-40. doi:10.1016/j.bbrc.2015.07.112

45. Schöndorf DC, Aureli M, McAllister FE, et al. iPSC-derived neurons from GBA1-associated Parkinson’s disease patients show autophagic defects and impaired calcium homeostasis. *Nat Commun*. 2014;5:4028. doi:10.1038/ncomms5028

46. Iwakura Y, Piao YS, Mizuno M, et al. Influences of dopaminergic lesion on epidermal growth factor-ErbB signals in Parkinson’s disease and its model: Neurotrophic implication in nigrostriatal neurons. *J Neurochem*. 2005;93(4):974-983. doi:10.1111/j.1471-4159.2005.03073.x

47. Gilmore TD. Introduction to NF-κB: Players, pathways, perspectives. *Oncogene*. 2006;25(51):6680-6684. doi:10.1038/sj.onc.1209954

48. Henderson-Smith A, Corneveaux JJ, De Both M, et al. Next-generation profiling to identify the molecular etiology of Parkinson dementia. *Neurol Genet*. 2016;2(3). doi:10.1212/NXG.0000000000000075

49. Goodwin S, McPherson JD, McCombie WR. Coming of age: Ten years of next-generation sequencing technologies. *Nat Rev Genet*. 2016;17(6):333-351. doi:10.1038/nrg.2016.49

50. Edgar R, Domrachev M, Lash AE. Gene Expression Omnibus: NCBI gene expression and hybridization array data repository. *Nucleic Acids Res*. 2002;30(1):207-210. doi:10.1093/nar/30.1.207

51. Parkinson H, Sarkans U, Shojatalab M, et al. ArrayExpress - A public repository for microarray gene expression data at the EBI. *Nucleic Acids Res*. 2005;33(DATABASE ISS.):553-555. doi:10.1093/nar/gki056

52. Taccioli C, Maselli V, Tegnér J, et al. ParkDB: A Parkinson’s disease gene expression database. *Database*. 2011;2011:1-6. doi:10.1093/database/bar007

53. Mei J, Desrosiers C, Frasnelli J. Machine Learning for the Diagnosis of Parkinson's Disease: A Review of Literature. *Front Aging Neurosci*. 2021;13(May):1-41. doi:10.3389/fnagi.2021.633752

54. Chicco D, Oneto L. An Enhanced Random Forests Approach to Predict Heart Failure from Small Imbalanced Gene Expression Data. *IEEE/ACM Trans Comput Biol Bioinforma*. 2021;18(6):2759-2765. doi:10.1109/TCBB.2020.3041527

55. Tylee DS, Kawaguchi DM, Glatt SJ. On the outside, looking in: A review and evaluation of the comparability of blood and brain "-omes." *Am J Med Genet Part B Neuropsychiatr Genet*. 2013;162(7):595-603. doi:10.1002/ajmg.b.32150

56. Pantaleo E, Monaco A, Amoroso N, et al. A Machine Learning Approach to Parkinson's Disease Blood Transcriptomics. *Genes (Basel)*. 2022;13(5):727. doi:10.3390/genes13050727

57. Zhang L, Li S, Hao C, et al. Extracting a few functionally reproducible biomarkers to build robust subnetwork-based classifiers for the diagnosis of cancer. *Gene*. 2013;526(2):232-238. doi:10.1016/j.gene.2013.05.011

58. Samper-González J, Burgos N, Bottani S, et al. Reproducible evaluation of classification methods in Alzheimer's disease: Framework and application to MRI and PET data. *Neuroimage*. 2018;183(March):504-521. doi:10.1016/j.neuroimage.2018.08.042

59. Holik AZ, Law CW, Liu R, et al. RNA-seq mixology: Designing realistic control experiments to compare protocols and analysis methods. *Nucleic Acids Res*. 2017;45(5). doi:10.1093/nar/gkw1063

5 Summary and Future Work

This thesis investigated the potential of cortical tissue obtained during deep brain stimulation surgery in patients with Parkinson's disease (PD) patients as a therapeutic and research tool. Chapter 2 established a rodent model to evaluate brain-derived progenitor cells (BDPCs) as a possible autologous cell therapy, demonstrating their derivation, survival and tracking after brain implantation. Chapter 3 used RNA-seq to analyze gene expression changes in the living PD cortex for the first time, revealing novel dysregulated pathways. Building on this, Chapter 4 identified alternative splicing events in PD and developed a machine learning classifier to identify the genetic signature of PD in brain, neuron, and blood samples.

5.1 Discussion and Conclusions

Together, this thesis demonstrates that valuable insights can be gained from accessing living PD brain tissue, opening new avenues for understanding disease mechanisms and developing diagnostic tools and cell-based therapies.

5.1.1 Chapter 2 - Establishing a rodent syngeneic graft model to examine the potential of novel cell-based therapeutics for Parkinson’s disease

Chapter 2 describes the establishment of a rodent syngeneic graft model to examine the potential of brain-derived progenitor cells (BDPCs) as a cell-based therapeutic for Parkinson's disease. The study was designed with the aim of generating and implanting rat BDPCs into the striatum of syngeneic Fischer rats to approximate the intended use of human BDPCs as an autologous cell-based therapy for PD. Cellular engineering of those BDPCs to express luciferase afforded the opportunity for tracking the cell graft longitudinally *in vivo* using BLI. The key findings in this chapter were:

1. Rodent BDPCs displayed similar characteristics to their human counterparts, including expression of neural progenitor and oligodendrocyte markers, and electrophysiological properties akin to neural progenitor cells or immature neurons.

2. Rodent BDPCs endogenously expressed and secreted important neurotrophic factors, suggesting they could provide trophic support to the diseased brain.

3. Engineered rodent BDPCs could be readily tracked in vivo using bioluminescence imaging after transplantation into a syngeneic rat model, demonstrating survival and engraftment after 5 weeks.

These findings indicate that BDPCs derived from rat brain possess comparable desirable properties for use as a cell-based therapy as human BDPCs derived from cortical tissue, including the ability to survive, integrate, and potentially provide neuroprotective support when transplanted. The ability to engineer these cells for BLI is particularly valuable, as it allows for non-invasive monitoring of graft survival and migration over time. The establishment of this rodent syngeneic graft model provides an important preclinical platform to further evaluate the therapeutic potential of autologous BDPCs, with broader implications for understanding disease mechanisms and developing personalized cell-based interventions for PD patients.

5.1.2 Chapter 3 - Expanding the search for genetic biomarkers of Parkinson's disease into the living brain

Chapter 3 of the thesis describes the use of RNA-seq to expand the search for genetic biomarkers of Parkinson's disease by analyzing gene expression changes in the living cortical tissue of patients with PD. This is the first study to perform gene expression analysis on cortical tissue biopsied directly from living PD patients during deep brain stimulation surgery, rather than relying on postmortem brain samples or peripheral tissues. This provided an unprecedented opportunity to interrogate the transcriptional landscape of the diseased brain *in vivo*, overcoming limitations of prior studies that had to make inferences about central nervous system changes based on more accessible samples. The key findings reported in this chapter were:

1. Differential gene expression analysis identified a set of 370 altered genes in patients with PD.

2. Differentially expressed genes were associated with pathways with known associations to PD including trophic factor signaling, apoptosis, inflammation, coagulation, and neuroendocrine function.

3. Our comparative analysis revealed very few consistent DEGs in the 7 RNA-Seq studies at the time of publication and gene expression changes in 123 DEGs never previously reported in other PD transcriptome studies.

These findings provide important new insights into the molecular changes occurring within the living PD brain. The identification of differentially expressed genes related to trophic factor signaling, inflammation, and other key biological processes suggests potential new avenues for understanding disease mechanisms and developing targeted therapies. The discovery that 123 of the DEGs were unique to the living brain and that consistent changes in any gene across the literature were nearly non-existent, underscored the importance of examining the living brain using an unbiased approach in the continued search for clinically relevant biomarkers and therapeutic targets. The ability to directly interrogate gene expression in the living PD brain represents a significant advance over prior work, overcoming the limitations of using postmortem samples or peripheral tissues to infer central nervous system changes. This chapter laid the groundwork for the next experiments to examine the role of alternative splicing in PD and to determine the value of the DEG signature we discovered for training a machine learning based diagnostic tool.

5.1.3 Chapter 4 - Alternative splicing in the living Parkinson's disease brain: probing for novel events and the development of a random forest classifier

Chapter 4 builds upon the gene expression analysis in Chapter 3 further expanding knowledge of the transcriptome in the living brain and taking steps towards the development of diagnostic tools for PD. Our approach moved beyond simply examining differential gene expression to also probe for changes in alternative splicing - a critical and understudied layer of transcriptional regulation that can have profound impacts on protein function and disease pathogenesis. Additionally, we leveraged the PD-associated gene expression signature identified in the previous chapter to train a machine learning model capable of discriminating PD samples from controls, demonstrating the translational potential for developing novel diagnostic tools. The main findings reported in this chapter were:

1. DEXSeq and SpliceSeq pipelines identified >600 statistically significant alternative splicing events each in the living PD frontal cortex compared to controls.

2. Quantitative PCR validation confirmed four of the differentially spliced transcripts identified by RNA-Seq.

3. A random forest classifier trained using the gene expression signature from Chapter 3, demonstrated high accuracy in distinguishing PD samples from controls not only in brain tissue, but also in neuron and blood-derived samples.

These findings indicate that alternative splicing is an important and underexplored mechanism contributing to the transcriptional dysregulation observed in the living PD brain. The identification of specific splicing events associated with the disease provides new candidate targets for further investigation, potentially uncovering novel pathways and therapeutic opportunities. Moreover, the development of a robust machine learning classifier is an approach that has the potential to enable earlier, more accurate diagnosis of PD, which is crucial given the progressive nature of the disease and the need for timely intervention.

5.2 Limitations

5.2.1 Qualitative nature of Chapter 2 and lack of necessary controls

One of the major limitations of this thesis lies in that much of the data presented in Chapter 2 is qualitative and lacks controls that limit proper interpretation of the results. For the immunocytochemistry experiments and for the rat brain histology, no labelling control was included to demonstrate that artifacts from autofluorescence were not responsible for the observed fluorescence. The Western blots for both lineage markers and neurotrophic factors are generally poor in quality, as well as lacking negative(no primary/no expression), and positive controls. This work would be significantly improved by adding those (e.g. samples with no/known expression of target protein or sample buffer) and by semi-quantitative analysis of multiple replicates to estimate the relative protein quantities detected. The blots probing for neurotrophic factors secreted in cell media by BDPCs in particular would benefit from using alternative complementary experimental methods such as ELISA (as discussed in Chapter 2). This would permit accurate quantification of protein whereby allowing determination of the biological relevance of secreted proteins BDNF and GDNF.

5.2.2 Syngeneic animal model limitations

Preclinical research in animal models is exceedingly valuable for understanding human disease and is widely used in translational research. However, use of any animal model cannot fully capture the complexity and nuances in the human brain, particularly as they manifest in PD. Neuroanatomical and physiological differences in models such as rats and mice can often impact the translatability of research findings. In Chapter 2, we established a transplant model using Fischer-rat derived BDPCs implanted into syngeneic Fischer rat striatum. As a transplant model attempting to mimic an autologous therapeutic transplant strategy for patients with PD, we recapitulated only a few aspects of the anticipated therapy. Grafts were implanted into the striatum of the rats, as performed in many human transplant trials (see Chapter 1.3).[1–3] Transplanting the BDPCs as a suspension into the rodent brain, while technically similar to what would be performed in humans, does not accurately reflect the native cellular niche and microenvironment that the cells would encounter in the human PD brain. The rat model we used lacked any underlying Parkinson's disease-related neurodegeneration that could influence the survival, integration, and function of the grafted cells. This does not capture the complex, progressive neurodegenerative milieu present in the Parkinson's disease brain that any grafted cells would need to contend with. In addition, without PD pathology in the rodent model (e.g. 6-OHDA or a genetic model[4,5]), we were unable to incorporate therapeutic intervention or measurement of any functional or behavioural outcomes, which would strengthen the translational relevance of any findings. In summary, while the rodent syngeneic graft model provides an important proof-of-concept for the BDPC approach, the inherent limitations of this animal system constrain the ability to fully recapitulate the complex pathophysiology of Parkinson's disease or evaluate the potential of any envisioned therapeutic intervention. Moving forward, incorporating a more sophisticated experimental protocol involving: (1) injections for a toxic model, or selection of a disease-relevant animal model, and (2) inclusion of outcome measures, will be the minimum needed to rigorously evaluate the inherent therapeutic potential of BDPCs.

5.2.3 Tissue sourcing

The analyses in Chapters 3 and 4 were conducted on a relatively small number of bulk brain tissue samples obtained from living PD patients and controls which poses several limitations. Firstly, as a bulk tissue sample, interpretation of results is impaired by the lack of specificity of gene expression since the expression of all cell types is conflated. This can now be overcome by using single-cell RNAseq (scRNAseq), which can sequence at a single-cell resolution, though at significantly increased cost.[6] Also of note, the average age at diagnosis for the PD sample group was 43.5 (SD 11.29), which is indicative of at least a very atypical PD sample group and likely means some of the patients did not have sporadic PD. As a result, the generalizability of our findings is impacted, though the smaller sample size already limits interpretation of our results to the general PD population. The limited sample size also effectively reduced the statistical power to detect alterations in gene expression. Sequencing to an average depth of approximately ninety million reads per sample and opting for longer 125-bp paired-end reads offset some of the downsides of the limited sample sizes. However, the literature shows that detecting fold changes of 1.5 or less with fewer than 10 samples is likely to succeed less than half the time at a significance level of 5%.[7] When analyzing splicing alterations this effect is amplified further with some studies suggesting up to 400 or 500 million reads are needed to detect 85% of splicing variations.[8,9] Ideally the study would have been performed in a larger number of age and sex-matched samples to an increased depth.

Limitations in the availability of these unique samples and the resources necessary to process, sequence and analyze a larger cohort precluded doing so at the time the experiments were conducted. Any future work will need to keep these limitations in mind.

5.2.4 Aging of the comparative literature review in Chapter 3

Due to the publication of Chapter 3 in 2020 many novel studies using RNAseq and scRNAseq in the context of PD have since been published, particularly as the prohibitive cost and lack of accessibility of RNAseq have continued to improve. Searching PubMed with the same terms used for that chapter for years 2021 to 2024 generated 40 results, many of which would have been relevant to include for an updated study. These data would likely be highly informative and interesting to include, particularly studies using scRNAseq given the limitations described in section 1.2.2.

5.2.5 Reliance on correlative evidence and lack of mechanistic insights

While this thesis identifies valuable PD-associated gene expression alterations and alternative splicing events, it does not provide direct experimental evidence for the functional roles of these changes in disease pathogenesis. Similarly, our findings highlight interesting transcriptional changes in the living PD brain, but the underlying molecular mechanisms driving these alterations are not known. Lacking further mechanistic studies, the correlative nature of the data limits the ability to pinpoint specific molecular pathways or targets for the development of novel therapeutic interventions. Additionally, without a clear understanding of how the identified genes and splicing events relate to disease pathogenesis, diagnostic tools like our random forest classifier lack the robustness and reliability offered by knowledge of the underlying biology driving the relevant gene signature. As such, for both therapeutic and diagnostic purposes our ability to extrapolate to the broader PD population without those insights is likely limited. Future studies will need to focus on establishing causal links between the identified molecular alterations and disease pathogenesis through functional experiments, both in vitro and in relevant animal models.

5.3 Future Directions

By leveraging this unique tissue source, we have uncovered new layers of molecular complexity underlying Parkinson's disease, opening promising avenues for improving disease understanding, diagnosis, and the development of targeted treatments. This thesis includes the first exploratory studies using cortical tissue from living patients with Parkinson’s disease and leaves areas suitable for further research. Among those, several areas of future research appear to be most meaningful to advance. First, we will expand on the rat BDPC model from Chapter 2 to evaluate the nature of BDPCs and their endogenous therapeutic potential. Secondly, key genes or alternative splicing events will need to be selected from Chapters 3 and 4 to perform functional and mechanistic experiments.

5.3.1 Determining the exact nature of BDPCs

An important question remaining after the work included in this thesis is regarding the exact cell type of BDPCs. The experiments in Chapter 2 expanded on the original work describing BDPCs derived from the human frontal cortex with markers of progenitor cells, as well as neural and mesenchymal proteins, by exploring their electrophysiological properties. Together with BDPCs derived from rat frontal cortex, BDPCs from humans once again exhibited properties consistent with neural precursor cells. However, establishing BDPCs as a pluripotent stem cell or multipotent neural progenitor still requires further experimentation. The current standard for establishing pluripotency for the purpose of cell characterization is the generation of embryoid bodies.[10] This can be performed in neutral (undirected) conditions without any exogenous growth factors or with conditions to promote differentiation into ecto-, meso- or endoderm lineages. Assuming the embryoid bodies can be formed, many downstream analyses can then be performed to confirm the “stemness” of the cells, which can be as simple as immunocytochemistry for pluripotency markers like SOX2 or NANOG, but would ideally consist of a quantitative method such as using an established qPCR panel (e.g. ScoreCard[11]) which uses a gene expression signature to establish functional pluripotency.

The more likely possibility is that BDPCs are not pluripotent, but more mature multipotent neural progenitor cells. Neural progenitors still have the ability to differentiate into neurons, glial cells and oligodendrocytes, and form neurospheres in non-adherent culture conditions. Experiments not included in this thesis were able to determine that BDPCs could be cultured in neural progenitor media in what qualitatively appeared to be neurospheres. Future experiments will need to take this one step further attempting to differentiate BDPCs using exogenous growth factors like fibroblast growth factor 8/sonic hedgehog (neurons) or ciliary neurotrophic factor (astrocytes) in appropriate culture conditions.[12] Expression of lineage specific markers for each mature cell type could then be confirmed experimentally.

5.3.2 Assess therapeutic potential of BDPCs

In Chapter 2, we established a syngeneic transplant model in Fischer rats and demonstrated longitudinal tracking of genetically engineered BDPCs over a period of five weeks. First, we would need to refine BDPC isolation, expansion, and transplantation protocols to enhance graft survival, integration, and functional outcomes. Though we determined that larger grafts (i.e., 240k cells) did not survive long-term in Chapter 2, optimization of isolation and culture methods (e.g., cell passage, culture conditions, addition of growth factors, and cell differentiation) should be evaluated first to improve survival of BDPCs once transplanted.

After optimization of the culture and transplantation protocol, we will use the 6-hydroxydopamine toxin model of PD in rats to determine if BDPCs have any endogenous therapeutic potential. As our results from Chapter 2 indicate, BDNF and GDNF are natively expressed and secreted by both human and rat BDPCs. These NTFs, particularly GDNF, are among the most widely investigated trophic agents for PD with robust preclinical research showing protective and regenerative effects on dopaminergic neurons (see Chapter 1.3.4).[13,14] As such, we'd like to use neuroprotective and neurorestorative graft protocols to determine whether BDPCs protect against dopaminergic cell loss and can restore motor function after a toxic insult. Following the results of those experiments, strategies could then be investigated to enhance the therapeutic potential of BDPCs, or if they have none, genetically engineer BDPCs to express other therapeutic molecules. Future *in vivo* studies to assess long-term survival, integration, and functional benefit of BDPCs will also be crucial for demonstrating safety and efficacy, paving the way for clinical translation as an autologous cell-based therapy approach for PD.

5.3.3 Conduct validation studies based on transcriptome analysis findings

In the discussions of Chapters 3 and 4 we highlighted many genes of interest related to PD or the processes that may be underlying disease. This is an important first step in improving our understanding of PD. Nonetheless, these findings are largely correlative in nature, requiring functional experiments to determine any causative or contributory role in the pathogenesis and progression of PD. In future studies, we will need to select key genes, perhaps focusing on a particular pathway of interest, and investigate the nature of their potential role in PD. For gene expression changes seen in PD this could take the form of *in vitro* experiments, modulating gene expression in cells either genetically or altering their protein products pharmacologically. For alternative splicing events of interest, engineered nuclease strategies like CRISPR or zinc-finger nucleases can be used to target genetic regions of interest, artificially replicating RNA-seq findings *in vitro*. Functional effects of those splicing variations can then be measured in a cell culture model, and further evaluation of their potential impact in PD can be assessed using an *in vitro* toxic model(e.g. 6-OHDA, rotenone or MPTP) with either differentiated or undifferentiated neural cell lines like SH-SY5Y or iPSCs.[15] Alternatively, 3D cell models such as brain organoids could better replicate the interactions that control physiological cell function and improve translational value of any experimental results.[16] ScRNAseq would not only address the limitations described in 1.2.2 by allowing deconvolution of cellular signals identifying which cells are driving any larger changes that were detected by bulk RNAseq, but can also advance our understanding of how each cell type may be contributing to or protective against PD when comparing cell-type specific gene expression changes against controls.

5.4 Significance and Overall Conclusions

This thesis has demonstrated the power of directly accessing and interrogating the living brain tissue of Parkinson's disease patients to uncover valuable insights that can advance both our understanding of the disease and the development of new therapeutic approaches. We established an important preclinical platform to evaluate the potential of autologous BDPCs grafts as a therapeutic strategy for PD, leveraging the unique opportunity to study BDPCs derived from the PD cortex. Moreover, transcriptomic analyses of this tissue have revealed novel dysregulated pathways, alternative splicing events, and a gene expression signature that holds promise as a diagnostic biomarker. Collectively, these findings open new avenues for targeted intervention, earlier diagnosis, and personalized treatment of this devastating neurodegenerative disorder. As the field of Parkinson's research continues to evolve, the ability to directly examine the living diseased brain offers many advantages in helping to unraveling the complex mechanisms underlying the disease and translating these insights into meaningful clinical impact.

5.5 References

1. Backlund EO, Granberg PO, Hamberger B, et al. Transplantation of adrenal medullary tissue to striatum in parkinsonism. *J Neurosurg*. 1985;62(2):169-173. doi:10.3171/jns.1985.62.2.0169

2. Wenning GK, Odin P, Morrish P, et al. Short- and long-term survival and function of unilateral intrastriatal dopaminergic grafts in Parkinson's disease. *Ann Neurol*. 1997;42(1):95-107. doi:10.1002/ana.410420115

3. Brundin P, Pogarell O, Hagell P, et al. Bilateral caudate and putamen grafts of embryonic mesencephalic tissue treated with lazaroids in Parkinson's disease. *Brain*. 2000;123(7):1380-1390. doi:10.1093/brain/123.7.1380

4. Tieu K. A guide to neurotoxic animal models of Parkinson's disease. *Cold Spring Harb Perspect Med*. 2011;1(1):1-20. doi:10.1101/cshperspect.a009316

5. Creed RB, Goldberg MS. New Developments in Genetic rat models of Parkinson's Disease. *Mov Disord*. 2018;33(5):717-729. doi:10.1002/mds.27296

6. Fiorini MR, Dilliott AA, Thomas RA, Farhan SMK. Transcriptomics of Human Brain Tissue in Parkinson's Disease: a Comparison of Bulk and Single-cell RNA Sequencing. *Mol Neurobiol*. 2024;(0123456789). doi:10.1007/s12035-024-04124-5

7. Conesa A, Madrigal P, Tarazona S, et al. A survey of best practices for RNA-seq data analysis. *Genome Biol*. 2016;17(1):1-19. doi:10.1186/s13059-016-0881-8

8. Liu Y, Ferguson JF, Xue C, et al. Evaluating the Impact of Sequencing Depth on Transcriptome Profiling in Human Adipose. *PLoS One*. 2013;8(6):1-10. doi:10.1371/journal.pone.0066883

9. Toung JM, Morley M, Li M, Cheung VG. RNA-sequence analysis of human B-cells. *Genome Res*. 2011;21:991-998. doi:10.1101/gr.116335.110.21

10. Allison TF, Andrews PW, Avior Y, et al. Assessment of established techniques to determine developmental and malignant potential of human pluripotent stem cells. *Nat Commun*. 2018;9(1):1-15. doi:10.1038/s41467-018-04011-3

11. Tsankov AM, Akopian V, Pop R, et al. An improved ScoreCard to assess the differentiation potential of human pluripotent stem cells. *Nat Biotechnol*. 2016;33(11):1182-1192. doi:10.1038/nbt.3387.An

12. Dhara SK, Stice SL. Neural differentiation of human embryonic stem cells. *J Cell Biochem*. 2008;105(3):633-640. doi:10.1002/jcb.21891

13. Paul G, Sullivan AM. Trophic factors for Parkinson's disease: Where are we and where do we go from here? *Eur J Neurosci*. 2019;49(4):440-452. doi:10.1111/ejn.14102

14. Staudt MD, Di Sebastiano AR, Xu H, et al. Advances in neurotrophic factor and cell-based therapies for Parkinson's disease: A mini-review. *Gerontology*. 2016;62(3):371-380. doi:10.1159/000438701

15. Cetin S, Knez D, Gobec S, Kos J, Pišlar A. Cell models for Alzheimer's and Parkinson's disease: At the interface of biology and drug discovery. *Biomed Pharmacother*. 2022;149(March). doi:10.1016/j.biopha.2022.112924

16. McComish SF, MacMahon Copas AN, Caldwell MA. Human Brain-Based Models Provide a Powerful Tool for the Advancement of Parkinson's Disease Research and Therapeutic Development. *Front Neurosci*. 2022;16(May):1-15. doi:10.3389/fnins.2022.851058

Appendices

Appendix A: Supplementary Figures

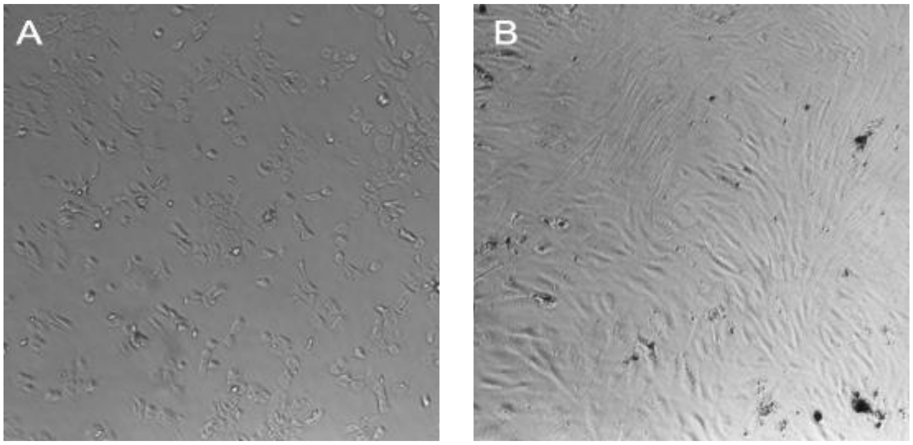

Supplementary Figure 2-1 Representative photomicrographs (10x objective) showing rat BDPCs with a flat polygonal shape at subconfluence (A) and narrow spindle like morphology at higher confluence (B).

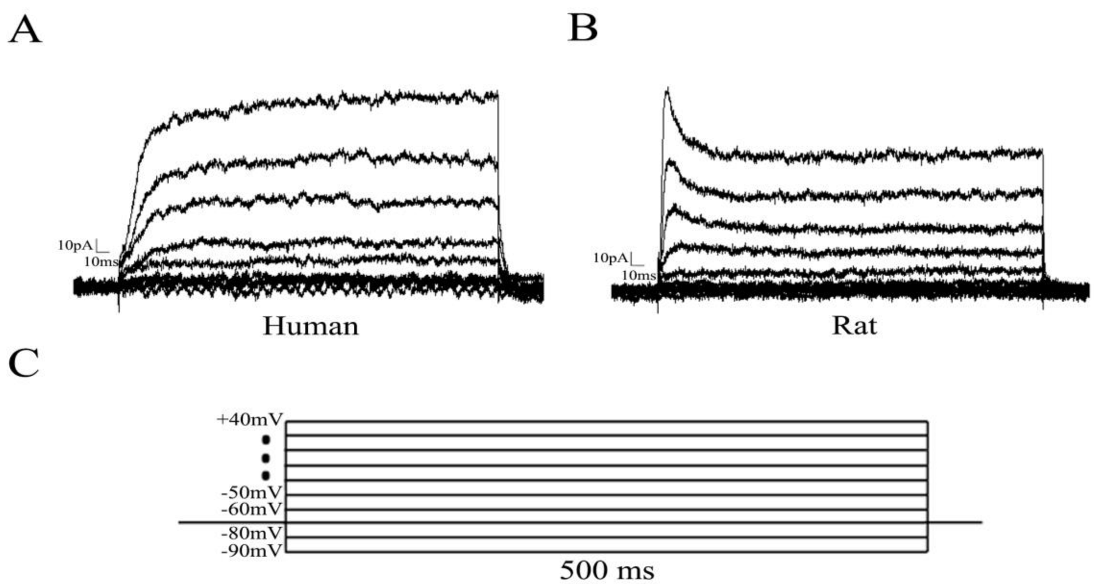

Supplementary Figure 2-2 Average voltage clamp recordings for (A) human and (B) rat BDPCs shown with (C) a representation of the stimulation protocol.

Appendix B: Supplementary Tables

Supplementary Table 2-1 Rodent neurotrophic factor primers

Gene	Direction	Primer Sequence	Predicted Product length (bases)
BDNF-1	Forward	TACCTGGATGCCGCAAACAT	182
	Reverse	TGGCCTTTTGATACCGGGAC	
BDNF-2	Forward	GTTCGAGAGGTCTGACGACG	220
	Reverse	GACATGTTTGCGGCATCCAG	
BDNF-3	Forward	GCTGAGCGTGTGTGACAGTA	282
	Reverse	ATGAACCGCCAGCCAATTCT	
CDNF-1	Forward	AAGAGGCAACCTCCGCTACT	121
	Reverse	TGGTTGGAGATCCAAAGCCC	
CDNF-2	Forward	CGAGGGCTGACTGTGAAGTA	192
	Reverse	CTAGGATCTTGGTGGCCGAG	
CDNF-3	Forward	TCCGCTACTGTAAGCAAGGTG	119
	Reverse	GCCAGCACATGGTTGGAGAT	
GDNF-1	Forward	CGCTGACCAGTGACTCCAATA	268
	Reverse	TCGTAGCCCAAACCCAAGTC	
GDNF-2	Forward	CCGGACGGGACTCTAAGATG	104
	Reverse	GAGAAGCCTCTTACCGGCG	
GDNF-3	Forward	GCCGGACGGGACTCTAAGAT	111
	Reverse	CGCTTCGAGAAGCCTCTTAC	

Supplementary Table 2-2 Primary Antibodies

Antibody	Vendor	Product ID	Host species	Dilution
BDNF	Abcam (Cambridge, MA, USA)	ab108383	Rabbit (polyclonal)	1:100 ICC, 1:1000 WB
CDNF	Bioss	BS-11499R	Rabbit (polyclonal)	1:100 ICC, 1:1000 WB
GDNF	Abcam	ab18956	Rabbit (polyclonal)	1:100 ICC, 1:1000 WB
β-Actin	Abcam	ab49900	Mouse (monoclonal)	1: ICC, 1:5000 WB
Nestin	Proteintech	66259-2-IG	Mouse (monoclonal)	1:100 ICC, 1:1000 WB
NG2	Millipore	MAB5384	Mouse (monoclonal)	1:500 ICC, 1:500 WB
CD133	Invitrogen	PA5-38014	Rabbit (polyclonal)	1:400 ICC, 1:200 WB
$p75^{NTR}$	Abcam	ab38335	Rabbit (polyclonal)	1:200 ICC, 1:1000 WB
Olig1	Millipore	MAB5540	Mouse (monoclonal)	1:100 ICC, 1:500 WB
GalC	Millipore	MAB342	Mouse (monoclonal)	1:100 ICC, 1:500 WB
Iba1	Abcam	ab15690	Mouse (monoclonal)	1:100 ICC, 1:1000 WB
Fibronectin	Sigma-Aldrich (St. Louis, MO, USA)	F3648	Rabbit (polyclonal)	1:200 ICC, 1:2000 WB

Collagen III	Abcam	ab7778	Rabbit (polyclonal)	1:200 ICC, 1:1000 WB
β III Tubulin	Promega (Madison, WI, USA)	G7121	Mouse (monoclonal)	1:100 ICC, 1:1000 WB
GFAP	Abcam	ab10062	Mouse (monoclonal)	1:200 ICC, 1:1000 WB

Supplementary Table 3-1 qPCR primers used for DEG validation

Gene	Direction	Primer Sequence	Predicted Product Length (bases)
CSN1S1	Forward	GGCACCTAATCAGAGGGTATTAAA	96
	Reverse	TGATGGCACTTACAGAACTGG	
GADD45G	Forward	AATTGCAGCATCATATAAGC	331
	Reverse	ACGCTGCGCGCCCTTATATAG	
GDNF	Forward	CGGACGGGACTTTAAGATGA	276
	Reverse	GGAAGCACTGCCATTTGTTT	
SGK1	Forward	CCGCTAGATTCTCCATCCCG	273
	Reverse	GAGGAGCCGGTGTACTTCAG	
TFAP2D	Forward	CCTACGACATCAGCCAAAGAA	114
	Reverse	CTTGCCTCGTACCCACTTAAA	
ZFP36	Forward	GGGAGGCAATGAACCCTCTC	204
	Reverse	GCAACGGCTTTGGCTACTTG	

Supplementary Table 3-2 RNA sequencing report

Sample	Reads	Reads Post-trimming	Nuclear rRNA(%), no 45S	45S rRNA (%)	Mitochondrial rRNA (%)	Mitochondrial, other RNA (%)	mRNA (%)	Overall Read Mapping Rate	Mapped to Exons (%)	Mapped to Introns (%)	Mapped Intergenic (%)	Reads Counted Towards Genes	Reads Not Aligned to Genes
C1	8.8E+07	8.8E+07	0.24	0.24	3.01	11.72	85.03	95.3	86.37	6.91	6.72	6.0E+07	2.4E+07
C2	9.6E+07	9.6E+07	0.38	0.38	4.05	16.15	79.42	95	87.62	4.86	7.51	6.2E+07	2.9E+07
C3	9.0E+07	9.0E+07	0.54	0.54	2.44	10.01	87.01	95.4	88.2	5.11	6.69	6.5E+07	2.1E+07
C4	9.0E+07	9.0E+07	0.82	0.82	2.5	9.35	87.33	95.1	88.8	4.65	6.55	6.6E+07	2.1E+07
C5	9.1E+07	9.1E+07	0.4	0.4	3	10.04	86.56	95.3	89.78	4.09	6.13	6.6E+07	2.1E+07
PD1	9.6E+07	9.6E+07	0.49	0.5	4.03	13.74	81.73	94.9	86.83	6.13	7.03	6.3E+07	2.8E+07
PD2	8.8E+07	8.8E+07	0.57	0.57	3.81	14.14	81.48	95.3	87.81	5.14	7.05	5.9E+07	2.5E+07
PD3	8.4E+07	8.3E+07	0.66	0.66	2.64	11.75	84.95	95.1	89.03	4.68	6.29	5.9E+07	2.1E+07
PD4	9.1E+07	9.1E+07	0.61	0.62	5.03	17.27	77.08	95.1	88.35	5.38	6.27	5.7E+07	3.0E+07
PD5	8.3E+07	8.3E+07	0.54	0.55	3.27	10.33	85.85	95.3	89.67	4.26	6.07	6.0E+07	2.0E+07
PD6	8.5E+07	8.4E+07	0.56	0.57	4.02	14.35	81.06	95.2	89.03	3.93	7.05	5.7E+07	2.4E+07

Supplementary Table 3-3 Expression of individual genes with causative linkage to Parkinson's disease

Gene Symbol	Alternate Name	Full Gene Name	Mode of Inheritance	Fold Change (log2)	Adjusted P-value
SNCA	PARK1/PARK4	synuclein alpha	AD	-0.164	0.399
PRKN	PARK2	parkin RBR E3 ubiquitin ligase	AR	-0.006	0.99
UCHL1	PARK5	ubiquitin C-terminal hydrolase L1	AD	0.037	0.92
PINK1	PARK6	PTEN induced putative kinase 1	AR	0.104	0.63
DJ-1	PARK7	parkinsonism associated deglycase	AR	0.081	0.75
LRRK2	PARK8	leucine-rich repeat kinase 2	AD	-0.021	0.98
ATP13A2	PARK9	ATPase 13A2	AR	0.201	0.15
GIGYF2	PARK11	GRB10 interacting GYF protein 2	AD	-0.002	1.00
HTRA2	PARK13	HtrA serine peptidase 2	AD	0.071	0.83
PLA2G6	PARK14	phospholipase A2 group VI	AR	-0.06	0.88
FBX07	PARK15	F-box protein 7	AR	-0.062	0.87
VPS35	PARK17	VPS35, retromer complex component	AD	0.107	0.59
EIF4G1	PARK18	eukaryotic translation initiation factor 4 gamma 1	AD	0.069	0.76
DNAJC6	PARK19	DNAJ heat shock protein family (Hsp40) member C6	AR	-0.093	0.72
SYNJ1	PARK20	synaptojanin 1	AR	0.005	0.99
TMEM230	PARK21	transmembrane protein 230	AD	0.101	0.61
CHCHD2	PARK22	coiled-coil-helix-coiled-coil-helix domain containing 2	AD	0.162	0.42
VPS13C	PARK23	vacuolar protein sorting 13 homolog C	AR	-0.001	1.00
RIC3		RIC3 acetylcholine receptor chaperone	AD	-0.061	0.84

Abbreviations: AD, autosomal dominant; AR, autosomal recessive

Supplementary Table 3-4 Expression of known mitochondrial genes

Gene Symbol	Gene Name	Fold Change (log2)	Corrected *P*-value
MT-ATP6	Mitochondrially Encoded ATP Synthase Membrane Subunit 6	0.275	0.52
MT-ATP8	Mitochondrially Encoded ATP Synthase Membrane Subunit 8	0.212	0.65
MT-CO1	Mitochondrially Encoded Cytochrome C Oxidase I	0.244	0.53
MT-CO2	Mitochondrially Encoded Cytochrome C Oxidase II	0.301	0.47
MT-CO3	Mitochondrially Encoded Cytochrome C Oxidase III	0.258	0.57
MT-CYB	Mitochondrially Encoded Cytochrome B	0.176	0.71
MT-ND1	Mitochondrially Encoded NADH:Ubiquinone Oxidoreductase Core Subunit 1	0.129	0.84
MT-ND2	Mitochondrially Encoded NADH:Ubiquinone Oxidoreductase Core Subunit 2	0.228	0.60
MT-ND3	Mitochondrially Encoded NADH:Ubiquinone Oxidoreductase Core Subunit 3	0.289	0.51
MT-ND4	Mitochondrially Encoded NADH:Ubiquinone Oxidoreductase Core Subunit 4	0.211	0.68
MT-ND4L	Mitochondrially Encoded NADH:Ubiquinone Oxidoreductase Core Subunit 4L	0.149	0.76
MT-ND5	Mitochondrially Encoded NADH:Ubiquinone Oxidoreductase Core Subunit 5	0.101	0.87
MT-ND6	Mitochondrially Encoded NADH-Ubiquinone Oxidoreductase Core Subunit 6	0.294	0.51

Supplementary Table 3-5 Complete dataset of DEGs identified in the frontal lobe transcriptome of living PD patients

Symbol	Gene Name	Fold Change (log2)	Corrected *P*-value
A2ML1	alpha-2-macroglobulin like 1	0.68	3.10E-03
ABI3BP	ABI family member 3 binding protein	-0.79	3.79E-02
ACAT2	acetyl-CoA acetyltransferase 2	0.32	1.33E-02
ACSBG1	acyl-CoA synthetase bubblegum family member 1	0.40	6.13E-04
ACSL1	acyl-CoA synthetase long chain family member 1	-0.29	4.03E-02
ACSL5	acyl-CoA synthetase long chain family member 5	0.72	3.03E-02
ACSS1	acyl-CoA synthetase short chain family member 1	0.32	1.69E-02
ACSS3	acyl-CoA synthetase short chain family member 3	0.44	1.43E-02
ADGRA1	adhesion G protein-coupled receptor A1	-0.27	1.96E-02
ADI1	acireductone dioxygenase 1	0.33	1.96E-02
AHI1	Abelson helper integration site 1	-0.41	1.70E-02
AHNAK2	AHNAK nucleoprotein 2	0.43	2.50E-02
AKAP12	A-kinase anchoring protein 12	0.34	9.01E-03
AKR1C1	aldo-keto reductase family 1 member C1	0.60	8.59E-03
ALCAM	activated leukocyte cell adhesion molecule	-0.26	2.78E-02
ALDH2	aldehyde dehydrogenase 2 family member	0.32	3.78E-02
ALDH6A1	aldehyde dehydrogenase 6 family member A1	0.29	3.46E-02
ALDOC	aldolase, fructose-bisphosphate C	0.35	2.26E-02
AMOT	angiomotin	0.37	5.95E-04
ANKRD22	ankyrin repeat domain 22	-3.19	1.32E-03
ANKRD37	ankyrin repeat domain 37	0.53	4.57E-02
APC	APC regulator of WNT signaling pathway	0.33	3.46E-02
APOLD1	apolipoprotein L domain containing 1	-1.55	1.06E-09
AQP1	aquaporin 1 (Colton blood group)	-1.23	3.24E-03
ARRDC2	arrestin domain containing 2	-1.06	6.80E-19
ARRDC3	arrestin domain containing 3	-0.54	3.32E-04
ATOH8	atonal bHLH transcription factor 8	-0.62	1.49E-02
ATP1A2	ATPase Na+/K+ transporting subunit alpha 2	0.37	9.51E-04
ATP1B2	ATPase Na+/K+ transporting subunit beta 2	0.28	3.24E-02
AVPR1A	arginine vasopressin receptor 1A	-1.25	4.47E-05
AXL	AXL receptor tyrosine kinase	0.35	5.24E-03
BAMBI	BMP and activin membrane bound inhibitor	0.61	4.81E-03
BCOR	BCL6 corepressor	-0.55	1.56E-04

BRINP3	BMP/retinoic acid inducible neural specific 3	-0.34	7.69E-03
BTNL9	butyrophilin like 9	0.73	2.98E-05
C17orf102	chromosome 17 open reading frame 102	-0.45	3.78E-02
C1orf61	chromosome 1 open reading frame 61	0.30	1.83E-03
C1R	complement C1r	-0.44	4.42E-02
C5AR2	complement component 5a receptor 2	-0.96	1.59E-02
CA10	carbonic anhydrase 10	0.28	4.67E-02
CA9	carbonic anhydrase 9	-1.26	4.23E-02
CAPN9	calpain 9	-1.61	1.08E-02
CAVIN2	caveolae associated protein 2	-0.86	2.17E-09
CBLN2	cerebellin 2 precursor	0.33	2.72E-03
CCBE1	collagen and calcium binding EGF domains 1	0.81	1.84E-02
CCDC38	coiled-coil domain containing 38	2.01	5.53E-06
CCDC85C	coiled-coil domain containing 85C	0.33	2.06E-02
CCP110	centriolar coiled-coil protein 110	-0.25	4.06E-02
CD320	CD320 molecule	0.38	3.64E-02
CD44	CD44 molecule (Indian blood group)	-0.94	1.69E-02
CDH20	cadherin 20	0.29	4.30E-02
CDKN1A	cyclin dependent kinase inhibitor 1A	-0.68	1.59E-02
CEBPD	CCAAT enhancer binding protein delta	-0.95	1.55E-09
CHN2	chimerin 2	-0.44	4.46E-03
CHRM1	cholinergic receptor muscarinic 1	-0.29	1.62E-02
CHRM4	cholinergic receptor muscarinic 4	-0.44	4.40E-02
CHST3	carbohydrate sulfotransferase 3	-0.73	1.41E-07
CHSY1	chondroitin sulfate synthase 1	-0.45	1.62E-03
CIART	circadian associated repressor of transcription	-0.59	3.00E-02
CITED2	Cbp/p300 interacting transactivator with Glu/Asp rich carboxy-terminal domain 2	0.45	3.00E-02
CLCN5	chloride voltage-gated channel 5	0.39	2.08E-02
CLDN5	claudin 5	-0.50	1.76E-02
CLEC4E	C-type lectin domain family 4 member E	-1.67	4.53E-03
CLK1	CDC like kinase 1	0.60	3.87E-02
CNTN3	contactin 3	-0.65	2.12E-08
CNTN6	contactin 6	0.67	8.37E-05
COL13A1	collagen type XIII alpha 1 chain	-0.95	3.83E-02
COL5A1	collagen type V alpha 1 chain	-0.78	1.48E-02
COX6A1	cytochrome c oxidase subunit 6A1	0.36	6.97E-03

CP	ceruloplasmin	-1.16	1.37E-03
CPT1A	carnitine palmitoyltransferase 1A	0.38	2.79E-02
CREB5	cAMP responsive element binding protein 5	-0.47	5.00E-03
CSDC2	cold shock domain containing C2	0.47	3.71E-02
CSGALNACT1	chondroitin sulfate N-acetylgalactosaminyltransferase 1	-0.29	1.82E-02
CSN1S1	casein alpha s1	2.29	1.37E-04
CSRNP1	cysteine and serine rich nuclear protein 1	-0.75	3.53E-06
CTAG2	cancer/testis antigen 2	-7.27	5.97E-08
CTXN3	cortexin 3	0.89	1.01E-11
CX3CR1	C-X3-C motif chemokine receptor 1	0.70	4.45E-05
CXADR	CXADR Ig-like cell adhesion molecule	-0.30	2.78E-02
CXXC5	CXXC finger protein 5	-0.35	1.45E-03
DACH1	dachshund family transcription factor 1	-0.42	3.48E-02
DCSTAMP	dendrocyte expressed seven transmembrane protein	-1.46	5.24E-03
DDIT4	DNA damage inducible transcript 4	-0.67	2.55E-05
DDR2	discoidin domain receptor tyrosine kinase 2	0.70	1.83E-03
DPH1	diphthamide biosynthesis 1	-0.33	3.86E-02
DUSP6	dual specificity phosphatase 6	0.72	1.24E-05
ENAH	ENAH actin regulator	0.23	4.03E-02
EPCAM	epithelial cell adhesion molecule	1.12	3.15E-02
EYA3	EYA transcriptional coactivator and phosphatase 3	0.30	4.75E-02
F2RL3	F2R like thrombin or trypsin receptor 3	-3.06	6.08E-06
F5	coagulation factor V	1.02	3.46E-02
FABP3	fatty acid binding protein 3	0.27	4.03E-02
FABP7	fatty acid binding protein 7	0.43	1.21E-02
FADS2	fatty acid desaturase 2	0.31	1.44E-03
FAM13B	family with sequence similarity 13 member B	-0.42	2.41E-05
FAM189B	family with sequence similarity 189 member B	0.31	7.69E-03
FAM87A	family with sequence similarity 87 member A	-0.88	8.37E-04
FASN	fatty acid synthase	0.24	4.06E-02
FBLN5	fibulin 5	-0.58	3.42E-04
FBXL19	F-box and leucine rich repeat protein 19	0.24	3.74E-02
FBXO2	F-box protein 2	0.26	1.69E-02
FGF18	fibroblast growth factor 18	-0.85	2.16E-02
FGF7P3	fibroblast growth factor 7 pseudogene 3	0.40	1.48E-02

FOXC1	forkhead box C1	1.13	7.89E-08
FOXF2	forkhead box F2	0.99	6.66E-05
FOXP2	forkhead box P2	-0.53	1.46E-02
FOXQ1	forkhead box Q1	1.39	3.23E-07
FPR1	formyl peptide receptor 1	-0.88	1.34E-02
FRAT1	FRAT regulator of WNT signaling pathway 1	-0.70	4.01E-04
FREM3	FRAS1 related extracellular matrix 3	0.97	2.41E-05
FSTL5	follistatin like 5	-0.34	2.28E-02
FZD1	frizzled class receptor 1	0.47	7.69E-03
GADD45G	growth arrest and DNA damage inducible gamma	-2.00	2.97E-16
GALNT14	polypeptide N-acetylgalactosaminyltransferase 14	-0.45	1.82E-02
GAP43	growth associated protein 43	0.29	1.08E-02
GATC	glutamyl-tRNA amidotransferase subunit C	0.55	6.98E-04
GDNF	glial cell derived neurotrophic factor	-0.96	1.87E-02
GNA14	G protein subunit alpha 14	0.67	2.13E-03
GNG4	G protein subunit gamma 4	-0.38	2.53E-03
GOLGA8S	golgin A8 family member S	-0.86	9.66E-03
GPR143	G protein-coupled receptor 143	0.57	4.03E-02
GPR37L1	G protein-coupled receptor 37 like 1	0.37	1.83E-03
GPX3	glutathione peroxidase 3	0.49	3.71E-07
GRAMD1C	GRAM domain containing 1C	0.31	4.75E-02
GRASP	general receptor for phosphoinositides 1 associated scaffold protein	-0.41	5.45E-04
GREM1	gremlin 1, DAN family BMP antagonist	-0.49	1.60E-02
GREM2	gremlin 2, DAN family BMP antagonist	-0.44	6.95E-03
GRIK3	glutamate ionotropic receptor kainate type subunit 3	-0.40	3.70E-04
GRM7	glutamate metabotropic receptor 7	-0.35	1.62E-02
H3-3B	H3.3 histone B	-0.33	3.23E-03
HAS2-AS1	HAS2 antisense RNA 1	-1.24	2.45E-02
HCN4	hyperpolarization activated cyclic nucleotide gated potassium channel 4	0.52	1.45E-02
HEG1	heart development protein with EGF like domains 1	0.38	1.34E-02
HERC2P3	hect domain and RLD 2 pseudogene 3	0.81	1.21E-02
HERPUD1	homocysteine inducible ER protein with ubiquitin like domain 1	-0.37	2.42E-03
HES5	hes family bHLH transcription factor 5	1.16	1.32E-03

HHEX	hematopoietically expressed homeobox	1.42	5.96E-07
HPCA	hippocalcin	-0.25	4.03E-02
HRK	harakiri, BCL2 interacting protein	-0.61	3.10E-03
HS3ST4	heparan sulfate-glucosamine 3-sulfotransferase 4	-0.50	1.82E-04
HSPA1B	heat shock protein family A (Hsp70) member 1B	0.73	1.44E-02
HYAL2	hyaluronidase 2	-0.45	7.16E-03
ID1	inhibitor of DNA binding 1, HLH protein	0.82	1.39E-03
ID3	inhibitor of DNA binding 3, HLH protein	0.72	1.88E-03
IDH1	isocitrate dehydrogenase (NADP(+)) 1	0.43	3.20E-04
IGFL4	IGF like family member 4	-0.96	3.53E-02
IL1R2	interleukin 1 receptor type 2	-2.19	2.76E-02
IL1RAPL2	interleukin 1 receptor accessory protein like 2	-0.57	4.93E-02
INKA2	inka box actin regulator 2	-0.43	1.38E-05
IP6K3	inositol hexakisphosphate kinase 3	-0.75	3.10E-03
IRF8	interferon regulatory factor 8	0.69	1.76E-02
ISLR	immunoglobulin superfamily containing leucine rich repeat	-0.46	3.86E-02
ISLR2	immunoglobulin superfamily containing leucine rich repeat 2	-0.36	4.77E-02
ITPR2	inositol 1,4,5-trisphosphate receptor type 2	0.42	1.67E-02
ITPRIP	inositol 1,4,5-trisphosphate receptor interacting protein	-0.92	6.30E-07
ITPRIPL2	ITPRIP like 2	0.36	4.45E-02
JAKMIP3	Janus kinase and microtubule interacting protein 3	-0.50	2.20E-02
KANK4	KN motif and ankyrin repeat domains 4	1.01	3.27E-03
KCNH8	potassium voltage-gated channel subfamily H member 8	-0.72	4.23E-02
KCNK10	potassium two pore domain channel subfamily K member 10	-0.37	3.58E-02
KCNN1	potassium calcium-activated channel subfamily N member 1	0.26	4.35E-02
KIF19	kinesin family member 19	-0.61	4.03E-02
KLF9	Kruppel like factor 9	-0.46	1.14E-05
KLHL14	kelch like family member 14	-0.89	6.22E-03
KLK5	kallikrein related peptidase 5	1.06	2.95E-02
KLK7	kallikrein related peptidase 7	1.03	1.57E-06
KRTAP5-AS1	KRTAP5-1/KRTAP5-2 antisense RNA 1	-0.53	8.74E-03
L3MBTL4	L3MBTL histone methyl-lysine binding protein 4	-0.42	3.88E-02

LAMA2	laminin subunit alpha 2	0.51	1.72E-04
LAMB3	laminin subunit beta 3	-0.47	2.20E-02
LCN15	lipocalin 15	-0.96	3.52E-02
LDLR	low density lipoprotein receptor	0.47	3.58E-02
LGALS1	galectin 1	0.36	3.83E-02
LGR5	leucine rich repeat containing G protein-coupled receptor 5	-0.59	1.52E-02
LHFPL1	LHFPL tetraspan subfamily member 1	0.93	1.28E-02
LIMK1	LIM domain kinase 1	0.33	1.58E-02
LINC00086	small integral membrane protein 10 like 2A	0.29	3.22E-02
LINC00443	long intergenic non-protein coding RNA 443	1.45	1.28E-02
LINC00634	long intergenic non-protein coding RNA 634	0.44	1.67E-02
LINC00883	DPPA2 upstream binding RNA	-0.43	5.03E-03
LINC00925	MIR9-3 host gene	-0.42	3.59E-02
LMCD1	LIM and cysteine rich domains 1	0.79	7.02E-03
LMO2	LIM domain only 2	0.74	7.12E-04
LOC100507351	uncharacterized	-0.47	4.16E-02
LOC100507534	uncharacterized	0.69	2.14E-02
LOC100996609	uncharacterized	2.77	1.18E-02
LOC101928358	uncharacterized	-0.78	4.48E-02
LOC101929555	uncharacterized	-0.86	5.95E-03
LOC441081	uncharacterized	2.03	1.17E-09
LONRF1	LON peptidase N-terminal domain and ring finger 1	0.38	1.83E-03
LPAR5	lysophosphatidic acid receptor 5	0.53	4.45E-02
LPAR6	lysophosphatidic acid receptor 6	0.91	5.04E-08
LRMP	lymphoid restricted membrane protein	-0.47	2.48E-03

LRP4	LDL receptor related protein 4	0.29	3.59E-02
LRRC8C	leucine rich repeat containing 8 VRAC subunit C	0.34	1.71E-02
LRRTM2	leucine rich repeat transmembrane neuronal 2	-0.31	7.69E-03
LRTM2	leucine rich repeats and transmembrane domains 2	-0.39	2.78E-03
LYNX1	Ly6/neurotoxin 1	0.27	2.34E-02
MAF	MAF bZIP transcription factor	0.28	2.22E-02
MAP4K5	mitogen-activated protein kinase kinase kinase 5	-0.47	1.04E-02
MARCHF1	membrane associated ring-CH-type finger 1	-0.39	9.66E-03
MARCO	macrophage receptor with collagenous structure	-3.24	2.08E-05
MARVELD2	MARVEL domain containing 2	0.76	4.25E-02
MCTP2	multiple C2 and transmembrane domain containing 2	-0.62	6.87E-03
MEF2D	myocyte enhancer factor 2D	-0.29	1.95E-02
MET	MET proto-oncogene, receptor tyrosine kinase	-0.93	2.31E-06
MGAM	maltase-glucoamylase	-1.25	1.95E-02
MGST1	microsomal glutathione S-transferase 1	0.53	4.77E-02
MICAL3	microtubule associated monooxygenase, calponin and LIM domain containing 3	-0.25	2.58E-02
MIR3648	microRNA 3648-1	2.54	4.18E-05
MIR3687	microRNA 3687-1	2.70	4.90E-06
MMD2	monocyte to macrophage differentiation associated 2	0.51	8.22E-04
MSMO1	methylsterol monooxygenase 1	0.48	9.51E-04
MT1F	metallothionein 1F	0.56	4.72E-03
MT1G	metallothionein 1G	0.84	3.57E-05
MTRNR2L2	MT-RNR2 like 2	1.46	4.56E-02
MYORG	myogenesis regulating glycosidase (putative)	0.34	4.82E-03
N4BP2L1	NEDD4 binding protein 2 like 1	-0.31	2.31E-02
NEFH	neurofilament heavy	0.59	6.52E-03
NEFM	neurofilament medium	0.53	3.63E-03
NELL1	neural EGFL like 1	-0.46	5.95E-03
NF2	neurofibromin 2	0.27	4.04E-02
NFKBIA	NFKB inhibitor alpha	-0.88	2.29E-12
NKAIN1	sodium/potassium transporting ATPase interacting 1	-0.51	6.87E-03
NKX2-2	NK2 homeobox 2	0.61	1.81E-02
NPAS4	neuronal PAS domain protein 4	2.30	3.83E-02

NPTX1	neuronal pentraxin 1	-0.29	1.65E-02
NR2F1	nuclear receptor subfamily 2 group F member 1	-0.27	1.28E-02
NUMBL	NUMB like endocytic adaptor protein	-0.30	1.76E-02
OLFM2	olfactomedin 2	0.28	7.16E-03
OLFML2B	olfactomedin like 2B	-0.77	2.82E-04
OLIG2	oligodendrocyte transcription factor 2	-0.44	2.44E-02
OPALIN	oligodendrocytic myelin paranodal and inner loop protein	-0.42	4.30E-02
OPRL1	opioid related nociceptin receptor 1	-0.54	1.58E-04
OPRM1	opioid receptor mu 1	0.42	4.24E-02
OTOGL	otogelin like	-0.58	3.69E-03
PCDH11X	protocadherin 11 X-linked	-0.70	7.16E-05
PCDH17	protocadherin 17	0.27	2.20E-02
PCF11	PCF11 cleavage and polyadenylation factor subunit	-0.27	1.52E-02
PCYT2	phosphate cytidylyltransferase 2, ethanolamine	0.28	2.20E-02
PDE1A	phosphodiesterase 1A	-0.31	2.95E-02
PDE1C	phosphodiesterase 1C	-0.29	3.83E-02
PDE4B	phosphodiesterase 4B	-0.30	3.10E-03
PDK4	pyruvate dehydrogenase kinase 4	-0.56	1.32E-05
PDZRN4	PDZ domain containing ring finger 4	-0.51	1.24E-02
PER1	period circadian regulator 1	-0.53	4.01E-04
PHYHIPL	phytanoyl-CoA 2-hydroxylase interacting protein like	-0.28	1.11E-02
PI4KAP2	phosphatidylinositol 4-kinase alpha pseudogene 2	-0.64	1.32E-02
PIK3CG	phosphatidylinositol-4,5-bisphosphate 3-kinase catalytic subunit gamma	0.56	4.37E-02
PLA2G3	phospholipase A2 group III	1.16	1.33E-02
PLEKHO2	pleckstrin homology domain containing O2	0.49	3.70E-04
PNPT1	polyribonucleotide nucleotidyltransferase 1	-0.33	3.00E-02
POU3F2	POU class 3 homeobox 2	0.27	2.65E-02
PPL	periplakin	-0.44	4.21E-04
PPP1R15A	protein phosphatase 1 regulatory subunit 15A	-0.39	1.11E-02
PPP1R3C	protein phosphatase 1 regulatory subunit 3C	0.77	1.06E-09
PREX2	phosphatidylinositol-3,4,5-trisphosphate dependent Rac exchange factor 2	0.49	5.79E-03
PRKAB2	protein kinase AMP-activated non-catalytic subunit beta 2	-0.29	3.71E-02
PRR18	proline rich 18	-0.79	5.36E-07

PTGIS	prostaglandin I2 synthase	-0.73	8.80E-03
PTK7	protein tyrosine kinase 7 (inactive)	-0.61	2.55E-03
PTPRR	protein tyrosine phosphatase receptor type R	-0.40	2.48E-03
RAB3D	RAB3D, member RAS oncogene family	0.38	1.45E-03
RAPGEF6	Rap guanine nucleotide exchange factor 6	-0.36	3.71E-02
RARA	retinoic acid receptor alpha	-0.37	3.53E-02
RASD1	ras related dexamethasone induced 1	-0.57	6.08E-06
RASL10B	RAS like family 10 member B	0.37	3.83E-02
RELL2	RELT like 2	0.34	1.73E-02
REM2	RRAD and GEM like GTPase 2	-0.97	1.22E-04
RETREG1	reticulophagy regulator 1	-0.26	1.76E-02
RGS1	regulator of G protein signaling 1	-3.05	1.32E-08
RHOB	ras homolog family member B	-0.32	1.45E-03
RHOU	ras homolog family member U	-0.59	5.75E-05
RPRM	reprimo, TP53 dependent G2 arrest mediator homolog	-0.65	2.48E-03
RPRML	reprimo like	-0.47	2.66E-02
RRN3	RRN3 homolog, RNA polymerase I transcription factor	-0.29	2.48E-02
RTN4R	reticulon 4 receptor	-0.33	2.26E-02
RXFP1	relaxin family peptide receptor 1	-0.33	2.88E-03
RYR1	ryanodine receptor 1	0.32	1.85E-02
S100A1	S100 calcium binding protein A1	0.43	2.36E-03
SCG2	secretogranin II	-0.26	4.13E-02
SCN4B	sodium voltage-gated channel beta subunit 4	0.44	5.24E-03
SCRG1	stimulator of chondrogenesis 1	0.56	1.31E-06
SEMA3E	semaphorin 3E	-0.58	1.04E-05
SEMA4C	semaphorin 4C	-0.44	6.44E-04
SERPINE1	serpin family E member 1	-2.09	2.36E-06
SERPINF1	serpin family F member 1	-0.36	6.87E-03
SERPINH1	serpin family H member 1	0.68	4.81E-03
SETD4	SET domain containing 4	-0.35	3.78E-02
SGK1	serum/glucocorticoid regulated kinase 1	-1.10	3.50E-23
SH2D3C	SH2 domain containing 3C	-0.34	4.35E-02
SH3TC1	SH3 domain and tetratricopeptide repeats 1	-0.59	1.08E-02
SHANK3	SH3 and multiple ankyrin repeat domains 3	0.27	2.59E-02
SHB	SH2 domain containing adaptor protein B	-0.53	1.85E-02
SIM2	SIM bHLH transcription factor 2	1.12	3.50E-03

SIRPB1	signal regulatory protein beta 1	-1.94	1.97E-02
SLA	Src like adaptor	-0.96	6.08E-06
SLAIN1	SLAIN motif family member 1	-0.31	1.62E-02
SLC15A2	solute carrier family 15 member 2	0.29	3.87E-02
SLC19A3	solute carrier family 19 member 3	1.35	9.02E-06
SLC22A10	solute carrier family 22 member 10	-1.03	1.96E-02
SLC31A2	solute carrier family 31 member 2	-0.60	1.54E-03
SLC35E2A	solute carrier family 35 member E2A	-0.80	1.88E-06
SLC35E2B	solute carrier family 35 member E2B	0.58	2.17E-06
SLC4A4	solute carrier family 4 member 4	0.38	1.83E-02
SLC6A10P	solute carrier family 6 member 10, pseudogene	-1.24	2.26E-02
SLC7A1	solute carrier family 7 member 1	0.29	4.21E-03
SNAR-C3	small NF90 (ILF3) associated RNA C3	8.00	1.55E-07
SNCG	synuclein gamma	0.46	1.22E-04
SORCS3	sortilin related VPS10 domain containing receptor 3	-0.29	4.77E-02
SOX18	SRY-box transcription factor 18	1.44	9.16E-06
SOX9	SRY-box transcription factor 9	0.29	4.03E-02
SPACA6P-AS	SPACA6P antisense RNA	1.33	5.03E-03
SPAG6	sperm associated antigen 6	-0.70	5.45E-03
SPHK2	sphingosine kinase 2	0.49	5.95E-04
SPRED2	sprouty related EVH1 domain containing 2	0.29	1.10E-02
SPRY1	sprouty RTK signaling antagonist 1	0.55	1.99E-02
SPRY2	sprouty RTK signaling antagonist 2	0.55	2.27E-07
SPRY4	sprouty RTK signaling antagonist 4	0.73	1.57E-06
SRGN	serglycin	-0.47	4.53E-03
SRSF5	serine and arginine rich splicing factor 5	-0.51	2.85E-05
SRSF6	serine and arginine rich splicing factor 6	-0.34	1.53E-03
SSTR2	somatostatin receptor 2	-0.41	5.09E-04
STARD8	StAR related lipid transfer domain containing 8	-0.67	5.20E-04
STOX1	storkhead box 1	0.27	3.47E-02
SYT15	synaptotagmin 15	0.75	7.97E-03
TFAP2C	transcription factor AP-2 gamma	1.10	4.23E-02
TFAP2D	transcription factor AP-2 delta	-1.85	1.49E-05
THEMIS	thymocyte selection associated	-0.51	3.83E-02
THSD1	thrombospondin type 1 domain containing 1	0.59	4.23E-02

TIPARP	TCDD inducible poly(ADP-ribose) polymerase	-0.66	1.07E-06
TLE4	TLE family member 4, transcriptional corepressor	-0.32	3.10E-03
TLR2	toll like receptor 2	-0.87	2.92E-02
TMEM151B	transmembrane protein 151B	0.25	1.87E-02
TMEM200A	transmembrane protein 200A	0.67	1.53E-02
TMEM220-AS1	TMEM220 antisense RNA 1	1.02	1.69E-02
TMEM229B	transmembrane protein 229B	0.28	4.03E-02
TMEM233	transmembrane protein 233	-0.80	1.69E-02
TMTC2	transmembrane O-mannosyltransferase targeting cadherins 2	-0.33	3.81E-02
TNC	tenascin C	-1.30	3.81E-02
TNFRSF10A	TNF receptor superfamily member 10a	0.97	3.97E-02
TNFSF10	TNF superfamily member 10	0.69	1.95E-02
TOMM34	translocase of outer mitochondrial membrane 34	0.39	6.16E-04
TPD52L1	TPD52 like 1	0.40	1.81E-03
TRH	thyrotropin releasing hormone	-0.94	3.73E-02
TRIB1	tribbles pseudokinase 1	0.48	3.10E-03
TRIM22	tripartite motif containing 22	-0.37	4.93E-02
TRIM29	tripartite motif containing 29	1.39	1.15E-04
TRIM36	tripartite motif containing 36	0.27	3.58E-02
TRMT9B	tRNA methyltransferase 9B (putative)	-0.40	4.81E-03
TSHZ2	teashirt zinc finger homeobox 2	-0.55	4.49E-03
TSHZ3	teashirt zinc finger homeobox 3	-0.67	2.90E-09
TSPAN1	tetraspanin 1	-1.07	1.02E-02
TSPYL2	TSPY like 2	-0.30	3.00E-02
TUBB2B	tubulin beta 2B class IIb	0.32	1.59E-02
TUNAR	TCL1 upstream neural differentiation-associated RNA	0.63	4.54E-07
U2SURP	U2 snRNP associated SURP domain containing	-0.25	1.73E-02
USP2	ubiquitin specific peptidase 2	-0.62	1.31E-06
WHRN	whirlin	-0.55	2.36E-03
ZC3H7A	zinc finger CCCH-type containing 7A	-0.24	3.58E-02
ZCCHC14	zinc finger CCHC-type containing 14	-0.25	3.87E-02

ZDHHC22	zinc finger DHHC-type palmitoyltransferase 22	-0.28	1.59E-02
ZFP36	ZFP36 ring finger protein	-0.86	1.28E-02
ZFP36L1	ZFP36 ring finger protein like 1	0.58	2.77E-06
ZFP36L2	ZFP36 ring finger protein like 2	0.57	6.44E-04
ZIC2	Zic family member 2	0.45	2.17E-02
ZNF366	zinc finger protein 366	0.92	1.69E-02
ZNF488	zinc finger protein 488	-0.46	1.83E-03
ZNF711	zinc finger protein 711	-0.27	3.90E-02

Supplementary Table 3-6. Complete list of DEGs uniquely identified in brain specimens from living PD patients

Symbol	Gene Name	Fold Change (log2)	Corrected *P*-value
ACAT2	acetyl-CoA acetyltransferase 2	0.32	1.33E-02
ACSL5	acyl-CoA synthetase long-chain family member 5	0.72	3.03E-02
ADI1	acireductone dioxygenase 1	0.33	1.96E-02
AHI1	Abelson helper integration site 1	-0.41	1.70E-02
ALDOC	aldolase, fructose-bisphosphate C	0.35	2.26E-02
ARRDC3	arrestin domain containing 3	-0.54	3.32E-04
BAMBI	BMP and activin membrane bound inhibitor	0.61	4.81E-03
BRINP3	BMP/retinoic acid inducible neural specific 3	-0.34	7.69E-03
C1orf61	chromosome 1 open reading frame 61	0.30	1.83E-03
C1R	complement C1r	-0.44	4.42E-02
C5AR2	complement component 5a receptor 2	-0.96	1.59E-02
CCDC38	coiled-coil domain containing 38	2.01	5.53E-06
CD320	CD320 molecule	0.38	3.64E-02
CHSY1	chondroitin sulfate synthase 1	-0.45	1.62E-03
CIART	circadian associated repressor of transcription	-0.59	3.00E-02
CNTN6	contactin 6	0.67	8.37E-05
CSDC2	cold shock domain containing C2	0.47	3.71E-02
CTAG2	cancer/testis antigen 2	-7.27	5.97E-08
CXADR	coxsackie virus and adenovirus receptor	-0.30	2.78E-02
DCSTAMP	dendrocyte expressed seven transmembrane protein	-1.46	5.24E-03
DPH1	diphthamide biosynthesis 1	-0.33	3.86E-02
DUSP6	dual specificity phosphatase 6	0.72	1.24E-05
EPCAM	epithelial cell adhesion molecule	1.12	3.15E-02
EYA3	EYA transcriptional coactivator and phosphatase 3	0.30	4.75E-02
F2RL3	F2R like thrombin/trypsin receptor 3	-3.06	6.08E-06
FAM134B	family with sequence similarity 134 member B	-0.26	1.76E-02
FAM13B	family with sequence similarity 13 member B	-0.42	2.41E-05
FAM189B	family with sequence similarity 189 member B	0.31	7.69E-03
FAM212B	family with sequence similarity 212 member B	-0.43	1.38E-05
FAM87A	family with sequence similarity 87 member A	-0.88	8.37E-04
FASN	fatty acid synthase	0.24	4.06E-02
FRAT1	frequently rearranged in advanced T-cell lymphomas 1	-0.70	4.01E-04
GADD45G	growth arrest and DNA damage inducible gamma	-2.00	2.97E-16

GALNT14	polypeptide N-acetylgalactosaminyltransferase 14	-0.45	1.82E-02
GDNF	glial cell derived neurotrophic factor	-0.96	1.87E-02
GNG4	G protein subunit gamma 4	-0.38	2.53E-03
GOLGA8S	golgin A8 family member S	-0.86	9.66E-03
GPR123	adhesion G protein-coupled receptor A1	-0.27	1.96E-02
GPR37L1	G protein-coupled receptor 37 like 1	0.37	1.83E-03
GPX3	glutathione peroxidase 3	0.49	3.71E-07
H3F3B	H3 histone family member 3B	-0.33	3.23E-03
HAS2-AS1	HAS2 antisense RNA 1	-1.24	2.45E-02
HERC2P3	hect domain and RLD 2 pseudogene 3	0.81	1.21E-02
HERPUD1	homocysteine inducible ER protein with ubiquitin like domain 1	-0.37	2.42E-03
HRK	harakiri, BCL2 interacting protein	-0.61	3.10E-03
HYAL2	hyaluronoglucosaminidase 2	-0.45	7.16E-03
IDH1	isocitrate dehydrogenase) 1, cytosolic	0.43	3.20E-04
KCNK10	potassium two pore domain channel subfamily K member 10	-0.37	3.58E-02
KGFLP2	fibroblast growth factor 7 pseudogene 3	0.40	1.48E-02
KIAA1456	tRNA methyltransferase 9B	-0.40	4.81E-03
LAMA2	laminin subunit alpha 2	0.51	1.72E-04
LAMB3	laminin subunit beta 3	-0.47	2.20E-02
LCN15	lipocalin 15	-0.96	3.52E-02
LINC00086	small integral membrane protein 10 like 2A	0.29	3.22E-02
LINC00443	long intergenic non-protein coding RNA 443	1.45	1.28E-02
LINC00883	DPPA2 upstream binding RNA	-0.43	5.03E-03
LINC00925	MIR9-3 host gene	-0.42	3.59E-02
LMCD1	LIM and cysteine rich domains 1	0.79	7.02E-03
LMO2	LIM domain only 2	0.74	7.12E-04
LOC100507351	uncharacterized	-0.47	4.16E-02
LOC100507534	uncharacterized	0.69	2.14E-02
LOC100996609	uncharacterized	2.77	1.18E-02
LOC101928358	uncharacterized	-0.78	4.48E-02
LOC101929555	uncharacterized	-0.86	5.95E-03
LONRF1	LON peptidase N-terminal domain and ring finger 1	0.38	1.83E-03
LRRC8C	leucine rich repeat containing 8 family member C	0.34	1.71E-02
MARVELD2	MARVEL domain containing 2	0.76	4.25E-02
MEF2D	myocyte enhancer factor 2D	-0.29	1.95E-02
MICAL3	microtubule associated monooxygenase, calponin and LIM domain containing 3	-0.25	2.58E-02
MIR3648	microRNA 3648-1	2.54	4.18E-05

MIR3687	microRNA 3687-1	2.70	4.90E-06
MMD2	monocyte to macrophage differentiation associated 2	0.51	8.22E-04
MSMO1	methylsterol monooxygenase 1	0.48	9.51E-04
MTRNR2L2	MT-RNR2-like 2	1.46	4.56E-02
N4BP2L1	NEDD4 binding protein 2 like 1	-0.31	2.31E-02
NF2	neurofibromin 2	0.27	4.04E-02
NKAIN1	Na+/K+ transporting ATPase interacting 1	-0.51	6.87E-03
NKX2-2	NK2 homeobox 2	0.61	1.81E-02
NUMBL	NUMB like, endocytic adaptor protein	-0.30	1.76E-02
OPRM1	opioid receptor mu 1	0.42	4.24E-02
PCDH11X	protocadherin 11 X-linked	-0.70	7.16E-05
PCF11	PCF11 cleavage and polyadenylation factor subunit	-0.27	1.52E-02
PCYT2	phosphate cytidylyltransferase 2, ethanolamine	0.28	2.20E-02
PDZRN4	PDZ domain containing ring finger 4	-0.51	1.24E-02
PER1	period circadian clock 1	-0.53	4.01E-04
PHYHIPL	phytanoyl-CoA 2-hydroxylase interacting protein like	-0.28	1.11E-02
PI4KAP2	phosphatidylinositol 4-kinase alpha pseudogene 2	-0.64	1.32E-02
PLEKHO2	pleckstrin homology domain containing O2	0.49	3.70E-04
PNPT1	polyribonucleotide nucleotidyltransferase 1	-0.33	3.00E-02
PRKAB2	protein kinase AMP-activated non-catalytic subunit beta 2	-0.29	3.71E-02
PTGIS	prostaglandin I2 synthase	-0.73	8.80E-03
RAB3D	RAB3D, member RAS oncogene family	0.38	1.45E-03
RARA	retinoic acid receptor alpha	-0.37	3.53E-02
RASD1	ras related dexamethasone induced 1	-0.57	6.08E-06
REM2	RRAD and GEM like GTPase 2	-0.97	1.22E-04
RRN3	RRN3 homolog, RNA polymerase I transcription factor	-0.29	2.48E-02
S100A1	S100 calcium binding protein A1	0.43	2.36E-03
SEMA4C	semaphorin 4C	-0.44	6.44E-04
SETD4	SET domain containing 4	-0.35	3.78E-02
SH2D3C	SH2 domain containing 3C	-0.34	4.35E-02
SHANK3	SH3 and multiple ankyrin repeat domains 3	0.27	2.59E-02
SIM2	single-minded family bHLH transcription factor 2	1.12	3.50E-03
SLC22A10	solute carrier family 22 member 10	-1.03	1.96E-02
SLC6A10P	solute carrier family 6 member 10, pseudogene	-1.24	2.26E-02
SNAR-C3	small ILF3/NF90-associated RNA C3	8.00	1.55E-07
SPACA6P-AS	SPACA6P antisense RNA	1.33	5.03E-03
SPHK2	sphingosine kinase 2	0.49	5.95E-04

SPRY4	sprouty RTK signaling antagonist 4	0.73	1.57E-06
SRSF6	serine and arginine rich splicing factor 6	-0.34	1.53E-03
STARD8	StAR related lipid transfer domain containing 8	-0.67	5.20E-04
SYT15	synaptotagmin 15	0.75	7.97E-03
TFAP2D	transcription factor AP-2 delta	-1.85	1.49E-05
TLE4	transducin like enhancer of split 4	-0.32	3.10E-03
TMEM220-AS1	TMEM220 antisense RNA 1	1.02	1.69E-02
TMEM229B	transmembrane protein 229B	0.28	4.03E-02
TNFSF10	tumor necrosis factor superfamily member 10	0.69	1.95E-02
TOMM34	translocase of outer mitochondrial membrane 34	0.39	6.16E-04
TRIB1	tribbles pseudokinase 1	0.48	3.10E-03
TSHZ3	teashirt zinc finger homeobox 3	-0.67	2.90E-09
USP2	ubiquitin specific peptidase 2	-0.62	1.31E-06
ZC3H7A	zinc finger CCCH-type containing 7A	-0.24	3.58E-02
ZDHHC22	zinc finger DHHC-type containing 22	-0.28	1.59E-02
ZNF488	zinc finger protein 488	-0.46	1.83E-03

Supplementary Table 3-7: Comparative analysis of published idiopathic PD RNA-Seq studies

	Fold Change (log2)*							
	This Study	**Dumitriu et al. (2016)**	**Henderson et al. (2016)**	**Riley et al. (2014)**	**Riley et al. (2014)**	**Riley et al. (2014)**	**Planken et al. (2017)**	**Infante et al. (2016)**
Gene Symbol	**Frontal Cortex**	**Frontal Cortex**	**Cingulate Cortex**	**Unspecified Cortex**	**Substantia Nigra**	**Striatum**	**Skin Fibroblasts**	**Whole Blood**
A2ML1	0.68	**0.48**				**2.57**		
ABI3BP	-0.79		0.68	**-2.33**	**-1.37**	1.70		
ACSBG1	0.40				-1.02	**1.19**	-1.09	
ACSL1	-0.29		0.84			1.15		
ACSS1	0.32					**1.21**	-0.58	
ACSS3	0.44				-1.58	**2.47**		
AHNAK2	0.43					**3.11**		
AKAP12	0.34						**0.56**	
AKR1C1	0.60				**2.12**			
ALCAM	-0.26		0.74					
ALDH2	0.32					**1.48**		
ALDH6A1	0.29				-1.80	**1.73**		
AMOT	0.37					**1.58**		
ANKRD22	-3.19							**-1.24**
ANKRD37	0.53	**0.60**			**1.31**			
APC	0.33					**1.50**		
APOLD1	-1.55					1.02		

AQP1	-1.23		0.87	4.19		1.18		
ARRDC2	-1.06						**-0.88**	
ATOH8	-0.62	0.62						
ATP1A2	0.37				-1.06	**1.72**		
ATP1B2	0.28					**1.42**		
AVPR1A	-1.25		1.17					
AXL	0.35					**1.33**		
BCOR	-0.55				**-1.39**			
BTNL9	0.73					**1.28**		**0.63**
C17orf102	-0.45		**-1.30**		**-3.24**			
CA10	0.28					**1.18**		
CA9	-1.26		**-2.94**	**-1.17**				
CAPN9	-1.61			**-1.19**	**-2.21**			
CBLN2	0.33		-0.90					
CCBE1	0.81		-0.95					
CCDC85C	0.33					**1.01**		
CD44	-0.25		1.84	1.86		5.55		
CDH20	-0.94				-1.46	**1.33**		
CDKN1A	0.29					1.74		
CEBPD	-0.68	0.58		**-1.99**				
CHN2	-0.95			1.10				
CHRM1	-0.44		**-1.46**					
CHRM4	-0.29		**-1.51**		**-3.30**	1.42		
CHST3	-0.44		0.80					
CITED2	-0.73		-0.94					

CLCN5	0.45					**1.19**	
CLDN5	0.39				1.03		**-0.71**
CLEC4E	-0.50						**-1.59**
CLK1	-1.67					**1.32**	
CNGA4	0.60					**1.56**	
CNTN3	-0.65		**-0.60**			1.17	
COL13A1	-0.95	**-0.71**			**-1.26**	1.18	
COL5A1	-0.78					1.56	
COX6A1	0.36						-0.61
CP	-1.16		0.74	1.18		2.22	
CPT1A	0.38					**1.02**	
CREB5	-0.47		0.85		**-1.85**		0.64
CSGALNACT1	-0.29					1.41	
CSN1S1	2.29			**2.03**			-2.47
CSRNP1	-0.75			**-1.01**			
CTXN3	0.89		-1.39		**1.68**		
CX3CR1	0.70			**1.44**	-1.26	**2.83**	
CXXC5	-0.35				**-1.59**	1.57	
DACH1	-0.42			1.51			
DDIT4	-0.67	1.01				2.30	**-0.99**
DDR2	0.70		**1.52**		-2.37	**3.49**	
DFNB31	-0.55			1.29			
ENAH	0.23					**1.32**	
F5	1.02		**1.13**			**1.40**	

FABP3	0.27				**1.27**		
FABP7	0.43					**2.02**	-0.67
FADS2	0.31					**1.91**	
FBLN5	-0.58					1.85	
FBXL19	0.24		-0.97			**1.12**	
FBXO2	0.26	**0.43**				**1.78**	
FGF18	-0.85		**-1.08**	**-1.26**			
FOXC1	1.13			-3.34			
FOXF2	0.99						-0.87
FOXP2	-0.53					1.17	
FOXQ1	1.39				**1.01**		
FPR1	-0.88			1.92	**-1.37**	3.23	**-1.26**
FREM3	0.97		-2.02				
FSTL5	-0.34					1.31	
FZD1	0.47			-1.27		**1.76**	
GAP43	0.29		-0.78		-1.01	**1.31**	
GATC	0.55		**0.75**				
GNA14	0.67				-1.51		
GPR143	0.57					**1.13**	
GRAMD1C	0.31					**1.25**	
GRASP	-0.41		**-0.75**		1.16		
GREM1	-0.49		0.88		**-1.04**		
GREM2	-0.44		**-1.07**				
GRIK3	-0.40					1.65	
GRM7	-0.35		**-0.90**				

HCN4	0.52		-1.31					
HEG1	0.38		1.01			**1.00**		
HES5	1.16				-1.73		-1.14	
HHEX	1.42					**1.18**		
HPCA	-0.25		**-1.02**					
HS3ST4	-0.50			1.80		2.67	0.96	
HSPA1B	0.73	**1.29**			**1.57**	-1.47		
ID1	0.82			-1.10	1.27		-1.32	
ID3	0.72					2.47		
IGFL4	-0.96		**-0.87**					
IL1R2	-2.19	0.92	1.61					**-0.69**
IL1RAPL2	-0.57		**-1.09**					
IP6K3	-0.75		1.07	1.18	**-1.04**			
IRF8	0.69			**1.30**	-1.09	**2.08**		
ISLR	-0.46			**-2.28**				
ISLR2	-0.36		**-0.84**					
ITPR2	0.42					1.85		
ITPRIP	-0.92			**-1.46**		1.23		
ITPRIPL2	0.36					**1.02**		
JAKMIP3	-0.50			1.53	**-2.16**	2.10		
KANK4	1.01		**0.68**					
KCNH8	-0.72			1.36	**-2.88**			0.68
KCNN1	0.26		-0.92					
KIAA1161	0.34				-1.38	**1.31**		
KIF19	-0.61			3.12		1.59		

KLF9	-0.46				1.48		
KLHL14	-0.89	**-1.08**					
KLK5	1.06	-1.59					
KLK7	1.03	-0.80			**1.90**		
KRTAP5-AS1	-0.53	**-1.01**					
L3MBTL4	-0.42			**-1.65**			
LDLR	0.47	**1.03**	-1.10				
LGALS1	0.36				**1.02**	-0.85	
LGR5	-0.59	0.88	1.11	**-1.79**			
LHFPL1	0.93				**1.55**		
LIMK1	0.33	-0.90			**1.22**		
LINC00634	0.44	-0.64					
LOC441081	2.03						-0.86
LPAR5	0.53				**1.44**		
LPAR6	0.91				**1.53**		
LRMP	-0.47				2.52		
LRP4	0.29				**1.20**		
LRRTM2	-0.31			**-1.99**			
LRTM2	-0.39	**-1.32**					
LYNX1	0.27				**1.14**		
MAF	0.28				**1.46**		
MAP4K5	-0.47			**-1.38**			
MARCH1	-0.39						**-0.47**
MARCO	-3.24		**-4.26**	**-1.14**	2.55	**-1.10**	
MCTP2	-0.62				1.45		

MET	-0.93		**-0.98**	**-2.47**	**-1.69**	1.57		
MGAM	-1.25		1.24			1.55		
MGST1	0.53					**1.75**		
MT1F	0.56	**0.82**		**1.77**	**1.87**	**2.24**		
MT1G	0.84	**0.68**		**1.26**	**1.56**	**2.34**	-1.19	
NEFH	0.59		-0.95			**1.46**		
NEFM	0.53		-0.95					
NELL1	-0.46				**-2.31**			
NFKBIA	-0.88	0.53				1.48		
NPAS4	2.30			-2.09		-5.32		
NPTX1	-0.29		**-0.87**					
NR2F1	-0.27				**-1.10**	2.11		
OLFM2	0.28					**1.26**		
OLFML2B	-0.77			**-1.55**	**-1.07**			**-0.56**
OLIG2	-0.44							0.60
OPALIN	-0.42				**-1.58**			
OPRL1	-0.54		**-1.03**					
OTOGL	-0.58		**-0.67**	1.41				
PCDH17	0.27				-1.08	**1.03**		
PDE1A	-0.31				**-1.95**	1.35		
PDE1C	-0.29		0.93		**-2.15**			
PDE4B	-0.30				**-1.19**			
PDK4	-0.56				**-1.26**			
PIK3CG	0.56		**1.00**			**2.27**		
PLA2G3	1.16			-1.28	**3.09**		-0.77	

POU3F2	0.27				**1.22**		
PPL	-0.44	**-0.99**			2.79		
PPP1R15A	-0.39		**-1.95**		**-2.07**		
PPP1R3C	0.77		-1.15				
PREX2	0.49			-1.65			
PRR18	-0.79			**-1.63**			
PTK7	-0.61			**-1.06**	1.62		
PTPRR	-0.40	**-0.82**		**-1.02**			
RAPGEF6	-0.36			**-1.19**			
RASL10B	0.37				**1.33**		
RELL2	0.34	-1.08			**1.67**		
RGS1	-3.05			**-3.46**	3.99		
RHOB	-0.32			**-1.08**		**-0.72**	
RHOU	-0.59	0.77		**-1.47**			
RPRM	-0.65						2.28
RPRML	-0.47	**-0.74**					
RTN4R	-0.33	**-1.06**					
RXFP1	-0.33	**-0.58**	1.44		2.72		
RYR1	0.32			-1.04	**1.57**		
SCN4B	-0.26	-0.95					
SCRG1	0.44				**1.77**		
SDPR	0.56				1.13		
SEMA3E	-0.86		1.15		1.17		
SERPINE1	-0.58	0.95	**-1.39**				
SERPINF1	-2.09	**-0.84**					

SERPINH1	-0.36	**1.29**	**0.87**	-3.15	**1.57**	-2.44	
SGK1	0.68		0.66		**-1.51**		
SH3TC1	-1.10	0.60				1.25	
SHB	-0.59			1.06			
SIRPB1	-0.53				**-2.12**	3.36	-1.10
SKAP1	-1.94				**1.51**		
SLA	-0.96					2.38	
SLAIN1	-0.31				**-1.20**		
SLC15A2	0.29				-1.12	**1.53**	
SLC19A3	1.35	**0.48**					
SLC31A2	-0.60				**-1.22**		
SLC35E2	-0.80					1.35	
SLC35E2B	0.58				-1.14		
SLC4A4	0.38			-2.44	-1.56	**1.17**	
SLC7A1	0.29					**1.08**	
SNCG	0.46		-0.83		**1.03**		
SORCS3	-0.29				**-1.19**		
SOX18	1.44				**1.39**		
SOX9	0.29				-1.52	**1.06**	
SPAG6	-0.70	**-0.73**	0.79			3.15	
SPRED2	0.29				-1.10	**1.67**	
SPRY1	0.55				-1.24		
SPRY2	0.55				-1.00	**1.02**	
SRGN	-0.47		0.91			2.28	
SRSF5	-0.51					1.00	

SSTR2	-0.41			**-1.44**				
STOX1	0.27				-1.06	**1.61**		**0.97**
TFAP2C	1.10	**0.77**						
THEMIS	-0.51			2.27				
THSD1	0.59					**1.09**		
TIPARP	-0.66		1.02					
TLR2	-0.87				**-1.31**	2.15		
TMEM151B	0.25		-1.10					
TMEM200A	0.67				-1.65	**2.18**		
TMEM233	-0.80		**-0.83**	1.81				
TMTC2	-0.33		0.85		**-1.92**			
TNC	-1.30		1.66	2.56	**-1.70**	4.44		
TNFRSF10A	0.97		**1.07**					
TPD52L1	0.40	**0.55**				**1.27**		
TRH	-0.94			**-1.44**	**-1.89**			
TRIM22	-0.37		0.86			1.38		
TRIM29	1.39			-1.82	**1.42**	**3.17**		
TRIM36	0.27					**1.07**		
TSHZ2	-0.55					1.67		
TSPAN1	-1.07					1.55		
TSPYL2	-0.30		**-0.69**					
TUBB2B	0.32					**1.00**		
TUNAR	0.63		-1.18					
U2SURP	-0.25				**-1.02**			
ZCCHC14	-0.25					1.01		

ZFP36	-0.86	**-2.42**	**-1.16**	1.70
ZFP36L1	0.58			**2.43**
ZFP36L2	0.57			**1.62**
ZIC2	0.45	-1.23		
ZNF366	0.92	**2.46**	-1.42	**1.82**
ZNF711	-0.27		**-1.26**	

***Fold change values with corresponding direction of change compared to this study are highlighted as bold text.**

Supplementary Table 3-8 DEGs identified with common directional changes within frontal lobe and peripheral tissues in living PD patients

		Fold Change (log2)		
Symbol	**Gene Name**	**This Study**	**Planken et al. (2017) - Skin Fibroblasts[5]**	**Infante et al. (2016) - Whole Blood[2]**
AKAP12	A-kinase anchoring protein 12	0.35	0.56	
ARRDC2	arrestin domain containing 2	-1.06	-0.88	
CLDN5	claudin 5	-0.49	-0.71	
CLEC4E	C-type lectin domain family 4 member E	-1.67	-1.59	
DDIT4	DNA damage inducible transcript 4	-0.66	-0.99	
FPR1	formyl peptide receptor 1	-0.87	-1.26	
MARCO	macrophage receptor with collagenous structure	-3.24	-1.10	
RHOB	ras homolog family member B	-0.31	-0.72	
SIRPB1	signal regulatory protein beta 1	-1.94	-1.10	
ANKRD22	ankyrin repeat domain 22	-3.18		-1.24
BTNL9	butyrophilin like 9	0.74		0.63
IL1R2	interleukin 1 receptor type 2	-2.19		-0.69
MARCH1	membrane associated ring-CH-type finger 1	-0.38		-0.47
OLFML2B	olfactomedin like 2B	-0.77		-0.56
STOX1	storkhead box 1	0.27		0.97

Supplementary Table 4-1 Primers used for qPCR validation of ASEs

Transcript	Direction	Primer Sequence	Predicted Product Length (bases)
AXIN2 AS (Exon 7)	Forward	GAAGCATGTCCACCACCACT	208
	Reverse	TTTGGGCAAGGTACTGCCTC	
AXIN2 NS (Exons 9-10)	Forward	GGACAGGAATCATTCGGCCA	100
	Reverse	ACCTGCCAGTTTCTTTGGCT	
CLK1 AS (Exon 5)	Forward	AAAGAGACCATGAAAGCCGGT	140
	Reverse	TTTCCTTCGGTGACTCTTCCC	
CLK1 NS (Exons 9-11)	Forward	GTCTGACTACACAGAGGCGT	179
	Reverse	GGGACCACCCTAGGGCTAAA	
FOS AS (intron 2.3)	Forward	GGTGGAACAGGTGAGGAACTCTAGC	168
	Reverse	GAGTTGGGATGGAATGGGCTT	
FOS NS (exon 1)	Forward	CCTAACCGCCACGATGATGT	117
	Reverse	TCTGCGGGTGAGTGGTAGTA	
SERPINH1 AS (Exon 2.2)	Forward	AGTAGAATCGTGTCGCGGCT	97
	Reverse	CTCAGAGGGAGGTCAATGCC	
SERPINH1 NS (Exon 3)	Forward	TGGTGCACGCAAACCACT	505
	Reverse	TTGGAGTGCTCGCAGTTGTA	

Abbreviations: AS, alternatively spliced; NS, Non-spliced.

Supplementary Table 4-2 – significant ASEs identified by SpliceSeq (*p*<0.01)

Gene	RPKM Control	RPKM PD	Splice Type	Exons	dPSI	Magnitude	*P*-value
ABCC5	10.64	10.23	ES	7.3:7.4	-0.077	0.05	8.63E-03
ABCC5	10.64	10.23	ES	24	0.018	0.95	9.05E-03
ABCD3	12.57	12.8	ES	3	-0.021	0.35	3.74E-03
ABCG1	5.74	4.93	AD	16.2	-0.093	0.98	3.11E-03
ABI2	28.15	26.33	ES	5.1:5.2:5.3	0.005	1	8.74E-03
ACAD9	9.48	9.6	AD	1.2	-0.065	0.63	4.27E-04
ACOT8	13.03	15.06	AA	6.1	-0.031	0.81	9.49E-04
ACSS1	12.34	16.38	ES	12.2:13:14:15.1	-0.002	1	8.30E-03
ADAM11	16.52	15.88	AD	9.2	0.040	0.72	7.90E-03
ADAMTS10	3.11	2.86	AP	1	-0.128	0.17	2.41E-03
ADAMTS16	0.29	0.31	AT	23	-0.229	0.91	2.64E-03
ADAMTS16	0.29	0.31	AT	11.2	0.229	0.43	2.64E-03
ADAMTS4	3.9	2.93	AT	2.4	0.070	0.06	1.47E-04
ADAMTS4	3.9	2.93	AT	8	-0.070	0.55	1.47E-04
ADHFE1	4.78	6.16	AA	11.1	-0.159	0.91	8.59E-03
AFAP1	4.77	3.99	AP	2.1	-0.155	0.1	7.86E-04
AFAP1	4.77	3.99	AP	1	0.155	0.27	7.86E-04
AFMID	9.12	9.29	ES	5:6:10:11.1:12	-0.076	0.37	7.07E-03
AHDC1	4.88	4.33	ES	3	0.177	0.87	2.20E-03
AK2	10.96	11.63	AT	10	0.073	0.47	1.00E-04
AK2	10.96	11.63	AT	8.2	-0.074	0.73	3.68E-05
AKAP17A	4.96	4.9	ES	4.3	-0.172	0.59	7.02E-05
AKAP17A	4.96	4.9	AD	4.2:4.3	-0.161	0.71	4.79E-03
AKAP17A	4.96	4.9	RI	4.2	0.116	0.66	7.47E-03
AMY2B	9.65	7.59	ES	10	-0.026	0.99	8.57E-03
ANK3	17.65	17.45	ES	5:6:7:8:9:10:11:12:13:14:15:16:17:18:19:20:21:22:23:24:25:26:27:29.1:30:31:32:33:34:35:36:37:38:39:40:41	0.145	0.01	7.69E-04
ANKH	31.86	31.69	AT	13.3	0.006	0.34	4.40E-04
ANKH	31.86	31.69	AT	2	-0.006	0	4.39E-04
ANKRD49	2.05	1.82	AD	2.5:2.6	-0.249	0.61	4.75E-03
ANKRD54	6.31	6.56	ES	8	0.014	1	4.20E-03
APBB1	111.61	106.78	AP	2	-0.030	0.32	5.02E-03
APOL2	26.13	23.7	AP	2.1	0.090	0.25	3.80E-03
APOL2	26.13	23.7	AP	1	-0.090	0.03	3.80E-03
APOLD1	12.74	12.38	AT	4	-0.249	1	1.79E-04
APOLD1	12.74	12.38	AT	17	0.249	1	1.79E-04
ARID5A	2.94	2.25	ES	4	0.145	0.95	2.50E-03

ARL13B	1.87	1.77	ES	3.2	0.109	0.53	2.45E-03
ARPC4	54.37	55.55	ES	3	-0.014	0.72	5.97E-03
ARPP21	16.41	16.38	ES	18	-0.074	0.79	7.59E-04
ASCC3	2.32	2.46	AT	4	0.062	0.24	1.14E-03
ASCC3	2.32	2.46	AT	43	-0.062	1	1.14E-03
ATAD1	27.06	27.68	AT	9	-0.004	0	9.89E-03
ATAD1	27.06	27.68	AT	11	0.004	0.93	9.89E-03
ATF5	2.59	2.63	AP	2.1	-0.121	0.28	1.67E-03
ATF5	2.59	2.63	AP	1	0.121	0.14	1.67E-03
ATMIN	13.66	12.85	AP	2	-0.019	0.02	3.41E-03
ATP5J	76.1	86.56	AD	1.2:1.3:1.4	-0.083	0.02	8.57E-03
ATRNL1	28.56	26.92	ES	2:3:4:5:6:7:8.1	-0.003	1	1.89E-03
ATXN2	12.1	12.29	ES	21	-0.049	0.88	8.53E-04
ATXN2	12.1	12.29	ES	24	-0.019	0.67	7.89E-03
ATXN2	12.1	12.29	ES	12	0.016	0.98	8.16E-03
ATXN7L1	1.74	1.3	ES	14	0.160	0.8	7.22E-03
AUTS2	4.31	4.48	ES	13	0.118	1	7.59E-04
AXIN2	3.7	3.04	ES	7	0.246	0.5	8.36E-04
BAHD1	4.78	4.31	AP	2	-0.060	0.21	5.01E-03
BAHD1	4.78	4.31	AP	1	0.060	0.02	5.01E-03
BAZ2A	5.81	5.99	AP	2	0.169	0.11	6.45E-03
BAZ2A	5.81	5.99	AP	1	-0.169	0.08	6.45E-03
BBS1	10.3	9.88	ES	4	-0.009	1	6.86E-03
BCAR1	10.73	9.7	ES	09:10.1	0.016	0.89	2.96E-03
BCKDHA	10.05	10.75	AP	1	-0.119	0.21	2.45E-03
BCKDHA	10.05	10.75	AP	2.1	0.119	0.23	2.45E-03
BCLAF1	28.24	24.53	AA	5.1	-0.009	1	7.06E-03
BOD1	14.56	14.05	ES	3	0.019	1	1.64E-05
BSCL2	132.42	131.08	ES	5	-0.001	0.98	6.61E-03
BTAF1	5.14	4.51	ES	25:26.1	-0.057	0.85	8.01E-03
C11orf30	2.53	2.19	AT	22	-0.074	1	7.60E-05
C11orf30	2.53	2.19	AT	4.2	0.074	0.37	7.60E-05
C12orf10	18.03	20.41	ME	3|4	-0.074	0.21	6.07E-03
C14orf23	1.69	1.68	AT	4	0.061	0.68	4.29E-03
C14orf79	3.93	3.39	ES	2.4	0.032	0.76	9.99E-03
C14orf80	2.54	3.14	AP	1	-0.036	0.05	9.73E-03
C1orf50	4.95	5.22	RI	1.2	-0.104	0.41	7.28E-03
C1orf63	12.07	14.33	ES	5.1:5.2:5.3	-0.439	0.2	3.76E-04
C3orf17	7.19	6.89	AD	3.2	-0.052	0.65	9.05E-03
C3orf38	4.68	4.83	AA	3.1	0.008	1	1.47E-03
C5orf63	0.49	0.49	ES	4	-0.126	1	9.36E-03
C6orf203	10.75	11.76	ES	1.2:2	-0.033	0.4	2.53E-03
C6orf211	8.78	8.26	ES	2	0.013	0.77	4.86E-03
C7orf63	0.74	0.73	ES	8	0.134	1	9.11E-03

CACNA1G	4.03	3.57	AA	31.1	0.026	0.85	7.00E-03
CACNB2	11.66	11.49	AP	6	-0.059	0.58	2.38E-03
CAD	2.62	2.6	ES	13	0.146	0.89	9.52E-03
CALU	12.49	13.78	ES	2	-0.095	0.48	4.11E-03
CAMK1	26.59	25.86	ES	11	0.003	1	3.19E-03
CAMTA1	19.38	19.17	AT	26	-0.046	1	4.83E-03
CAMTA1	19.38	19.17	AT	5	0.042	0.62	5.55E-03
CARF	3.54	3.1	AA	4.1	-0.232	0.14	9.24E-03
CASP6	0.58	0.66	ES	2:03	-0.400	0.36	3.46E-03
CBR1	44.17	39.83	AA	3.1	0.101	0.08	9.50E-03
CBX7	31.59	32.41	AA	5.1	-0.010	1	8.10E-03
CBY1	5.94	6.49	ES	2	-0.089	0.64	2.27E-03
CCBL1	5.53	5.55	ES	2:03	0.087	0.36	1.88E-04
CCBL1	5.53	5.55	ES	3	0.141	0.13	8.77E-03
CCDC107	7.44	7.17	RI	3.8	-0.055	1	7.56E-03
CCDC25	20.05	20.84	ES	7	0.026	1	7.41E-03
CCDC57	2.1	1.82	AT	22	-0.072	1	6.49E-03
CCDC65	1.46	1.38	AT	9	-0.050	1	9.55E-03
CCDC65	1.46	1.38	AT	8.2	0.050	1	9.55E-03
CCDC66	2.32	2.07	ES	13	-0.094	0.97	8.46E-03
CCDC66	2.32	2.07	AT	8	-0.134	0.11	1.51E-03
CCDC74A	2.83	2.8	AA	3.3	0.140	0.83	4.82E-03
CCDC74B	1.04	1.56	AA	3.3:3.4	0.187	0.98	6.42E-03
CCL28	0.66	0.54	ES	4	-0.063	0.84	2.87E-03
CCND3	16.11	17.26	ES	3.2:4	0.397	0.02	1.17E-03
CCNG2	15.94	14.35	AP	2.1	-0.179	0.03	2.05E-03
CCNG2	15.94	14.35	AP	1.1	0.179	0.05	2.05E-03
CCNI	208.97	227.12	ME	2|3	-0.191	0	9.37E-03
CCNT1	3.08	3.02	ES	7	0.178	0.98	4.27E-03
CCPG1	18.23	18.15	RI	9.4	0.057	0.93	1.20E-03
CDH24	2.34	1.84	ES	9	0.161	0.74	3.53E-03
CDK13	6.02	5.87	AA	13.1	-0.089	1	5.07E-03
CEP192	2.81	2.3	ES	13:14	0.044	0.59	2.94E-03
CHD5	25.5	25.09	ES	40	0.038	0.86	1.64E-03
CHGA	122.42	103.47	ES	6	0.015	1	8.01E-03
CHID1	15.89	16.25	ES	4.2	0.056	0.58	7.52E-03
CHL1	50.25	51	ES	9	0.020	0.63	7.86E-03
CHTF18	1.4	1.18	AD	10.2	-0.149	0.73	1.42E-03
CIRBP	92.61	84.54	AD	9.4:9.5:9.6	-0.219	0.05	6.08E-03
CIRBP	92.61	84.54	ES	9.5:9.6	-0.271	0.18	2.79E-03
CLK1	12.22	17.41	AP	1	0.408	0.31	7.07E-03
CLK1	12.22	17.41	ES	5	0.087	0.4	5.57E-05
CLK3	7.19	8.48	AP	1	0.061	0.02	7.38E-03
CLK3	7.19	8.48	ES	5	-0.083	0.77	1.22E-05

CLK3	7.19	8.48	AP	2	0.083	0.12	7.38E-03
CLK4	6.58	6.8	ES	2.3:3	0.153	0.87	9.04E-04
CLK4	6.58	6.8	RI	2.2	-0.327	0.48	3.64E-05
CNOT2	10.82	10.18	RI	11.3	0.010	0.88	1.11E-04
CNOT2	10.82	10.18	ES	3.2	0.048	0.84	3.20E-03
CNR1	7.22	6.06	AP	1.1	-0.061	0.57	3.34E-03
CNTN1	81	77.78	AP	1	-0.045	0.41	8.21E-03
CNTN1	81	77.78	AP	2	0.045	0.09	8.21E-03
CNTROB	3.64	3.53	AA	18.1	-0.114	0.77	7.35E-03
COA1	13.76	15.69	AT	7.2	0.090	0.85	5.54E-03
COL24A1	2.13	2.17	ES	55:56:00	-0.109	0.91	5.79E-03
COMMD4	9.73	9.72	AT	10	-0.085	0.1	3.99E-03
COMMD4	9.73	9.72	AT	9.2	0.085	0.34	3.99E-03
COX15	8.03	8.55	AT	10	-0.015	1	7.12E-03
COX15	8.03	8.55	AT	9	0.015	0.9	7.12E-03
CPEB2	10.96	10.73	ES	6	-0.024	0.95	1.74E-03
CREBRF	8	7.23	AA	2.1	0.033	0.48	3.55E-03
CRELD1	24	23.16	ES	10	0.013	1	5.60E-03
CTNNA2	49.95	50.42	AP	16	0.006	0	9.27E-03
CTNNAL1	3.06	3.15	AA	21.1	0.028	1	7.18E-03
CX3CR1	1.4	2.66	AP	3	0.011	0.03	8.74E-03
DAPK1	11.83	11.67	ES	24	0.016	1	5.85E-03
DDAH1	54.19	61.05	AP	4	-0.009	0.01	4.59E-03
DDX11	1.57	1.53	RI	29.2	0.140	0.77	6.40E-03
DDX49	8.56	8.93	AA	10.1	0.009	0.89	8.68E-04
DENND3	4.04	3.65	AA	2.1	-0.114	0.42	7.92E-03
DHX32	6.04	5.45	ES	4.2	0.012	1	6.98E-03
DIDO1	3.95	3.86	AP	1	-0.137	0.34	2.39E-03
DIDO1	3.95	3.86	AP	2.1	0.137	0.68	2.39E-03
DNAJC16	6.03	5.75	ES	2	0.049	0.61	3.30E-03
DNAJC27	5.22	5.61	ES	5	-0.057	0.89	2.74E-03
DNPH1	13.13	14.29	RI	3.2	-0.036	0.85	2.35E-03
DPAGT1	5.23	4.96	ES	3	-0.045	0.77	8.87E-03
DPF2	9.93	10.51	ES	7	-0.079	1	4.39E-03
DPP8	14.83	15.14	ME	17|19	-0.008	0.13	9.13E-03
DPP8	14.83	15.14	ES	17	-0.063	0.81	3.28E-03
DTNA	27.64	31.38	AP	1	-0.013	0.15	8.70E-03
DTNA	27.64	31.38	ES	31	-0.038	0.25	5.30E-03
DYM	10.24	9.83	AA	15.1	0.030	0.72	5.42E-03
E2F6	4.5	4.58	ES	2:03	-0.180	0.24	5.75E-03
ECHDC2	2.32	2.34	ES	04:05.1	-0.122	0.34	3.59E-03
EEF1D	25.22	25.92	ES	8.3:9:10.1:10.2:11:12.1:12.2:13.1	0.030	1	2.43E-03
EEF1D	25.22	25.92	ES	8.3:10.1:10.2:11:12.1:12.2:13.1	0.004	0.19	1.76E-03
EEF1D	25.22	25.92	ES	8.3:9:10.1:10.2:11:12.2:13.1	0.162	0.04	7.57E-03

EEF1D	25.22	25.92	ES	8.3:9:10.1:11:12.1:12.2:13.1	0.298	0.02	9.46E-03
EEF1E1	17.95	17.62	AT	5	-0.014	0.03	3.12E-03
EFCAB6	0.6	0.55	ME	2|3	0.450	0.44	4.24E-03
EML3	3.46	3.41	AP	1	-0.096	0.33	1.67E-03
EML3	3.46	3.41	AP	2.1	0.096	0.14	1.67E-03
EPB41L1	50.89	53.41	ME	7|3	0.159	0.04	5.53E-03
EPS15	49.68	46.27	AP	13	-0.107	0.02	8.11E-03
EPS15	49.68	46.27	AP	1	0.107	0.07	8.11E-03
ERBB2	1.44	1.6	ES	5	-0.131	0.36	4.93E-03
ERBB3	5.42	4.47	AP	24.1	-0.047	0.07	2.42E-03
ERGIC1	12.72	12.53	ES	5	-0.012	1	4.76E-03
ERO1LB	3.55	3.12	AT	7.2	0.040	0.17	8.16E-03
ERO1LB	3.55	3.12	AT	16	-0.040	1	8.16E-03
ESRRA	8.9	10.84	AP	2	-0.029	0.05	8.03E-03
ESRRA	8.9	10.84	AP	1	0.029	0.59	8.03E-03
F3	25.48	26.36	ES	5	0.021	1	1.58E-03
FAAH	10.66	9.54	ES	2	0.010	0.61	5.58E-03
FAIM	3.54	4.05	ME	4|3	-0.233	0.33	7.08E-03
FAM131A	38.66	38.57	AP	5	0.024	0.09	7.40E-03
FAM13A	7.37	6.53	AA	16.1	-0.074	1	6.73E-03
FAM13C	11.31	10.3	AA	14.1	-0.094	0.91	1.64E-03
FAM214A	4.91	4.15	AD	12.2	0.144	0.76	4.92E-04
FAM222B	1.6	1.85	ES	08:09.1	-0.285	0.22	3.27E-03
FAM3A	8	8.68	AA	5.2	0.044	1	5.22E-03
FASTK	15.2	15.82	RI	5.1	-0.025	1	2.48E-03
FASTK	15.2	15.82	AD	3.2	0.015	0.9	3.98E-03
FDFT1	48.55	53.92	AA	8.1	0.003	1	6.84E-03
FGF12	36.14	35.77	AP	4	0.034	0.2	6.59E-04
FGF12	36.14	35.77	AP	2	-0.034	0.43	5.37E-04
FGF5	0.37	0.35	ES	2	-0.217	0.85	1.27E-03
FKBP5	13.08	10.03	AT	10.2	0.019	0.03	7.13E-03
FKBP5	13.08	10.03	AT	13	-0.019	1	7.13E-03
FLCN	8.84	7.39	AT	14	-0.077	1	3.94E-03
FLCN	8.84	7.39	AT	8.2	0.077	0.42	3.94E-03
FLJ27365	0.16	0.17	AT	8.2	-0.141	1	7.05E-03
FLJ27365	0.16	0.17	AT	6	0.141	1	7.05E-03
FN1	7.84	8.98	ES	40.2	-0.163	0.41	4.29E-04
FN1	7.84	8.98	AA	40.2:40.3	-0.097	0.35	4.63E-03
FN1	7.84	8.98	AA	40.1	0.073	0.95	5.90E-03
FNBP1L	4.84	4.74	ES	10:11	-0.186	0.79	2.14E-03
FNTA	20.77	20.68	AP	2	0.027	0.01	8.08E-03
FNTA	20.77	20.68	AP	1	-0.027	0.27	8.08E-03
FNTB	4.89	4.82	AP	4	-0.053	0.54	6.97E-03
FNTB	4.89	4.82	AP	1	0.053	0.85	6.97E-03

FOLH1	8.68	6.74	ME	3|4	0.032	0.08	5.45E-03
FOLH1	8.68	6.74	ES	4	-0.118	0.29	8.11E-04
FOS	2.96	6.61	RI	2.3	0.211	0.8	7.04E-03
FRS2	4.57	5.12	ES	4	-0.162	0.68	9.61E-03
FRYL	5.14	4.84	ES	47	0.043	1	8.42E-03
GALK1	1.96	2.12	RI	4.2	-0.092	0.98	7.64E-03
GBA2	24.04	27.46	RI	14.5	-0.058	0.97	6.70E-03
GDAP2	1.33	1.49	AT	13.2	-0.115	0.42	2.51E-04
GDAP2	1.33	1.49	AT	14	0.115	0.57	2.51E-04
GGACT	0.35	0.5	ES	2	-0.144	0.95	1.51E-03
GMFG	3.2	3.66	ES	3.2:4	-0.047	0.74	7.28E-03
GOLGA6L4	2.43	2.13	RI	6.2	-0.053	1	3.02E-04
GPS2	17.11	17.4	RI	1.2	-0.059	0.31	9.38E-03
GRB2	44.8	43.3	ME	5|6	0.212	0.01	1.02E-03
GSN	34.34	31.27	AP	13	0.011	0.01	4.39E-03
GTF2H2C	6.28	6.53	AT	9	0.003	0.01	3.39E-03
HACL1	6.23	5.56	ES	10	0.021	0.99	7.50E-03
HARS	43.06	42.05	AD	6.2	0.007	0.99	1.19E-03
HENMT1	9.06	7.68	ES	5:06	-0.008	1	6.82E-03
HES2	0.01	0	AT	5	0.617	0.8	7.95E-03
HES2	0.01	0	AT	4.3	-0.617	0.67	7.95E-03
HIPK3	7.63	7.53	ES	14	-0.139	0.69	7.10E-05
HIVEP3	1.26	1.31	AA	9.1	-0.124	0.56	4.77E-03
HMGB1	122.01	119.11	AP	3	0.006	0.01	5.78E-03
HMGCR	24.25	28.5	ES	14	0.036	1	1.32E-04
HNRNPUL2	89.31	88.77	ES	12	0.006	0.71	2.35E-03
HOPX	41.7	51.1	ES	1.2:2	-0.036	0.03	3.17E-03
HS1BP3	2.96	3.32	AT	3.2	0.017	0.04	9.19E-03
HSPA14	4.9	4.27	AT	15	-0.070	0.88	5.49E-03
HSPA14	4.9	4.27	AT	4	0.070	0.78	5.49E-03
IFFO1	11.01	10.75	ES	7:08:09	0.150	0.2	3.86E-03
IFNAR2	3.99	4.02	ES	9	0.099	0.87	5.00E-03
IFRD2	2.99	2.97	RI	7.2	-0.133	0.6	7.12E-03
IFT122	7.74	7.08	AA	25.1	-0.093	0.92	9.88E-03
IL32	0.86	0.9	ES	1.4:1.5:1.6:1.7:1.8:1.9	0.089	0.12	4.87E-03
ILF3	21.57	20.65	AA	14.1	-0.027	1	6.17E-03
ILK	19.31	21.88	ES	2:03	-0.010	0.15	3.85E-03
ILK	19.31	21.88	ES	2	-0.045	0.43	1.30E-03
ILK	19.31	21.88	ES	3	0.043	0.9	9.60E-03
ING4	18.1	18	AA	6.1	-0.048	0.65	8.64E-03
INPP5J	4.9	5.22	ES	11	0.023	1	6.04E-03
INPP5K	9.24	9.43	ES	5.1:5.2	0.032	0.82	7.70E-03
IP6K2	12.49	10.63	AD	11.3:11.4:11.5	0.089	0.34	9.52E-03

IP6K3	1.48	0.83	ES	2	0.120	0.76	2.81E-03
IRF7	0.43	0.4	RI	2.4	0.286	0.94	4.24E-03
IRF7	0.43	0.4	ES	4	-0.348	0.9	1.31E-03
JKAMP	16.36	16.12	ES	1.2:2.1	-0.136	0.19	5.62E-03
JKAMP	16.36	16.12	AD	4.2	0.004	1	9.14E-03
JMJD1C	7.07	7.17	AA	17.1	0.028	0.95	9.04E-03
KCNJ6	1.67	1.73	AP	2	0.055	0.05	6.64E-03
KCNJ6	1.67	1.73	AP	1	-0.055	0.84	6.64E-03
KCNQ2	24.49	24.83	ES	9	-0.042	0.87	2.92E-03
KDM6B	2.18	2.1	RI	22.2	0.148	0.76	5.16E-03
KIAA1191	29.6	30.62	ES	2:04	0.194	0.07	8.13E-03
KIAA1191	29.6	30.62	ES	2:4:5:6	0.168	0.1	4.95E-03
KIAA1211	3.12	3.22	ES	4	0.137	0.91	9.68E-04
KIAA1217	6.23	5.11	AP	1	0.108	0.18	2.69E-03
KIAA1324	5.07	4.35	ES	2	0.021	0.55	7.06E-04
KIAA1324L	9.25	8.07	ES	3	-0.047	0.3	9.98E-03
KIAA2013	8.96	10.36	AT	2.2	-0.044	0.29	7.63E-03
KIAA2013	8.96	10.36	AT	3	0.044	1	7.63E-03
KIF12	0.55	0.61	ES	15	0.200	0.78	7.84E-03
KIF13A	4.26	4.31	AT	41.2	-0.019	0.06	2.13E-03
KIF1B	40.69	44.11	ES	16:17.1	-0.041	0.86	8.68E-03
KIF21A	45.71	47.91	ES	30:32:00	-0.032	0.4	6.37E-03
KIF22	4.8	4.42	AD	1.2:1.3	0.032	0.45	6.64E-04
KITLG	6.67	8.18	ES	6	0.027	0.88	2.72E-03
KLC1	217.72	201.57	ES	15:16	0.114	0.01	7.24E-03
KMT2E	14.76	13.78	ES	26	0.127	0.61	4.31E-04
LCORL	1.59	1.67	AT	8	-0.054	0.67	9.31E-03
LCORL	1.59	1.67	AT	9	0.054	0.97	9.31E-03
LDB2	33.12	34.78	ES	9.2:11.1	-0.067	0.36	4.60E-03
LENG8	17.51	14.31	ES	1.2:2	-0.042	0.55	1.27E-03
LEPROTL1	11.23	10.97	AP	1	0.006	0.62	9.74E-03
LEPROTL1	11.23	10.97	AP	2	-0.006	0	9.73E-03
LGALS1	88.66	112	ES	3	0.002	1	1.22E-03
LIMA1	2.2	2.4	AP	4.1	0.067	0.25	7.03E-03
LMO4	128.89	143.55	AP	1	-0.028	0.46	1.04E-03
LMO4	128.89	143.55	AP	2	0.028	0.08	1.04E-03
LONRF1	5.83	7.63	ES	7	-0.114	0.8	1.53E-03
LPHN2	10.04	9.57	AP	4	-0.054	0.01	9.23E-03
LRRC20	6.15	6.53	AP	2	0.097	0.02	5.48E-03
LRRC20	6.15	6.53	AP	1.1	-0.032	0.35	5.48E-03
LRRC20	6.15	6.53	ME	4|5	0.032	0.27	4.08E-03
LTBP1	1.84	1.73	AP	1	-0.076	0.06	1.58E-03
LTBP1	1.84	1.73	AP	5.1	0.076	0.66	1.58E-03
LUC7L	15.17	13.11	RI	1.2	0.143	0.31	3.71E-04

LYRM9	15.55	11.64	RI	6.2:6.3:6.4	0.032	0.99	5.80E-03
LYST	2.92	2.77	ES	29	-0.053	0.98	4.92E-03
MAATS1	1.07	0.8	ES	2	0.193	0.56	1.51E-03
MAF1	21.09	21.56	AP	1	0.017	0.46	5.04E-03
MAF1	21.09	21.56	AP	2	-0.017	0.01	5.04E-03
MAGOH	17.52	17.45	ES	3	-0.033	1	2.00E-03
MAP3K9	7.29	8.38	AD	9.2	0.074	0.65	1.07E-03
MAP4	39.01	42.87	ES	15	0.046	1	6.91E-03
MAP4	39.01	42.87	ES	19	0.064	0.69	7.51E-03
MAP7D2	32.55	32.63	AA	9.1	-0.026	0.7	7.69E-03
MAPK8	17.14	16.42	ES	07:11.1	0.003	1	7.43E-03
MAPK8	17.14	16.42	ES	08:11.1	0.021	0.19	9.25E-03
MARK2	12.73	11.96	AP	2	-0.008	0.01	5.79E-03
MATR3	155.37	136.93	ES	8	0.004	0.59	3.42E-03
MATR3	155.37	136.93	AD	7.2	0.094	0.02	5.11E-03
MBD1	9.83	9.68	RI	18.2:18.3	0.062	1	7.02E-03
MBD4	8.88	8.43	AD	7.2	0.029	0.88	6.66E-03
MCRS1	14.54	14.48	ES	2	0.037	0.73	3.34E-03
MDFIC	1.36	1.47	AT	6	0.044	1	1.66E-03
MDFIC	1.36	1.47	AT	3	-0.044	0.15	1.66E-03
ME1	11.92	13.89	ES	2:03	0.010	0.95	4.50E-03
MED12L	1.92	2.21	AT	44	-0.009	1	5.23E-03
MED12L	1.92	2.21	AT	15.2	0.009	0.02	5.23E-03
MED6	9.27	9.03	AA	5.1	-0.021	0.78	5.75E-03
METTL21A	4.06	4.33	AA	8.1	0.066	1	9.41E-04
METTL8	1.84	1.92	ME	3|2	0.195	0.29	4.34E-03
MID1	1.54	1.97	AP	3.1	0.119	0.45	8.42E-03
MINK1	30.07	30.07	ES	19	-0.022	0.49	6.51E-03
MKRN3	0.42	0.63	AT	3	-0.122	0.47	3.20E-03
MLLT10	3.45	2.72	AT	26	-0.077	1	3.28E-04
MLLT10	3.45	2.72	AT	5	0.077	0.71	3.28E-04
MON1B	6.81	7.18	AA	3.1	-0.011	0.94	6.00E-03
MRPL48	10.08	10.11	AT	11.2	-0.012	0.01	3.67E-04
MRPL48	10.08	10.11	AT	13	0.012	0.62	3.67E-04
MRPL49	10.95	11.77	AA	3.1:3.2:3.3:3.4:3.5	-0.005	0.01	1.93E-03
MRPL49	10.95	11.77	ES	3.1:3.3:3.4:3.5	-0.327	1	1.75E-03
MRPL55	7.61	8.22	AD	1.2	-0.065	0.46	4.26E-03
MS4A6A	0.59	0.51	RI	9.2	0.191	1	1.06E-03
MSTO1	5.2	5.11	ES	4.2:5	0.015	0.99	3.98E-03
MT1E	45.53	60.91	RI	2.2	-0.016	1	6.48E-03
MTMR10	13.82	15.39	ES	8	-0.028	0.58	7.99E-03
MUS81	5.88	5.95	AP	2	0.025	0.92	8.53E-03
MUS81	5.88	5.95	AP	1	-0.025	0.05	8.53E-03
MUTYH	1.2	1.3	ES	11:12:13:14:15	0.044	1	6.37E-03

MX1	9.79	9.49	AP	1	0.063	0.02	6.52E-03
NAB2	13.05	11.61	ES	6	-0.010	0.94	8.00E-03
NARFL	7.21	7.19	RI	1.2	0.181	0.06	6.02E-03
NARG2	3.35	3.24	AA	4.1	0.084	0.89	9.40E-03
NASP	16.74	13.25	ES	9	0.112	0.99	4.94E-04
NBPF12	1.66	1.07	ES	24.3:25	0.205	0.58	7.15E-03
NBPF12	1.66	1.07	ES	29:30:31:32:33:34:35:36:37:38:39:40:41:42:43:44:45:46:47:48:49:50:51:52:53:54:55:56	0.059	0.67	1.08E-03
NDRG4	201.26	197.24	AP	2	-0.008	0.03	7.94E-03
NDUFAF5	10.19	10.17	AA	4.1	-0.070	1	6.74E-04
NDUFB6	38.76	41.28	ES	3	-0.180	0.02	3.97E-03
NEDD4L	14.1	13.84	ES	25	-0.040	0.98	8.90E-03
NEK4	7.26	7.54	ES	2.1:2.2	0.009	0.95	1.11E-04
NFATC1	0.5	0.57	AD	10.2	0.285	0.61	3.91E-03
NFU1	17.22	16.46	AD	1.2	0.024	0.42	6.00E-03
NGLY1	8.21	8	ES	7	0.227	0.03	2.84E-03
NIM1	7.61	6.99	AP	2	-0.072	0.15	1.42E-03
NIM1	7.61	6.99	AP	1	0.072	0.3	1.42E-03
NIN	5.37	4.54	ES	29	-0.124	0.9	8.61E-04
NMD3	10.36	10.31	AP	1	-0.020	0.5	6.24E-03
NMD3	10.36	10.31	AP	2.1	0.020	0.02	6.24E-03
NPIPB3	6.74	6.72	AP	8.1	0.155	0.58	9.88E-03
NPIPB4	3.42	2.4	AD	2.2	-0.169	0.41	4.84E-03
NPRL3	7.57	7.43	ES	4:05	0.145	0.75	5.93E-03
NPRL3	7.57	7.43	ES	3:04:05	0.059	0.27	4.23E-03
NR1D2	30.52	27.56	ES	6	-0.011	0.72	2.44E-04
NR2C2AP	2.71	2.59	ES	3	0.104	0.98	2.21E-03
NRP1	3.87	4.53	AT	11.2	0.005	0.02	9.76E-03
NUMA1	19.22	17.53	ES	3:04	0.112	0.01	7.14E-03
NUP98	4.97	4.81	AT	20.2	-0.063	0.38	2.00E-03
NUP98	4.97	4.81	AT	35	0.063	1	2.00E-03
PACSIN1	104.65	104.2	AP	1	-0.044	0.31	1.23E-04
PACSIN1	104.65	104.2	AP	2	0.044	0.27	1.23E-04
PARD3	1.99	2.36	ES	20	0.098	0.64	8.20E-03
PBRM1	4.12	3.95	ES	15	-0.106	0.72	7.68E-03
PCBP2	94.98	92.76	ES	15	-0.056	0.97	9.26E-03
PCBP4	22.35	20.5	AD	9.2:9.3	-0.176	0.07	6.94E-03
PCCB	17.43	18.33	AT	19.2	-0.029	0.23	3.76E-03
PCCB	17.43	18.33	AT	18.2	0.029	0.93	3.76E-03
PDCD4	13.89	13.43	ES	2	0.035	0.59	4.90E-03
PDLIM5	5.63	6.55	AT	3	-0.005	0.01	1.15E-03
PEX5L	20.91	19.41	ME	3|4	-0.058	0.24	6.68E-03
PFKFB3	13.66	13.91	ES	18.1	-0.187	0.45	1.11E-03
PHF15	9.94	8.86	ES	12	0.078	0.54	1.35E-03

PHF20L1	7.21	6.76	AA	6.1	0.414	0.05	1.24E-03
PIGN	2.59	2.43	ES	3	-0.202	0.38	1.28E-03
PIKFYVE	5.82	5.73	ES	3:05	-0.129	0.09	3.83E-03
PIKFYVE	5.82	5.73	ES	3:04	-0.311	0.18	5.27E-04
PLD2	2.54	3.01	RI	18.2	-0.105	0.98	6.08E-03
PLOD2	5.56	5.55	ES	15	-0.072	0.96	1.90E-03
PLSCR1	3.52	3.32	ES	3:04	-0.869	0.04	9.85E-05
PLSCR1	3.52	3.32	ES	3	-0.041	0.74	4.44E-03
PODXL	7.65	8.9	ES	3	-0.075	0.88	8.85E-03
POLK	4.66	4.65	ES	14.1:14.2	0.100	0.95	8.28E-03
POLM	1.27	1.08	AD	9.3:9.4:9.5	0.190	0.56	5.74E-03
POMT1	6.85	6.1	ES	2:03	0.090	0.5	2.28E-03
POU2F2	0.49	0.34	AA	5.1	0.347	1	9.67E-03
POU6F1	8.35	9.19	AP	6.1	-0.078	0.1	5.46E-03
PPAP2C	5.27	4.52	AP	2	-0.040	0.04	7.59E-04
PPAP2C	5.27	4.52	AP	1.1	0.040	0.47	7.59E-04
PPAPDC1B	2.71	2.49	AT	7	-0.039	1	5.08E-03
PPP1R1B	49.78	54.74	AP	1.1	-0.068	0.08	9.90E-03
PPP1R1B	49.78	54.74	AP	2.1	0.068	0.03	9.90E-03
PPP1R7	55.4	55.57	ES	2	0.010	0.55	3.80E-03
PPP1R8	11.55	11.38	ES	4	0.004	1	2.65E-03
PPP2R4	61.2	63.8	ES	3.1:4:5	-0.057	0.04	8.04E-03
PPP2R4	61.2	63.8	ES	3.1	-0.085	0.04	1.38E-03
PPWD1	6.12	6.33	ES	2	-0.041	0.53	9.66E-03
PRDM15	1.13	1.23	ES	2:3:4:5:7:8	0.088	0.12	4.58E-03
PRKAR1A	120.52	114.31	AP	3.1	-0.002	0	2.97E-03
PRKCG	25.42	27.93	RI	19.2	-0.006	0.63	6.37E-04
PRPF4	6.69	6.87	AA	2.1	-0.048	0.76	1.63E-03
PRRX1	1.82	1.91	ES	4	-0.122	0.86	2.89E-03
PRRX1	1.82	1.91	AT	5	-0.032	1	6.55E-03
PRRX1	1.82	1.91	AT	3.2	0.032	0.59	6.55E-03
PSEN2	6.35	6.51	AD	13.3	-0.014	0.68	3.93E-03
PTPN13	4.5	4.73	ES	21	-0.074	0.71	2.51E-03
PTPN5	30.82	25.83	AP	5.1	0.011	0.01	2.90E-03
PTPRA	50.18	47.4	ES	22:23	0.005	1	5.09E-03
PTPRU	5.65	4.41	AA	31.1	-0.020	0.99	2.54E-04
PYCR1	2.2	2.39	ME	6|7	-0.109	0.29	1.93E-03
QKI	69.27	68.82	AT	9	-0.013	0.14	6.18E-03
QKI	69.27	68.82	AT	8.7	0.013	1	6.18E-03
QPCTL	3.13	3.17	ES	3	0.018	1	7.01E-03
RABGEF1	5.05	4.44	ES	5	-0.058	0.22	9.63E-03
RABGGTA	6.53	6.52	RI	1.2:1.3	0.064	0.43	3.86E-03
RABL5	10.47	11.38	ES	3.2	-0.035	0.98	2.12E-03
RAP1GDS1	41.53	43.42	ES	5	0.005	0.31	5.87E-03

RASGRP2	5.73	6.44	AP	1	0.081	0.14	5.52E-03
RBFOX2	23.11	21.33	AP	1	-0.107	0.23	5.99E-04
RBFOX2	23.11	21.33	AP	3	0.107	0.29	5.99E-04
RBM23	13.74	13.05	ES	4	-0.071	0.79	7.56E-03
RBM26	10.74	10.36	AA	13.1	-0.046	0.87	7.56E-03
RBM39	28.99	27.25	ES	9	-0.027	0.63	1.47E-03
RBM39	28.99	27.25	AP	2	0.003	0	9.99E-03
RBM39	28.99	27.25	AP	1	-0.003	0.52	9.98E-03
RBM6	13.7	11.37	AA	3.1	0.048	0.65	3.34E-03
RC3H1	1.53	1.56	AA	18.1	-0.188	0.81	6.92E-03
RELA	5.53	5.3	RI	10.2	0.086	0.87	8.03E-03
RGL3	0.65	0.69	AT	21	-0.135	0.62	5.77E-03
RGL3	0.65	0.69	AT	20	0.135	0.98	5.77E-03
RHOC	14.72	18.21	ES	4	0.015	1	3.24E-03
RHOT2	12.59	12.26	ES	3	0.007	1	8.66E-03
RIOK2	5.05	5.42	AT	8.2	-0.031	0.03	9.72E-03
RIOK2	5.05	5.42	AT	10	0.031	0.59	9.72E-03
RIPK2	2.61	2.37	ES	3	0.175	0.61	1.63E-03
RLTPR	16.27	15.5	ES	36	-0.064	0.83	5.43E-03
RNF10	39.54	39.16	AA	10.1	-0.022	1	1.77E-03
RNF146	13.63	12.94	ES	5.1	-0.079	1	3.34E-03
RNF220	41.77	41.51	AT	17	-0.013	1	5.78E-03
RNF220	41.77	41.51	AT	10.2	0.013	0.1	5.78E-03
RNMTL1	5.2	5.21	ES	2	0.050	1	4.38E-03
RPAIN	16.17	15.53	ME	4|5	0.134	0.29	9.18E-03
RPAIN	16.17	15.53	ES	5	-0.068	0.24	8.34E-03
RPGRIP1L	2.86	2.5	AT	28	0.067	0.86	5.39E-03
RPGRIP1L	2.86	2.5	AT	4	-0.105	0.53	4.42E-03
RPL17	142.11	128.87	AA	3.2:3.3	0.035	0.53	6.85E-03
RPL17-C18orf32	5.06	4.85	ES	6	-0.065	0.67	4.69E-03
RPRD2	9.38	8.78	ES	4	-0.139	0.94	2.44E-04
RPS3	116.41	119.78	ES	4.1:4.2:4.3	-0.325	0	6.39E-03
RPS6KB1	7.17	6.57	RI	14.2	0.018	0.75	5.63E-03
RPS6KL1	7.39	6.84	ES	9	0.160	0.13	5.36E-03
RPS7	103.97	107.42	AA	2.1	-0.005	0.4	2.96E-03
RRNAD1	4.04	3.84	AA	2.1:2.2	-0.021	0.53	9.00E-03
RRNAD1	4.04	3.84	ES	2.1	-0.036	0.8	5.35E-03
RUNX1T1	2.78	3.09	ES	3.2:5:6.2:6.3	0.684	0.03	9.98E-03
S100B	109.57	134.39	ES	3	0.011	1	9.43E-03
SAP30BP	22.44	22.07	AT	5	0.020	0.02	4.01E-03
SAP30BP	22.44	22.07	AT	14	-0.020	0.52	4.01E-03
SART3	11.54	10.56	ES	7	-0.036	0.73	8.42E-05
SCAF11	5.2	5.47	AT	18	0.057	1	8.95E-03
SCD	123.99	144.17	ES	5	0.002	1	8.25E-03

SCMH1	5.09	5.18	ES	6	0.119	0.33	5.31E-03
SCNN1D	2.23	2.32	ES	1.5	-0.143	0.26	2.94E-03
SDC4	19.17	22.15	ES	2	0.013	0.79	4.68E-03
SEC22A	3.27	3.33	ES	3.2:4:5	-0.950	0.02	4.61E-05
SEC22A	3.27	3.33	AA	3.1	0.013	0.98	1.67E-03
SEC31A	16.09	15.92	AA	5.1	-0.058	0.43	3.59E-03
SEMA6D	7.19	6.62	ES	22	0.159	0.66	4.14E-03
SEMA6D	7.19	6.62	ES	23.1:23.2	0.146	0.59	1.53E-03
SEMA6D	7.19	6.62	AA	21.1	-0.140	0.98	4.76E-04
SEPT5	181.4	194.47	AA	11.1	0.004	0.96	1.74E-03
SERPINH1	1.15	2.21	ES	2.2	-0.358	0.57	4.64E-03
SEZ6L2	48.39	47.59	ES	15	-0.041	1	6.57E-03
SGCE	13.21	13.83	ES	10	0.063	1	3.78E-03
SGK1	30.56	11.59	AP	6.1	0.118	0.73	3.74E-03
SGK1	30.56	11.59	AP	1	-0.102	0.28	8.10E-04
SGK2	2.12	1.65	AA	7.1	-0.105	0.72	8.81E-03
SH2D6	0.11	0.12	AA	22.1	-0.130	1	9.13E-03
SIRPA	110.41	101.22	AD	9.2	-0.011	0.7	8.36E-03
SKP1	299.56	299.63	ES	3	-0.004	0.52	2.77E-03
SLC25A46	21.96	21.27	ES	8	-0.009	1	3.80E-03
SLC26A6	0.92	0.93	AA	18.2	-0.363	0.81	2.61E-04
SLC29A3	1.52	1.28	ES	3	0.150	0.85	6.94E-03
SLC35A3	2.84	2.88	ES	3	0.161	0.46	8.72E-03
SLC43A1	0.42	0.4	ES	7:08	0.204	0.97	1.44E-03
SLC52A2	2.86	3.01	AD	1.2:1.3	0.327	0.08	2.43E-03
SLC7A6	2.17	2.05	RI	13.2	-0.096	1	4.63E-03
SLC9A3R1	18.76	23.41	AP	1	0.008	0.96	4.64E-03
SLC9A3R1	18.76	23.41	AP	2.1	-0.008	0.01	4.64E-03
SLCO4A1	2.22	2.09	RI	8.4	-0.199	1	4.56E-04
SLMAP	8.17	7.82	AP	16	-0.075	0.01	4.38E-03
SLMAP	8.17	7.82	AP	1	0.068	0.18	7.81E-03
SMARCA2	39.39	42.05	AP	1	0.097	0.12	8.76E-03
SMARCD3	33.72	37.88	AD	7.2	0.002	0.8	8.60E-03
SMEK1	7.91	7.5	AD	7.2	-0.130	0.74	2.37E-03
SNAP47	24.52	24.8	AP	2	0.054	0.14	9.87E-03
SNAP47	24.52	24.8	AP	1	-0.054	0.01	9.87E-03
SNRPF	14.55	15.57	AT	7	0.017	0.01	9.11E-04
SNRPN	248.68	230.9	AP	3	-0.024	0.04	4.45E-03
SNURF	66.71	86.46	ES	6	0.003	1	6.86E-03
SNX27	11.47	12.36	AA	12.1	0.056	0.94	5.42E-03
SORBS1	16.53	16.43	ES	32.1:32.2:33	0.044	0.8	8.64E-03
SP110	1.53	1.39	ES	20	-0.295	0.14	8.02E-03
SPARCL1	789.54	892.29	ES	11	0.000	1	5.68E-03
SPATA6L	0.83	0.7	ES	3	-0.293	0.47	3.93E-03

SPATA7	5.59	5.49	ES	7:08	-0.038	0.52	9.37E-03
SPECC1	11.31	12	AT	10	-0.092	0.25	9.49E-05
SPECC1	11.31	12	AT	18	0.092	0.61	9.49E-05
SPEG	3.35	3.32	AT	16	-0.044	1	1.70E-04
SPEG	3.35	3.32	AT	48	0.044	1	1.70E-04
SPHK2	9.7	13.57	AP	1.1	0.072	0.1	3.46E-04
SPHK2	9.7	13.57	AP	3.1	-0.072	0.68	3.46E-04
SREBF2	51.77	54.98	ES	10	-0.008	0.73	8.31E-03
SRP19	12.56	11.31	AA	5.1	-0.056	0.98	8.23E-03
SRP68	32.58	33.18	ES	1.2:2.2	-0.314	0.02	5.14E-03
SRSF1	32.77	32.45	AA	3.3:3.4	0.256	1	7.98E-03
SRSF1	32.77	32.45	ES	3.3	0.134	0.19	5.22E-03
SRSF1	32.77	32.45	AD	3.2:3.3	0.027	0.07	4.29E-04
SRSF2	31.14	28.79	RI	2.6	-0.012	1	1.88E-03
SSR2	25.51	26.77	ES	4.1:5:6.1:6.2	-0.178	0.02	1.73E-03
STAT3	11.66	11.82	AA	2.1:2.2	0.074	0.36	3.63E-03
STK24	27.51	29.18	AP	1	0.149	0.26	2.43E-03
STK24	27.51	29.18	AP	2	-0.149	0.15	2.43E-03
STOML2	21.93	22.96	ES	6	0.002	1	2.99E-03
STRAP	78.62	76.97	ES	10	-0.001	1	8.22E-03
STX5	8.66	8.4	AA	12.1	0.015	1	9.62E-03
STX8	17.74	17.94	ES	3:04	-0.022	1	5.14E-03
SULF1	2.84	2.48	AP	1	-0.149	0.12	9.25E-03
SULF1	2.84	2.48	AP	2	0.149	0.36	9.25E-03
SUPT20H	4.46	3.87	ES	26	-0.156	0.98	2.14E-03
SYBU	27.87	24.03	AP	1	0.060	0.16	3.58E-05
TAF1D	14.4	15.69	AA	8.1	0.161	0.44	1.54E-03
TAF5L	3.51	3.71	AT	4.2	0.026	0.39	7.05E-04
TAOK2	17.32	17.62	AT	19	-0.031	0.65	7.94E-03
TAOK2	17.32	17.62	AT	16.3	0.031	0.49	7.94E-03
TATDN3	7.6	7.14	AT	10.2	0.017	1	2.62E-03
TATDN3	7.6	7.14	AT	6.2	-0.017	0.03	2.62E-03
TBC1D3	2.26	1.86	AD	18.2	0.040	0.68	7.47E-03
TBC1D3F	2.41	2.2	AD	11.2	0.042	0.78	8.72E-03
TBXAS1	1.42	1.45	AP	5.1	-0.153	0.25	8.08E-03
TBXAS1	1.42	1.45	AP	1	0.153	0.13	8.08E-03
TCEA1	23.55	23.47	ES	3.2	-0.035	0.73	7.41E-03
THAP9	1.21	1.07	ES	5	-0.959	0.09	1.73E-04
THNSL2	4.02	3.2	ES	10	0.290	0.69	5.60E-03
THNSL2	4.02	3.2	ES	7:08:10	0.053	0.1	2.39E-03
TIA1	9.01	7.48	ES	5:06	-0.256	0.3	6.77E-03
TIA1	9.01	7.48	ES	6	-0.139	0.34	7.27E-03
TMEM107	3.41	3.34	ES	2:3.2:3.4	-0.126	0.42	2.14E-03
TMEM131	6.39	6.15	ES	30	0.027	1	9.36E-03

TMEM184B	22.88	23.2	ES	4.1:4.2:5	-0.015	0.04	2.33E-03
TMEM184B	22.88	23.2	ES	4.1:4.2	-0.288	0.58	9.81E-04
TMEM234	1.63	1.99	RI	5.2:5.3	0.140	1	7.68E-04
TMPO	6.54	5.9	ES	6:07:08	-0.114	0.97	1.42E-03
TNIK	9.82	11.34	ES	22	-0.125	0.64	1.41E-04
TNPO2	38.29	39.82	AP	4	-0.026	0.1	4.12E-03
TNRC6A	7.15	7.11	ES	13	0.156	0.92	1.58E-03
TRAPPC4	16.07	16.98	ES	3.1:3.2	0.017	1	3.99E-03
TRMU	7.84	7.23	AA	6.1:6.2	-0.069	0.84	3.30E-03
TRO	16.2	14.18	ES	3	-0.015	1	3.63E-03
TRPC4AP	26.15	24.13	AA	9.1	-0.061	0.59	6.00E-03
TSC2	12.01	11.48	ES	5	0.006	0.89	5.78E-04
TTC18	0.55	0.46	ES	25	0.152	1	5.50E-03
TTC18	0.55	0.46	AA	15.1	0.071	0.79	4.08E-03
TTC39A	1.74	1.91	AA	10.1	0.106	0.67	7.71E-03
UBE2D3	44.87	48.83	AP	3.1	-0.067	0.13	1.40E-03
UBE2D3	44.87	48.83	AP	2.1	0.056	0.06	3.98E-03
UBE3A	24.51	24.84	ES	5.1:5.2	0.128	0.29	9.35E-05
UBR2	5.39	4.93	ES	43	0.018	1	3.25E-03
UCHL5	21.45	20.59	ES	13.2	-0.178	0.07	3.27E-03
USHBP1	0.53	0.74	RI	3.2	-0.282	0.76	1.98E-03
USP35	4.49	4.38	AP	1	0.082	0.72	9.81E-03
USP35	4.49	4.38	AP	4.1	-0.082	0.14	9.81E-03
USP45	1.93	1.84	AT	22	-0.067	1	5.98E-03
USP53	3.65	3.23	ES	13	-0.036	0.8	7.12E-03
USPL1	5.62	5.52	ES	2	0.167	0.54	8.84E-03
UTP23	4.94	4.64	ES	2.2:4:5.1	-0.348	0.06	8.22E-04
VDAC2	79.93	80.76	ES	7	-0.007	0.85	1.58E-03
WDR20	4.35	4.82	AT	8	-0.032	0.35	2.06E-03
WDR33	6.3	5.74	RI	6.2	0.090	1	7.18E-03
WDR45B	21.88	21.9	ES	3	-0.010	0.96	3.73E-03
WFIKKN2	0.14	0.08	AP	1	0.489	0.48	9.38E-03
WFIKKN2	0.14	0.08	AP	2	-0.489	0.4	9.38E-03
YPEL4	17.76	15.71	RI	1.4:1.5	0.065	0.6	5.87E-03
YWHAE	385.44	394.62	ES	4:05	0.002	1	4.56E-04
ZBTB45	3.73	4.43	AP	1.1	-0.071	0.32	8.84E-03
ZBTB45	3.73	4.43	AP	2	0.071	0.66	8.84E-03
ZGLP1	0.93	0.93	RI	1.4	0.290	0.98	2.03E-03
ZKSCAN3	0.79	0.89	ES	3	0.178	0.94	3.32E-03
ZNF138	1.45	1.37	ES	4.1:4.2:5	-0.257	0.56	8.93E-04
ZNF177	1.27	1.32	AA	18.3	-0.113	0.96	1.69E-03
ZNF189	3.22	3.23	ES	2	0.132	0.37	6.20E-03
ZNF189	3.22	3.23	AA	3.1	-0.121	0.92	1.68E-03

ZNF197	2.92	2.97	ES	3	-0.111	0.61	2.91E-03
ZNF222	1.05	0.86	ES	2	-0.212	1	4.07E-03
ZNF233	1.72	1.52	AT	7.2	0.048	1	3.43E-03
ZNF233	1.72	1.52	AT	6	-0.048	0.24	3.43E-03
ZNF236	2.04	2.13	AP	1	-0.141	0.13	7.97E-03
ZNF236	2.04	2.13	AP	2	0.141	0.35	7.97E-03
ZNF263	3.01	3.19	ES	3:4:5.1:6	0.175	0.93	9.73E-03
ZNF286A	1.95	2.43	RI	1.2:1.3	-0.116	0.5	5.76E-03
ZNF3	3.68	3.76	AP	3	0.081	0.09	2.86E-03
ZNF3	3.68	3.76	AP	1	-0.081	0.51	2.86E-03
ZNF329	4.24	4.05	ES	3:04	0.102	0.14	8.60E-03
ZNF346	4.29	4.36	ES	04:05.1	0.055	1	7.52E-03
ZNF346	4.29	4.36	ES	5.1:5.2:6.2	0.187	0.88	1.84E-03
ZNF346	4.29	4.36	ES	5.1:5.2:6.1:6.2	0.013	0.22	5.97E-03
ZNF385B	10.6	9.63	AP	7	0.012	0.01	1.15E-03
ZNF397	4.06	4.26	AT	6	-0.029	0.45	5.19E-03
ZNF418	1.6	1.4	ES	03:04.1	-0.145	0.5	3.79E-04
ZNF449	1.33	1.47	RI	2.2	0.264	0.96	5.93E-03
ZNF462	2.24	2.3	AA	5.2	0.081	0.68	7.52E-03
ZNF507	3.05	3.03	ES	6	0.023	0.98	3.15E-03
ZNF544	4.27	4.42	ES	7.1:7.2:9:10.1	0.153	0.2	3.89E-03
ZNF550	1.83	1.55	ES	5.1:5.2	0.279	0.73	1.21E-03
ZNF570	1.85	1.9	AP	2.1	0.090	0.39	2.46E-03
ZNF570	1.85	1.9	ES	3	-0.123	0.91	1.79E-03
ZNF570	1.85	1.9	AP	1.1	0.123	0.17	2.46E-03
ZNF606	1.59	1.53	AT	3.2	-0.014	0.08	8.48E-03
ZNF608	2.94	2.78	ES	9	-0.304	0.7	7.97E-03
ZNF615	1.32	1.5	ES	7.1:7.2	-0.239	0.59	4.84E-04
ZNF667	4.21	3.23	ES	9	0.322	0.98	1.59E-03
ZNF667	4.21	3.23	ME	11|9	0.023	0.06	1.08E-03
ZNF714	1.84	2.09	ES	5:6.1:6.2	0.095	0.5	8.08E-03
ZNF76	5.27	4.8	AA	12.1:12.2	0.122	0.52	6.34E-03
ZNF76	5.27	4.8	RI	12.4	0.092	1	2.13E-03
ZNF792	0.16	0.15	AP	3.1	-0.425	0.65	3.47E-03
ZNF792	0.16	0.15	AP	1	0.425	0.82	3.47E-03
ZNF814	0.75	0.81	AT	4.2	-0.044	1	5.45E-03
ZNF836	1.69	1.67	AT	5	-0.114	0.98	5.06E-03
ZNF836	1.69	1.67	AT	4.2	0.114	0.61	5.06E-03
ZNF837	0.33	0.35	AD	2.2	0.263	1	5.67E-03
ZNF846	2.49	2.16	ES	2.1:2.2:3.1:3.2:4.1:4.2	0.614	0.06	7.26E-03
ZSCAN18	25.45	22.1	AA	9.1	-0.033	0.86	9.38E-03

Abbreviations: AD, alternate donor; AP, alternate promoter; AT, alternate terminator, dPSI, delta percent spliced in; ES, exon skipping; RI, retained intron; RPKM, reads per kilobase of transcript per million aligned reads

Supplementary Table 4-3 – significant ASEs identified by DEXSeq (*p*<0.05)

Gene	RPKM Control	RPKM PD	Fold Change (log2)	Ensemble Transcript(s)	Corrected *P*-value
AATK	20.00	14.14	-1.03	ENST00000326724	2.04E-02
ABCA2	6.91	9.37	0.88	ENST00000464876, ENST00000398207, ENST00000476211	2.43E-02
ABCA2	6.91	9.37	0.88	ENST00000464876, ENST00000398207, ENST00000476211	2.43E-02
ABCA8	18.32	20.86	0.39	ENST00000269080, ENST00000586292, ENST00000430352, ENST00000589980, ENST00000586539	2.96E-02
ABHD17A	33.44	35.54	0.19	ENST00000292577, ENST00000250974	2.14E-02
ABHD17B	7.93	10.34	0.77	ENST00000377041	1.40E-02
ABLIM1	18.10	20.59	0.38	ENST00000369266, ENST00000428430, ENST00000369253, ENST00000392952	5.47E-03
ACSL5	4.39	1.82	-2.55	ENST00000369410	1.64E-02
ADAM28	10.47	7.43	-1.00	ENST00000523236	1.56E-02
ADAP1 COX19	50.83	43.91	-0.50	ENST00000344111	2.56E-08
ADIRF AGAP11 FAM25A BMS1P3	15.95	13.49	-0.49	ENST00000437689, ENST00000444431, ENST00000433214	3.33E-02
ADPRH	0.75	3.27	4.24	ENST00000465513	2.80E-02
AGBL3	4.67	1.94	-2.53	ENST00000435976, ENST00000436302, ENST00000275763, ENST00000458078	4.99E-03
AHCTF1	20.88	18.60	-0.34	ENST00000470300, ENST00000326225, ENST00000391829, ENST00000366508	1.63E-02
AHCTF1	20.88	18.60	-0.34	ENST00000470300, ENST00000326225, ENST00000391829, ENST00000366508	1.63E-02
AHDC1	19.93	23.50	0.49	ENST00000374011	7.66E-03
AKAP17A	15.09	12.51	-0.55	ENST00000381261, ENST00000474361	3.22E-03
AKAP9	4.49	2.23	-2.02	ENST00000493453	4.69E-02

ALDH4A1 IFFO2 TAS1R2	18.57	20.84	0.34	ENST00000375341, ENST00000290597, ENST00000432718	2.94E-02
ANKDD1 A PLEKHO2	20.32	24.81	0.60	ENST00000323544, ENST00000502574, ENST00000437723	1.80E-02
ANKDD1A PLEKHO2	22.94	27.57	0.56	ENST00000323544, ENST00000502574, ENST00000437723	9.04E-03
ANKDD1A PLEKHO2	21.54	25.95	0.56	ENST00000323544, ENST00000502574, ENST00000437723	1.34E-03
ANKDD1A PLEKHO2	51.70	59.89	0.53	ENST00000323544	2.86E-05
ANKDD1A PLEKHO2	15.67	13.90	-0.35	ENST00000395720, ENST00000395723, ENST00000487867, ENST00000488082, ENST00000357698, ENST00000380230	1.65E-02
ANKDD1A PLEKHO2	16.81	15.09	-0.32	ENST00000395720, ENST00000395723, ENST00000487867, ENST00000488082, ENST00000357698, ENST00000380230	9.96E-03
ANKDD1A PLEKHO2	21.17	18.79	-0.36	ENST00000487867	1.70E-05
ANKDD1A PLEKHO2	19.82	17.49	-0.37	ENST00000487867, ENST00000380230, ENST00000395723, ENST00000357698	9.92E-04
ANKDD1A PLEKHO2	41.77	38.77	-0.24	ENST00000487867, ENST00000380230, ENST00000357698	6.77E-04
ANKRD32	8.11	11.06	0.90	ENST00000450932	3.51E-02
ANKRD42	7.55	10.19	0.87	ENST00000533342, ENST00000393392	3.95E-03
AP2M1	36.98	39.82	0.24	ENST00000292807, ENST00000382456, ENST00000461733	5.68E-03
AP2M1	26.68	29.23	0.28	ENST00000292807, ENST00000382456	3.57E-03
AP3B2	9.76	16.02	1.45	ENST00000535385	4.10E-02
APC SRP19 ZRSR1	27.20	22.82	-0.53	ENST00000503445, ENST00000512790, ENST00000506997, ENST00000515755, ENST00000505459, ENST00000282999, ENST00000445150, ENST00000515463	5.78E-03
APC SRP19 ZRSR1	32.15	27.65	-0.47	ENST00000520401, ENST00000503445, ENST00000512790, ENST00000506997, ENST00000506987, ENST00000515755,	9.72E-03

				ENST00000505459, ENST00000282999, ENST00000509024, ENST00000445150	
APC SRP19 ZRSR1	33.37	28.56	-0.49	ENST00000515755, ENST00000512790, ENST00000503445, ENST00000520401, ENST00000506987, ENST00000506997, ENST00000505459, ENST00000282999, ENST00000509024, ENST00000445150, ENST00000515463	5.85E-03
APC SRP19 ZRSR1	38.60	33.74	-0.43	ENST00000512790, ENST00000520401, ENST00000506987, ENST00000515755, ENST00000505459, ENST00000504696, ENST00000282999, ENST00000509024, ENST00000445150, ENST00000515463	2.73E-03
APC SRP19 ZRSR1	10.97	7.09	-1.27	ENST00000445150, ENST00000515755	1.78E-02
APC SRP19 ZRSR1	11.67	7.85	-1.15	ENST00000445150	3.06E-02
APC SRP19 ZRSR1	13.99	9.13	-1.25	ENST00000282999	6.75E-03
APC SRP19 ZRSR1	48.98	44.00	-0.37	ENST00000504696, ENST00000520401, ENST00000506987, ENST00000505459, ENST00000282999, ENST00000515463	2.60E-02
APC SRP19 ZRSR1	48.05	43.04	-0.37	ENST00000515463, ENST00000506987, ENST00000504696, ENST00000282999, ENST00000505459	2.94E-02
APC SRP19 ZRSR1	33.02	28.81	-0.43	ENST00000505459, ENST00000282999, ENST00000515463	3.68E-02
APC SRP19 ZRSR1	35.44	30.67	-0.46	ENST00000505459, ENST00000282999	3.56E-02
APH1A	12.23	8.15	-1.18	ENST00000486720	4.61E-03
APH1A	10.72	7.58	-1.01	ENST00000461320, ENST00000486308	2.20E-04
APH1A	11.76	8.25	-1.03	ENST00000486308	1.34E-03
APOL2	18.03	15.06	-0.53	ENST00000358502	4.26E-03
APOL2	18.50	15.47	-0.53	ENST00000358502, ENST00000489186	2.32E-03
APOL2	19.40	16.71	-0.44	ENST00000358502, ENST00000484830, ENST00000489186	3.34E-03
APOLD1 DDX47	89.76	63.65	-1.45	ENST00000356591, ENST00000326765	6.16E-06

APOLD1 DDX47	17.71	10.72	-1.47	ENST00000356591	1.12E-02
APOLD1 DDX47	28.52	29.00	0.05	ENST00000541537, ENST00000358007, ENST00000534843, ENST00000540583, ENST00000426619, ENST00000544400, ENST00000544032, ENST00000352940, ENST00000545038, ENST00000542123, ENST00000544497	2.74E-04
APOLD1 DDX47	33.25	33.78	0.05	ENST00000541537, ENST00000358007, ENST00000534843, ENST00000540583, ENST00000426619, ENST00000544400, ENST00000544032, ENST00000352940, ENST00000545038, ENST00000542123, ENST00000544497	3.25E-10
APOLD1 DDX47	31.62	32.39	0.08	ENST00000541537, ENST00000544400, ENST00000534843, ENST00000545038, ENST00000426619, ENST00000358007, ENST00000544032, ENST00000352940, ENST00000542123, ENST00000544497	8.79E-12
APOLD1 DDX47	36.02	36.82	0.07	ENST00000541537, ENST00000534843, ENST00000545038, ENST00000426619, ENST00000358007, ENST00000542832, ENST00000544032, ENST00000352940, ENST00000392155	3.25E-10
APOLD1 DDX47	29.79	30.55	0.08	ENST00000541537, ENST00000534843, ENST00000545038, ENST00000426619, ENST00000358007, ENST00000542832, ENST00000544032, ENST00000352940	7.04E-07
APOLD1 DDX47	29.36	30.53	0.12	ENST00000541537, ENST00000544400, ENST00000534843, ENST00000545038, ENST00000426619, ENST00000358007, ENST00000542832, ENST00000544032, ENST00000352940, ENST00000542123	1.91E-11
APOLD1 DDX47	23.70	24.66	0.12	ENST00000541537, ENST00000544400, ENST00000534843, ENST00000545038, ENST00000426619, ENST00000358007, ENST00000542832, ENST00000544032, ENST00000352940, ENST00000542123	7.04E-07
APOLD1 DDX47	28.40	29.62	0.13	ENST00000541537, ENST00000358007, ENST00000534843, ENST00000545038, ENST00000544400, ENST00000542832, ENST00000544032, ENST00000352940, ENST00000542123	1.07E-03
APOLD1 DDX47	26.95	27.74	0.09	ENST00000541537, ENST00000358007, ENST00000534843, ENST00000545038,	1.86E-02

				ENST00000544400, ENST00000542832, ENST00000352940, ENST00000542123	
APOLD1 DDX47	28.05	28.33	0.03	ENST00000541537, ENST00000358007, ENST00000534843, ENST00000545038, ENST00000544400, ENST00000542832, ENST00000352940, ENST00000542123	3.51E-02
APOLD1 DDX47	27.88	28.11	0.02	ENST00000541537, ENST00000358007, ENST00000534843, ENST00000545038, ENST00000544400, ENST00000352940, ENST00000542123	2.65E-02
APOLD1 DDX47	33.52	33.38	-0.01	ENST00000358007, ENST00000541537, ENST00000534843, ENST00000542123, ENST00000545038	1.97E-03
APOLD1 DDX47	28.79	28.57	-0.02	ENST00000541537, ENST00000358007, ENST00000534843, ENST00000545038, ENST00000544400, ENST00000535722, ENST00000352940, ENST00000542123	8.34E-07
APOLD1 DDX47	32.42	31.51	-0.09	ENST00000541537, ENST00000534843, ENST00000545038, ENST00000358007, ENST00000535722, ENST00000352940, ENST00000542123	6.75E-05
APOLD1 DDX47	30.99	30.10	-0.09	ENST00000534843, ENST00000545038, ENST00000358007, ENST00000535722, ENST00000352940, ENST00000542123	8.57E-04
APOLD1 DDX47	35.84	36.18	0.03	ENST00000358007, ENST00000352940, ENST00000534843, ENST00000542123, ENST00000545038	1.17E-04
APOLD1 DDX47	44.53	45.64	0.08	ENST00000358007, ENST00000352940, ENST00000534843, ENST00000545038, ENST00000542123	2.47E-08
ARHGAP4 NAA10 L1CAM	9.27	4.97	-1.80	ENST00000496122	5.83E-03
ARHGAP42	9.36	11.70	0.65	ENST00000298815, ENST00000529535, ENST00000524892	2.00E-02
ARHGEF1	15.66	19.60	0.67	ENST00000600387	1.48E-03
ARHGEF10	13.74	16.12	0.47	ENST00000398560, ENST00000398564, ENST00000518288, ENST00000520359, ENST00000349830, ENST00000262112	2.05E-02
ARID4B RBM34	8.85	5.70	-1.28	ENST00000494543, ENST00000471257	2.96E-02

ARRB2	4.22	7.63	1.71	ENST00000575131	6.11E-03
ARRDC2	6.74	9.88	1.11	ENST00000595712, ENST00000600788	3.34E-02
ARRDC2	4.51	7.21	1.36	ENST00000595712	3.01E-03
ASCC3	17.41	13.38	-0.78	ENST00000369143	9.00E-04
AS-LRRK1	10.09	9.33	-0.23	ENST00000558979	2.96E-02
ASPH	13.73	16.56	0.55	ENST00000389204, ENST00000445642, ENST00000517661, ENST00000517903, ENST00000518306, ENST00000541428, ENST00000522343, ENST00000522603, ENST00000517847, ENST00000522349, ENST00000522835	2.14E-02
ASXL1	5.27	1.68	-3.31	ENST00000470145	6.88E-04
ATP1A2	11.62	14.10	0.57	ENST00000468587	3.06E-02
ATP1A3	15.41	17.63	0.40	ENST00000302102, ENST00000545399	4.55E-02
ATP6V0A2	8.61	4.39	-1.95	ENST00000534943	4.71E-04
AXIN1	10.79	14.66	0.90	ENST00000461023	2.93E-02
BAZ2A	4.55	7.56	1.47	ENST00000551812, ENST00000549506, ENST00000379441, ENST00000179765, ENST00000550730	1.47E-02
BAZ2A	2.47	5.10	2.10	ENST00000551812, ENST00000379441, ENST00000179765	9.43E-03
BEX2	80.61	82.11	0.08	ENST00000372674, ENST00000372677, ENST00000536889	4.79E-02
BFAR	20.20	16.67	-0.57	ENST00000562442, ENST00000566520	2.47E-02
BLOC1S6 SQRDL	10.11	6.94	-1.09	ENST00000568816	3.64E-03
BRAF	10.25	12.99	0.69	ENST00000469930	7.57E-03
BRD8	8.11	4.67	-1.60	ENST00000483805	3.95E-02
BRI3	8.76	5.61	-1.29	ENST00000485422	4.93E-02
BRINP3	18.30	20.66	0.36	ENST00000445957	4.70E-02
BRPF3	4.69	2.15	-2.25	ENST00000527657	3.78E-02
C11orf30	8.46	10.90	0.74	ENST00000533988	1.43E-02

C18orf32 SNORD58C SNORD58A RPL17-C18orf32 RPL17 SNORD58B	41.32	44.48	0.25	ENST00000580387, ENST00000581305, ENST00000579408, ENST00000418495	9.46E-04
C18orf32 SNORD58C SNORD58A RPL17-C18orf32 RPL17 SNORD58B	42.16	45.37	0.25	ENST00000580387, ENST00000580210, ENST00000418495, ENST00000579408, ENST00000581305	1.71E-03
C18orf32 SNORD58C SNORD58A RPL17-C18orf32 RPL17 SNORD58B	42.49	45.96	0.26	ENST00000580387, ENST00000581305, ENST00000607313, ENST00000418495, ENST00000579408, ENST00000580210	2.73E-03
C1orf27	8.05	5.43	-1.14	ENST00000478571	1.47E-02
C1orf63	25.85	30.95	0.56	ENST00000498238, ENST00000570063, ENST00000568212	1.77E-02
C3orf14	64.34	61.47	-0.17	ENST00000494481	6.10E-03
C3orf17	7.94	5.18	-1.24	ENST00000496206, ENST00000472637, ENST00000469809, ENST00000491121, ENST00000496340, ENST00000460410, ENST00000393857	1.12E-02
C9orf114	44.94	42.91	-0.16	ENST00000361256	5.68E-03
CABIN1	29.01	26.42	-0.29	ENST00000337989, ENST00000405822, ENST00000398319, ENST00000263119	2.84E-02
CACUL1	9.96	5.79	-1.58	ENST00000481360	5.29E-06
CACUL1	6.65	4.39	-1.20	ENST00000493518	3.68E-02
CALU	16.60	12.24	-0.89	ENST00000479257, ENST00000542996, ENST00000535623	1.49E-04

CAMK2A	16.32	11.33	-1.07	ENST00000508662	4.46E-02
CAMTA1	34.42	37.61	0.28	ENST00000486138, ENST00000303635, ENST00000473578, ENST00000467404, ENST00000557126, ENST00000461311, ENST00000490738, ENST00000476163, ENST00000439411	3.77E-02
CAMTA1	29.71	32.63	0.29	ENST00000486138, ENST00000303635, ENST00000473578, ENST00000557126, ENST00000461311, ENST00000439411	3.64E-03
CAMTA1	25.84	28.49	0.30	ENST00000473578, ENST00000303635, ENST00000467404, ENST00000557126, ENST00000490738, ENST00000476163, ENST00000439411	1.13E-02
CASC3	13.55	8.52	-1.35	ENST00000579238, ENST00000577605	3.68E-02
CASKIN2	5.83	3.30	-1.65	ENST00000581870	2.28E-02
CASP1 CARD16 CARD17	6.94	9.26	0.84	ENST00000525374, ENST00000528513, ENST00000375704, ENST00000375706	3.51E-02
CBWD1	20.94	25.57	0.60	ENST00000382389, ENST00000377447, ENST00000382447, ENST00000382393, ENST00000314367, ENST00000377400, ENST00000431099, ENST00000356521	3.51E-02
CBWD1	23.05	26.00	0.37	ENST00000382389, ENST00000377447, ENST00000382447, ENST00000382393, ENST00000314367, ENST00000377400, ENST00000465014, ENST00000431099, ENST00000356521	1.16E-02
CCDC144 B FAM106A USP32P2	6.12	8.80	1.05	ENST00000457330, ENST00000285176, ENST00000608141, ENST00000425211	3.06E-02
CCDC38	5.29	3.78	-0.97	ENST00000546386	3.41E-02
CCDC38	3.95	8.27	2.14	ENST00000344280	2.56E-03
CCDC66	5.24	2.26	-2.42	ENST00000422788, ENST00000472582, ENST00000473322	1.96E-02
CCDC74B	6.95	9.56	0.93	ENST00000392984, ENST00000457413, ENST00000496704, ENST00000434929, ENST00000310463, ENST00000423263	1.34E-02

CCDC74B	4.70	6.91	1.11	ENST00000392984, ENST00000496704, ENST00000457413, ENST00000434929, ENST00000310463	4.90E-02
CCNL1	19.18	16.69	-0.41	ENST00000483789, ENST00000471247, ENST00000474539	8.26E-03
CCNL2	9.15	11.60	0.69	ENST00000463260	1.93E-02
CDK12	13.24	10.93	-0.56	ENST00000559545, ENST00000558240	3.28E-02
CDK4	7.00	3.42	-2.07	ENST00000552254, ENST00000552388	3.24E-02
CDK4	8.15	4.22	-1.90	ENST00000552254	1.93E-02
CDK4	7.76	4.51	-1.57	ENST00000547853	1.11E-03
CDK4	9.66	6.13	-1.32	ENST00000551706	2.04E-04
CDK9 MIR3960	9.29	6.53	-1.02	ENST00000480353	3.17E-02
CDKL3 SKP1 PPP2CA	16.53	12.17	-0.90	ENST00000520417, ENST00000523359, ENST00000517625, ENST00000522855, ENST00000519054	2.03E-02
CFLAR	54.08	50.98	-0.21	ENST00000309955	5.87E-03
CGRRF1	8.92	6.31	-1.00	ENST00000556216	4.97E-02
CHD1	9.45	6.36	-1.15	ENST00000505982	3.21E-04
CHD8	5.13	2.86	-1.69	ENST00000554384	4.69E-02
CHGA	26.20	16.39	-1.41	ENST00000553866	2.47E-02
CHGA	70.48	71.88	0.08	ENST00000556876, ENST00000556076, ENST00000216492, ENST00000553866	4.95E-02
CHGA	73.12	74.60	0.08	ENST00000556876, ENST00000216492, ENST00000553866	1.34E-02
CLDN10	39.34	36.96	-0.20	ENST00000376873	1.03E-02
CLK1	14.54	10.60	-0.92	ENST00000461981	1.37E-02
CLK1	14.54	10.60	-0.92	ENST00000461981	1.37E-02
CLK1	10.51	7.91	-0.83	ENST00000496205	7.57E-03
CLK1	10.51	7.91	-0.83	ENST00000496205	7.57E-03
CLK2	12.59	9.08	-0.95	ENST00000497188	1.88E-02

CLK4 RN7SKP70	19.88	16.07	-0.63	ENST00000521621, ENST00000522556, ENST00000522749	1.04E-03
CLK4 RN7SKP70	26.82	20.39	-0.83	ENST00000521621, ENST00000522556	8.97E-10
CLK4 RN7SKP70	17.07	13.95	-0.59	ENST00000521621, ENST00000520957, ENST00000523013	3.21E-04
CLK4 RN7SKP70	7.77	10.60	0.90	ENST00000520957	3.64E-03
CLK4 RN7SKP70	20.39	24.03	0.49	ENST00000316308, ENST00000520199, ENST00000519132, ENST00000519583, ENST00000521621, ENST00000520878	2.78E-02
CLK4 RN7SKP70	21.29	25.24	0.51	ENST00000521621, ENST00000316308, ENST00000520878, ENST00000519583, ENST00000520199	1.74E-03
CLK4 RN7SKP70	20.12	17.00	-0.50	ENST00000519583, ENST00000522749, ENST00000521621, ENST00000520878, ENST00000522556, ENST00000516655	1.23E-03
CLK4 RN7SKP70	19.58	15.44	-0.70	ENST00000521621, ENST00000522556, ENST00000522749, ENST00000516655	5.29E-05
CNDP2	13.37	8.33	-1.38	ENST00000577409, ENST00000584581	1.72E-04
CNOT2	3.06	6.79	2.30	ENST00000551483	3.16E-06
CNOT7	48.46	45.81	-0.19	ENST00000523917	2.13E-02
CNOT7	48.46	45.81	-0.19	ENST00000523917	2.13E-02
CNTN1	22.86	26.28	0.42	ENST00000552913, ENST00000547849	4.69E-02
COASY NAGLU	9.70	6.75	-1.05	ENST00000588353	3.37E-02
COBLL1	5.87	8.59	1.10	ENST00000493868	2.12E-02
COG1 SSTR2	31.28	33.09	0.18	ENST00000299886, ENST00000582512, ENST00000438720, ENST00000582973	2.92E-02
COL5A1	1.16	3.57	3.24	ENST00000371817	2.71E-02
COMMD4	10.42	7.88	-0.81	ENST00000567935, ENST00000480484	8.02E-03
COMMD4	8.88	11.92	0.86	ENST00000564068, ENST00000566843, ENST00000568034, ENST00000565834, ENST00000564587, ENST00000562310	3.24E-02

COMMD4	7.10	9.58	0.87	ENST00000565834, ENST00000567935, ENST00000566843, ENST00000568034, ENST00000562310, ENST00000564587, ENST00000564068	2.92E-02
COQ10A	8.51	6.20	-0.92	ENST00000546614, ENST00000551566	4.93E-02
COX4I1	48.47	44.54	-0.29	ENST00000569997, ENST00000564903, ENST00000568339	4.37E-02
COX6A1 GATC	17.57	13.94	-0.68	ENST00000549525	7.57E-03
CPNE1 NFS1 RBM12	8.04	4.28	-1.82	ENST00000471137, ENST00000480655	1.21E-02
CPNE1 NFS1 RBM12	7.17	3.62	-1.98	ENST00000480655	4.10E-02
CPNE1 NFS1 RBM12	8.30	5.06	-1.43	ENST00000480655	4.88E-02
CPOX CLDND1	20.43	12.16	-1.53	ENST00000507411	3.84E-05
CPOX CLDND1	19.92	12.85	-1.29	ENST00000513988	8.05E-04
CREBZF	41.99	39.88	-0.17	ENST00000490820, ENST00000398294, ENST00000527447, ENST00000528889	8.31E-03
CREG2	33.37	38.33	0.44	ENST00000495455	4.54E-02
CSDE1	34.99	37.09	0.19	ENST00000358528, ENST00000534699, ENST00000438362	3.56E-02
CSRNP2	12.44	14.61	0.47	ENST00000548981, ENST00000548206	2.84E-02
CSRP1	19.39	13.22	-1.13	ENST00000533402, ENST00000458271, ENST00000527573, ENST00000532313	1.39E-03
CSRP1	16.71	12.74	-0.80	ENST00000533402	3.24E-02
CSRP1	19.85	14.06	-1.02	ENST00000533402, ENST00000529975, ENST00000532313	1.02E-03
CSRP1	33.61	24.60	-0.97	ENST00000533402, ENST00000458271, ENST00000532313	9.30E-04
CSRP1	36.68	26.77	-0.99	ENST00000533402, ENST00000532313	5.21E-05
CSRP1	23.68	17.57	-0.89	ENST00000533402, ENST00000532313, ENST00000533188	3.84E-04

CSRP1	34.98	25.73	-0.96	ENST00000533402, ENST00000532313	8.19E-05
CSRP1	29.10	21.34	-0.94	ENST00000533402, ENST00000532313	2.20E-04
CSRP1	21.35	16.67	-0.74	ENST00000533402, ENST00000527662	3.02E-05
CTNNA2	60.06	58.80	-0.08	ENST00000466387, ENST00000541047, ENST00000343114, ENST00000496558, ENST00000402739, ENST00000361291, ENST00000540488	4.77E-02
CTSD IFITM10	55.97	48.49	-0.51	ENST00000340134, ENST00000382123	1.21E-02
CYB5R2	11.99	8.13	-1.13	ENST00000526084	9.73E-03
DAAM1	5.88	9.13	1.27	ENST00000555651	9.51E-03
DDR1 MIR4640	7.54	4.63	-1.41	ENST00000514534	2.00E-02
DGCR6	24.71	26.76	0.24	ENST00000480608, ENST00000331444, ENST00000608842, ENST00000483718, ENST00000427407	3.25E-02
DGCR6	33.74	25.94	-0.82	ENST00000483718	6.16E-06
DGCR6	9.76	6.91	-1.00	ENST00000331444, ENST00000483718, ENST00000413981	3.21E-03
DICER1-AS1	5.53	8.72	1.32	ENST00000439999	1.59E-04
DIEXF	16.11	18.49	0.41	ENST00000457820, ENST00000491415	1.63E-03
DMTF1	10.61	7.76	-0.91	ENST00000425406, ENST00000480982	3.24E-02
DMTF1	22.78	16.28	-1.00	ENST00000480982	1.22E-02
DNM2	3.31	6.07	1.75	ENST00000590806	4.53E-02
DNMT1 S1PR2	6.20	3.76	-1.44	ENST00000587604	1.79E-02
DPH1 OVCA2	18.22	20.60	0.37	ENST00000572195, ENST00000571710, ENST00000263084, ENST00000572684	3.06E-02
DST	4.93	2.37	-2.12	ENST00000523943	3.28E-02
DST	4.93	2.37	-2.12	ENST00000523943	3.28E-02
DYNC2LI1	20.55	15.63	-0.81	ENST00000398823	2.93E-02
E2F4	9.08	11.94	0.80	ENST00000567007	2.96E-02

E2F6	28.02	25.17	-0.33	ENST00000428221, ENST00000444832, ENST00000381525	2.83E-02
EDRF1	10.22	7.12	-1.05	ENST00000368813	1.45E-02
EEF1E1 BLOC1S5 TXNDC5 BLOC1S5-TXNDC5 EEF1E1-BLOC1S5	4.76	2.22	-2.20	ENST00000460138	1.15E-02
EIF2AK1	6.33	3.41	-1.79	ENST00000470168	2.09E-02
EIF2AK3	7.23	2.93	-2.61	ENST00000478003	4.53E-02
EIF2AK3	7.23	2.93	-2.61	ENST00000478003	4.53E-02
EIF3F	66.97	61.66	-0.32	ENST00000533626	5.12E-05
EPB41L2	30.82	33.43	0.25	ENST00000337057, ENST00000368128, ENST00000527659, ENST00000529208, ENST00000527423, ENST00000456097, ENST00000530481, ENST00000527411, ENST00000524581	2.77E-02
EPHB6	9.82	16.70	1.56	ENST00000486511	3.62E-02
ERBB2IP	13.38	11.15	-0.54	ENST00000284037	4.01E-02
EXOC5	5.91	2.52	-2.47	ENST00000554011	1.49E-04
FADS2 FEN1	45.39	38.07	-0.58	ENST00000305885	8.91E-03
FADS2 FEN1	37.96	39.47	0.13	ENST00000521849, ENST00000278840	3.97E-02
FAM115A	17.41	3.91	-4.34	ENST00000355951, ENST00000479870	5.99E-04
FAM115A	5.04	7.80	1.26	ENST00000355951, ENST00000392900, ENST00000479870	2.28E-02
FAM115A	3.13	6.54	2.13	ENST00000355951	1.75E-04
FAM13C	22.99	20.72	-0.31	ENST00000489341, ENST00000419214, ENST00000373868, ENST00000442566, ENST00000468840, ENST00000435852	1.87E-02
FAM211A	14.46	16.88	0.46	ENST00000409887	9.73E-03
FAM49B	27.59	25.30	-0.26	ENST00000522746, ENST00000517654, ENST00000519540, ENST00000522250,	2.13E-02

				ENST00000401979, ENST00000519110, ENST00000523509, ENST00000519824, ENST00000523288	
FAM49B	27.59	25.30	-0.26	ENST00000522746, ENST00000517654, ENST00000519540, ENST00000522250, ENST00000401979, ENST00000519110, ENST00000523509, ENST00000519824, ENST00000523288	2.13E-02
FAM49B	72.60	70.00	-0.15	ENST00000519824	2.00E-03
FAM49B	72.60	70.00	-0.15	ENST00000519824	2.00E-03
FAM49B	27.80	25.49	-0.27	ENST00000522746, ENST00000523288, ENST00000519110, ENST00000523509, ENST00000519824, ENST00000401979	4.69E-02
FAM49B	27.80	25.49	-0.27	ENST00000522746, ENST00000523288, ENST00000519110, ENST00000523509, ENST00000519824, ENST00000401979	4.69E-02
FAM49B	28.48	26.09	-0.27	ENST00000522746, ENST00000517654, ENST00000522250, ENST00000401979, ENST00000519110, ENST00000523509, ENST00000519824, ENST00000523288	3.33E-02
FAM49B	28.48	26.09	-0.27	ENST00000522746, ENST00000517654, ENST00000522250, ENST00000401979, ENST00000519110, ENST00000523509, ENST00000519824, ENST00000523288	3.33E-02
FAM76B	4.45	2.15	-2.10	ENST00000540054	3.62E-02
FAM91A1	8.46	3.28	-2.75	ENST00000518333	2.67E-03
FANCL	5.49	8.38	1.22	ENST00000470506, ENST00000540646	3.25E-02
FEZ1	8.35	11.51	0.94	ENST00000577924	4.34E-02
FKBP4	10.55	12.94	0.60	ENST00000540260, ENST00000543769	3.69E-02
FKBP5	19.84	9.71	-2.10	ENST00000542713	1.75E-06
FLCN PLD6	21.61	31.46	1.15	ENST00000466317	8.72E-03
FLCN PLD6	15.47	21.38	0.96	ENST00000389169, ENST00000466317	1.36E-03
FNBP4	20.22	23.11	0.40	ENST00000530207	1.20E-02
FNBP4	7.22	9.47	0.79	ENST00000530207, ENST00000363220	4.46E-02
FNBP4	9.56	12.33	0.74	ENST00000363220	1.63E-03

FOS	4.24	8.54	2.03	ENST00000555242	4.42E-02
FOS	3.61	7.39	2.07	ENST00000554617	4.42E-02
FOS	4.58	10.01	2.27	ENST00000555347	9.73E-08
FOS	3.74	9.33	2.64	ENST00000555347, ENST00000554617	1.00E-04
FRYL	10.49	4.70	-2.33	ENST00000513401	1.04E-11
FRYL	12.36	7.94	-1.29	ENST00000514783	3.34E-03
GAB1	6.21	3.80	-1.42	ENST00000515388, ENST00000505913	2.33E-02
GAPDH	42.82	40.61	-0.17	ENST00000496049, ENST00000229239	5.22E-03
GAPDH	43.08	40.91	-0.17	ENST00000396856, ENST00000496049, ENST00000229239	6.65E-03
GAPDH	28.23	25.11	-0.36	ENST00000229239	1.77E-05
GBGT1 RALGDS	17.99	13.98	-0.74	ENST00000469972, ENST00000498797	2.37E-03
GBGT1 RALGDS	14.44	10.50	-0.93	ENST00000469972	9.78E-04
GBGT1 RALGDS	6.82	9.76	1.04	ENST00000540636, ENST00000470431, ENST00000472281, ENST00000372043, ENST00000372040, ENST00000372038	1.06E-02
GCDH	8.22	4.90	-1.50	ENST00000591050	4.13E-03
GCSH C16orf46	6.66	4.21	-1.33	ENST00000564477	4.80E-02
GIGYF1	33.00	30.46	-0.25	ENST00000275732	3.51E-02
GIMAP5 GIMAP1	11.27	14.04	0.64	ENST00000464461, ENST00000307194	5.65E-03
GIMAP5 GIMAP1	25.10	27.85	0.32	ENST00000307194	1.56E-02
GIMAP5 GIMAP1	12.85	9.66	-0.83	ENST00000476324	1.22E-03
GLYR1	3.52	6.39	1.72	ENST00000586095	2.49E-03
GMPR2	14.23	11.37	-0.66	ENST00000560517	2.16E-02

GNAS	121.45	122.16	0.03	ENST00000476935, ENST00000477931, ENST00000371095, ENST00000480232, ENST00000468895, ENST00000470512, ENST00000464624, ENST00000496934, ENST00000371075, ENST00000493958, ENST00000488546, ENST00000492907, ENST00000472183, ENST00000354359, ENST00000476196, ENST00000479025, ENST00000306090, ENST00000464788, ENST00000487862, ENST00000371102, ENST00000481039, ENST00000371100, ENST00000467321, ENST00000313949, ENST00000265620, ENST00000487981, ENST00000488652, ENST00000371085, ENST00000604005, ENST00000480975	3.95E-02
GNB2L1 SNORD95 SNORD96 A	11.97	9.07	-0.81	ENST00000514183, ENST00000502548	4.57E-02
GNL1	53.04	54.37	0.09	ENST00000462708, ENST00000376621, ENST00000464231	2.09E-02
GNL1	48.66	50.41	0.12	ENST00000462708, ENST00000376621, ENST00000487166	1.04E-03
GOLGA6L 9 UBE2Q2P2	3.46	1.03	-3.49	ENST00000300515	4.88E-02
GPCPD1	24.45	26.70	0.27	ENST00000481038, ENST00000379019, ENST00000481690	3.17E-02
GPR123	11.51	14.56	0.69	ENST00000392606	5.31E-03
GPR56	13.62	15.94	0.46	ENST00000456916, ENST00000566164, ENST00000388813, ENST00000388812, ENST00000538815, ENST00000568487, ENST00000567702, ENST00000565338, ENST00000563374, ENST00000568645, ENST00000567154, ENST00000562558, ENST00000568234, ENST00000564338, ENST00000566271, ENST00000565770, ENST00000563007, ENST00000562631	2.01E-02
GPR56	13.62	15.94	0.46	ENST00000456916, ENST00000566164, ENST00000388813, ENST00000388812, ENST00000538815, ENST00000568487, ENST00000567702, ENST00000565338, ENST00000563374, ENST00000568645, ENST00000567154, ENST00000562558, ENST00000568234, ENST00000564338,	2.01E-02

				ENST00000566271, ENST00000565770, ENST00000563007, ENST00000562631	
GPS2 NEURL4	9.93	5.66	-1.63	ENST00000576485	8.74E-08
GPX3	14.04	16.41	0.46	ENST00000388825	2.48E-02
GSTM4	0.77	3.21	4.13	ENST00000369833	3.41E-02
GUSBP13	5.21	3.43	-1.21	ENST00000506490	2.21E-02
H2AFY	4.40	6.78	1.25	ENST00000512507	2.80E-02
HBB	1.54	4.33	3.00	ENST00000475226	3.67E-02
HDAC6	9.83	13.46	0.92	ENST00000489352, ENST00000476625, ENST00000462730, ENST00000477528, ENST00000465269	3.78E-03
HECTD3	18.57	13.07	-1.03	ENST00000486132	3.95E-02
HGS	4.47	7.08	1.33	ENST00000576393	6.57E-03
HINT2	7.90	5.36	-1.12	ENST00000474908	9.96E-03
HIPK3	12.76	9.28	-0.93	ENST00000303296	2.80E-02
HK1	70.92	72.32	0.08	ENST00000360289, ENST00000448642, ENST00000359426, ENST00000404387, ENST00000494253, ENST00000298649	3.06E-02
HNRNPDL	19.81	17.83	-0.31	ENST00000502762, ENST00000295470, ENST00000602300, ENST00000349655	4.88E-02
HSPA14	28.69	32.19	0.36	ENST00000437161	4.46E-03
HSPA8 SNORD14C SNORD14D	25.90	22.49	-0.43	ENST00000527983, ENST00000453788, ENST00000533238, ENST00000534624	3.01E-03
HTR7P1	1.84	4.37	2.49	ENST00000543321	1.56E-02
HYAL2 TUSC2	71.48	73.34	0.11	ENST00000232496	1.60E-02
HYAL2 TUSC2	37.72	39.91	0.18	ENST00000454201, ENST00000417867, ENST00000421918, ENST00000463304, ENST00000462137, ENST00000232496	5.02E-03
HYAL2 TUSC2	34.44	30.36	-0.40	ENST00000395139, ENST00000447092, ENST00000357750, ENST00000442581	2.77E-04

HYAL2 TUSC2	33.38	29.22	-0.42	ENST00000395139, ENST00000447092, ENST00000442581, ENST00000357750, ENST00000481597	1.34E-02
HYAL2 TUSC2	20.32	18.12	-0.34	ENST00000428028, ENST00000442581, ENST00000462137, ENST00000395139, ENST00000424190, ENST00000447092, ENST00000458018, ENST00000481597, ENST00000426286, ENST00000357750	2.89E-02
IER3IP1 HDHD2	12.98	10.50	-0.62	ENST00000588705	1.21E-02
INPP5F	20.13	23.59	0.48	ENST00000361976	7.04E-07
INPP5F	18.20	20.57	0.37	ENST00000361976	7.47E-03
INPP5F	23.85	26.18	0.28	ENST00000361976	4.23E-03
INPP5F	13.07	15.53	0.51	ENST00000369083, ENST00000361976	8.98E-03
INPP5F	20.12	22.60	0.35	ENST00000361976	1.25E-02
ITM2C	25.04	27.26	0.26	ENST00000541852, ENST00000457215	2.34E-02
ITPKB	16.56	11.99	-0.95	ENST00000366784	4.56E-04
JMJD1C	9.57	5.69	-1.51	ENST00000497922, ENST00000483298	9.63E-03
JMJD1C	9.57	5.69	-1.51	ENST00000497922, ENST00000483298	9.63E-03
JPH4 AP1G2	16.00	14.12	-0.37	ENST00000556152, ENST00000465445	4.10E-02
KATNBL1	8.24	11.53	0.98	ENST00000560671	1.89E-02
KAZN	53.65	49.09	-0.31	ENST00000376030	8.23E-03
KCNAB2	9.00	5.59	-1.38	ENST00000378087	4.72E-02
KCNN1	35.81	37.40	0.14	ENST00000609922, ENST00000222249	3.62E-02
KDM5B	19.73	17.63	-0.33	ENST00000472822	4.36E-02
KDM6A	3.60	6.05	1.50	ENST00000377967, ENST00000451692	4.87E-02
KDM6A	3.97	7.00	1.64	ENST00000377967, ENST00000451692, ENST00000433797	1.46E-02
KHDRBS3	32.29	28.34	-0.41	ENST00000522578, ENST00000522079, ENST00000521461	3.89E-05
KHDRBS3	37.16	32.59	-0.42	ENST00000522578, ENST00000522079, ENST00000521461	4.28E-06

KIAA0408 SOGA3	18.60	15.67	-0.51	ENST00000487331	3.51E-02
KIAA2013	18.83	16.30	-0.43	ENST00000376576	7.11E-03
KIFC2	5.89	2.98	-1.97	ENST00000533114	3.37E-02
KLC1 APOPT1	29.24	31.76	0.26	ENST00000556253, ENST00000458117, ENST00000557079, ENST00000492189, ENST00000477116, ENST00000409074, ENST00000476323, ENST00000473127, ENST00000247618, ENST00000440963	1.78E-02
KLC1 APOPT1	26.71	29.13	0.27	ENST00000458117, ENST00000557079, ENST00000492189, ENST00000477116, ENST00000409074, ENST00000476323, ENST00000473127, ENST00000247618, ENST00000440963	9.43E-03
KLC1 APOPT1	35.19	37.89	0.24	ENST00000556253, ENST00000474271, ENST00000473127, ENST00000555660, ENST00000458117, ENST00000554876, ENST00000492189, ENST00000472726, ENST00000409074, ENST00000476323, ENST00000247618, ENST00000440963, ENST00000489117, ENST00000477116	1.51E-02
KLF6	3.82	0.73	-4.78	ENST00000497571, ENST00000542957, ENST00000461124	4.18E-02
KLHL2	14.26	11.28	-0.69	ENST00000509028	9.30E-04
LARP6	5.04	2.11	-2.52	ENST00000560052	4.88E-02
LEMD2	9.32	12.20	0.79	ENST00000511171	9.78E-04
LGR4	6.00	3.25	-1.77	ENST00000489910	2.09E-02
LIMCH1	11.37	14.14	0.64	ENST00000509454, ENST00000396595, ENST00000509277, ENST00000381753	8.30E-03
LINC00599	36.04	41.49	0.46	ENST00000518557, ENST00000517675	1.63E-08
LINC00623	3.31	5.64	1.54	ENST00000439332, ENST00000441423, ENST00000440719	2.33E-02
LINC02609	18.32	15.26	-0.54	ENST00000606660, ENST00000455680	9.63E-03
LMBR1L	1.89	4.86	2.73	ENST00000551169	1.85E-03
LMBR1L	11.20	16.06	1.06	ENST00000549587	7.29E-05
LMNA	4.70	1.98	-2.50	ENST00000368298, ENST00000496738	8.32E-03

LONRF1	9.66	4.99	-1.92	ENST00000534446, ENST00000526680	1.01E-10
LRP4	9.77	6.72	-1.08	ENST00000529604	1.16E-02
LRPPRC	4.81	2.31	-2.12	ENST00000483489	1.16E-02
LRPPRC	4.81	2.31	-2.12	ENST00000483489	1.16E-02
LRRC8C LRRC8D	62.05	69.36	0.43	ENST00000370454	9.64E-03
LRRC8C LRRC8D	74.20	73.07	-0.06	ENST00000337338, ENST00000394593	5.73E-04
MAD1L1	12.35	16.04	0.77	ENST00000437877	5.72E-03
MAG	10.61	7.82	-0.89	ENST00000597162	1.34E-02
MAGI2	4.02	1.01	-3.98	ENST00000517762	1.04E-03
MAN2A1	8.87	6.16	-1.06	ENST00000508043	4.46E-03
MANBA	4.14	1.27	-3.42	ENST00000514430	6.39E-03
MAP3K12	5.86	10.56	1.71	ENST00000547020	2.65E-02
MAP3K12	11.44	5.89	-1.93	ENST00000547020	1.01E-04
MAP4K4	40.99	42.85	0.15	ENST00000476609, ENST00000347699, ENST00000413150, ENST00000324219, ENST00000417294, ENST00000425019, ENST00000350198, ENST00000350878	3.37E-02
MAPK8IP2	65.17	60.21	-0.30	ENST00000399908	3.54E-03
MAST4	5.79	8.14	0.99	ENST00000434115, ENST00000406374, ENST00000470421, ENST00000490016, ENST00000403666, ENST00000450827	2.59E-02
MAT2A	27.83	18.38	-1.25	ENST00000481412	4.99E-02
MBD5	15.27	12.44	-0.60	ENST00000404807, ENST00000416015	3.51E-02
MEG3	11.42	15.16	0.83	ENST00000521812, ENST00000452120	3.25E-02
MEG3	11.42	15.16	0.83	ENST00000521812, ENST00000452120	3.25E-02
MEG3	8.39	11.68	0.96	ENST00000455531, ENST00000524131, ENST00000398461, ENST00000524035	2.18E-02
MEG3	8.39	11.68	0.96	ENST00000455531, ENST00000524131, ENST00000398461, ENST00000524035	2.18E-02

MEG3	15.33	19.43	0.70	ENST00000455531, ENST00000398461, ENST00000524035	1.02E-02
MEG3	15.33	19.43	0.70	ENST00000455531, ENST00000398461, ENST00000524035	1.02E-02
MEG3	15.55	19.65	0.69	ENST00000455531, ENST00000398461, ENST00000524035	2.78E-02
MEG3	15.55	19.65	0.69	ENST00000455531, ENST00000398461, ENST00000524035	2.78E-02
METTL17	8.43	5.21	-1.40	ENST00000554751, ENST00000554283, ENST00000553564	6.22E-04
METTL17	8.43	5.21	-1.40	ENST00000554751, ENST00000554283, ENST00000553564	6.22E-04
MFSD1	14.25	8.69	-1.44	ENST00000465235	4.63E-03
MFSD1	10.09	6.20	-1.41	ENST00000465235, ENST00000468409	4.10E-02
MICAL3	8.81	11.18	0.69	ENST00000579997	3.37E-02
MICALL2	9.06	12.00	0.82	ENST00000496184, ENST00000470807	8.23E-03
MICALL2	18.67	21.72	0.45	ENST00000472100	4.42E-02
MIER1	7.81	10.11	0.75	ENST00000371012	3.34E-02
MLLT10	13.48	16.79	0.65	ENST00000377100, ENST00000377091	7.65E-04
MLLT6	7.43	11.20	1.19	ENST00000494578	4.54E-02
MROH8	13.07	10.85	-0.54	ENST00000417458, ENST00000441008, ENST00000217333, ENST00000343811, ENST00000400441	3.25E-02
MRPL13	7.85	4.16	-1.84	ENST00000523316	4.37E-02
MRPS24 URGCP URGCP-MRPS24	48.02	51.14	0.22	ENST00000603700, ENST00000418740, ENST00000317534	2.50E-02
MRPS24 URGCP URGCP-MRPS24	45.52	48.88	0.24	ENST00000483330, ENST00000603700, ENST00000418740, ENST00000317534	7.49E-03
MRPS24 URGCP URGCP-MRPS24	52.12	55.63	0.23	ENST00000483330, ENST00000603700, ENST00000467084, ENST00000418740, ENST00000317534	3.21E-04

MRPS24 URGCP URGCP-MRPS24	39.30	42.36	0.25	ENST00000483330, ENST00000467084, ENST00000317534, ENST00000603700, ENST00000414932, ENST00000418740	3.18E-07
MRPS24 URGCP URGCP-MRPS24	31.77	34.67	0.28	ENST00000414932, ENST00000603700, ENST00000467084, ENST00000418740, ENST00000317534	1.17E-04
MRPS24 URGCP URGCP-MRPS24	78.00	74.76	-0.18	ENST00000223341, ENST00000447717, ENST00000453200, ENST00000443736, ENST00000402306, ENST00000497914, ENST00000336086	4.84E-05
MRPS24 URGCP URGCP-MRPS24	39.57	37.00	-0.22	ENST00000223341, ENST00000447717, ENST00000439702, ENST00000453200, ENST00000455877, ENST00000443736, ENST00000467410, ENST00000402306, ENST00000426198, ENST00000497914, ENST00000474376, ENST00000336086	3.51E-02
MRPS24 URGCP URGCP-MRPS24	31.06	28.94	-0.22	ENST00000223341, ENST00000447717, ENST00000439702, ENST00000453200, ENST00000443736, ENST00000402306, ENST00000497914, ENST00000336086	3.68E-02
MRPS33	8.36	5.00	-1.49	ENST00000485202, ENST00000496641	3.26E-02
MRS2	44.15	40.43	-0.29	ENST00000378386, ENST00000274747	4.45E-02
MSI2	7.63	9.91	0.76	ENST00000581776	2.00E-02
MSTO1 MSTO2P	9.45	7.02	-0.87	ENST00000466815	6.39E-03
MT1X DPPA2P4	12.66	6.76	-1.83	ENST00000568370	4.45E-02
MTMR10	9.90	6.70	-1.13	ENST00000568611	2.86E-02
MTRR	9.06	6.38	-1.01	ENST00000509961	4.23E-03
MTUS1	27.61	31.77	0.44	ENST00000520196, ENST00000523718, ENST00000262102, ENST00000381862, ENST00000519263, ENST00000381869	1.16E-02
MTUS1	14.61	17.30	0.50	ENST00000520196, ENST00000523718, ENST00000262102, ENST00000381862, ENST00000519263, ENST00000381869	7.57E-03
MUC20 SDHAP2	14.39	18.20	0.69	ENST00000414625, ENST00000445430	4.10E-02

LINC0096 9					
NADSYN1	5.47	3.21	-1.55	ENST00000525245, ENST00000527538	4.24E-02
NASP	30.05	33.70	0.36	ENST00000453748, ENST00000537798, ENST00000470768, ENST00000350030, ENST00000402363	7.63E-03
NBL1 MINOS1 MINOS1-NBL1	9.44	6.84	-0.93	ENST00000486890	5.68E-03
NBPF24	2.63	4.58	1.61	ENST00000369228, ENST00000474625, ENST00000470042	4.79E-02
NCKAP5L	7.00	10.09	1.06	ENST00000477361	4.10E-04
NDRG1	24.67	15.48	-1.39	ENST00000519278	4.13E-02
NDRG2	18.21	16.01	-0.38	ENST00000556688, ENST00000557616, ENST00000557318, ENST00000556329, ENST00000554379, ENST00000554143, ENST00000397851, ENST00000557676, ENST00000397853, ENST00000555142	4.79E-02
NDUFA6-AS1	7.98	4.75	-1.51	ENST00000416037, ENST00000608491	2.92E-02
NDUFA6-AS1	7.21	4.04	-1.67	ENST00000416037, ENST00000608491, ENST00000439129	2.77E-02
NDUFA6-AS1	10.19	5.76	-1.65	ENST00000608288, ENST00000608491	1.67E-05
NDUFA6-AS1	12.62	7.52	-1.51	ENST00000608288, ENST00000608491	1.59E-02
NDUFA6-AS1	11.28	6.82	-1.46	ENST00000417586, ENST00000608288, ENST00000608491	4.88E-02
NDUFB5	8.26	4.10	-2.03	ENST00000477177	7.81E-04
NDUFB5	9.02	5.70	-1.33	ENST00000491054, ENST00000477177	4.05E-02
NDUFB5	9.02	4.99	-1.72	ENST00000482604, ENST00000491054	3.68E-02
NDUFB5	12.23	6.84	-1.69	ENST00000491054	3.97E-02
NEB	6.14	3.79	-1.39	ENST00000421461, ENST00000409198, ENST00000397345, ENST00000498015, ENST00000413693, ENST00000603639, ENST00000509223, ENST00000604864, ENST00000424585, ENST00000172853,	2.30E-02

				ENST00000434685, ENST00000427231, ENST00000397337	
NEMF	9.04	3.65	-2.63	ENST00000556074	6.16E-06
NFE2L1	22.68	24.97	0.29	ENST00000577431, ENST00000536222, ENST00000580050, ENST00000579537	3.17E-02
NFRKB	4.28	6.73	1.31	ENST00000304521, ENST00000524794	1.56E-02
NGFRAP1	55.34	52.01	-0.22	ENST00000299872, ENST00000372645, ENST00000372635	4.05E-02
NOC2L	2.78	5.32	1.88	ENST00000496938	4.46E-02
NOC3L	7.66	4.35	-1.64	ENST00000463649	4.22E-05
NONO	7.02	3.62	-1.91	ENST00000486613	7.43E-03
NONO	6.80	3.30	-2.09	ENST00000490044	2.08E-02
NOSTRIN	8.04	4.75	-1.53	ENST00000472260	4.47E-02
NOSTRIN	5.52	2.69	-2.08	ENST00000486873	1.50E-02
NOSTRIN	6.02	3.73	-1.38	ENST00000472260	3.56E-02
NR2C1	7.32	10.71	1.11	ENST00000549617	4.75E-02
NRXN2	6.97	4.62	-1.19	ENST00000466324	4.53E-02
NSMAF	5.92	3.62	-1.42	ENST00000519166	3.89E-02
NSMAF	7.59	4.78	-1.34	ENST00000519166, ENST00000524148	2.36E-02
OAT	11.01	8.27	-0.83	ENST00000492376, ENST00000490096	3.87E-02
ODF2L	37.86	35.97	-0.17	ENST00000359242, ENST00000294678	8.18E-03
OSBPL7	5.38	8.39	1.29	ENST00000583167	9.46E-04
OSBPL7	5.10	7.77	1.22	ENST00000583167, ENST00000580808	1.56E-02
OSGEP	9.31	5.48	-1.54	ENST00000555223	2.25E-03
OSGEP	9.31	5.48	-1.54	ENST00000555223	2.25E-03
P2RX5 TAX1BP3 P2RX5-TAX1BP3	3.61	7.48	2.11	ENST00000549063	3.41E-03
PACSIN1	41.12	43.89	0.22	ENST00000486120, ENST00000538621, ENST00000487760	1.34E-02

PALM3	22.61	25.28	0.34	ENST00000340790	1.05E-02
PCNX	4.67	2.44	-1.88	ENST00000557428	4.80E-02
PCSK1	59.57	61.38	0.11	ENST00000513085, ENST00000508626, ENST00000311106	1.56E-02
PCYOX1	4.38	7.03	1.37	ENST00000505044, ENST00000414812	2.65E-02
PDCD6IP	4.30	7.89	1.76	ENST00000489869	9.23E-05
PDCD6IP	4.30	7.89	1.76	ENST00000489869	9.23E-05
PDGFC	5.97	3.50	-1.54	ENST00000511985	1.48E-02
PER1 VAMP2	36.73	32.51	-0.39	ENST00000317276, ENST00000581082	5.78E-03
PER1 VAMP2	51.83	45.59	-0.44	ENST00000317276, ENST00000581082, ENST00000582719	2.01E-04
PER1 VAMP2	29.82	25.47	-0.48	ENST00000581082, ENST00000317276, ENST00000583677, ENST00000582719	2.73E-03
PER1 VAMP2	36.95	31.30	-0.53	ENST00000583677, ENST00000585284, ENST00000317276, ENST00000581082, ENST00000582719	5.78E-06
PER1 VAMP2	38.58	32.93	-0.51	ENST00000585284, ENST00000317276, ENST00000583677, ENST00000581082, ENST00000582719	1.21E-05
PER1 VAMP2	37.19	32.10	-0.47	ENST00000581082, ENST00000317276, ENST00000585284, ENST00000582719	1.95E-03
PER1 VAMP2	31.82	28.11	-0.39	ENST00000579098, ENST00000317276, ENST00000581082, ENST00000582719	4.14E-02
PER1 VAMP2	108.50	111.96	0.17	ENST00000316509, ENST00000498285, ENST00000404970, ENST00000481878, ENST00000488857	2.21E-02
PER1 VAMP2	27.63	24.44	-0.37	ENST00000354903, ENST00000317276, ENST00000578223, ENST00000581082, ENST00000582719, ENST00000581395	2.02E-02
PER1 VAMP2	27.95	24.96	-0.35	ENST00000354903, ENST00000317276, ENST00000578223, ENST00000581082, ENST00000582719, ENST00000581395	4.26E-02
PER1 VAMP2	27.83	22.85	-0.60	ENST00000354903, ENST00000317276, ENST00000581082, ENST00000581703, ENST00000582719, ENST00000577253, ENST00000581395, ENST00000579065	7.50E-03

PER1 VAMP2	20.59	18.52	-0.32	ENST00000354903, ENST00000317276, ENST00000581082, ENST00000583559, ENST00000578089, ENST00000582719	2.65E-02
PER1 VAMP2	27.24	23.63	-0.43	ENST00000354903, ENST00000578089, ENST00000317276, ENST00000581082, ENST00000582719	5.84E-04
PER1 VAMP2	27.54	22.78	-0.58	ENST00000354903, ENST00000317276, ENST00000581082, ENST00000581703, ENST00000582719, ENST00000581395, ENST00000579065	1.64E-03
PER1 VAMP2	25.35	22.67	-0.34	ENST00000354903, ENST00000581395, ENST00000579065, ENST00000317276, ENST00000582719	1.06E-02
PER1 VAMP2	23.74	20.06	-0.51	ENST00000354903, ENST00000317276, ENST00000581082, ENST00000582719, ENST00000581395, ENST00000579065	2.57E-02
PER1 VAMP2	26.71	23.31	-0.41	ENST00000354903, ENST00000581395, ENST00000317276, ENST00000581082, ENST00000582719	1.72E-02
PER1 VAMP2	24.91	20.82	-0.54	ENST00000354903, ENST00000317276, ENST00000581082, ENST00000581703, ENST00000582719, ENST00000581395, ENST00000579065	1.41E-02
PER1 VAMP2	25.56	21.95	-0.46	ENST00000354903, ENST00000581395, ENST00000317276, ENST00000581082, ENST00000582719	2.00E-02
PER1 VAMP2	30.45	26.95	-0.38	ENST00000354903, ENST00000317276, ENST00000581082, ENST00000582719, ENST00000581395, ENST00000585095	1.56E-02
PER1 VAMP2	27.44	23.82	-0.43	ENST00000354903, ENST00000317276, ENST00000578223, ENST00000581082, ENST00000582719, ENST00000581395	2.39E-02
PER1 VAMP2	29.77	25.65	-0.46	ENST00000354903, ENST00000317276, ENST00000581082, ENST00000582719, ENST00000581395, ENST00000579065	8.71E-03
PER1 VAMP2	27.27	23.60	-0.44	ENST00000354903, ENST00000317276, ENST00000581082, ENST00000579203, ENST00000582719, ENST00000581395, ENST00000577424, ENST00000585095	1.65E-02
PER1 VAMP2	30.20	25.88	-0.48	ENST00000354903, ENST00000317276, ENST00000581082, ENST00000578089, ENST00000582719, ENST00000581395	7.33E-04

PEX1	10.47	7.72	-0.89	ENST00000496420	1.68E-02
PFKFB3	25.74	23.52	-0.27	ENST00000461744, ENST00000360521, ENST00000317350, ENST00000379785, ENST00000414237, ENST00000379782, ENST00000490474, ENST00000467491	2.05E-02
PGAP2	7.06	9.36	0.82	ENST00000465237, ENST00000485602, ENST00000487112, ENST00000459679	2.90E-02
PI4KA	73.32	72.37	-0.05	ENST00000572273, ENST00000494113, ENST00000255882	3.68E-02
PI4KAP2	13.77	16.84	0.59	ENST00000479693, ENST00000360806, ENST00000467443, ENST00000450651, ENST00000462560, ENST00000480319, ENST00000546263	9.78E-03
PI4KAP2	8.73	11.62	0.83	ENST00000479693, ENST00000360806, ENST00000467443, ENST00000450651, ENST00000462560, ENST00000480319	2.69E-02
PILRA PILRB PVRIG2P STAG3L5P STAG3L5P -PVRIG2P-PILRB	7.63	10.83	1.02	ENST00000493091	2.30E-03
PIP4K2A	55.54	54.02	-0.10	ENST00000474335, ENST00000376573, ENST00000323883	4.75E-02
PKIA	84.09	81.92	-0.12	ENST00000396418	2.12E-02
PLEC	19.53	16.66	-0.47	ENST00000532346, ENST00000528025	3.71E-02
PLEKHM1 P	17.83	20.03	0.35	ENST00000582986, ENST00000397718, ENST00000580919, ENST00000578036, ENST00000440036, ENST00000584585, ENST00000582201	4.05E-02
PLOD2	8.21	4.81	-1.54	ENST00000478436	2.01E-02
PLP1	15.98	19.94	0.66	ENST00000303958, ENST00000361621	1.07E-03
PLXNB1	8.16	4.60	-1.66	ENST00000473996	1.21E-02
POLDIP3	7.29	4.28	-1.54	ENST00000454057, ENST00000491021	3.16E-03
PPA1	6.81	2.61	-2.77	ENST00000373230, ENST00000610026	3.95E-02
PPP2R5C	10.38	5.54	-1.82	ENST00000553730	8.98E-03

PRDM1	4.63	2.12	-2.25	ENST00000481163, ENST00000369089	3.51E-02
PRODH	8.49	12.01	1.01	ENST00000491604, ENST00000482858, ENST00000313755, ENST00000609229	4.31E-02
PRODH	8.49	12.01	1.01	ENST00000491604, ENST00000482858, ENST00000313755, ENST00000609229	4.31E-02
PRSS53 VKORC1	25.98	27.89	0.22	ENST00000532364, ENST00000354895, ENST00000300851, ENST00000529564, ENST00000319788, ENST00000394975	2.80E-02
PSEN2	0.78	3.48	4.33	ENST00000487450, ENST00000471728	1.12E-02
PSMC5	7.95	5.30	-1.18	ENST00000581764	4.46E-03
PTDSS1	28.45	23.99	-0.52	ENST00000517309	1.23E-04
PTK7	5.82	3.01	-1.90	ENST00000493339	2.68E-03
PTPRN	9.19	12.94	1.00	ENST00000486480	2.39E-02
PTPRN	8.58	12.73	1.15	ENST00000462351, ENST00000484986	1.47E-02
QKI	39.41	36.52	-0.25	ENST00000541696, ENST00000361752, ENST00000361758	2.01E-02
RAB3D TMEM205	49.33	54.02	0.32	ENST00000222120	2.09E-03
RAP1GAP2	8.01	5.21	-1.25	ENST00000254695, ENST00000542807, ENST00000366401	3.04E-03
RAP1GAP2	8.01	5.21	-1.25	ENST00000254695, ENST00000542807, ENST00000366401	3.04E-03
RAP1GAP2	6.46	4.06	-1.34	ENST00000254695, ENST00000366401	2.14E-02
RAP1GAP2	6.46	4.06	-1.34	ENST00000254695, ENST00000366401	2.14E-02
RAPGEF6 FNIP1	22.48	25.09	0.33	ENST00000307968, ENST00000307954, ENST00000510461, ENST00000511848	1.68E-02
RASSF4	15.13	9.97	-1.22	ENST00000471941	1.82E-07
RASSF4	7.53	4.82	-1.29	ENST00000428466, ENST00000471941	2.57E-02
RASSF4	8.60	5.79	-1.15	ENST00000428466	1.30E-02
RASSF4	11.92	9.14	-0.77	ENST00000471941	2.70E-03
RASSF4	11.65	9.02	-0.75	ENST00000462822, ENST00000471941	7.57E-03
RB1	11.23	14.52	0.75	ENST00000484879	2.32E-02

RBBP4	84.56	82.27	-0.12	ENST00000373493	1.46E-02
RBFOX2	20.41	24.29	0.52	ENST00000416721, ENST00000262829, ENST00000449924, ENST00000397305, ENST00000405409, ENST00000491982	4.23E-03
RBFOX2	20.56	23.89	0.45	ENST00000414461, ENST00000416721, ENST00000491982, ENST00000449924, ENST00000397305, ENST00000405409, ENST00000262829	1.30E-02
RBFOX2	18.47	22.45	0.58	ENST00000397305, ENST00000262829, ENST00000491982, ENST00000449924, ENST00000405409	4.71E-04
RDH11 VTI1B	4.50	7.32	1.41	ENST00000553578	4.46E-03
RDH5 BLOC1S1	46.45	47.88	0.10	ENST00000548556, ENST00000549147, ENST00000548925, ENST00000547076, ENST00000553100, ENST00000257899	3.95E-02
RELA	7.31	11.62	1.35	ENST00000525693	3.75E-02
RFNG	9.52	11.78	0.62	ENST00000582478	4.93E-02
RHOBTB2	6.68	3.15	-2.18	ENST00000517528	4.80E-02
RIT1	39.26	37.69	-0.13	ENST00000368323	4.75E-02
RLTPR	4.72	2.36	-2.00	ENST00000602321	2.89E-02
RNF125 RNF138	12.01	9.38	-0.72	ENST00000580863, ENST00000583814, ENST00000583384, ENST00000217740	4.45E-02
RNF19A	10.46	5.76	-1.73	ENST00000520071	2.04E-02
RNH1	9.52	6.49	-1.11	ENST00000525522, ENST00000524780	4.84E-02
RNPC3 ACTG1P4 AMY2B	8.22	13.61	1.47	ENST00000533834	8.19E-05
RPGRIP1L	20.60	24.17	0.48	ENST00000568653	1.46E-02
RPL13A ALDH16A1 SNORD35A SNORD32A SNORD34	5.51	3.20	-1.57	ENST00000476268, ENST00000363389, ENST00000488946, ENST00000476300, ENST00000472481	3.84E-02

FLT3LG SNORD33					
RPL37	74.60	75.52	0.05	ENST00000274242, ENST00000504562, ENST00000507642, ENST00000509877	5.47E-03
RPLP0	6.37	3.64	-1.62	ENST00000548495, ENST00000551783, ENST00000549242	4.76E-02
RPRD2	25.11	22.56	-0.32	ENST00000369068	1.10E-02
RPS11 SNORD35 B	70.44	72.20	0.10	ENST00000270625, ENST00000602252, ENST00000599167, ENST00000601216, ENST00000596873, ENST00000600027, ENST00000594493	4.46E-03
RPS25	19.36	13.19	-1.13	ENST00000524864, ENST00000532567, ENST00000527853	1.38E-02
RSBN1L	5.74	3.03	-1.85	ENST00000462800	7.47E-03
RSRC2	6.94	3.11	-2.32	ENST00000531639, ENST00000525335	1.54E-03
RSRC2	7.78	3.51	-2.30	ENST00000531639	3.21E-04
RSRC2	12.15	6.57	-1.79	ENST00000527173	4.47E-05
RTDR1	5.00	7.96	1.35	ENST00000216036	3.68E-02
RTDR1	4.21	6.95	1.45	ENST00000216036	7.50E-03
RTKN	10.71	6.11	-1.63	ENST00000472518, ENST00000464094	9.18E-03
RTKN	19.19	14.43	-0.84	ENST00000492013	3.94E-04
RYK	9.38	6.04	-1.28	ENST00000473208	3.97E-02
SAFB2	8.20	14.53	1.67	ENST00000591101	3.77E-02
SAFB2	12.00	18.70	1.31	ENST00000591310	2.32E-02
SAR1B	81.08	78.21	-0.16	ENST00000402673	3.06E-02
SARM1 TMEM199 MIR4723	40.51	37.29	-0.27	ENST00000457710	1.56E-02
SART3	6.53	4.22	-1.26	ENST00000547528	4.77E-02
SART3	6.53	4.22	-1.26	ENST00000547528	4.77E-02
SCHIP1 IQCJ IQCJ-SCHIP1	29.33	20.30	-1.12	ENST00000482885	4.42E-02

SCHIP1 IQCJ IQCJ-SCHIP1	20.82	14.40	-1.09	ENST00000482885, ENST00000472483	5.65E-03
SCRG1	33.28	31.05	-0.22	ENST00000296506	2.06E-02
SEMA6D	12.86	15.58	0.56	ENST00000358066, ENST00000559064, ENST00000560006, ENST00000537942, ENST00000389432, ENST00000558014	1.94E-03
SEMA6D	11.71	14.08	0.54	ENST00000558014, ENST00000358066, ENST00000559064, ENST00000537942, ENST00000389432	3.98E-02
SEPT3	6.72	9.35	0.96	ENST00000449288	1.95E-02
SEPW1	16.53	14.34	-0.42	ENST00000593892, ENST00000601048, ENST00000509570	4.45E-02
SEPW1	16.53	14.34	-0.42	ENST00000593892, ENST00000601048, ENST00000509570	4.45E-02
SERPINH1	5.41	2.54	-2.19	ENST00000528760, ENST00000532356, ENST00000524558, ENST00000525611, ENST00000530284, ENST00000533603, ENST00000533449	3.95E-03
SERPINH1	5.41	2.54	-2.19	ENST00000528760, ENST00000532356, ENST00000524558, ENST00000525611, ENST00000530284, ENST00000533603, ENST00000533449	3.95E-03
SETD5	9.10	5.35	-1.54	ENST00000488236	3.84E-07
SETD6	8.55	11.07	0.75	ENST00000491587	4.50E-02
SFSWAP	7.18	10.51	1.11	ENST00000539506	4.46E-03
SFSWAP	5.72	9.00	1.31	ENST00000539506	1.22E-03
SGK1	18.08	25.01	0.97	ENST00000533224, ENST00000524929, ENST00000367858	4.44E-05
SGK1	14.46	19.84	0.94	ENST00000461976, ENST00000484353, ENST00000367858, ENST00000524387, ENST00000531575	5.85E-04
SGK1	14.33	18.97	0.83	ENST00000524929, ENST00000367858	7.70E-03
SGK1	15.20	20.30	0.86	ENST00000461976, ENST00000524929, ENST00000367858, ENST00000484353, ENST00000460769	6.10E-03
SGK1	15.44	22.12	1.07	ENST00000461976, ENST00000533224, ENST00000524929, ENST00000367858	2.52E-05

SGK1	14.98	19.79	0.82	ENST00000367858	2.84E-02
SGK1	13.96	18.86	0.89	ENST00000460769, ENST00000533224, ENST00000461976, ENST00000524929, ENST00000367858	2.68E-04
SGK1	13.55	18.53	0.92	ENST00000460769, ENST00000524929, ENST00000461976, ENST00000367858	1.22E-03
SGSM3	12.90	17.72	0.93	ENST00000478085	1.43E-03
SH3BP2	48.61	46.77	-0.13	ENST00000442312, ENST00000503393, ENST00000356331	2.06E-02
SH3BP2	48.61	46.77	-0.13	ENST00000442312, ENST00000503393, ENST00000356331	2.06E-02
SH3KBP1	44.60	42.43	-0.17	ENST00000379726, ENST00000541422, ENST00000379716, ENST00000397821, ENST00000379698	1.89E-02
SH3TC2-DT	3.78	7.32	1.91	ENST00000507318	9.73E-03
SHANK2	7.64	11.36	1.15	ENST00000409530	3.62E-02
SLC1A3	5.63	2.83	-1.99	ENST00000506178	3.06E-03
SLC1A3	6.71	3.76	-1.68	ENST00000502864	1.22E-03
SLC35E2B	28.68	24.59	-0.47	ENST00000234800, ENST00000378662, ENST00000481276	2.57E-02
SLC35E2B	30.97	28.77	-0.23	ENST00000234800, ENST00000378662, ENST00000481276	4.02E-02
SLC38A3	6.60	3.40	-1.92	ENST00000417851	1.46E-02
SLC48A1	39.18	35.52	-0.32	ENST00000442892, ENST00000442218	4.84E-02
SLC6A8	16.57	8.44	-1.97	ENST00000476466	5.84E-04
SLC6A8	16.57	8.44	-1.97	ENST00000476466	5.84E-04
SLC6A8	15.86	9.16	-1.60	ENST00000466243	4.46E-02
SLC6A8	15.86	9.16	-1.60	ENST00000466243	4.46E-02
SLCO1A2	23.48	16.71	-1.02	ENST00000480394	8.55E-03
SLCO4A1	11.08	8.08	-0.92	ENST00000497209	3.68E-02
SMEK1	16.58	14.16	-0.47	ENST00000428424, ENST00000554574, ENST00000555029, ENST00000555462, ENST00000554943, ENST00000555470	1.64E-02

SMEK1	16.10	13.56	-0.51	ENST00000555029, ENST00000555462, ENST00000554943, ENST00000554574, ENST00000428424	7.67E-03
SMG1P1 NPIPB5	11.73	9.62	-0.58	ENST00000545375, ENST00000541154, ENST00000543407	4.25E-02
SMG1P1 NPIPB5	12.66	9.67	-0.79	ENST00000415654, ENST00000431681, ENST00000309865, ENST00000546168, ENST00000378955	6.57E-03
SMG1P2	11.10	18.42	1.49	ENST00000566127	3.37E-02
SNRNP40	7.50	3.89	-1.90	ENST00000489853	1.92E-04
SNRPA1	9.54	6.55	-1.09	ENST00000559686	2.15E-02
SNRPN SNURF SNHG14	46.91	41.56	-0.41	ENST00000553597, ENST00000400097, ENST00000400098, ENST00000400100	3.37E-02
SNRPN SNURF SNHG14	27.14	21.91	-0.65	ENST00000553597, ENST00000400097	4.79E-03
SNRPN SNURF SNHG14	40.80	36.46	-0.37	ENST00000553597, ENST00000400097, ENST00000400098, ENST00000400100	2.73E-03
SP3	24.62	22.29	-0.30	ENST00000310015, ENST00000455789	4.88E-02
SPECC1	19.50	16.52	-0.49	ENST00000582226, ENST00000395525, ENST00000584527, ENST00000395522, ENST00000395529	1.09E-03
SPECC1	19.50	16.52	-0.49	ENST00000582226, ENST00000395525, ENST00000584527, ENST00000395522, ENST00000395529	1.09E-03
SPECC1	30.86	25.58	-0.58	ENST00000395529	1.49E-08
SPECC1	30.86	25.58	-0.58	ENST00000395529	1.49E-08
SPECC1	14.98	11.88	-0.68	ENST00000395522, ENST00000395529	1.12E-04
SPECC1	14.98	11.88	-0.68	ENST00000395522, ENST00000395529	1.12E-04
SPEG	23.93	21.66	-0.30	ENST00000475921, ENST00000462545, ENST00000498378, ENST00000464989, ENST00000396695, ENST00000396698, ENST00000396689, ENST00000396688	1.30E-02
SPG20	8.74	6.09	-1.05	ENST00000482146	7.47E-03

SPHK2	20.23	17.29	-0.47	ENST00000245222, ENST00000340932, ENST00000601712, ENST00000598088, ENST00000600537	1.26E-03
SPHK2	19.55	22.46	0.42	ENST00000599029, ENST00000443164, ENST00000599748	1.34E-03
SPHK2	14.54	16.97	0.46	ENST00000599748, ENST00000443164	2.92E-02
SPHK2	20.57	23.29	0.37	ENST00000599748, ENST00000599029, ENST00000443164, ENST00000598574	2.09E-03
SPHK2	19.87	16.62	-0.53	ENST00000340932, ENST00000245222, ENST00000601712, ENST00000426514, ENST00000600537, ENST00000598088	8.55E-03
SPOP	12.62	9.88	-0.71	ENST00000509079, ENST00000503676, ENST00000507970, ENST00000347630, ENST00000508805, ENST00000514121, ENST00000505581	3.04E-03
SPP1	11.53	7.37	-1.30	ENST00000513981, ENST00000504310, ENST00000509659, ENST00000509334	4.97E-02
SPP1	9.85	6.00	-1.44	ENST00000505146	3.50E-02
SRSF5	47.73	45.58	-0.16	ENST00000557154, ENST00000394366, ENST00000553548, ENST00000554465, ENST00000556184, ENST00000557435, ENST00000553635, ENST00000553369, ENST00000553521, ENST00000451983	8.10E-04
SRSF5	48.50	46.26	-0.16	ENST00000394366, ENST00000556184, ENST00000557154, ENST00000554465, ENST00000557435, ENST00000553635, ENST00000553369, ENST00000557460, ENST00000451983, ENST00000553521, ENST00000553548	6.67E-04
SRSF5	49.09	47.00	-0.15	ENST00000557154, ENST00000394366, ENST00000553548, ENST00000556184, ENST00000554465, ENST00000557435, ENST00000553635, ENST00000556587, ENST00000553369, ENST00000557460, ENST00000553521, ENST00000451983	3.54E-03
SRSF5	45.13	43.18	-0.15	ENST00000394366, ENST00000553548, ENST00000557154, ENST00000554465, ENST00000557435, ENST00000553635, ENST00000553369, ENST00000553521, ENST00000451983	9.46E-04
SSBP1 TAS2R6	12.64	6.35	-2.00	ENST00000461433, ENST00000468267, ENST00000496622	2.69E-02

SSBP1 TAS2R6	9.02	4.40	-2.08	ENST00000469123, ENST00000465167	8.19E-03
SSBP1 TAS2R6	6.98	3.08	-2.37	ENST00000469123	3.21E-03
SSX2IP	9.98	4.51	-2.31	ENST00000460500	1.47E-02
STARD3NL	6.96	11.45	1.45	ENST00000471550	3.14E-02
STARD3NL	6.96	11.45	1.45	ENST00000471550	3.14E-02
STAT2	8.15	5.37	-1.21	ENST00000557156	1.90E-03
STK24	15.06	18.89	0.67	ENST00000376547	4.61E-03
STT3A CHEK1	2.21	4.73	2.20	ENST00000533778, ENST00000524737	3.71E-02
SYN1	71.63	73.25	0.09	ENST00000340666, ENST00000295987	1.47E-02
SYT1	12.92	15.40	0.52	ENST00000551304	1.46E-02
SYT17 ITPRIPL2	10.71	13.58	0.70	ENST00000562274	1.28E-02
TAF10	36.91	33.20	-0.34	ENST00000526743	2.14E-02
TAF1C	11.55	8.90	-0.76	ENST00000570270, ENST00000562330, ENST00000565279	3.37E-02
TAF1C	13.50	10.39	-0.77	ENST00000570270, ENST00000562330	7.57E-03
TAF1D SNORA32 SNORA1 SNORA25 SNORA18 SNORA8 SNORA40 MIR1304 SNORD5	33.82	30.61	-0.31	ENST00000448108, ENST00000534770, ENST00000527068, ENST00000323981, ENST00000532235, ENST00000526015, ENST00000527169	1.23E-03
TANC1	8.78	5.05	-1.60	ENST00000470074	1.84E-05
TAOK2	42.07	44.35	0.18	ENST00000566552, ENST00000416441, ENST00000543033, ENST00000308893	3.08E-02
TBC1D24 AMDHD2 ATP6V0C	35.20	32.96	-0.21	ENST00000569874, ENST00000293970, ENST00000564879, ENST00000567020	3.69E-02
TBCD	10.84	15.63	1.07	ENST00000571796, ENST00000576677	2.74E-04

TBCD	14.03	19.53	0.98	ENST00000576677	1.63E-02
TBX2	7.88	10.14	0.73	ENST00000477081	3.62E-02
TCF25 TUBB3 MC1R	48.31	46.64	-0.12	ENST00000566751, ENST00000263347, ENST00000263346, ENST00000562184, ENST00000562256	4.94E-02
TCF25 TUBB3 MC1R	47.76	46.11	-0.12	ENST00000263347, ENST00000263346, ENST00000562256, ENST00000568412, ENST00000566751, ENST00000568409, ENST00000562184	4.33E-02
TCF25 TUBB3 MC1R	46.87	45.20	-0.12	ENST00000263347, ENST00000263346, ENST00000562256, ENST00000568412, ENST00000566751, ENST00000568409, ENST00000562184, ENST00000563636	2.89E-02
TENC1	16.33	18.60	0.39	ENST00000552403, ENST00000379902, ENST00000546602, ENST00000552570, ENST00000451358, ENST00000314250, ENST00000549311, ENST00000549700, ENST00000551302, ENST00000549498, ENST00000314276	2.27E-02
TENC1	6.54	9.77	1.16	ENST00000552403	3.89E-02
TFRC	4.83	2.18	-2.30	ENST00000464011	3.92E-02
TFRC	4.83	2.18	-2.30	ENST00000464011	3.92E-02
THOC2	7.59	5.05	-1.18	ENST00000497887, ENST00000496830	1.02E-02
THOC2	7.59	5.05	-1.18	ENST00000497887, ENST00000496830	1.02E-02
TIE1	8.00	4.08	-1.95	ENST00000538015	3.74E-07
TIE1	8.00	4.08	-1.95	ENST00000538015	3.74E-07
TM9SF1 NEDD8 IPO4 MDP1 CHMP4A NEDD8-MDP1	15.26	12.66	-0.55	ENST00000531406	2.41E-03
TM9SF1 NEDD8 IPO4 MDP1 CHMP4A NEDD8-MDP1	12.50	10.28	-0.57	ENST00000396854	2.77E-02

TMBIM1	54.45	52.58	-0.12	ENST00000465082, ENST00000396809, ENST00000445635, ENST00000258412, ENST00000444881	4.71E-03
TMEM132A	9.98	12.61	0.68	ENST00000537110	8.70E-03
TMEM184 B	6.33	3.41	-1.79	ENST00000436674, ENST00000466117	2.65E-02
TMEM234	7.41	9.72	0.79	ENST00000466796, ENST00000373593	3.41E-02
TMEM70 RPS20P21	24.05	18.80	-0.74	ENST00000312184, ENST00000466859	3.94E-04
TMEM70 RPS20P21	18.10	14.22	-0.71	ENST00000312184	3.71E-02
TMX1	3.14	5.95	1.84	ENST00000555574	3.14E-02
TNNT2 LAD1	20.07	22.30	0.32	ENST00000360372, ENST00000421663, ENST00000367315, ENST00000476888, ENST00000367317, ENST00000367318, ENST00000458432, ENST00000460780, ENST00000367322, ENST00000236918, ENST00000491504, ENST00000367320, ENST00000509001	7.65E-04
TNNT2 LAD1	25.88	27.88	0.23	ENST00000360372, ENST00000421663, ENST00000367320, ENST00000476888, ENST00000367322, ENST00000367318, ENST00000458432, ENST00000460780, ENST00000367317, ENST00000509001, ENST00000479297, ENST00000491504, ENST00000367315, ENST00000236918	1.10E-02
TNNT2 LAD1	25.37	27.23	0.22	ENST00000360372, ENST00000421663, ENST00000476888, ENST00000367315, ENST00000438742, ENST00000367317, ENST00000367318, ENST00000458432, ENST00000460780, ENST00000367322, ENST00000236918, ENST00000479297, ENST00000491504, ENST00000367320, ENST00000509001	2.00E-02
TNNT2 LAD1	28.63	30.63	0.21	ENST00000360372, ENST00000421663, ENST00000476888, ENST00000367320, ENST00000438742, ENST00000367322, ENST00000367318, ENST00000367317, ENST00000460780, ENST00000458432, ENST00000509001, ENST00000479297, ENST00000491504, ENST00000367315, ENST00000236918	2.50E-02

TNNT2 LAD1	21.09	5.99	-3.68	ENST00000360372, ENST00000515042, ENST00000476888, ENST00000367317, ENST00000367318, ENST00000460780, ENST00000236918, ENST00000491504, ENST00000509001	1.78E-02
TNNT2 LAD1	23.93	16.47	-1.12	ENST00000360372, ENST00000421663, ENST00000367315, ENST00000438742, ENST00000476888, ENST00000515042, ENST00000367318, ENST00000367317, ENST00000460780, ENST00000458432, ENST00000367322, ENST00000509001, ENST00000479297, ENST00000491504, ENST00000367320, ENST00000236918	2.08E-05
TNNT2 LAD1	24.27	17.71	-0.94	ENST00000360372, ENST00000421663, ENST00000367320, ENST00000438742, ENST00000476888, ENST00000515042, ENST00000367318, ENST00000367317, ENST00000460780, ENST00000458432, ENST00000367315, ENST00000367322, ENST00000236918, ENST00000491504, ENST00000479297, ENST00000466570, ENST00000509001	2.91E-05
TNNT2 LAD1	22.62	18.17	-0.66	ENST00000360372, ENST00000421663, ENST00000367315, ENST00000438742, ENST00000367322, ENST00000515042, ENST00000367318, ENST00000458432, ENST00000460780, ENST00000367317, ENST00000236918, ENST00000479297, ENST00000491504, ENST00000367320, ENST00000466570, ENST00000509001	6.22E-04
TNPO2	45.03	47.70	0.20	ENST00000450764	1.21E-02
TNPO2	45.03	47.70	0.20	ENST00000450764	1.21E-02
TNRC6A	16.49	19.72	0.53	ENST00000395799, ENST00000462400, ENST00000568750, ENST00000491718	7.47E-03
TPGS2	13.03	10.67	-0.58	ENST00000590652	1.64E-02
TREX2 HAUS7	13.26	10.89	-0.58	ENST00000491286, ENST00000437046, ENST00000330912, ENST00000421080, ENST00000435662, ENST00000370212, ENST00000484394	2.00E-02
TRIP6	5.79	3.35	-1.58	ENST00000463125	2.12E-02
TTC37	15.05	10.43	-1.07	ENST00000506007	3.37E-02
TTLL4	13.39	10.43	-0.73	ENST00000480929, ENST00000491899	2.00E-02

TTLL4	8.94	6.25	-1.04	ENST00000480929	3.42E-02
TUBA1B	11.55	9.25	-0.65	ENST00000547476	4.87E-02
TUBB4A	102.87	102.04	-0.04	ENST00000264071, ENST00000595324, ENST00000598006, ENST00000540257, ENST00000601640, ENST00000598635, ENST00000594290, ENST00000597686, ENST00000596926, ENST00000596291, ENST00000601152	1.21E-02
TULP3 RHNO1	4.43	2.03	-2.25	ENST00000540184	2.55E-02
TXNIP	5.85	3.11	-1.83	ENST00000488537	9.51E-03
TYK2	9.79	13.41	0.92	ENST00000534228	6.77E-04
UBB	118.08	116.82	-0.06	ENST00000578649, ENST00000302182, ENST00000535788	9.43E-03
UBE2E2	14.45	8.84	-1.44	ENST00000427371, ENST00000396703	2.87E-03
UBXN6	7.36	3.76	-1.95	ENST00000587009, ENST00000588238	2.09E-02
UHRF2	13.81	10.20	-0.88	ENST00000479000, ENST00000485617	6.84E-04
UNC13B	15.28	18.74	0.60	ENST00000378496, ENST00000396787, ENST00000378495	3.51E-02
UNC45A	6.47	10.03	1.27	ENST00000487875	3.24E-02
UQCRB	70.39	71.26	0.05	ENST00000287022, ENST00000519322, ENST00000518406, ENST00000521036, ENST00000521948, ENST00000517603, ENST00000523920, ENST00000518876	1.29E-02
UQCRB	70.39	71.26	0.05	ENST00000287022, ENST00000519322, ENST00000518406, ENST00000521036, ENST00000521948, ENST00000517603, ENST00000523920, ENST00000518876	1.29E-02
USP14	17.12	10.76	-1.36	ENST00000578942	4.48E-02
USP4 C3orf62	26.99	23.84	-0.38	ENST00000343010, ENST00000479673	3.94E-04
VDAC2	10.20	7.61	-0.85	ENST00000535553, ENST00000498394, ENST00000470745, ENST00000475142, ENST00000468285, ENST00000472137	7.42E-03
VSTM2A	1.35	4.15	3.25	ENST00000466888	1.05E-02

WAC	64.77	63.13	-0.10	ENST00000354911, ENST00000439676, ENST00000375664, ENST00000375646, ENST00000345541, ENST00000347934, ENST00000480474	3.73E-02
WASF1	47.48	45.91	-0.11	ENST00000392588, ENST00000392589, ENST00000359451, ENST00000265601, ENST00000392587, ENST00000444391, ENST00000447287	3.62E-02
WDR33	23.83	21.68	-0.29	ENST00000436787, ENST00000322313	2.43E-02
WDR33	24.30	22.06	-0.29	ENST00000409658, ENST00000436787, ENST00000393006, ENST00000322313	1.04E-02
WDR53	3.52	1.06	-3.45	ENST00000425888	2.47E-02
WHSC1L1	5.81	9.59	1.46	ENST00000525081	4.99E-03
WSB1	11.12	14.32	0.74	ENST00000487603	1.36E-02
XPO1	9.51	5.16	-1.77	ENST00000481073	3.89E-02
YPEL4	4.58	7.28	1.34	ENST00000544993, ENST00000524669	7.70E-03
ZC3H11A ZBED6	26.37	29.61	0.36	ENST00000550078, ENST00000545588, ENST00000495527	2.65E-02
ZC3H11A ZBED6	30.05	35.48	0.52	ENST00000550078	2.33E-02
ZMYM6 ZMYM6NB	12.62	10.06	-0.66	ENST00000417456	1.46E-02
ZNF200	11.75	9.53	-0.61	ENST00000575285	3.51E-02
ZNF200	11.75	9.53	-0.61	ENST00000575285	3.51E-02
ZNF211	6.64	8.91	0.85	ENST00000347302, ENST00000240731	4.55E-02
ZNF211	6.69	8.97	0.85	ENST00000541801, ENST00000391703, ENST00000347302, ENST00000240731	4.80E-02
ZNF211	6.68	9.09	0.89	ENST00000347302	1.43E-02
ZNF263	19.39	15.10	-0.74	ENST00000575332	8.57E-04
ZNF263	9.79	7.47	-0.78	ENST00000575332, ENST00000574674	3.06E-02
ZNF263	12.12	8.79	-0.93	ENST00000574674, ENST00000575332	2.52E-05
ZNF263	12.80	15.34	0.53	ENST00000573578, ENST00000219069	5.47E-03

ZNF287	5.98	3.68	-1.40	ENST00000461555	4.10E-02
ZNF512B SOX18	16.21	26.13	1.43	ENST00000340356	3.94E-04
ZNF512B SOX18	8.51	14.25	1.50	ENST00000340356, ENST00000450537	4.60E-04
ZNF512B SOX18	11.73	18.07	1.27	ENST00000340356	3.51E-02
ZNF568	24.41	21.77	-0.35	ENST00000415168	1.98E-03
ZNF626 ZNF737	33.31	28.00	-0.54	ENST00000427401	7.04E-07
ZNF644	11.54	14.02	0.57	ENST00000479798	1.94E-02
ZNF681	3.81	6.06	1.35	ENST00000402377, ENST00000528059	2.65E-02
ZNF76	6.92	12.40	1.70	ENST00000498555, ENST00000229405	4.23E-04
ZNF76	5.58	9.61	1.57	ENST00000229405	4.11E-02
ZNF777	36.99	38.80	0.15	ENST00000247930	1.22E-02
ZNF841 ZNF432	30.57	33.27	0.27	ENST00000221315, ENST00000594154	1.44E-02
ZNF890P	13.63	10.59	-0.74	ENST00000530367	2.53E-02
ZNF91	40.47	35.88	-0.39	ENST00000596528	8.98E-03
ZNRF1	3.08	5.76	1.81	ENST00000566244	1.78E-02
ZNRF1	41.27	38.14	-0.26	ENST00000568844, ENST00000335325	1.16E-02
ZSCAN25	6.28	3.76	-1.49	ENST00000485586, ENST00000481424	1.43E-02
ZSCAN30	10.26	7.85	-0.78	ENST00000586922	1.93E-02

Abbreviations: ASE, alternative splicing event; RPKM, reads per kilobase per million mapped reads

Supplementary Table 4-4 – significant ASEs in genes identified by DEXSeq and SpliceSeq methods (*p*<0.01)*

Gene Symbol	RPKM Control	RPKM PD	Splice Type	Exons	dPSI	Magnitude	P-value
AHDC1	4.88	4.33	ES	3	0.177	0.87	2.20E-03
AHDC1	4.88	4.33	ES	3	0.177	0.87	2.20E-03
AKAP17A	4.96	4.90	ES	4.3	-0.172	0.59	7.02E-05
AKAP17A	4.96	4.90	AD	4.2:4.3	-0.161	0.71	4.79E-03
AKAP17A	4.96	4.90	RI	4.2	0.116	0.66	7.47E-03
AMY2B	9.65	7.59	ES	10	-0.026	0.99	8.57E-03
APOL2	26.13	23.70	AP	1	0.090	0.03	3.80E-03
APOL2	26.13	23.70	AP	2.1	-0.090	0.25	3.80E-03
APOLD1	12.74	12.38	AT	4	-0.249	1.00	1.79E-04
APOLD1	12.74	12.38	AT	17	0.249	1.00	1.79E-04
ASCC3	2.32	2.46	AT	43	0.062	1.00	1.14E-03
ASCC3	2.32	2.46	AT	4	-0.062	0.24	1.14E-03
BAZ2A	5.81	5.99	AP	1	0.169	0.08	6.45E-03
BAZ2A	5.81	5.99	AP	2	-0.169	0.11	6.45E-03

C11orf30	2.53	2.19	AT	22	-0.074	1.00	7.60E-05
C11orf30	2.53	2.19	AT	4.2	0.074	0.37	7.60E-05
C1orf63	12.07	14.33	ES	5.1:5.2:5.3	-0.439	0.20	3.76E-04
C3orf17	7.19	6.89	AD	3.2	-0.052	0.65	9.05E-03
CALU	12.49	13.78	ES	2	-0.095	0.48	4.11E-03
CAMTA1	19.38	19.17	AT	26	-0.046	1.00	4.83E-03
CAMTA1	19.38	19.17	AT	5	0.042	0.62	5.55E-03
CCDC66	2.32	2.07	AT	8	-0.094	0.11	1.51E-03
CCDC66	2.32	2.07	ES	13	-0.134	0.97	8.46E-03
CCDC74B	1.04	1.56	AA	3.3:3.4	0.187	0.98	6.42E-03
CHGA	122.42	103.47	ES	6	0.015	1.00	8.01E-03
CLK1	12.22	17.41	ES	5	0.408	0.40	5.57E-05
CLK1	12.22	17.41	AP	1	0.087	0.31	7.07E-03
CLK4	6.58	6.80	RI	2.2	0.153	0.48	3.64E-05
CLK4	6.58	6.80	ES	2.3:3	-0.327	0.87	9.04E-04
CNOT2	10.82	10.18	RI	11.3	0.010	0.88	1.11E-04

CNOT2	10.82	10.18	ES	3.2	0.048	0.84	3.20E-03
CNTN1	81.00	77.78	AP	1	-0.045	0.41	8.21E-03
CNTN1	81.00	77.78	AP	2	0.045	0.09	8.21E-03
COMMD4	9.73	9.72	AT	10	-0.085	0.10	3.99E-03
COMMD4	9.73	9.72	AT	9.2	0.085	0.34	3.99E-03
CTNNA2	49.95	50.42	AP	16	0.006	0.00	9.27E-03
E2F6	4.50	4.58	ES	2:03	-0.180	0.24	5.75E-03
EEF1E1	17.95	17.62	AT	5	-0.014	0.03	3.12E-03
FAM13C	11.31	10.30	AA	14.1	-0.094	0.91	1.64E-03
FKBP5	13.08	10.03	AT	13	0.019	1.00	7.13E-03
FKBP5	13.08	10.03	AT	10.2	-0.019	0.03	7.13E-03
FLCN	8.84	7.39	AT	14	-0.077	1.00	3.94E-03
FLCN	8.84	7.39	AT	8.2	0.077	0.42	3.94E-03
FOS	2.96	6.61	RI	2.3	0.211	0.80	7.04E-03
FRYL	5.14	4.84	ES	47	0.043	1.00	8.42E-03
GPS2	17.11	17.40	RI	1.2	-0.059	0.31	9.38E-03

HIPK3	7.63	7.53	ES	14	-0.139	0.69	7.10E-05
HSPA14	4.90	4.27	AT	15	-0.070	0.88	5.49E-03
HSPA14	4.90	4.27	AT	4	0.070	0.78	5.49E-03
JMJD1C	7.07	7.17	AA	17.1	0.028	0.95	9.04E-03
KIAA2013	8.96	10.36	AT	2.2	-0.044	0.29	7.63E-03
KIAA2013	8.96	10.36	AT	3	0.044	1.00	7.63E-03
KLC1	217.72	201.57	ES	15:16	0.114	0.01	7.24E-03
LONRF1	5.83	7.63	ES	7	-0.114	0.80	1.53E-03
MLLT10	3.45	2.72	AT	26	-0.077	1.00	3.28E-04
MLLT10	3.45	2.72	AT	5	0.077	0.71	3.28E-04
MSTO1	5.20	5.11	ES	4.2:5	0.015	0.99	3.98E-03
MTMR10	13.82	15.39	ES	8	-0.028	0.58	7.99E-03
NASP	16.74	13.25	ES	9	0.112	0.99	4.94E-04
PACSIN1	104.65	104.20	AP	1	-0.044	0.31	1.23E-04
PACSIN1	104.65	104.20	AP	2	0.044	0.27	1.23E-04
PFKFB3	13.66	13.91	ES	18.1	-0.187	0.45	1.11E-03

PLOD2	5.56	5.55	ES	15	-0.072	0.96	1.90E-03
PSEN2	6.35	6.51	AD	13.3	-0.014	0.68	3.93E-03
QKI	69.27	68.82	AT	9	-0.013	0.14	6.18E-03
QKI	69.27	68.82	AT	8.7	0.013	1.00	6.18E-03
RBFOX2	23.11	21.33	AP	1	-0.107	0.23	5.99E-04
RBFOX2	23.11	21.33	AP	3	0.107	0.29	5.99E-04
RELA	5.53	5.30	RI	10.2	0.086	0.87	8.03E-03
RLTPR	16.27	15.50	ES	36	-0.064	0.83	5.43E-03
RPGRIP1L	2.86	2.50	AT	4	0.067	0.53	4.42E-03
RPGRIP1L	2.86	2.50	AT	28	-0.105	0.86	5.39E-03
RPL17	142.11	128.87	AA	3.2:3.3	0.035	0.53	6.85E-03
RPL17-C18orf32	5.06	4.85	ES	6	-0.065	0.67	4.69E-03
RPRD2	9.38	8.78	ES	4	-0.139	0.94	2.44E-04
SART3	11.54	10.56	ES	7	-0.036	0.73	8.42E-05
SEMA6D	7.19	6.62	AA	21.1	0.159	0.98	4.76E-04
SEMA6D	7.19	6.62	ES	23.1:23.2	0.146	0.59	1.53E-03

SEMA6D	7.19	6.62	ES	22	-0.140	0.66	4.14E-03
SERPINH1	1.15	2.21	ES	2.2	-0.358	0.57	4.64E-03
SGK1	30.56	11.59	AP	1	0.118	0.28	8.10E-04
SGK1	30.56	11.59	AP	6.1	-0.102	0.73	3.74E-03
SKP1	299.56	299.63	ES	3	-0.004	0.52	2.77E-03
SLCO4A1	2.22	2.09	RI	8.4	-0.199	1.00	4.56E-04
SMEK1	7.91	7.50	AD	7.2	-0.130	0.74	2.37E-03
SNRPN	248.68	230.90	AP	3	-0.024	0.04	4.45E-03
SNURF	66.71	86.46	ES	6	0.003	1.00	6.86E-03
SPECC1	11.31	12.00	AT	10	-0.092	0.25	9.49E-05
SPECC1	11.31	12.00	AT	18	0.092	0.61	9.49E-05
SPEG	3.35	3.32	AT	16	-0.044	1.00	1.70E-04
SPEG	3.35	3.32	AT	48	0.044	1.00	1.70E-04
SPHK2	9.70	13.57	AP	3.1	0.072	0.68	3.46E-04
SPHK2	9.70	13.57	AP	1.1	-0.072	0.10	3.46E-04
SRP19	12.56	11.31	AA	5.1	-0.056	0.98	8.23E-03

STK24	27.51	29.18	AP	2	0.149	0.15	2.43E-03
STK24	27.51	29.18	AP	1	-0.149	0.26	2.43E-03
TAF1D	14.40	15.69	AA	8.1	0.161	0.44	1.54E-03
TAOK2	17.32	17.62	AT	19	-0.031	0.65	7.94E-03
TAOK2	17.32	17.62	AT	16.3	0.031	0.49	7.94E-03
TMEM184B	22.88	23.20	ES	4.1:4.2	-0.015	0.58	9.81E-04
TMEM184B	22.88	23.20	ES	4.1:4.2:5	-0.288	0.04	2.33E-03
TMEM234	1.63	1.99	RI	5.2:5.3	0.140	1.00	7.68E-04
TNPO2	38.29	39.82	AP	4	-0.026	0.10	4.12E-03
TNRC6A	7.15	7.11	ES	13	0.156	0.92	1.58E-03
VDAC2	79.93	80.76	ES	7	-0.007	0.85	1.58E-03
WDR33	6.30	5.74	RI	6.2	0.090	1.00	7.18E-03
YPEL4	17.76	15.71	RI	1.4:1.5	0.065	0.60	5.87E-03
ZNF263	3.01	3.19	ES	3:4:5.1:6	0.175	0.93	9.73E-03
ZNF76	5.27	4.80	RI	12.4	0.122	1.00	2.13E-03
ZNF76	5.27	4.80	AA	12.1:12.2	0.092	0.52	6.34E-03

Abbreviations: AD, alternate donor; AP, alternate promoter; ASE, alternative splicing event; AT, alternate terminator; DEGs, differentially expressed genes; dPSI, delta percent spliced in; ES, exon skipping; RI, retained intron; RPKM, reads per kilobase of transcript per million aligned reads

*data shown comprises 146 ASEs identified by SpliceSeq in the seventy-six genes found to be alternatively spliced by both analysis methods

Supplementary Table 4-5 – ASEs identified by SpliceSeq in significant DEGs from Chapter 3

Gene	RPKM Control	RPKM PD	Splice Type	Exons	dPSI	Magnitude	*P*-value
ACSS1	12.34	16.38	ES	12.2:13:14:15.1	-0.002	1.00	8.30E-03
APOLD1	12.74	12.38	AT	4	-0.249	1.00	1.79E-04
APOLD1	12.74	12.38	AT	17	0.249	1.00	1.79E-04
CLK1	12.22	17.41	ES	5	0.408	0.40	5.57E-05
CLK1	12.22	17.41	AP	1	0.087	0.31	7.07E-03
CX3CR1	1.40	2.66	AP	3	0.011	0.03	8.74E-03
IP6K3	1.48	0.83	ES	2	0.120	0.76	2.81E-03
LGALS1	88.66	112.00	ES	3	0.002	1.00	1.22E-03
LONRF1	5.83	7.63	ES	7	-0.114	0.80	1.53E-03
SERPINH1	1.15	2.21	ES	2.2	-0.358	0.57	4.64E-03
SGK1	30.56	11.59	AP	1	0.118	0.28	8.10E-04
SGK1	30.56	11.59	AP	6.1	-0.102	0.73	3.74E-03
SPHK2	9.70	13.57	AP	3.1	0.072	0.68	3.46E-04
SPHK2	9.70	13.57	AP	1.1	-0.072	0.10	3.46E-04

Abbreviations: AD, alternate donor; AP, alternate promoter; ASE, alternative splicing event; AT, alternate terminator; DEGs, differentially expressed genes; dPSI, delta percent spliced in; ES, exon skipping; RI, retained intron; RPKM, reads per kilobase of transcript per million aligned reads

Curriculum Vitae

Simon M. Benoit

EDUCATION

09/15-Present	Ph.D. Neuroscience University of Western Ontario, London, Ontario
09/13-04/15	B.Sc. (Hons) Psychology University of Ottawa, Ottawa, Ontario

SCHOLARSHIPS AND AWARDS

04/21 CNS Research Day 2021
Best Oral Presentation Award ($300)

Neuroscience Travel Award
2019-2020

Queen Elizabeth II Graduate Scholarship in Science and Technology
2019-2020

Neuroscience Travel Award
2018-2019

IDI in Stem Cells and Regenerative Medicine Grad Student/PDF Traineeship
2018-2019

International Congress Travel Grant Award, Movement Disorders Society
2018-2019

Neuroscience Travel Award
2017-2018

Raie and Nathan Pollack - Western Fund Ontario Graduate Scholarship/Queen Elizabeth II Graduate Scholarship in Science and Technology
2017-2018

Western Graduate Research Scholarship
2017-2018

Queen Elizabeth II Graduate Scholarship in Science and Technology
2016-2017

Western Graduate Research Scholarship
2016-2017

Western Graduate Research Scholarship
2015-2016

Related Work Experience	Teaching Assistant, Integrative Neuroscience The University of Western Ontario 2015, 2019

Publications:

Benoit SM, Xu H, Schmid S, Alexandrova R, Kaur G, Thiruvahindrapuram B, Pereira S, Jog M, Hebb MO (2020) Expanding the search for genetic biomarkers of Parkinson's Disease into the living brain. Submitted to Neurobiology of Disease.

Di Sebastiano AR, Deweyert A, **Benoit SM**, Iredale E, Xu H, De Oliviera C, Wong E, Schmid S, Hebb MO (2018) Preclinical outcomes of Intratumoral Modulation Therapy for glioblastoma. Scientific Reports 8(1): 1-11. doi:10.1038/s41598-018-25639-7.

De la Tremblaye PB, **Benoit SM**, Schock S, Plamondon H (2017) CRHR1 exacerbates the glial inflammatory response and alters BDNF / TrkB / pCREB signaling in a rat model of global cerebral ischemia : implications for neuroprotection and cognitive recovery. Prog Neuropsychopharmacol Biol Psychiatry 79:234–248 Available at: http://dx.doi.org/10.1016/j.pnpbp.2017.06.021.

Di Sebastiano AR, Staudt MD, **Benoit SM**, Xu H, Hebb MO, Schmid S (2016) Cell-Based Therapies for Parkinson's Disease: Preclinical and Clinical Perspectives. In: Challenges in Parkinson's Disease (Dorszewska J, ed). InTech. Available at: http://www.intechopen.com/books/challenges-in-parkinson-s-disease/cell-based-therapies-for-parkinson-s-disease-preclinical-and-clinical-perspectives.